# THE TRANSPARENCY OF SELECTED U.S. COASTAL WATERS WITH APPLICATIONS TO LASER BATHYMETRY

Maxim F. van Norden and Steven E. Litts

# NAVAL POSTGRADUATE SCHOOL
## Monterey, California

# THESIS

THE TRANSPARENCY OF SELECTED U.S. COASTAL WATERS WITH APPLICATIONS TO LASER BATHYMETRY

by

Maxim F. van Norden

and

Steven E. Litts

September 1979

Thesis Advisor: S. P. Tucker

Approved for public release; distribution unlimited.

UNCLASSIFIED

SECURITY CLASSIFICATION OF THIS PAGE (When Data Entered)

| REPORT DOCUMENTATION PAGE | | READ INSTRUCTIONS BEFORE COMPLETING FORM |
|---|---|---|
| 1. REPORT NUMBER | 2. GOVT ACCESSION NO. | 3. RECIPIENT'S CATALOG NUMBER |
| 4. TITLE (and Subtitle)<br>The Transparency of Selected U.S. Coastal Waters with Applications to Laser Bathymetry | | 5. TYPE OF REPORT & PERIOD COVERED<br>Master's Thesis; September 1979<br>6. PERFORMING ORG. REPORT NUMBER |
| 7. AUTHOR(s)<br>Maxim F. van Norden and Steven E. Litts | | 8. CONTRACT OR GRANT NUMBER(s) |
| 9. PERFORMING ORGANIZATION NAME AND ADDRESS<br>Naval Postgraduate School<br>Monterey, California 93940 | | 10. PROGRAM ELEMENT, PROJECT, TASK AREA & WORK UNIT NUMBERS |
| 11. CONTROLLING OFFICE NAME AND ADDRESS<br>Naval Postgraduate School<br>Monterey, California 93940 | | 12. REPORT DATE<br>September 1979<br>13. NUMBER OF PAGES<br>162 pages |
| 14. MONITORING AGENCY NAME & ADDRESS(if different from Controlling Office)<br>Naval Postgraduate School<br>Monterey, California 93940 | | 15. SECURITY CLASS. (of this report)<br>15a. DECLASSIFICATION/DOWNGRADING SCHEDULE |

16. DISTRIBUTION STATEMENT (of this Report)

Approved for public release; distribution unlimited.

17. DISTRIBUTION STATEMENT (of the abstract entered in Block 20, if different from Report)

18. SUPPLEMENTARY NOTES

19. KEY WORDS (Continue on reverse side if necessary and identify by block number)

Irradiance data, transparency, coastal waters, coastal zone, laser bathymetry, laser hydrography, Secchi data, light attenuation data, turbidity, beam transmittance data, irradiance attenuation lengths, marine optics, optical oceanography, Pacific Northwest & Gulf Coasts.

20. ABSTRACT (Continue on reverse side if necessary and identify by block number)

The operational effectiveness of airborne laser hydrography systems, considering the optical environment of the coastal waters of Oregon, Washington, and the Gulf Coast states, is examined. The best times of the year are predicted for conducting laser bathymetry considering the temporal and spatial variability of optical properties due to seasonal effects, and charts of seasonally averaged optical measurements are given. Original formulas to convert beam attenuation coefficients and Secchi depth measurements to irradiance

DD FORM 1 JAN 73 1473 (Page 1)

EDITION OF 1 NOV 65 IS OBSOLETE

S/N 0102-014-6601

UNCLASSIFIED

SECURITY CLASSIFICATION OF THIS PAGE (When Data Entered)

attenuation coeffients are included. The number of irradiance attenuation lengths to the bottom depth (Kd) are used as the indicator to estimate areas where laser hydrography systems would be successful and are shown by season and region. The conclusions of this thesis are that airborne laser hydrography is not practical in the coastal waters of Oregon and Washington, would be practical in limited areas of the western Gulf Coast, and would be very practical in the eastern Gulf Coast area. Along the eastern Gulf Coast a 38,800 $nmi^2$ area, delineated by a Kd = 4 contour, is judged surveyable by laser.

pproved for public release; distribution unlimited.

# The Transparency of Selected U.S. Coastal Waters with Applications to Laser Bathymetry

by

Maxim F. van Norden
Civil Engineer, U.S. Naval Oceanographic Office
B.S., University of Maryland, 1972

and

Steven E. Litts
Cartographer, Defense Mapping Agency
B.S., Pennsylvania State University, 1975

Submitted in partial fulfillment of the
requirements for the degree of

MASTER OF SCIENCE IN OCEANOGRAPHY (HYDROGRAPHY)

from the

NAVAL POSTGRADUATE SCHOOL
September 1979

ABSTRACT

The operational effectiveness of airborne laser hydrography systems, considering the optical environment of the coastal waters of Oregon, Washington, and the Gulf Coast states, is examined. The best times of the year are predicted for conducting laser bathymetry, considering the temporal and spatial variability of optical properties due to seasonal effects, and charts of seasonally averaged optical measurements are given. Original formulas to convert beam attenuation coefficients and Secchi depth measurements to irradiance attenuation coefficients are included. The number of irradiance attenuation lengths to the bottom depth (Kd) are used as the indicator to estimate areas where laser hydrography systems would be successful and are shown by season and region. The conclusionsof this thesis are that airborne laser hydrography is not practical in the coastal waters of Oregon and Washington, would be practical in limited areas of the western Gulf Coast, and would be very practical in the eastern Gulf Coast area. Along the eastern Gulf Coast a 38,800 $nmi^2$ area, delineated by a Kd = 4 contour, is judged surveyable by laser.

TABLE OF CONTENTS

LIST OF TABLES

LIST OF FIGURES

ACKNOWLEDGEMENTS

We would like to express our sincere gratitude to Assistant Professor Stevens P. Tucker, our thesis advisor, for his assistance and patience; Mr. David B. Enabnit for inspiring our thesis and providing funds for satellite imagery; and Lucia van Norden, an understanding wife, for her data key-punching and typing. Many people helped us in our search for data, and we are grateful to: Henry Odum of the National Oceanographic Data Center; Louis Hoelman of the Environmental Protection Agency; Gloria Richie of the Texas Natural Resources Information System; Dr. Murray Brown of the Bureau of Land Management; Dr. Hasong Pak and Dr. Lawrence Small of Oregon State University; John Grady of the National Marine Fisheries Service; V. Stewart of the Florida Department of Natural Resources; Gerald Shideler of the U.S. Geological Survey; and Larry Breaker of National Environmental Satellite Service. People who assisted us in the concepts of our thesis include: Andrew Bakun of the National Marine Fisheries Service and John Shannon and Howard Krumboltz of the Naval Air Development Center.

# I. INTRODUCTION

## A. HYDROGRAPHY AND THE DEVELOPMENT OF LASER BATHYMETRY

Hydrography has been defined as, "that science which deals with the measurement and description of the physical features of the oceans, seas, lakes, rivers, and other waters, and their adjoining coastal areas, with particular reference to their use for navigational purposes" (U.S. Naval Oceanographic Office, 1966). Hydrographic surveys are used to produce nautical charts and related information which satisfy navigational, engineering and marine scientific needs and contribute to national goals such as ocean resource management and national defense. However, these products may become quickly outdated, and new surveys are required because of changes caused by such natural processes as winds, tides, earthquakes and because of man-made changes resulting from construction of ports, channels, breakwaters, and pipelines. New surveys might also be needed because of changing requirements, for example those associated with deep draft tankers. Since the 1930s most hydrographic surveys have been performed by ships equipped with sonic depth sounders to obtain bathymetric data.

A new method for hydrographic surveying, airborne laser bathymetry, was shown to be a fast reliable technique to obtain bathymetric data by the U.S. Naval Oceanographic Office (NAVOCEANO) with their Pulsed Light Airborne Depth Sounder (PLADS) in 1969 (Bright, 1973). The PLADS system used a frequency-doubled Neodymium Yttrium Aluminum Garnet (Nd:YAG) laser (Rattman and

Cunningham, 1969). NAVOCEANO's interest in such a system resulted from immediate requirements stemming from the Vietnam War for better charts of shallow coastal waters within range of enemy controlled territory (Bright, 1973).

Since that time further work has been done by NAVOCEANO, NASA, National Ocean Survey (NOS), and the Australian Weapons Research Establishment. In 1974 NAVOCEANO tested a NASA-owned neon laser and in 1975 obtained a frequency-doubled Nd:YAG laser for their Coastal Aerial Photo-Laser Survey (CAPS) system (Crandall, 1976). In 1977 NASA, with DOD and NOS sponsorship, began testing their Airborne Oceanographic Lidar (AOL) as a hydrographic data acquisition system (Guenther and Enabnit, 1978). The success of these tests influenced the Naval Oceanographic Research and Development Agency (NORDA) to place their Hydrographic Airborne Laser Sounder (HALS) in the procurement stage in 1978 and influenced NOS to implement a development plan for a more sophisticated system in 1979. The Australian Weapons Research Establishment has built two systems, one for research and one for operational surveys (National Ocean Survey, 1979).

## B. MAJOR BENEFITS OBTAINABLE FROM LASER BATHYMETRY

The National Ocean Survey (1979) has evaluated airborne laser hydrography and has found four major benefits realizable over ship/sonar hydrography with this technique: cost savings, manpower savings, capability of increased production, and improvement in the quality of marine charts.

The NOS (1979) study showed that projected cost savings would be achieved through the speed with which an area could be surveyed. Figure 1 shows the costs per unit area as a function of area surveyed annually. The three curves represent amortized nonrecurring capital cost, operating cost, and total cost. The constant line approximates the cost of launch/sonar hydrography at $2730 per square nautical mile. The comparison of the projected laser cost per unit area of $438/nmi$^2$ to the launch/sonar cost per unit area of $2730/nmi$^2$ for a fully utilized system, 2000 nmi$^2$/yr, indicates that laser surveys would cost one-sixth of sonar surveys.

The NOS (1979) study also examined manpower and production. NOS concluded that manpower effectiveness of laser over launch/sonar would be five-to-one. Projected production for each NOS airborne laser system would be approximately 2000 nmi$^2$ per annum.

Finally, the NOS (1969) study suggested that the quality of marine charts would be improved by laser systems because of significantly increased spatial density and greater uniformity of distribution of soundings compared to sonar. The proposed NOS laser system was to collect 400-600 depth measurements per second with an average distribution of one per 20 m$^2$, yielding measurements 4.5 m apart in all directions. This would be 300 times the number of soundings per unit area of typical ship/sonar surveys. The increased density and more uniform distribution would provide a more representative chart.

## C. PURPOSE OF THE THESIS

NAVOCEANO and NASA have shown that laser bathymetry systems may be practical and reliable. NOS has shown that major benefits for hydrography may be possible with a laser system. The purpose of this thesis was to determine the most effective use of airborne laser hydrography systems considering the marine environment. Specifically, the questions to be answered are: which areas of U.S. coastal waters may be most effectively surveyed using airborne laser bathymetry and at what times of the year? This study was confined to the Gulf and West Coasts because major studies have already been conducted by NOS for the East Coast (Enabnit, 1979).

## II. ATTENUATION OF LASER BEAM POWER AS THE PARAMETER GOVERNING THE EFFECTIVENESS OF LASER BATHYMETRY

### A. INTRODUCTION

Laser penetration of ocean water is dependent on the optical properties of sea water. This thesis examines the optical properties which can be used to delineate those ocean areas which might be surveyed advantageously by laser bathymetry. Definitions and terms used to describe optical properties of sea water are those recommended by the Committee on Radiant Energy in the Sea and given by Jerlov (1976).

### B. OPTICAL CLASSIFICATION OF OCEAN WATERS

Jerlov (1976) has classified ocean waters in terms of the spectral transmittance of downward irradiance at high solar altitudes (Fig. 2). The Jerlov coastal water types 1-9 are characterized by increasingly higher amounts of yellow substance. Water types of decreasing irradiance transmittance indicate a spectral shift in the transmittance maximum toward longer wavelengths. Selective absorption by particles and yellow substance causes greater absorption at the shorter wavelengths and shifts the transmittance maximum from 470 nm, the blue region, for clear ocean type I water to 550 nm, the green region, for coastal type 7 water. Figure 3 is a similar graph of Jerlov's water types but gives instead of transmittance the irradiance attenuation coefficient (K) for downwelling daylight as a function of wavelength.

## C. TRANSMISSION WINDOWS AND LASER TYPES

The preference for a particular type of laser to be used for laser bathymetry depends upon the wavelength of maximum transmission. The transmission window for Jerlov's coastal water types 1-7 is approximately 510-580 nm (Figs. 2 and 3). Laser types that have operating wavelengths within that spectral band are: the frequency-doubled Nd:YAG laser (used in the proposed NORDA HALS and NOS systems), which operates at 532 nm; the neon laser (used in NASA's AOL), which operates at 540 nm; the argon laser, which operates at 514 nm; and the dye laser, which is tunable over the blue-green spectrum (Ferguson, 1975). The frequency-doubled Nd:YAG is preferred by NORDA and NOS for two primary reasons: (1) its high peak pulse power and high pulse rates, and (2) its small size and weight (NORDA, 1978).

## D. THE PRINCIPLE OF LASER BATHYMETRY

The technique of using a pulsed laser to measure water depths remotely can be explained with the aid of Figure 4. A short pulse of light is emitted from an airborne laser. The pulse of energy travels at the velocity of light and impinges upon the surface of the water. Approximately 3% of this energy is specularly reflected from the air/water interface and intercepted by the aircraft receiver. Half of the time difference between the initial laser pulse and this surface reflection yields the aircraft altitude. The remaining 97% of the laser energy is transmitted into the water, wherein its velocity is decreased by about 25%. (The transmission across the air/water interface is dependent on the angle of incidence, on polarization, and on sea state conditions. The value of 97% is an

average value for angles of incidence between $0^{\circ}$ and $45^{\circ}$ in calm seas [Witt, 1979]. In addition the signal is exponentially attenuated by absorption and scattering within the water column. If the signal is of sufficient intensity, it will be reflected from the water/sediment interface and be detected at the receiver. The time difference between the surface and bottom-sediment reflections is used to determine the water depth.

## E. THE IMPORTANCE OF THE SYSTEM ATTENUATION COEFFICIENT IN THE LASER SIGNAL EQUATION

A signal equation for a laser pulse transmitted from an airborne platform to the ocean floor may be given as follows (Avco Everett Research Laboratory, Inc., 1975):

$$Pr_B = \frac{P_t \, R(1-\rho) e^{-2a_1 h} e^{-2\gamma d} \, A_c \tau_{sB}}{\pi (h+\frac{d}{n})^2 \, n^2}$$

$P_{rB}$ = Received peak power [W]

$P_t$ = Transmitted peak power [W]

$R$ = Bottom reflectivity

$\rho$ = Surface reflectivity

$a_1$ = Atmospheric attenuation [$km^{-1}$]

$\gamma$ = System attenuation coefficient of sea water [$m^{-1}$]

$A_c$ = Area of collector [$m^2$]

$\tau_{sB}$ = System efficiency

$h$ = Aircraft altitude [km]

$d$ = Water depth [m]

$n$ = Index of refraction of sea water

This equation shows that the received signal is a function of environmental and system parameters. However, for a given appropriately designed and operated laser system, the major operational limitation is due to the environmental parameters. A simplified signal equation that indicates this is:

$$P_{rB} = SR\,(1-\rho)e^{-2a_1 h}\,e^{-2\gamma d}$$

$$\text{where } S = (P_t A_c \tau_{SB}) / [\pi (h+d/n)^2\, n^2]$$

For an aircraft altitude of 609 m (2000 ft), a water depth of 10 m, and representative values for the system and environmental parameters $P_t$ = 30 kW, R = 15%, $\rho$ = 2%, $a_1$ = 0.12/km, $\gamma$ = 0.2/m, $A_c$ = 0.073 $m^2$, $\tau_{sB}$ = 1.27%, and n = 1.33 (Avco Everett Research Laboratory, Inc., 1975) the following values are obtained:

$$S = 1.32 \times 10^{-5} W, \quad R = 0.15, \quad 1-\rho = 0.98, \quad e^{-2a_1 h} = 0.86,$$
$$e^{-2\gamma d} = 0.02, \quad P_{rB} = 3.33 \times 10^{-8} W.$$

The system parameter, S, is fixed for a given system or survey operation. Therefore, the ultimate environmental parameter is the product of the system attenuation coefficient and water depth ($\gamma$d) since it dominates all other terms.

## F. THE IRRADIANCE ATTENUTATION COEFFICIENT AS AN APPROXIMATION

Witt (1979) showed that the system attenuation coefficient ($\gamma$) may best be approximated by the irradiance attenuation coefficient (K), for downwelling light, an apparent optical oceanographic property readily measured in situ. This approximation was further confirmed by Krumboltz (1979) in a series of

tests for NORDA's HALS system. The coefficient K best approximates $\gamma$ because after traversing several attenuation lengths, the photons of a laser beam undergo multiple scattering, spreading the shape of the beam and ultimately giving it an asymptotic radiance distribution equivalent in shape to the irradiance distribution of downwelling daylight.

Witt (1979) and Krumboltz (1979) have shown that receiver field of view (FOV) and altitude affect the accuracy of this approximation. Figure 5 shows the variation of $\gamma$ as a function of FOV and receiver altitude at one test site. At a receiver altitude of 500 ft, $\gamma \approx K$ with a FOV of 80 mrad, but at 1500 ft, $\gamma \simeq K$ with a FOV of 40 mrad. The better approximation at higher receiver altitudes is due to the greater laser divergence with distance. The NASA AOL system had a FOV of 5-20 mrad (Avco Everett Research Laboratory, Inc., 1975), the NORDA HALS system a FOV of 0-30 mrad (Naval Oceanographic Research and Development Agency, 1978), and the proposed NOS system a FOV of 0-50 mrad (Avco Everett Research Laboratory, Inc., 1978). Figure 5 indicates that for the NASA AOL, the NORDA HALS, and the projected NOS systems the approximation is good for airborne laser bathymetry systems operating at 500 ft or higher but should be used with discretion at lower altitudes.

## G. IRRADIANCE ATTENUATION LENGTHS AND PERFORMANCE OF LASER BATHYMETRY SYSTEMS

The performance of laser bathymetry systems may be specified using irradiance attenuation lengths, L, which are the reciprocals of irradiance attenuation coefficients, i.e., $L = 1/K$, the

distance in which the irradiance decreases by a factor 1/e. The number of irradiance attenuation lengths to the bottom depth (d/L = Kd) that various laser bathymetry systems can attain or are projected to attain is shown in Fig. 6.

The NASA AOL system has achieved two attenuation lengths in the daytime and three at night (Enabnit, 1979), the NORDA HALS system was contracted to achieve 3.2 (Houck, 1979), and the proposed NOS system has a goal of four attenuation lengths (Enabnit, 1979). A higher value can be attained at night due to the lack of background noise caused by sunlight. It must be noted that in most studies of laser bathymetry, beam attenuation lengths have been used in describing the capability of laser systems, even though Krumboltz (1979) has shown that the system attenuation coefficient was better approximated by the irradiance attenuation coefficient. (The problem resulting from the use of beam attenuation lengths is apparent from Figure 5.) Thus some investigators have reported attenuation lengths five times greater than those given here (Guenther and Enabnit, 1978).

## H. NATURE OF THE PROBLEM

The first thesis objective was to determine where in U.S. coastal waters laser bathymetry can be effective, using the irradiance attenuation length as the best indicator of the expected performance of airborne laser bathymetry systems.

The second objective was to predict the best times of the year for using laser bathymetry. The optical properties of coastal waters may have temporal and spatial variability due

to seasonal changes in currents, winds, runoff, upwelling and other physical processes, as well as to biological activity. Other effects of shorter duration and more limited extent are storms, plankton blooms, tides, and man-made pollutants. Only the temporal and spatial variability due to seasonal effects were investigated. These are summarized by figures of seasonally plotted optical data.

## III. DATA COLLECTION AND PROCESSING

### A. LIMITATIONS OF MARINE OPTICAL DATA IN COASTAL WATERS

One of the major tasks in this study was the collection of marine optical data. Optical data for coastal waters are scarce; this is especially true for irradiance attenuation data. The most common type of optical measurement, the Secchi depth ($Z_s$), is usually obtained by marine biologists studying the euphotic zone. The next most common type of optical measurement for the Gulf Coast area is beam attenuation. Irradiance attenuation measurements, the optical data actually sought, are almost nonexistent for U.S. coastal waters. This scarcity of irradiance attenuation data required the use of Secchi depths and beam attenuation data. Other marine optical measurements such as volume scattering and turbidity measurements such as those recorded in Jackson or Formazin turbidity units were not considered. The in situ data sources used are listed in Appendix A. A limiting condition on all optical data used was that the water depth at the ocean station where the optical measurements were made had to be less than 200 meters. Since laser bathymetry systems will probably be limited to approximately four irradiance attenuation lengths (Enabnit, 1979), (80 m depth for a K of 0.05 $m^{-1}$), 200 meters was considered more than sufficient.

Satellite data may be indicative of the optical quality of coastal waters. Therefore, selected Landsat and NOAA-3 satellite imagery were qualitatively examined for turbidity patterns that correlated with in situ beam attenuation data.

Another necessary task was to find conversion formulas to convert Secchi depths ($Z_s$) and beam attenuation coefficients (C) to irradiance attenuation coefficients (K), because irradiance attenuation length was the chosen operational parameter. A related problem arose due to the spectral dependency of optical measurements. The optical data would be most useful if it were obtained for a wavelength of approximately 532 nm (wavelength of the frequency doubled Nd:YAG laser), but such data are scarce. This scarcity required the use of optical data measured with broad bandwidths or at wavelengths other than 532 nm and the formulation of the necessary conversion relations.

The third major task was the establishment of a data base with common optical and measurement parameters. Data from sites within a certain ocean region and collected during the same optical season were averaged.

## B. DATA REDUCTION AND CONVERSION

### 1. Irradiance Attenuation Coefficient (K) Data

The irradiance attenuation coefficient, $K(\lambda)$, is an apparent, spectrally dependent optical property that measures the extent to which diffuse downwelling daylight diminishes exponentially with depth in water. Thus,

$$H_z = H_o e^{-K(\lambda) Z}$$

where: $H_o$ = solar irradiance at sea surfaces

$H_z$ = downwelling irradiance at depth Z

Z = depth of measurement

$K(\lambda)$ = irradiance attenuation coefficient*

*Normally $(\lambda)$ will not be written, as it will generally be assumed that K is for a specific wavelength.

Depth averaged values of irradiance attenuation coefficients ($\bar{K}$) were required. Data were usually obtained in percent transmissions ($\%T = 100\ H_z/H_o$) for a series of depths. To obtain a depth-averaged value, $\bar{K}$, for the entire water column the following equation was used in a linear regression using the method of least squares:

$$\ln(T_n) = \ln(H_z/H_o)_n = -\bar{K}Z_n$$

n = index of data pairs

$\bar{K}$ in units of $m^{-1}$ was the slope of the straight-line model with depths, $z_n$, in meters as the independent variable and the corresponding transmissions, $T_n$, as the dependent variable.

Ideally, irradiance attenuation data used for this study should have been measured at $\lambda \simeq 532$ nm. However, few such data were found and irradiance data at other wavelengths had to be used. Most of these data were taken with irradiance meters having a photopic response with a peak transmission near 555 nm. The broad bandwidth of a photopic response coupled with the water's selective absorption by wavelength with increasing depth yields an effective response which is shifted towards the wavelength of maximum transmission for the given water. For this reason photopic K measurements were considered useful.

Other K measurements used in this study were obtained with a quantum irradiance meter. A quantum meter is normally sensitive in the 350-700 nm bandwidth interval and has a spectral energy sensitivity directly proportional to wavelength (Jerlov, 1976). To convert from quantum values, $K_Q$, to K the curves of Figs. 7 and 8 (Jerlov, 1976) were used. Given quantum transmission

measurements at a station, Fig. 7 was used to determine a water type. Figure 8 was then used to determine the $K/K_Q$ ratio. This ratio was then multiplied by the depth-averaged quantum irradiance attenuation coefficient ($\bar{K}_Q$) to obtain the irradiance attenuation coefficient ($\bar{K}$). Again the broad bandwidth of the quantum meter becomes narrowed to a green band with depth in coastal waters.

2. Beam Attenuation Coefficient (C) Data

The beam attenuation coefficient, $C(\lambda)$, is an inherent, spectrally dependent, optical property that characterizes the attenuation due to absorption and scattering by a collimated beam of monochromatic light traversing a fixed path-length of homogeneous water. Thus,

$$F_t = F_o \, e^{-C(\lambda)r}$$

where: $F_o$ = initial radiant power from projector

$F_t$ = residual radiant power measured by receiver

$r$ = path length of measurement

$C(\lambda)$ = beam attenuation coefficient*

Depth averaged values of beam attenuation coefficients ($\bar{C}$) were computed for this study. Data were usually expressed in percent transmission per meter, $\%T = 100 \, F_t/F_o$, for a series of depths. To obtain a depth-averaged $\bar{C}$ for a water column, numerical integration of the transmittance profile with depth was performed. First, the water column at each observation station was divided into layers so that each beam attenuation measurement was at the center of that layer. Two exceptions to

*Normally ($\lambda$) will not be written as it will generally be assumed that C is for a specific wavelength.

this procedure were the surface and bottom layers, because layer boundaries between measurements were kept equidistant. Second, each layer was assumed to contain homogeneous water, and the beam attenuation coefficient was calculated for each layer using the equation:

$$C_n = -\ln(F_t/F_o) \quad [m^{-1}]$$

Third, the transmittance of the entire water column was calculated using an iterative procedure:

$$T_n = T_{n-1} \exp(-C_n r_n)$$

where $C_n$ = coefficient for the layer ($m^{-1}$) in question

$r_n$ = width of the layer (m) in question

$T_{n-1}$ = incoming transmission to the layer in question and outgoing transmission of the previous layer.

$T_n$ = outgoing transmission of the layer in question and incoming transmission to the next layer.

$T_o$ = 100%

n = number of layers

Fourth, the depth averaged $\bar{C}$ was calculated by using the equation:

$$\bar{C} = -1/r_z \ln(T/100)$$

where $\bar{C}$ = depth averaged beam attenuation coefficient ($m^{-1}$)

$r_z$ = water depth at the station (m)

T = final $T_n$ of previous equation

Not all the beam attenuation data used for this study were measured at $\gamma \simeq 532$ nm. Beam attenuation data obtained for Oregon coastal waters (Pak, 1979) were measured at 660 nm and

had to be converted. A procedure to convert this data to 532 nm was formulated using data collected by Zaneveld, et al. (1978) in Monterey Bay, California. They used a spectral beam transmissometer that simultaneously measured at six wavelengths at various depths. From these beam attenuation data those for 45 stations at three wavelengths (500, 550, and 650 nm) measured at six different depths (0-1, 5, 10, 20, 40, and 60 meters) were selected for this study. Linear regression models were computed (x, y: $y = mx + b$) for the following sets of variables: [C(650), C(500)], [C(500), C(650)], [C(650), C(550)], and [C(550), C(650)] at each depth. Table I summarizes the procedure followed in computing a mean slope ($\bar{m}$) and a mean y-intercept ($\bar{b}$) to obtain the two equations:

$$C(500) = 1.12\ C(650) - 0.42$$

$$C(550) = 1.09\ C(650) - 0.35$$

The final equation, obtained by interpolating between the above two equations, was used to convert C(660) to C(532).

$$C(532) = 1.10C(650) - 0.37$$

where $C(650)$: $0.425 \leq C(650) \leq 2.00\ [m^{-1}]$

Beam attenuation coefficients were converted to irradiance attenuation coefficients using a relation computed by Shannon (1975) for C(532).

$$\bar{K} = 0.2\bar{C} + 0.04\ [m^{-1}]$$

where C: $0.11 \leq C \leq 1.6\ [m^{-1}]$

3. Secchi Depth ($Z_s$) Data

Most of the optical oceanographic measurements used were Secchi depths. This is the depth at which a white Secchi disc, usually 30 cm in diameter, lowered into the sea and viewed from

directly above, disappears from view. Unfortunately, the procedure has never really been standardized (Tyler, 1968; Williams, 1968; Holmes, 1970). Factors affecting the visibility of a Secchi disc include solar altitude, cloud cover, sea surface reflection and refraction, ship shadow, water color, observer's visual acuity, and height above the water surface (Tyler, 1968). Thus, Secchi disc measurements are somewhat subjective and imprecise.

As are the beam and irradiance attenuation measurements, the Secchi disc measurement is spectrally dependent. For the purpose of this study, the observers should have worn eye glasses with, for example, Wratten 61 filters (Williams, 1968). Again, such spectrally homogeneous data are not available. Williams (1968) investigated the relative response of the photopic eye (555 nm peak response) with and without a Wratten #61 filter (dominant wavelength 530 nm). Because of the selective absorption with depth of ocean water, the errors generated in using the photopic Secchi measurements were not thought to be of significance for this study.

Secchi depth measurements were converted to irradiance attenuation coefficients by methods based on geographic region. Formulas published by Poole and Atkins (1929), Graham (1966), Otto (1966), and Holmes (1970) were not considered adequate for this study because of poor statistical procedures or because the data were obtained in a different type of water. Instead, data from various sources were used to develop regional formulas to convert $Z_s$ to K.

The conversion formula used for Eastern Pacific coastal waters was based on photopic irradiance and Secchi depth data published by Callaway and McGary (1959) and Holmes (1970). The data selected from Callaway and McGary were from 19 stations approximately 150 nautical miles off the U.S. coast and north of $35^{o}$N latitude (Table II). Added to these were 13 stations in Goleta Bay near Santa Barbara, California, observed by Holmes. These 32 stations were used and processed in the following manner. First, the Callaway and McGary irradiance attenuation data were transformed to a depth-averaged value for the same water layer as the Secchi depth measurement. This value ($\bar{K}_s$) was computed by using only those irradiance transmission values which were measured or interpolated at depths equal to or shallower than the Secchi depth. The procedure used to calculate $\bar{K}_s$ from these transmission values was the same linear regression technique mentioned in Section III.B.1. The Holmes irradiance data were already in the correct form. Second, two linear regression models were used to compute conversion formulas. The first linear regression model used the Secchi depth reciprocal ($Z_s^{-1}$) as the independent variable and $\bar{K}_s$ as the dependent variable. The equation obtained was:

$$\bar{K}_s = 1.21\ Z_s^{-1} + 0.06 \quad [m^{-1}]$$

95% confidence interval

$m = 1.21 \pm 0.10$

$b = 0.06 \pm 0.02$

$r = .98$

In the second linear regression model $Z_s^{-1}$ was interchanged with $\bar{K}_s$. The equation obtained was:

$$Z_s^{-1} = 0.78\ \bar{K}_s - 0.04 \quad [m^{-1}]$$

95% confidence interval

$m = 0.78 \pm 0.07$

$b = -0.04 \pm 0.02$

$r = .98$

The final conversion formula used is the mean of the above two equations:

$$\bar{K}_s = 1.25 Z_s^{-1} + 0.05 \quad [m^{-1}]$$

where $Z_s$: $1.9 \leq Z_s \leq 32$ [m]

Figure 9 is a graph of the data points and the regression lines.

The conversion formula used for the western Gulf Coast waters (Longitude $\geq 89.5^{o}$W) was based on data published by Kamykowski, et al. (1978), quantum irradiance and Secchi depth data for one station off Texas observed on four different cruises. Eleven of the twelve published measurements were used. First, the data were transformed from quantum irradiance transmission to depth-averaged quantum irradiance attentuation coefficients for the same layer of water as the Secchi depth measurements. Second, these coefficients were converted from the $\bar{K}_Q$ to $\bar{K}$ by using Figs. 7 and 8 from Jerlov (1976). Table III summarizes the results. Third, linear regression models were computed resulting in the following equations:

$$\bar{K}_s = 1.14 Z_s^{-1} + 0.04 \quad [m^{-1}]$$

95% confidence interval

$m = 1.14 \pm 0.39$

$b = 0.04 \pm 0.05$

$r = .91$

$$Z_s^{-1} = 0.73\bar{K}_s - 0.01 \quad [m^{-1}]$$

95% confidence interval

$m = 0.73 \pm 0.25$

$b = -0.01 \pm 0.05$

$r = .91$

The final conversion formula used is the mean of the above two equations:

$$\bar{K}_s = 1.26\ Z_s^{-1} + 0.03 \quad [m^{-1}]$$

where $Z_s$: $3.5 \leq Z_s \leq 26$ [m]

Figure 10 is a graph of the data points and the regression lines.

The conversion formula used for the Eastern Gulf coastal waters (Longitude < 89.5°W) was computed by Shannon (Witt, et al., 1976) from optical measurements taken in the West Pacific and Eastern U.S. coastal waters.

$$\bar{K}_s = 1.15\ Z_s^{-1} + 0.03 \quad [m^{-1}]$$

$r = .95$

where $Z_s$: $4 \leq Z_s \leq 43$ [m]

The $\bar{K}_s$ data used were measured with two types of irradiance meters--photopic response or a peak response at 533.5 nm (Witt, 1979). This formula was determined by a linear regression model with $Z_s^{-1}$ the independent variable and $\bar{K}_s$ the dependent variable (Shannon, 1979). The weakness of this equation was that $Z_s^{-1}$ as the independent variable was assumed to be error free.

The Poole and Atkins (1929) data were examined due to the wide use of their formula,

$$\bar{K} = 1.7\ Z_s^{-1} \quad [m^{-1}]$$

Poole and Atkins used an irradiance meter with a photopic response and made fourteen series of observations mostly at one station in the English Channel over the course of one year. An average $\bar{K}$ was calculated for the surface water layer (0-20 m) for each series, and this was multiplied by $Z_s$, giving the product $\bar{K}_{0-20}\ Z_s$. Poole and Atkins then found the mean value of the fourteen $\bar{K}_{0-20}\ Z_s$ products to be 1.7. The same Poole and Atkins data were used to recalculate a formula using linear regression and to verify the conversions of this thesis. The two computed linear regression equations are:

$$\bar{K}_{0-20} = 1.11\ Z_s^{-1} + 0.04 \quad [m^{-1}]$$

95% confidence interval

$m = 1.11 \pm 0.35$

$b = 0.04 \pm 0.03$

$r = .90$

$$Z_s^{-1} = 0.72\ \bar{K}_{0-20} - 0.01 \quad [m^{-1}]$$

95% confidence interval

$m = 0.75 \pm 0.22$

$b = -0.01 \pm 0.03$

$r = .90$

The mean equation from the above two is:

$$\bar{K}_{0-20} = 1.25\ Z_s^{-1} + 0.03 \quad [m^{-1}]$$

where $Z_s$: $6.5 \leq Z_s \leq 22$ [m]

Figure 11 is a graph of the data points and the regression lines.

The close agreement between these equations verified the conversion formulas used to estimate the irradiance attenuation coefficient from the Secchi depth. Table IV summarizes the regression equations, and Fig. 12 shows the final conversion formulas.

C. REMOTELY SENSED DATA

Three types of satellites are able to provide data that indicate the optical quality of ocean waters: Landsat series, NOAA series and Nimbus 7. Selected imagery from Landsat and NOAA series were examined.

Landsat data have been used with some success by numerous investigators studying currents tagged by suspended sediments, plumes, and dispersal patterns of suspended sediments (Jarman, 1973; Pirie and Steller, 1973; Hunter, 1973; Erb, 1974; Carlson, et al., 1975; Maul and Gordon, 1975; Rouse and Coleman, 1976). The most successful studies have used image enhancement processes with in situ data simultaneously collected for calibration purposes. However, such enhancement was not available for this study, and only B&W imagery as received from the EROS data center of the U.S. Geological Survey were used.

For the coastal region off Oregon MSS4 and MSS5 Landsat imagery taken during the March 11, March 28, May 12, and May 13, 1975, overpasses were compared to beam attenuation data ($\lambda$ = 660 nm) collected on April 23-May 1, 1975 by Pak and Zaneveld (1977). No noticeable correlations were observed.

For the region off Texas MSS5 Landsat imagery taken during the November 12-13, 1975, and May 28-29, 1976, overpasses were

compared to beam attenuation data ($\lambda$ = 528 nm) published by Berryhill, et al. (1976) and collected on November 15-21, 1975 and May 21-25, 1976, respectively. Turbidity patterns were much more noticeable for the Texas imagery and some trends between the satellite imagery and the beam attenuation data were observed. These turbidity patterns observed in the andsat imagery were used as an aid in contouring the Texas beam attenuation coefficient data. Shideler (1979) extensively examined the data of all six cruises published in Berryhill, et al. (1976) and Berryhill, et al.(1978) with the related B&W Landsat imagery and indicated that turbid water masses throughout the inner shelf depths (less than 45 m) were apparent in the imagery.

The NOAA-3 imagery for selected days throughout 1975 were used to observe upwelling off the U.S. West Coast. The relationship of upwelling to seasonal variation of optical properties off the Northwest Coast is discussed in the next chapter.

Coastal Zone Color Scanner (CZCS) data from the Nimbus 7 satellite were not available at the time of the writing of this thesis. However, it is mentioned here because of its enormous potential as an optical data source for the marine environment. Data can be obtained on magnetic tape, CRCST (Calibrated Radiance, Pigment, Diffuse Attenuation Coefficient, and Temperature Tape), or film format. The irradiance (diffuse) attenuation coefficient is a computer parameter obtained on tape or film image. Since this scanner views a swath 1566 km wide, K data for enormous ocean areas could be obtained (Goddard Space Flight Center, 1978).

D. DATA PROCESSING

Each measurement datum was keypunched onto a standard 80-character computer card along with its latitude, longitude, date, bottom depth (when available), measurement unit (meters, feet, etc.), converted K value, and the source for the data. The latitude and longitude were given to a tenth of a minute.

The data on magnetic tape from NODC, EPA and Texas Natural Resources, required special processing due to limitations on processing resources and the wealth of data measurements recorded over relatively small areas. The NODC tape data was punched one card per measurement. The EPA "Storet" tape gave monthly data covering a span of three years. These data were averaged according to monthly means per station. The Texas Natural Resources tape was averaged by predetermined optical seasons (detailed in Chapter IV.C) per station.

These data cards were then used as input for the plotting program. A copy of this program is included in Appendix B. The data points were plotted on a Mercator projection at the same scale as available charts of the area. The plots were then overlayed onto the charts to trace the coastlines and bathymetric contours. Because of the irregular spacing of the data, a spatial averaging routine was used for areas where a dense spacing of points would have caused values to overprint one another. This was accomplished by a straight averaging of all points which were spaced within one plotted number width of one another. Contours were developed for plots by using the smallest plottable number, which was .04 inches for the NPS Versatec Plotter. These contours were

then transferred using a light table to a same scale plot which used a number size of .10 inches, the minimum reproducible size for thesis presentation. Therefore, the data contours represent an averaging of values plotted within 1.9 miles of one another on the West Coast, and within 3.4 miles on the Gulf Coast. However, data values on the final plots represent an averaging of values plotted within 4.7 miles of one another on the West Coast and within 8.5 miles on the Gulf Coast plots. No averaging was performed for individual data points positioned beyond these limits. Figures 14 through 16 show the locations of all the data points used in the plots.

For some months data were so sparse that meaningful plots could be obtained only by dividing the year into seasons. The determination of these seasons is the topic of the next chapter.

## IV. TEMPORAL VARIATION OF OPTICAL PROPERTIES BY REGION

### A. INTRODUCTION

The months of lead time required for laser bathymetric mission planning make it important to determine which times of the year provide optimum water clarity. The sparcity of data for certain months leads to a grouping of months into seasons.

Seasonal trends were estimated by comparing the month-to-month variations of oceanographic factors known to affect turbidity with the optical measurements of those few stations which provided monthly optical data. Oceanographic parameters which correlated best with the optical measurements were used to delimit the seasonal boundaries during those months with insufficient data. Secular variations were not studied due to the lack of repetitive optical measurements at the same location over a number of years.

Coastal water turbidity can be influenced by physical, chemical, and biological processes occurring both in the water column and in adjacent land areas. A major contributor to turbidity is particulate matter produced by land runoff and plankton, especially in areas of upwelling. Phytoplankton blooms can produce sudden increases in turbidity, which may be closely related to upwelling which in turn may be seasonal. Sea surface temperature measurements can be useful in identifying areas of upwelling, and salinity measurements have been used to trace the outflow from large rivers such as the Columbia

River (Pruter and Alverson 1972). York in (1974) demonstrated an inverse relationship between Secchi depths and Bakun's (1975) upwelling index. This upwelling index was helpful in determining optical seasons for the west coast of the U.S. Other factors such as large storms may increase turbidity over shorter time frames.

Data for the northwest coastal waters of the U.S. were assembled for the region from 42°N to 49°N out to a depth of 200 m. The California coast was not covered due to the narrowness of the Continental Shelf there.*

Data from the Gulf of Mexico were divided into two groups, one for the area west of 89° 30'W and the other to the east of that line. The Western Gulf region comprised that area along the coasts of Texas and Louisiana out to a depth of 200 m. The Eastern Gulf region started at 24°N, 80°W and included the southern and western coasts of Florida and the coasts of Alabama and Mississippi out to a depth of 200 m.

B. NORTHWEST COAST

Discharge from the Columbia and other rivers and seasonal upwelling along the coast dominate the turbidity observed along the northwest coast of the U.S. Upwelling affects most of the coast during the summer and the river discharges produce turbidity plumes which affect the coastal areas near river mouths. Brown (1973) correlated Secchi depths for the northwest coast with other simultaneously measured oceanographic parameters and found

---

*For the California coast there are a number of optical observations to which the reader can refer. References to California data which have either beam attenuation or diffuse attenuation measurements may be found in reports by the Allan Hancock Foundation (1963); Drake (1972); Frederick (1970); Karl (1976); and Winzler and Kelly (1977).

coefficients of .610 correlation with water depth, -.598 with observed Forel-Ule color codes, -.591 with $SiO_4$ and .504 with salinity. Other parameters such as surface temperature, density, and oxygen levels did not show as good correlations.

Bakun (1975) has attempted to quantify upwelling through the use of an upwelling index which is an estimate of the component of computed Ekman transport directed offshore. This transport is calculated from daily mean surface atmospheric pressure data. Figure 13 (Bakun, 1975) shows the upwelling indices computed by month versus latitude for the western coast of the U.S. Shaded areas represent upwelling in units of cubic meters per second per 100 m of coastline. Negative values indicate downwelling. The figure was compiled from an average of 20 years of wind observations. Upwelling occurs as a result of change in wind patterns from southwesterly in winter to northerly in summer. Although the upwelling is not constant but varies with wind variations, this same annual cycle of summer upwelling has been observed over the course of many years.

The Columbia River is the only major river source of turbidity along the Northwest coast. It ranks second among U.S. rivers in volume of discharge at its mouth with an average of 640,000 cubic feet per second (or approximately 7,300 $m^3$/sec) (Boone 1978). Peak discharges occur from May to July with lowest flows from August to October. Surface currents along this coast flow southerly from May through September, and northerly from mid-November through February (U.S. Navy Hydrographic Office 1967). This movement pushes the plume of the Columbia

River to the south during the months of peak discharge. Most of the remaining streams of the Northwest coastline originate in the Coast Range and produce highest stream flows in February through March and lowest flows from August to September (Geraghty 1973).

The preceding oceanographic factors along with K data from the area (Small, 1979) are summarized in Table V. The table shows upwelling from May to September, also the period of peak discharge of the Columbia River. Upwelling and river discharge act together to assure higher K values at this time. A season of relatively lower K was established from October to January when oceanic and coastal waters meet near shore and little or no upwelling occurs. February through April shows variability with upwelling occasionally establishing itself for short periods. Seasonal plots, figures 17 through 36, were generated using this division scheme.

Figures 17 through 25 show Secchi values obtained for this area. Of particular interest is the delineation of the Columbia River plume. Figure 21 shows the 5 m contour being extended south across the 46$^{o}$ parallel towards deeper waters. Figure 22 shows the same contour bulge as much smaller and directed northerly with the current at that time of year. Figure 20 shows the 5 m contour bulging straight out from the river mouth during the time of year when the surface currents are weak and variable in direction.

Figure 26 shows all the beam attenuation measurements obtained for the Northwest coast for all seasons. Figure 27 shows all the irradiance measurements obtained for all seasons.

Figures 28 through 36 show all measurements after their conversion to irradiance K according to the methods detailed in Chapter 3. Due to the abundance of Secchi measurements as opposed to any other type, these plots mainly reflect the trends indicated in the raw Secchi plots.

C. WESTERN GULF OF MEXICO

Winter storms and their associated winds and resulting high seas appear to be the most efficient mechanism in generating turbidity in the Western Gulf. Besides being able to resuspend bottom sediment, these storms apparently cause efficient tidal flushing of local estuaries and lagoons as suggested by Shideler (1979). These lagoons are laden with sediments from local rivers. However, peak discharges of turbid water from these lagoons is not related to high stream flows. Instead, the majority of sediment is trapped by the lagoons until storm conditions can aid high tides in discharging it.

The discharges of the Mississippi and Atchaflaya Rivers dominate the turbidity regime along the Louisiana Coast. Peak discharges for both rivers are from March to May, with lowest stream flows from September to November (Perret, et al 1971). These flows dominate the nearshore coast of Louisiana with diminishing effect towards the outer continental shelf. Other stream flows show peak discharges from January to May and lowest stream flows from August to October.

Coastal currents are generally weak (less than 1 m/sec over 95% of the time) but do play a role in directing turbidity

flows. From October to June the longshore currents are from the east and flow west, then south, along the Texas Coast (U.S. Naval Oceanographic Office, 1972). This causes the Atchaflaya and most of the Mississippi water to follow the Louisiana coast and keep turbidities high in this area. These currents also direct discharges from Texas lagoons to follow nearshore shallow waters. From July to September a longshore current from the south invades the southern Texas coast until it meets the previously described current at about 29° latitude. Incursions of the Loop Current of the Gulf of Mexico onto the continental shelf have been observed (Shideler, 1979). This shoreward incursion of deep water confines turbid coastal waters to the shallow inner shelf and results in lower turbidities elsewhere.

Upwelling, which plays an important role in turbidity levels for the Northwest coast, is not thought to be important for the Western Gulf. Winds from the south to southwest (for Texas coast) and from the west (for the Louisiana coast) which would be needed to produce an offshore Ekman transport are infrequent and generally weak.

Berryhill, et al. (1976) report finding a prevalent two-layer turbidity structure in their study of the South Texas outer continental shelf. This structure consisted of a nepheloid layer below a less turbid layer. This nepheloid layer varied in both thickness and distribution but in general became thickest toward the outer shelf. This type of structure casts doubt on the validity of the use of Secchi measurements to obtain K for the entire water column because they only indicate transparency near the surface.

Table VI illustrates the variables used in determining optical seasons. Wind data were obtained from a Summary of Synoptic Meteorological Observations (U.S. Naval Weather Service Command, 1970). Sea heights were obtained from a U.S. Naval Oceanographic Atlas (1972). Zooplankton counts were obtained from a study done by the Louisiana Wild Life and Fisheries Commission (Perret, 1971). Secchi transects were from a study of the South Texas outer continental shelf (Kamykowski, 1979).

A season from November to February was chosen to represent that time of year when storms are most prevalent and an efficient tidal flushing of lagoons is thought to occur. There is a variable season from March to May when winds are occasionally strong and outflows from the larger streams are high. June to October is the third season, when winds and streamflow are lowest. This third season is thought to consistently provide the best overall water visibility. Hurricanes which occur during this season could raise turbidities substantially, but are infrequent and usually short term in their effects.

Figures 37 through 39 show Secchi measurements made in the Western Gulf. Within the lagoons of Texas and the nearshore area of Louisiana, visibility is most related to streamflow and therefore March to May is generally the period of shallowest Secchi depths and when streamflows are highest. June to October is generally that period when the deepest Secchi depths were found, but a sparcity of data during these months makes comparisons difficult. November through February generally are the months when highest turbidities are encountered in the offshore deeper waters.

Figures 40 and 41 show the only beam attenuation data collected for this area. The more turbid waters of November to February of the two figures provide a further indication of tidal flushing of lagoons during this stormy season.

Figures 43 through 45 show the conversion of all the data to the common parameter K. Secchi depths less than 2 m were not dealt with by the $^{Z}$ to K conversion formula which was derived from measurements deeper than 2 m. Therefore, the Texas lagoon measurements do not appear on these figures. These plots display the same seasonal variations mentioned before. Shideler (1975) notes that secular variations were thought to be related mainly to annual stream flow variations and storm occurrences for those years.

D. EASTERN GULF OF MEXICO

The eastern Gulf data indicate similar mechanisms of turbidity generation as were present in the Western Gulf. The main differences are due to the appearance of some upwelling during winter months and a change of the months of highest stream flow along the Florida coast.

Alexander, et al. (1977) attribute mixing of the water column over the eastern Gulf's continental shelf to wind stress which can be linked to the frequency of low pressure disturbances (storms) crossing this area. In winter when storms are most frequent the water column was observed to be unstable and well mixed. By contrast, in summer and fall the water column is stable with established thermoclines and haloclines. Alexander, et al. (1977) also noted that the passage of Hurricane

Eloise did not raise turbidity levels to the degree that persistent winter storms had. Also, the rise in turbidity caused by the hurricane disappeared after one week.

Monthly Ekman transports for 2 degree squares in the Eastern Gulf have been computed by Ichiye, et al. (1973). Their results show transports to be lowest from June to August with averages less than 3,000 gm/cm-sec. Transport is generally alongshore except from December to February when offshore transports result from scattered areas of upwelling along the Florida coast, especially near De Soto Canyon. In other months there may be occasional periods of offshore transport but of smaller magnitudes.

Surface currents generally flow in a northwesterly direction along the coast in the nearshore areas. This directs Mississippi River flow away from the Eastern Gulf except from April to September when a reversal in flow direction occurs from the Mississippi River mouth to the Florida panhandle. Incursions of pockets of Mississippi outflow were observed by Alexander, et al. (1977) along with Loop Current eddies which had intruded onto the continental shelf during these summer months. No Loop Current intrusions were found during other seasons.

Table VII summarizes the main parameters used to delineate optical seasons. Wind mixing occurring during winter storms and a simultaneous increase in upwelling makes January to March a season of highest K. Lowest K values can be expected from June to September when the water column is most stable and clear water from the Loop Current intrudes upon the outer shelf. Exceptions to this occur along the Mississippi, Alabama,

and western Florida coasts where turbid Mississippi River outflows make K higher. The two remaining seasons are transition periods where K is variable and less predictable. Stream flows other than the Mississippi do not appear to influence turbidity levels greatly.

Figures 46 through 53 show the Secchi measurements obtained for the Eastern Gulf. Figures 54 through 59 show beam and irradiance attenuation measurements and figures 60 through 66 show all measurements converted to irradiance K. Overall, these plots show the lowest K values encountered in this study.

# V. CONCLUSIONS AND RECOMMENDATIONS

## A. CONCLUSIONS

The present and near-future water penetration capability of laser systems is limited to about four attenuation lengths (Enabnit, 1979) as was discussed in Chapter II (see also Fig. 6). Seasonal Kd values were plotted in nineteen figures for Pacific Northwest and Gulf coastal areas. These figures indicate where and when laser bathymetry systems would be successful, given the $Kd \leq 4$ criterion. These seasonal Kd values were derived from optical data collected over different years. However, inter-annual variations may change the utility of laser bathymetry systems in a particular area.

In the coastal areas of Oregon and Washington laser bathymetry would probably not be successful at any time over significant areas as is shown in Figures 67 to 75. A Kd value of ten was contoured (the lowest contourable value) as an indicator of possible areas surveyable by laser. The area within the Kd=10 contour is small for all seasons; the even smaller area with a $Kd \leq 4$ is too small for practical laser hydrographic operations.

In the Western Gulf, limited areas are candidates for laser bathymetry as shown by Figures 76 to 78. The southern half of Laguna Madre, Texas, is surveyable by laser bathymetry from November through February. The area from Matagorda Bay to Sabine Pass off Texas is surveyable all year up to depths of 10 to 20 fathoms as indicated by the Kd=4 contours. West of the

Mississippi Delta, possibly to Sabine Pass, a strip from outside local estuaries and bays to the 10-fm depth contour is available to laser bathymetry from March to October.

The Eastern Gulf coastal area is the area best suited to laser bathymetry as indicated in Figures 79 to 85 by the Kd=4 contour. Off Florida from Panama City to the Florida Keys, an area of 30,000 $nmi^2$ bordered by the 30-fm depth contour may be surveyed by laser bathymetry during June through September, and a reduced area bordered by the 20-fm depth contour all year. This 30,000 $nmi^2$ area alone represents 15 years of work for one laser system and represents a costs savings of $69 million (1977 dollars) over launch/sonar surveys. From Panama City to the eastern Mississippi Delta an area of 8,800 $nmi^2$ bordered by the 20-fm depth contour is surveyable from October through December.

B. RECOMMENDATIONS

1. More optical measurements, especially irradiance and beam attenuation data, should be collected throughout the year in U.S. coastal waters.
2. More simultaneous measurements of $Z_s$, K, and C at the same wavelength should be taken and more investigations of the relationships between them should be made. Universal relationships should not be expected due to regional variation in suspended particles and yellow substance (Gordon and Wouters, 1978) and, therefore, such studies should be regional.

3. Investigators should send optical measurements to the National Oceanographic Data Center, especially measurements made in the Gulf Coast area. NODC should establish irradiance and beam attenuation data categories as part of the Ocean Stations Data Base.
4. This thesis studied seasonal variation of marine optical properties in U.S. coastal waters; others should investigate long term trends and their cause.
5. Investigators should always state the wavelength at which their optical data were taken.
6. Prior to the commencement of laser hydrographic survey operations, Nimbus 7-CZCS data for the areas of interest should be examined and used to update the figures presented here.
7. This thesis did not examine the bottom reflectivities of coastal waters because of their generally relatively minor effect compared to attenuation lengths as a limiting parameter for laser bathymetry operations. However, in areas of marginal utility for laser bathymetry, bottom reflectivity may become significant. This suggests further study of this effect is needed.
8. The National Ocean Survey should consider the west coast of Florida for airborne laser hydrographic operations due to the favorable marine optical environment there.

## APPENDIX A

## DATA SOURCE OF IN-SITU OPTICAL MEASUREMENTS IN COASTAL WATERS

1. Data Source: CDS Data Base

   Institution: Texas Natural Resources Information System

   Geographic Area: Texas

   Date of Tape Generation: May 1979

   Data Range: 1968-77

   Optical Data Type: $Z_s$

   Number of Data Observations: 14,232

   Data Reduction Procedures: Data was on magnetic tape. Converted to $\bar{K}$ by methods of Section III.B.3.

2. Data Source: SD-2 Oceanographic Stations (Master Records) Data Base

   Institution: National Oceanographic Data Center

   Geographic Area: Primarily Oregon and Washington

   Date of Tape Generation: March 1979

   Data Range: 1952-74

   Optical Data Type: $Z_s$

   Number of Data Observations: 1329

   Data Reduction Procedures: Data was on magnetic tape. Converted to $\bar{K}$ by methods of Section III.B.3.

3. Data Source: STORET Data Base

   Institution: Environmental Protection Agency

   Geographic Area: Florida

   Date of Tape Generation: June 1979

   Data Range: 1966-79

   Optical Data Type: $Z_s$

   Number of Data Observations: 3,000

   Data Reduction Procedures: Data was on magnetic tape for selected stations off Florida. Converted to $\bar{K}$ by methods of Section III.B.3.

4. Investigator: Barret, Barney B.

   Data Source: Barret (1971)

   Institution: Louisiana Department of Wildlife and Fisheries

   Geographic Area: Louisiana

Date of Data Collection: 1968-1969

Optical Data Type: $Z_s$

Data Reduction Procedure: Computed $\bar{K}$ from $Z_s$ by method outlined in Section III.B.3.

Investigators: Barret, Barney B. et al

Data Source: Barret et al (1978)

Institution: Louisiana Department of Wildlife and Fisheries

Geographic Area: Louisiana

Date of Data Collection: 1974-76

Optical Data Type: $Z_s$

Data Reduction Procedure: Computed $\bar{K}$ from $Z_s$ by method outlined in Section III.B.3.

Investigators: Berryhill, Henry L., Jr., et al

Data Sources: Berryhill et al (1976) and Berryhill et al (1978)

Institution: U.S. Geological Survey

Geographic Area: Texas

Date of Data Collection: 1975-1977

Optical Data Type: C

Instrument: Martek Transmissometer (528nm)

Data Reduction Procedure: Integrated $\bar{C}$ computed by method outlined in Section III.B.2 for 28 stations sampled six different times. Most stations had the beam transmission measurements (surface, middle, and bottom) per profile but some lacked bottom measurements. For these stations the middle value was used to the bottom depth. $\bar{K}$ was then computed from $\bar{c}$.

Investigators: Carder, K. L., and Haddad, K. D.

Data Source: Carder and Haddad (1979)

Institution: University of South Florida

Geographic Area: Mississippi, Alabama, and Florida

Date of Data Collection: 1976-1978

Optical Data Type: C

Instrument: Hydro Products Transmissometer (550nm)

Data Reduction Procedure: The original data were given as suspended particles beam attenuation coefficient ($C_p$) contours on profile figures. The use of this data required special processing. First, values of $C_p$ had to be picked off the figures for the $C_p$ vs depth profile at each ocean station. Second, $C_p$ was converted to C for each layer by using the relation $C_p + .06935 = C$ (Carder and Haddad, 1979). Third, the methods of Section III.B.2. were used to obtain $\bar{K}$.

. Investigator: El-Sayed, Sayed Z.

Data Source: Unpublished Data (El-Sayed 1974)

Institution: Texas A&M University

Geographic Area: Gulf of Mexico

Date of Data Collection: 1971-73

Optical Data Type: $Z_s$

Data Reduction Procedure: Computed $\bar{K}$ from $Z_s$ by method outlined in Section III.B.3.

. Investigators: Godcharles, Mark F. and Jaap, Walter C.

Data Source: Godcharles and Jaap (1973)

Institution: Florida Department of Natural Resources Marine Research Laboratory

Geographic Area: Florida

Date of Data Collection: 1970-71

Optical Data Type: $Z_s$

Data Reduction Procedure: Computed $\bar{K}$ from $Z_s$ by method outlined in Section III.B.3.

0. Investigators: Gordon, Howard R. and Dera Jerzy

Data Source: Gordon and Dera (1969)

Institution: Institute of Marine Sciences, University of Miami

Geographic Area: Florida

Date of Data Collection: December 1967

Optical Data Type: $\bar{K}$

Instrument: Irradiance meter with a selenium photocell covered by a 525nm filter and a diffuse screen.

Data Reduction Procedure: None

11. Investigator: Grady, John R.

Data Source: Grady (1979). Five Cruises of GUS III

Institution: National Marine Fisheries Service

Geographic Area: Louisiana and Texas

Date of Data Collection: Jan-May 1966

Optical Data Type: $Z_s$

Data Reduction Procedures: $Z_s$ converted to $\bar{K}$ by methods of Section III.B.3.

12. Investigators: James, W. P., et al.

Data Source: James (1977)

Institution: Texas A&M University

Geographic Area: Florida

Date of Data Collection: 2/76, 3/76, 7/76

Optical Data Type: K, $Z_s$

Instrument: Kahl Scientific Co. Universal Radiometric Submarine Photometer (Green filter)

Data Reduction Procedures: K data reduced to a depth averaged $\bar{K}$ by method of Section III.B.1. $Z_s$ data converted to $\bar{K}$ by method of Section III.B.3.

13. Investigators: Joyce, Edwin A. and Williams, Jean

Data Source: Joyce and Williams (1969)

Institution: Florida Department of Natural Resources

Geographic Area: Florida

Date of Data Collection: 1966-69

Optical Data Type: $Z_s$

Data Reduction Procedure: Computed $\bar{K}$ from $Z_s$ by method outlined in Section III.B.3.

4. Investigators: Kamykowski, Daniel et al.

Data Source: Kamykowski et al (1978)

Institutions: University of Texas Marine Science Institute
Port Aransas Marine Laboratory

Geographic Area: South Texas

Date of Data Collection: 6/78-11/78

Optical Data Type: Quantum K, C, and $Z_s$

Instrument: Lambda Photometer (quantum)
Martek Transmissometer (528nm)

Data Reduction Procedure: Quantum K reduced to K by procedure outlined in Section III.B.1. Integrated $\bar{C}$ computed by method outlined in Section III.B.2. Quantum $\bar{K}_s$ and $Z_s$ were used to compute the conversion formula, $Z_s$ to $\bar{K}_s$, for the Western Gulf Coast and the procedure is described in Section III.B.3. All data for one oceanographic station.

5. Investigators: Manheim, Frank T.; Steward, Robert G., and Carder, Kendall L.

Data Source: Manheim, Steward and Carder (1977).

Institution: University of South Florida

Geographic Area: Mississippi, Alabama, and Florida

Date of Data Collection: 1975-1976

Optical Data Type: C

Instrument: Hydro Products Transmissometer (550nm)

Data Reduction Procedures: $\bar{C}$ and $\bar{K}$ computed by methods of Section III.B.2.

6. Investigators: McGrail, David W.; Huff, David; Jenkins, Stacy

Data Source: McGrail, Huff and Jenkins (1978)

Institution: Texas A&M University

Geographic Area: Texas and Louisiana

Date of Data Collection: 1977

Optical Data Type: C

Instruments: Martek Transmissometer

Data Reduction Procedures: The data published were transmittance profiles graphed for each ocean station. Thus, inflection points were picked off and the methods of Section III.B.2 were used to computer $\bar{C}$ and $\bar{K}$.

17. Investigator: Oregon State University Cruises

Data Source: Unpublished data (Pak 1974)

Institution: Oregon State University

Geographic Area: Oregon

Date of Data Collection: 1968-1971.

Optical Data Type: $Z_s$

Date Reduction Procedure: Computed $\bar{K}$ from $\bar{Z}_s$ by method outlined in Section III.B.3.

18. Investigators: Pak, Hasong and Zaneveld, Ronald V.

Date Source: Unpublished data (Pak 1979) Conclusions of this data were published by Pak and Zaneveld (1977).

Institution: Oregon State University

Geographic Area: Oregon

Date of Data Collection: 8/74-5/75

Optical Data Type: C

Instrument: OSU Transmissometer (660nm)

Data Reduction Procedure: Computed $\bar{C}$ at 660nm converted to $\bar{C}$ (532nm), and converted to $\bar{K}$ by methods outlined in Section III.B.2.

19. Investigator: Saloman, Carl H.

Data Source: Saloman (1974)

Institution: National Marine Fisheries Service

Geographic Area: Florida

Date of Data Collection: 11/70-9/71

Optical Data Type: $Z_s$

Data Reduction Procedure: Computed $\bar{K}$ from $Z_s$ by method outlined in Section III.B.3.

20. Investigators: Saloman, Carl H. and Collins, L. Alan

Data Source: Saloman and Collins (1974)

Institution: National Marine Fisheries Service

Geographic Area: Tampa Bay, Florida

Date of Data Collection: 1/71-12/72

Optical Data Type: $Z_s$

Date Reduction Procedure: Computed $\bar{K}$ from $Z_s$ by method outlined in Section III.B.3.

21. Investigators: Small, Lawrence F. and Curl, Herbert, Jr.

Data Source: Unpublished Data (Small 1979). Conclusions of this data were published by Small and Curl (1968).

Institution: Oregon State University

Geographic Area: Oregon

Date of Data Collection: 4/62-4/65

Optical Data Type: K

Instrument: Kahl Scientific Irradiance Meter (photopic)

Data Reduction Procedure: None

22. Investigators: Stevenson, W. H., and Pastula, E. J.

Data Source: Stevenson and Pastula (1973)

Institution: National Marine Fisheries Service

Geographic Area: Mississippi Sound

Date of Data Collection: August 1972

Optical Data Type: $Z_s$

Data Reduction Procedure: Computed $\bar{K}$ from $Z_s$ by method outlined in Section III.B.3.

```
CCCCCCCCCCCCCCCCCCCCCCCCCCCCCCCCCCCCCCCCCCCCCCCCCCCCCCCCCCCCCCCCCCCCCCCCCCCC
C                                                                             C
C   PROGRAM PLOTS OPTICAL DATA BY LATITUDE AND LONGITUDE ON TO A MERCATOR     C
C   PROJECTION.  IT SEPARATES THE DATA BY PREDETERMINED OPTICAL SEASONS       C
C   AND AVERAGES DATA WHEN MORE THAN ONE OBSERVATION HAS BEEN TAKEN AT        C
C   A STATION DURING THE SAME OPTICAL SEASON.  IT ASSUMES THAT THE DATA       C
C   CARDS ARE SORTED BY INCREASING LATITUDE.                                  C
C                                                                             C
CCCCCCCCCCCCCCCCCCCCCCCCCCCCCCCCCCCCCCCCCCCCCCCCCCCCCCCCCCCCCCCCCCCCCCCCCCCC
C
      INTEGER*4   XD,XM,KTM,YD,YM,YTM,DEP,Q
      INTEGER*4   MONTH
      INTEGER*4   SEASON(4000)
      DIMENSION   X(4000),Y(4000),YLAT(5),VIS(4000)
      REAL*4      KCONV
      DATA         MAXXD/31/,MINYD/-98/,MAXYD/-88/,LMASK/Z55555555/
      DATA         DELX/10.42/,DELY/10.21/,MINXD/26/
      DATA         SIZENO/.10/,QSCC/'SCC'/,QC/'C'/,QF/'F'/
      DATA       ZERO/-0.06/,QIRR/'IRR'/,QATT/'ATT'/
      COMMON  R,RAD,PI4
      PI4=0.7854
      RAD=0.0174533
C
C   COMPUTE MINIMUM X AND Y FROM SPECIFIED CHART LIMITS.
      ALAT1=RAD*(FLOAT(MINXD))
      ALAT2=RAD*(FLOAT(MAXXD))
      ALON1=FLOAT(MINYD)
      R=DELX/(ALOG(TAN(PI4+(ALAT2/2)))-(ALOG(TAN(PI4+(ALAT1/2)))))
      XMIN=R*(ALOG(TAN(PI4+(ALAT1/2))))
      AY=DELY/(MAXYD-MINYD)
C
C   READ DATA FROM DISK.
      N=0
      IDEG=0
C
C
      DO 100 I=1,6000
      READ(4,10) XD,XM,KTM,YD,YM,YTM,MONTH,DEP,TYP,DAT,UNIT,KCONV
10    FORMAT(I2,I2,I1,1X,I3,I2,I1,3X,I2,8X,I4,1X,A3,6X,F4.0,1X,A1,6X,F4.
     10,25X)
      IF(XD.EQ.99) GO TO 201
      IF(YD.LT.89) GO TO 100
      IF(YD.EQ.89.AND.YM.LT.30) GO TO 100
      IF(YD.GE.98) GO TO 100
      IF(XD.GE.31) GO TO 100
      IF(XD.LT.26) GO TO 100
      IF(MONTH.EQ.0) GO TO 100
      IF(DEP.EQ.0) GO TO 100
```

```
C  CONVERT ALL MEASUREMENTS TO METRIC.
      IF(UNIT.EQ.QC)  DAT=DAT/100
      IF(UNIT.EQ.QC)  DEP=DEP/100
      IF(UNIT.EQ.QF)  DAT=DAT*.305
      IF(UNIT.EQ.QF)  DEP=DEP*.305
C
C  CONVERT ALL MEASUREMENTS TO K.
      IF(TYP.EQ.QSCC.AND.DAT.LE.2) GO TO 100
      IF(TYP.EQ.QSCC)  DAT=(1.26/DAT)+0.03
      IF(TYP.EQ.QATT)  DAT=KCONV/1000
      IF(TYP.EQ.QIRR)  DAT=DAT/1000
      DAT =DAT*DEP
C
C  COMPUTE X AND Y FOR DATA LOCATIONS, WHERE X=LAT, AND Y=LONG.
      CALL MLAT(XD,XM,XTM,AX)
      ALON=FLOAT(YD)+(FLOAT(YM)+(FLOAT(YTM)*0.1))/60.0
      ALON=-ALON
      N=N+1
      X(N)=AX-XMIN
      Y(N)=AY*(ALON-ALON1)
C  SHIFT COORDINATES SO THAT PLOTTED NUMBER WILL BE CENTERED.
      X(N)=X(N)-(.5*SIZENO)
      Y(N)=Y(N)-(.30*SIZENO)

      IF(DAT.GE.10)  Y(N)=Y(N)-(.45*SIZENO)
      VIS(N)=DAT
C
C  DETERMINE WHICH OPTICAL SEASON DATA WAS TAKEN IN.
      IF(MONTH.LE.5)  SEASON(N)=1
      IF(MONTH.EQ.6.OR.MONTH.EQ.12)  SEASON(N)=2
      IF(MONTH.GE.7.AND.MONTH.LE.11)  SEASON(N)=3
C
C  CHECK TO SEE IF THIS LATITUDE HAS MORE THAN ONE OBSERVATION.
      JA=N-1
      IF(XD.EQ.IDEG) GO TO 50
      IDEG=XD
      CALL MLAT(IDEG,0,),AX)
      ADEG=AX-XMIN
      GO TO 100
C
C  LOOP50 SEARCHES BACK THRU LATITUDE XD FOR DUPLICATE STATIONS (PLUS OR
C  MINUS THE SIZE OF A PLOTTED NUMBER).
50    DUPA=X(JA)+(SIZENO*1.5)
      DUPB=X(JA)-(SIZENO*1.5)
      IF(X(N).LE.DUPA.AND.X(N).GE.DUPB) GO TO 60
C  CONTINUE SEARCH.
55    JA=JA-1
      IF(JA.EQ.0) GO TO 100
      DIFF=X(JA)-ADEG
      IF(DIFF.GE.ZERO) GO TO 50
      GO TO 100
```

```
C  STATEMENT 60 IS BRANCHED TO WHEN A DUPLICATE LATITUDE STATION HAS BEEN
C  FOUND.  NOW MUST CHECK IF LONGITUDE ALSO MATCHES.  IF NOT, BRANCH BACK
C  INTO LATITUDE SEARCH (LOOP 50).
60     DUPA=Y(JA)+(SIZENO*2.5)
       DUPB=Y(JA)-(SIZENO*2.5)
       IF(Y(N).GT.DUPA.OR.Y(N).LT.DUPB) GO TO 55
C
C  A DUPLICATE POSITION HAS BEEN FOUND.  CHECK TO SEE IF THE OBSERVATION
C  WAS TAKEN DURING THE SAME OPTICAL SEASON.
       IF(SEASON(N).NE.SEASON(JA)) GO TO 55
C
C  A DUPLICATE STATION OBSERVATION HAS BEEN FOUND.  ADD THIS DATA TO THE
C  PREVIOUS OBSERVATION TO BE AVERAGED LATER.  TO SAVE STORAGE, 10,000 IS
C  ADDED TO THE SUM AS A COUNTER TO INDICATE THE NUMBER OF OBSERVATIONS
C  (MINUS 1) THAT HAVE BEEN SUMMED TOGETHER AT A PARTICULAR POSITION.
       VIS(JA)=VIS(JA)+DAT+10000
C  DELETE LAST DUPLICATE OBSERVATION.
       N=N-1
100    CONTINUE
C
C
201    NPTS=N
C
C
C  A FINAL AVERAGE IS MADE OF ALL POSITIONS WITH MORE THAN ONE OBSERVATION.
       DO 210 I=1,NPTS
       IF(VIS(I).LT.10000) GO TO 210
       ND=VIS(I)/10000
       VIS(I)=VIS(I)-(ND*10000)
       ND=ND+1
       VIS(I)=VIS(I)/ND
210    CONTINUE
C
C...DATA POINTS ARE PLOTTED ACCORDING TO THEIR POSITIONS IN ARRAYS X AND Y.
C...PROJECTION.
C...X AND Y MEASURE IN A POSITIVE DIRECTION FROM THE SOUTHWEST CORNER OF THE
C...INITIALIZE PLOTTING.
       CALL PLOTS (0,0,0)
       CALL SETMSG (2)
C
C...DRAW GRID OVERLAY OF LAT AND LONG LINES.
C...DETERMINE INTERVAL SPACING FOR LATITUDE GRID.
       DLAT=XMIN
       I=1
       DO 300 K=27,31
```

APPENDIX B (cont'd)

```
      Q=K
      CALL MLAT(Q,0,0,AK)
      YLAT(I)=AX-DLAT
      DLAT=AX
      I=I+1
300   CONTINUE
C
C...PLOT EACH SEASON SEPARATELY.
      DO 410 JB=1,3
      CALL GRID (0.,0.,10,1.82,1005,YLAT,LMASK)
C
      DO 400 J=1,NPTS
      IF(SEASON(J).NE.JB) GO TO 400
      CALL NUMBER (Y(J),X(J),.09,VIS(J),0.0,-1)
400   CONTINUE
C
      IF(JB.EQ.3) GO TO 900
      CALL PLOT (0.,0.,-999)
410   CONTINUE
C
C  END ALL PLOTTING
900   CALL PLOT (0.,0.,+999)
      STOP
      END
```

```
      SUBROUTINE MLAT(LD,LM,LTM,ALAT)
C
C  THIS SUBROUTINE COMPUTES THE MERCATOR LATITUDE (ALAT), GIVEN A SPECIFIED
C  RADIUS R, AND LATITUDE IN DEGREES (LD), MINUTES (LM), AND TENTHS OF
C  MINUTES (LTM).
C
      COMMON  R,RAD,PI4
      ALAT=RAD*(FLOAT(LD)+(FLOAT(LM)+(FLOAT(LTM)*0.1))/60.0)
      ALAT=R*(ALOG(TAN(PI4+(ALAT/2))))
      RETURN
      END
```

TABLE I.* SUMMARY OF LINEAR REGRESSIONS FOR SPECTRAL BEAM ATTENUATION DATA AT VARIOUS DEPTHS TAKEN IN MONTEREY BAY, CALIFORNIA

| Depth (M) | C(500)=mC(650)+b | | C(650)=nC(500)+a | | Corr. Coef. | C(550=mC(650)+b | | C(650)=nC(550)+a | | Corr. Coef. |
|---|---|---|---|---|---|---|---|---|---|---|
| | m | b | n | a | | m | b | n | a | |
| 0-1 | .997 | -.322 | .948 | .352 | .97 | .950 | -.230 | .901 | .330 | .93 |
| 5 | 1.087 | -.399 | .875 | .390 | .98 | 1.112 | -.369 | .854 | .357 | .97 |
| 10 | 1.101 | -.403 | .845 | .399 | .96 | 1.042 | -.311 | .915 | .323 | .98 |
| 20 | .975 | -.331 | .837 | .406 | .90 | .970 | -.272 | .847 | .356 | .91 |
| 40 | 1.192 | -.463 | .809 | .394 | .98 | 1.096 | -.346 | .878 | .325 | .98 |
| 60 | 1.147 | -.442 | .855 | .389 | .99 | 1.089 | -.344 | .908 | .319 | .99 |
| MEAN | 1.083 | -.393 | .862 | .388 | | 1.043 | -.312 | .883 | .335 | |
| | | | TRANSF C(500) TO L.HAND SIDE | | | | | TRANSF C(550) TO L.HAND SIDE | | |
| MEAN | 1.083 | -.393 | 1.160 | -.450 | | 1.043 | -.312 | 1.133 | -.379 | |
| FINAL EQUAT | C(500)=1.12C(650)-0.42 | | | | | C(550)=1.09C(650)-0.35 | | | | |

*OSU Stations used were: 0501, 0502, 0610, 0611, 0701, 0901, 1006, 1007, 1103, 1104, 1105, 1106, 1303, 0602, 0605, 0803, 0805, 0806, 0901, 0902, 0903, 1006, 1007, 1009, 1014, 1103, 1104, 1105, 1202, 1203, 1204, 1305, 1306, 1401, 1402, 1403, 1404, 1406, 1501, 1502, 1503, 1504, 1605, 1606, 1607. (Zaneveld, et al., OSU Ref. 78-13, Aug 78).

TABLE II. DATA USED TO CONVERT SECCHI DEPTH TO IRRADIANCE ATTENUATION ($Z_s$ TO $\bar{K}_s$) FOR EASTERN PACIFIC COASTAL WATERS

| Station | 1957 Date | North Latitude | North Longitude | $Z_s$ (m) | $\bar{K}_s$ ($m^{-1}$) |
|---|---|---|---|---|---|
| 49A | 7/9 | 39° 59' | 126° 38' | 32 | .0718 |
| 51 | 7/10 | 40° 02' | 127° 07' | 32 | .0363 |
| 61 | 7/15 | 44° 50' | 126° 11' | 22 | .1114 |
| 64 | 7/23 | 44° 18' | 126° 38' | 20 | .1117 |
| 65 | 7/23 | 43° 51' | 127° 22' | 32 | .0708 |
| 66 | 7/24 | 43° 43' | 127° 51' | 32 | .0747 |
| 67 | 7/24 | 43° 13' | 127° 12' | 26 | .0903 |
| 83 | 7/30 | 39° 01' | 126° 26' | 28 | .0674 |
| 88 | 8/4 | 38° 56' | 125° 42' | 26 | .0651 |
| 89 | 8/4 | 38° 57' | 126° 10' | 24 | .0900 |
| 91 | 8/5 | 38° 14' | 125° 40' | 20 | .1096 |
| 92 | 8/5 | 38° 05' | 125° 25' | 16 | .1327 |
| 93 | 8/5 | 38° 14' | 125° 44' | 22 | .0938 |
| 95 | 8/6 | 37° 06' | 125° 07' | 24 | .0999 |
| 96 | 8/6 | 36° 58' | 124° 56' | 18 | .1291 |
| 98 | 8/6 | 36° 45' | 124° 34' | 20 | .1340 |
| 101 | 8/7 | 36° 45' | 124° 34' | 22 | .1123 |
| 102 | 8/8 | 36° 08' | 123° 24' | 20 | .1151 |
| 103 | 8/8 | 35° 19' | 123° 23' | 10 | .2577 |

Original station data from Callaway and McGary (1959); $\bar{K}_s$ computed by van Norden.

TABLE III. DATA USED TO CONVERT SECCHI DEPTH TO IRRADIANCE ATTENUATION ($Z_s$ TO $\bar{K}_s$) FOR WESTERN GULF COASTAL WATERS

| Date | Local Time | $Z_s$ (m) | Quanta $\bar{K}_s$ | $K/K_Q$ | $\bar{K}_s$ ($m^{-1}$) |
|---|---|---|---|---|---|
| 6/29/78 | 1300 | 23.75 | .0609 | 1.085 | .0661 |
| 6/29/78 | 1700 | 20 | .0909 | 1.06 | .0964 |
| 7/24/78 | 1200 | 26 | .0683 | 1.095 | .0748 |
| 7/25/78 | 0800 | 19 | .0587 | 1.08 | .0634 |
| 7/25/78 | 1200 | 20 | .0442 | 1.12 | .0495 |
| 9/25/78 | 1345 | 4 | .387 | .975 | .377 |
| 9/26/78 | 0000 | 3.5 | .295 | .975 | .299 |
| 11/08/78 | 1200 | 9 | .233 | .990 | .231 |
| 11/08/78 | 1600 | 9 | .183 | .980 | .180 |
| 11/09/78 | 0800 | 14 | .187 | .950 | .177 |
| 11/09/78 | 1200 | 14 | .158 | .950 | .143 |

All observations at N 27° 34' Latitude and W 96° 50' Longitude. Original station data from Kamykowski, et al. (1978); Quanta $\bar{K}_Q$ and $\bar{K}_s$ computed by van Norden and $K/K_Q$ obtained from Jerlov (1976).

TABLE IV. SUMMARY OF LINEAR REGRESSIONS TO CONVERT SECCHI DEPTH TO IRRADIANCE ATTENUATION ($Z_s$ TO $\bar{K}_s$) FOR SELECTED U.S. COASTAL WATERS

| Location | $Z_s^{-1}$ as Independent Variable | $\bar{K}_s$ as Independent Variable | Mean Equation |
|---|---|---|---|
| U.S. West Coast | $\bar{K}_s = 1.21 Z_s^{-1} + 0.06$ | $Z_s^{-1} = 0.78 K_s - 0.04$ | $\bar{K}_s = 1.25 Z_s^{-1} + 0.05$ |
| U.S. West Gulf | $\bar{K}_s = 1.14 Z_s^{-1} + 0.04$ | $Z_s^{-1} = 0.73 \bar{K}_s - 0.01$ | $\bar{K}_s = 1.26 Z_s^{-1} + 0.03$ |
| Shannon's Equation (Witt, et al, 1976) | $\bar{K}_s = 1.15 Z_s^{-1} + 0.03$ | | |
| English Channel Poole-Atkins Data | $\bar{K}_{0-20} = 1.11 Z_s^{-1} + 0.04$ | $Z_s^{-1} = 0.72 \bar{K}_{0-20} - 0.01$ | $\bar{K}_{0-20} = 1.25 Z_s^{-1} + 0.03$ |

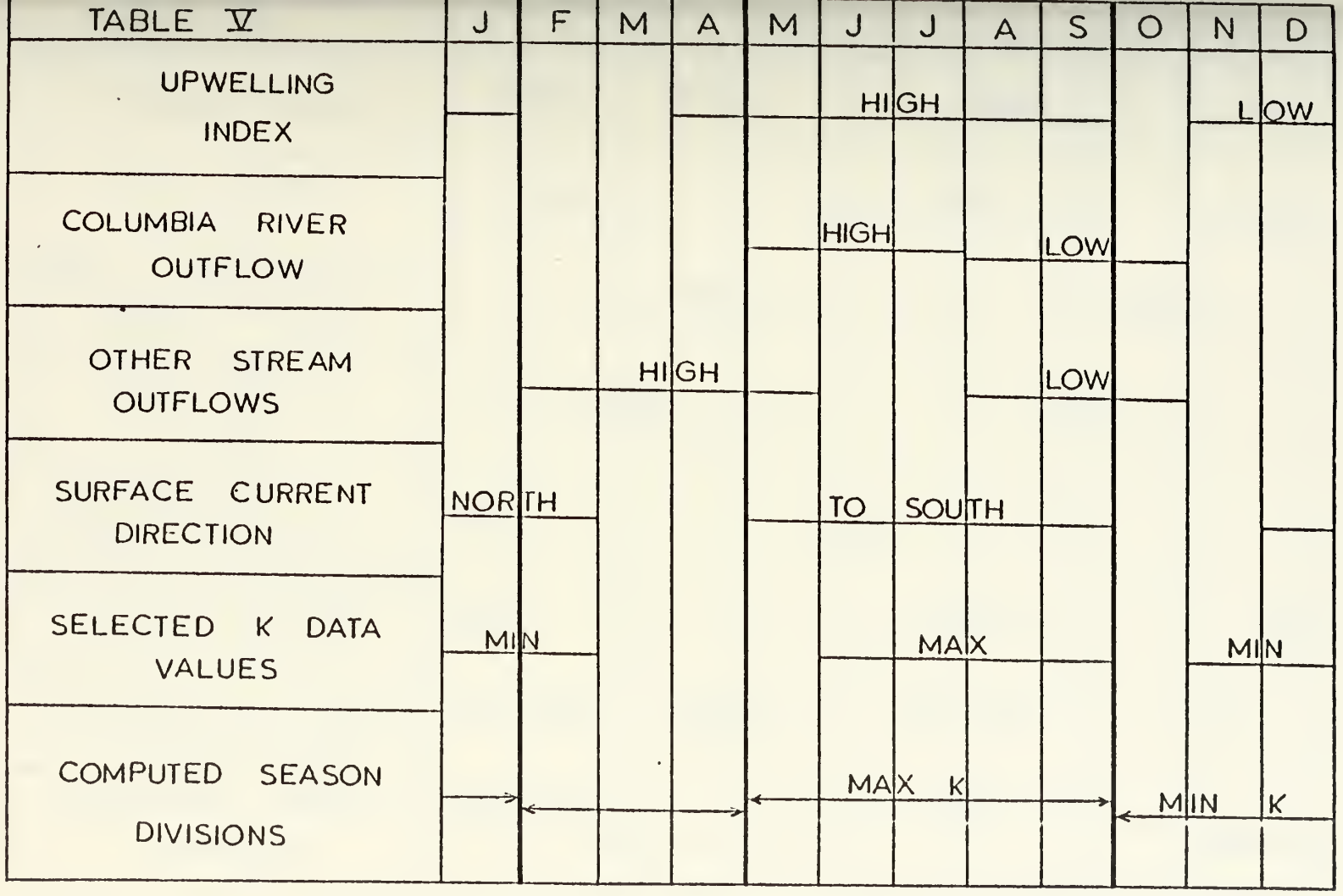


TABLE V. PACIFIC NORTHWEST COAST PARAMETERS USED TO DETERMINE OPTICAL SEASONS

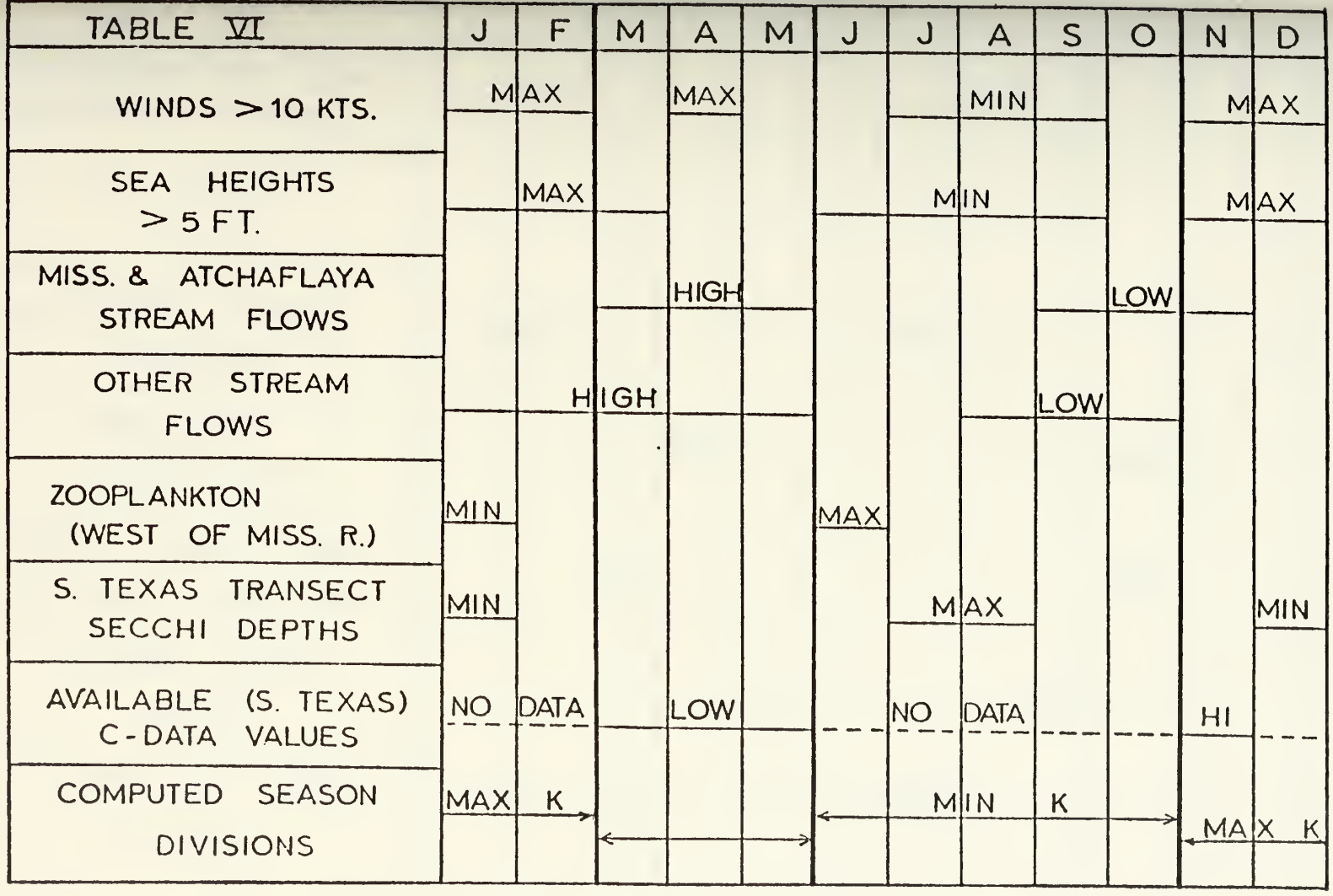


TABLE VI. WESTERN GULF PARAMETERS USED TO DETERMINE OPTICAL SEASONS

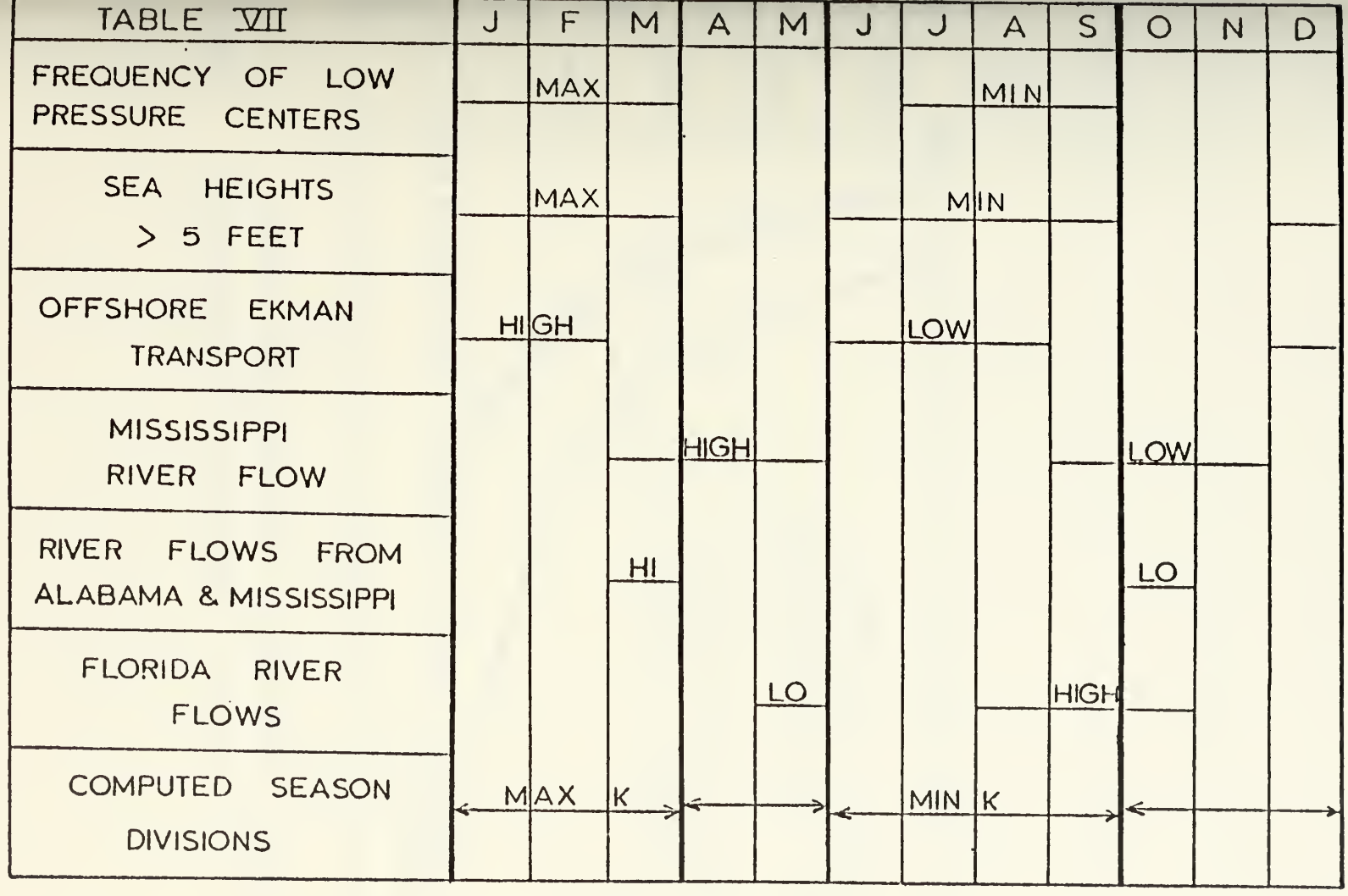


TABLE VII. EASTERN GULF PARAMETERS USED TO DETERMINE OPTICAL SEASONS

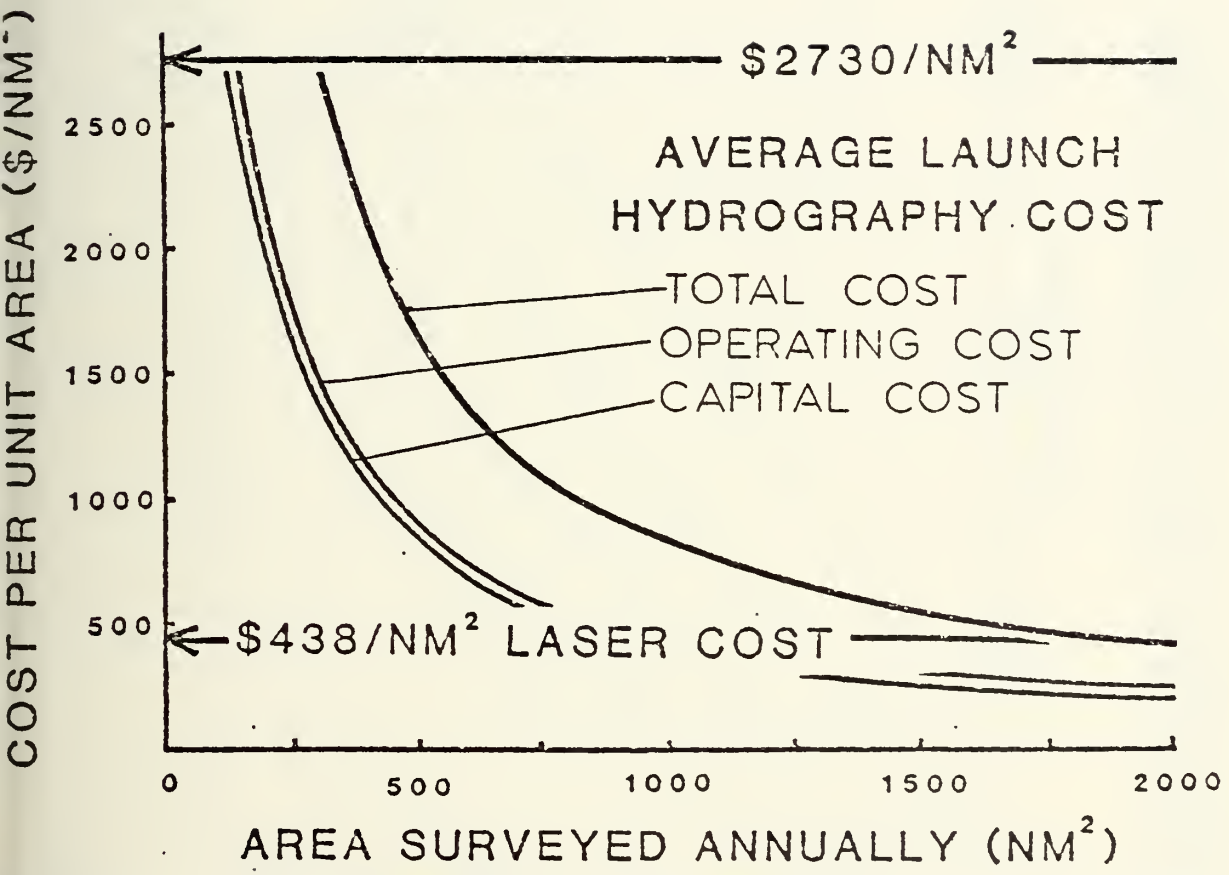


FIGURE 1. LASER/SONAR COST COMPARISON, COSTS IN 1977 DOLLARS (NOS, 1979).

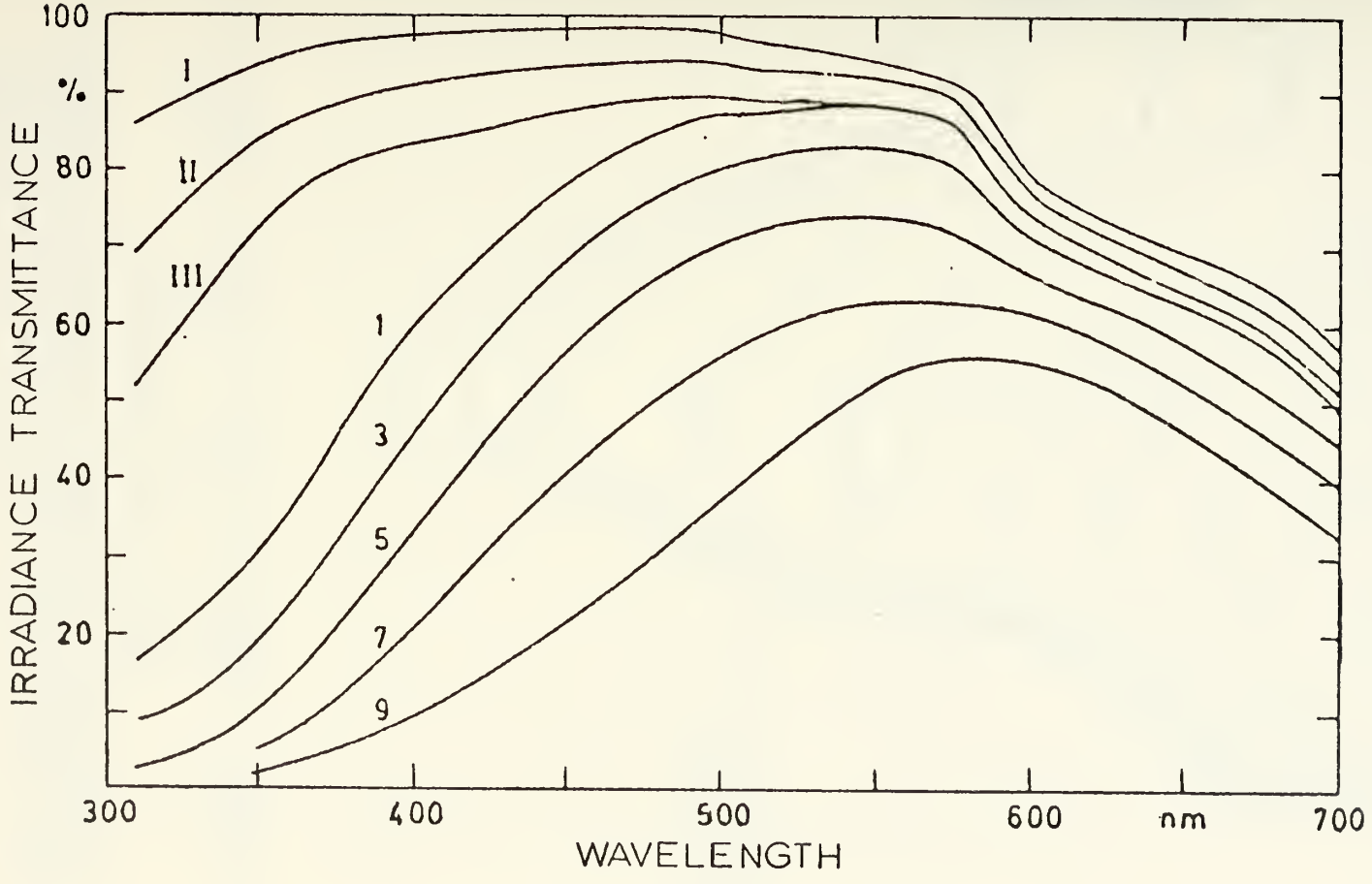


FIGURE 2. TRANSMITTANCE PER METER OF DOWNWARD IRRADIANCE IN THE SURFACE LAYER FOR OPTICAL WATER TYPES. OCEANIC TYPES I, II, III AND COASTAL TYPES 1, 3, 5, 7, 9 (JERLOV, 1976).

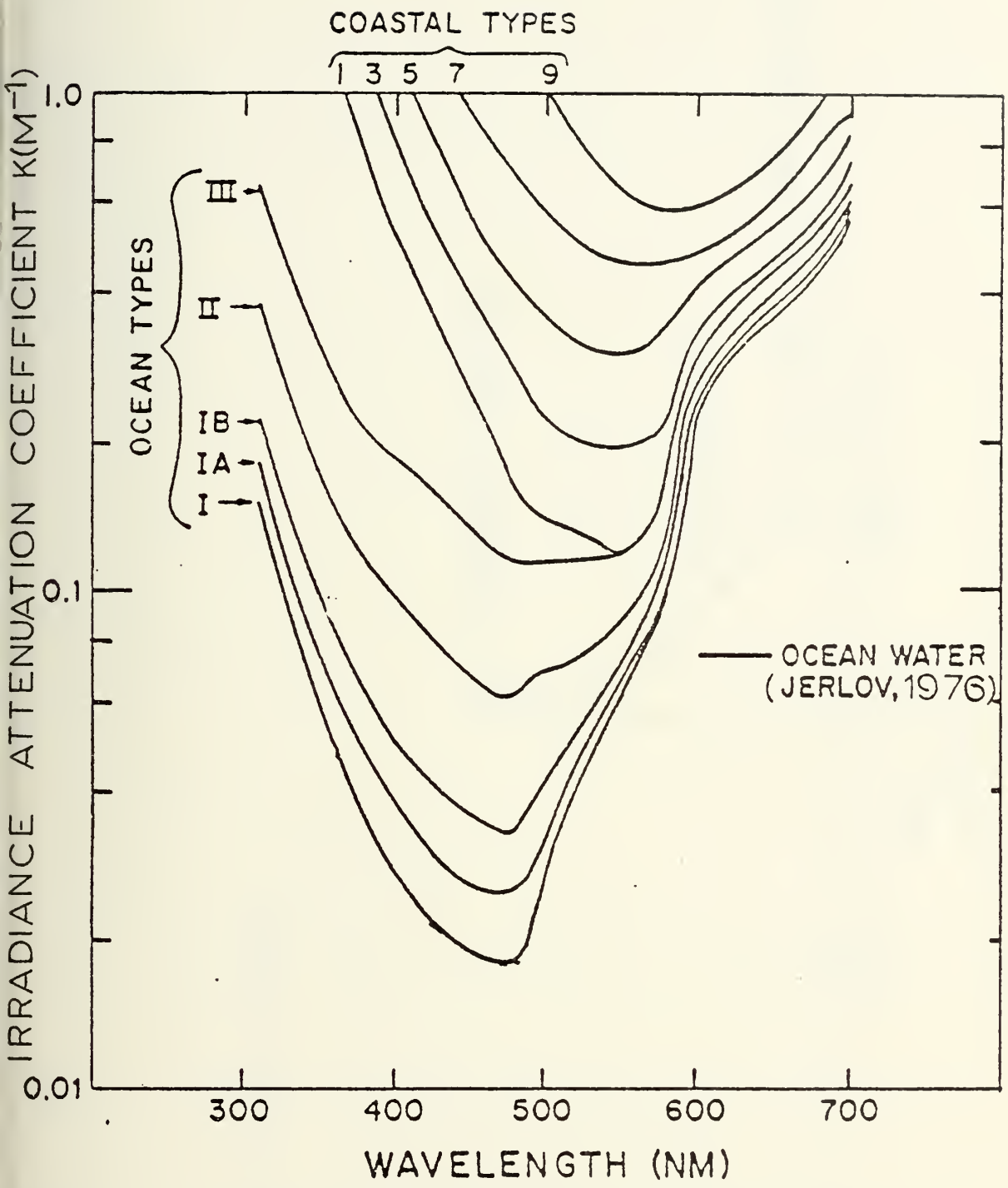


FIGURE 3. SPECTRAL IRRADIANCE ATTENUATION COEFFICIENTS OF DOWNWARD IRRADIANCE IN THE SURFACE LAYER FOR JERLOV OPTICAL WATER TYPES (AVCO EVERETT RESEARCH LABORATORY, INC., 1978).

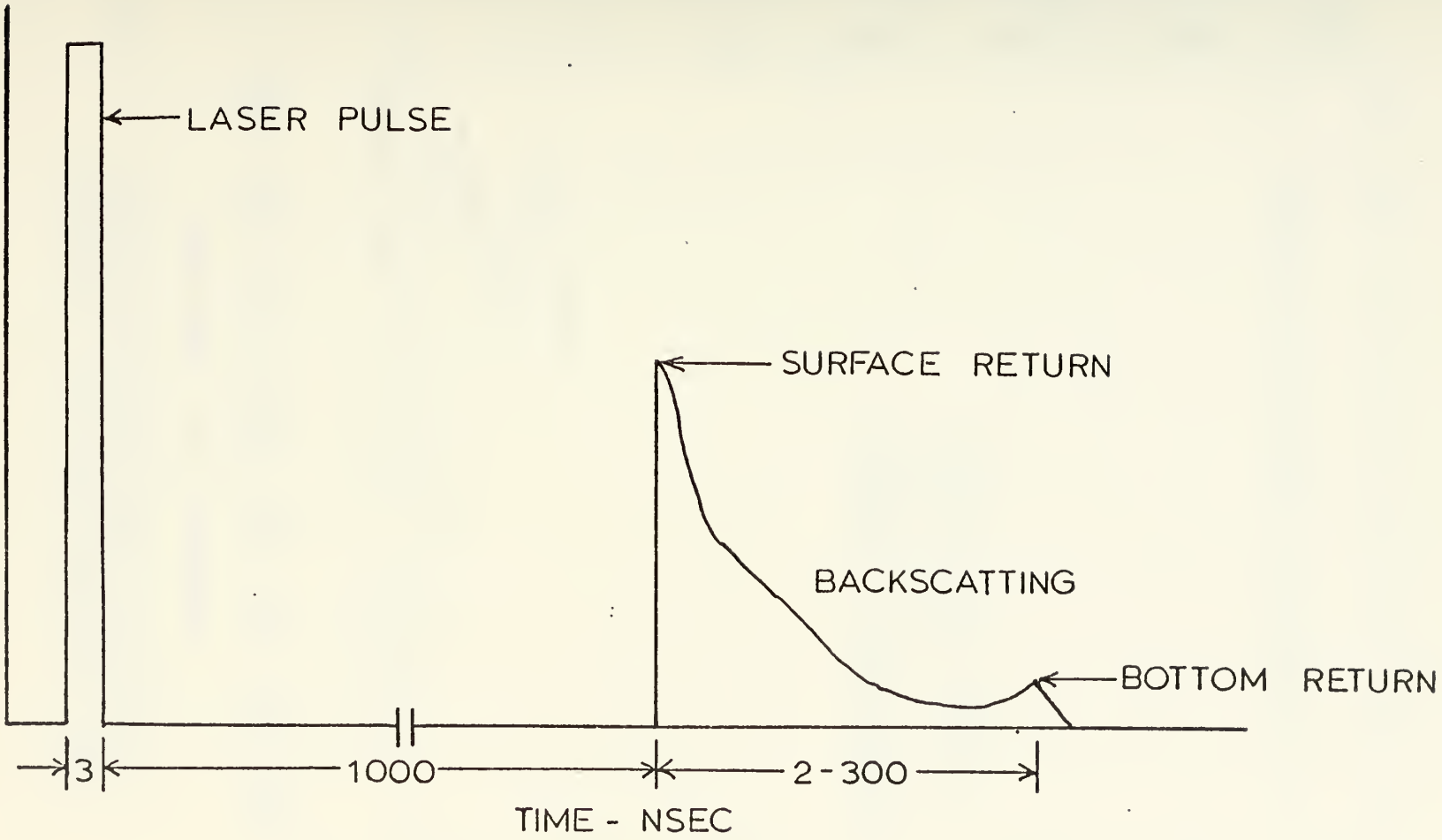


FIGURE 4

LASER PULSE AND RETURN SIGNALS

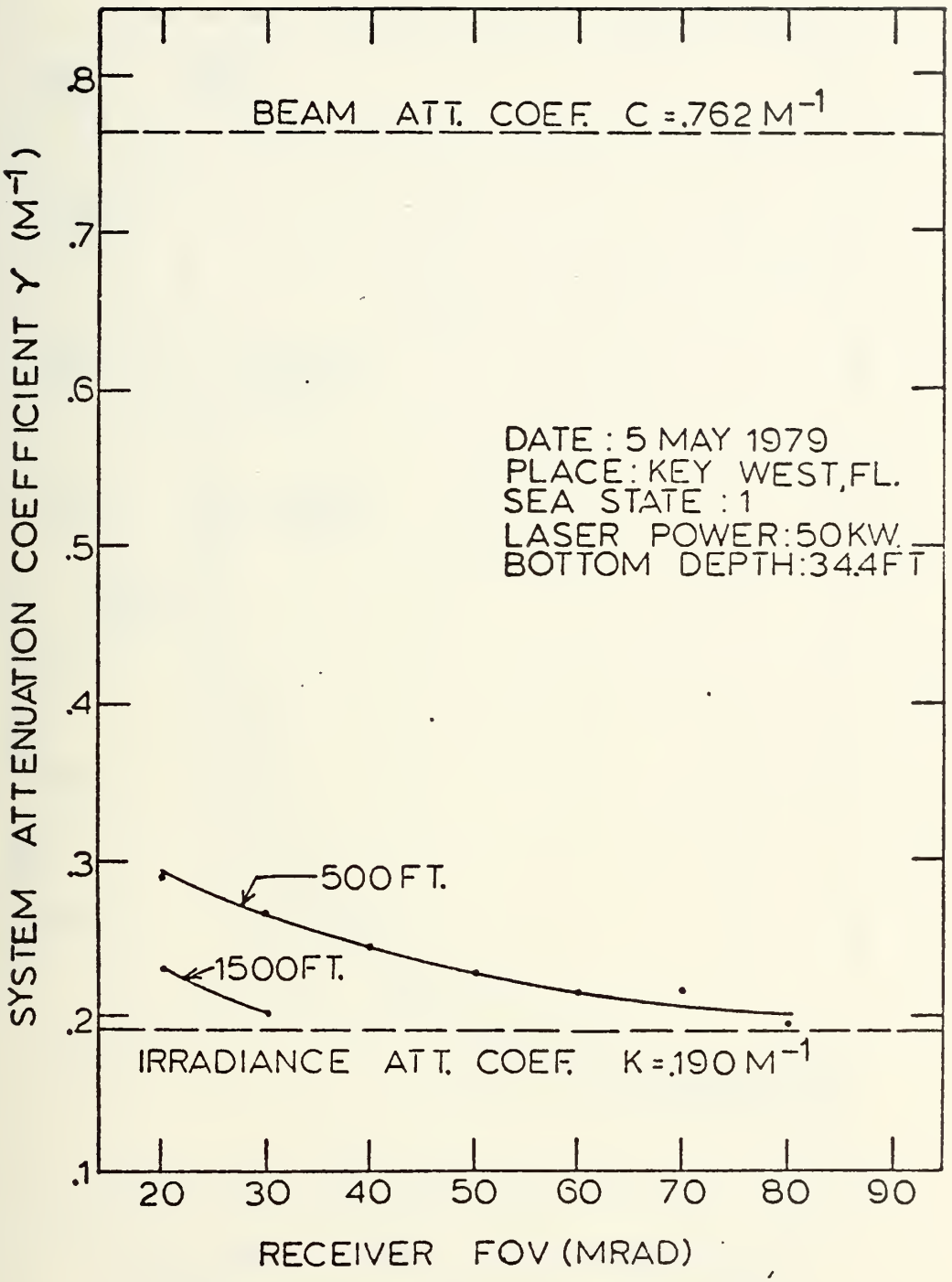


FIGURE 5. SYSTEM ATTENUATION COEFFICIENTS AS A FUNCTION OF RECEIVER FOV AND AIRCRAFT ALTITUDE. DATA FROM KRUMBOLTZ (1979).

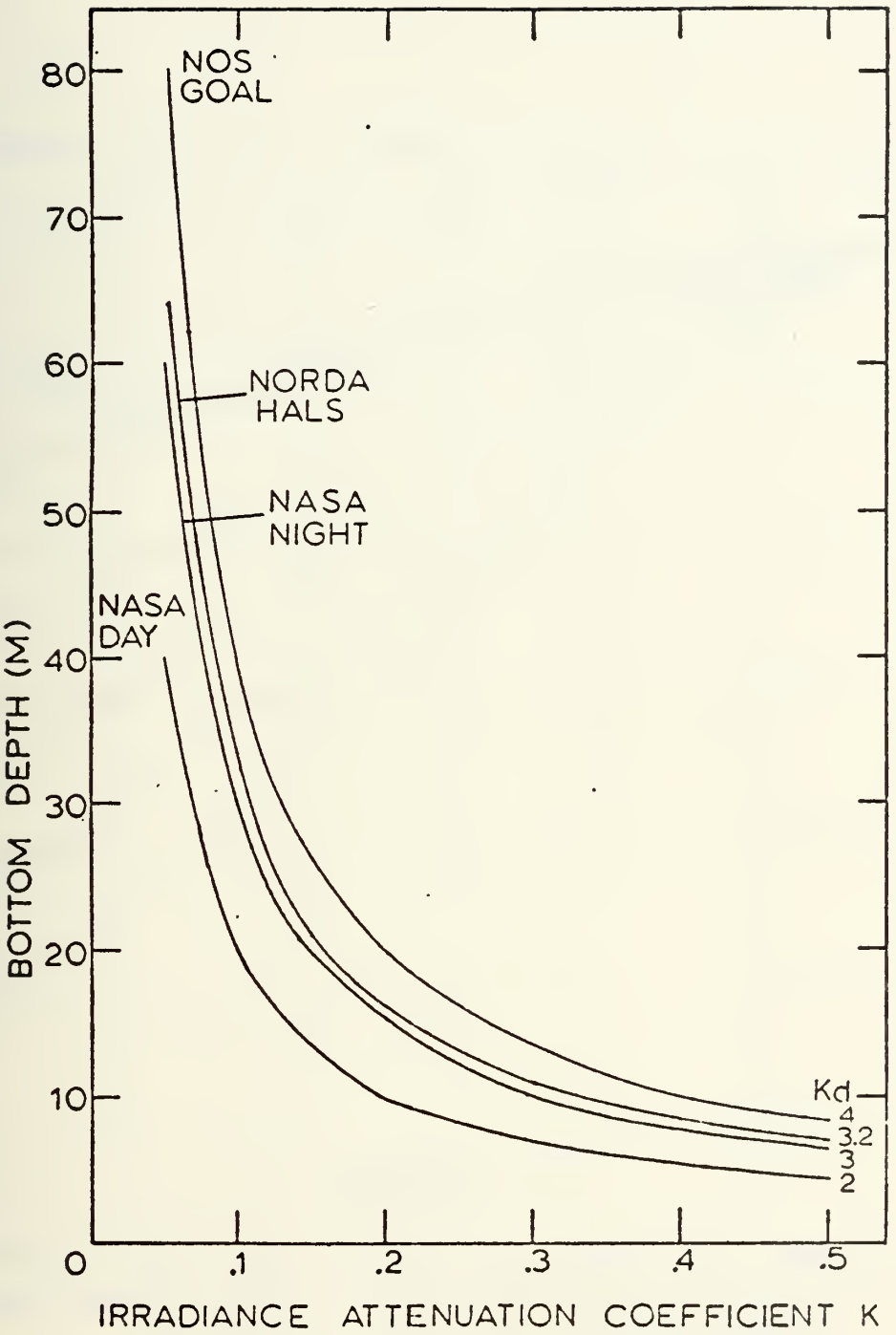


FIGURE 6. EXPECTED PENETRATION OF DIFFERENT LASER SYSTEMS AS SPECIFIED BY IRRADIANCE ATTENUATION LENGTHS TO THE BOTTOM.

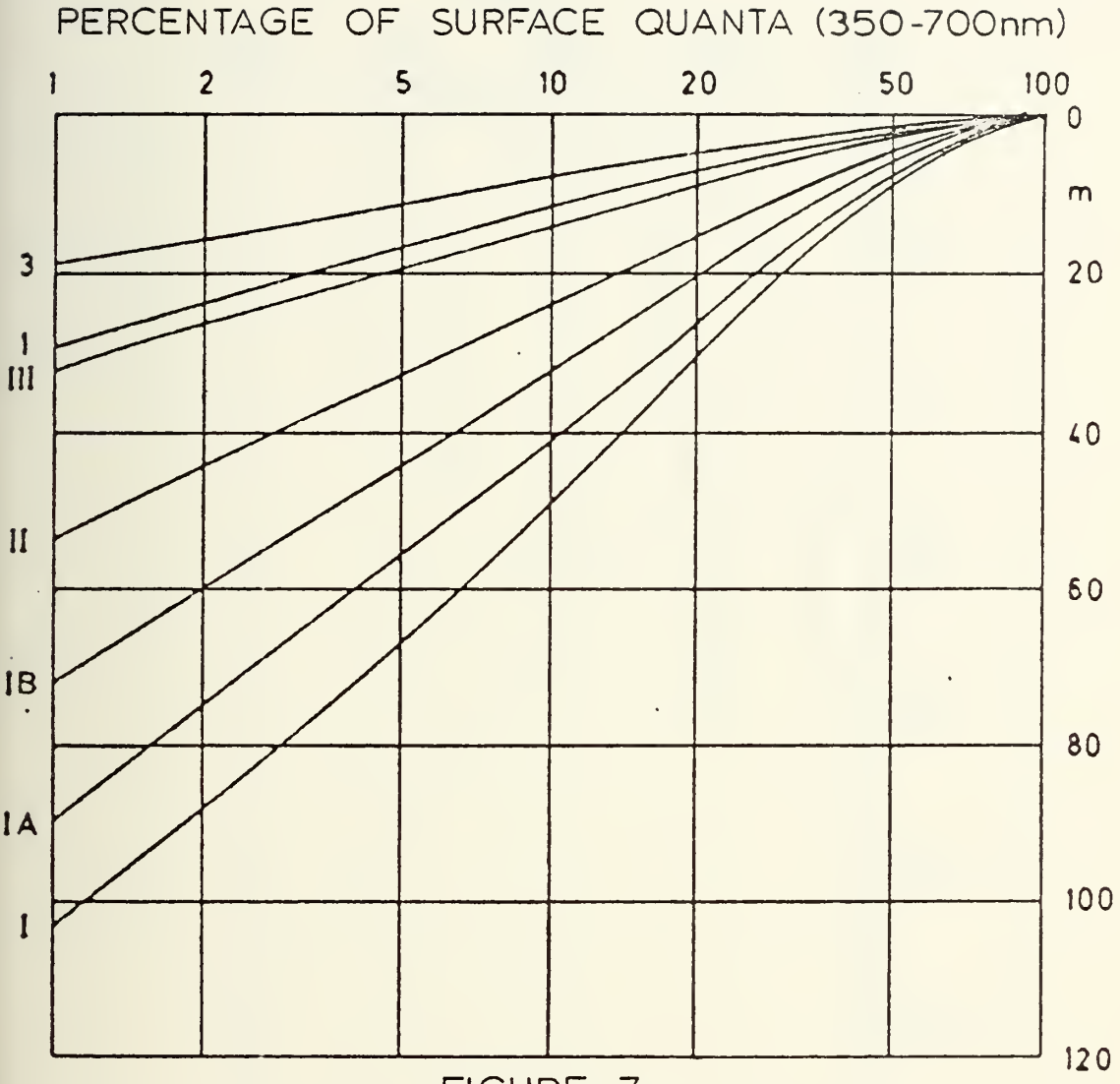


FIGURE 7

DEPTH PROFILES OF PERCENTAGE OF SURFACE QUANTA(350-700nm) FOR DIFFERENT WATER TYPES (JERLOV,1976)

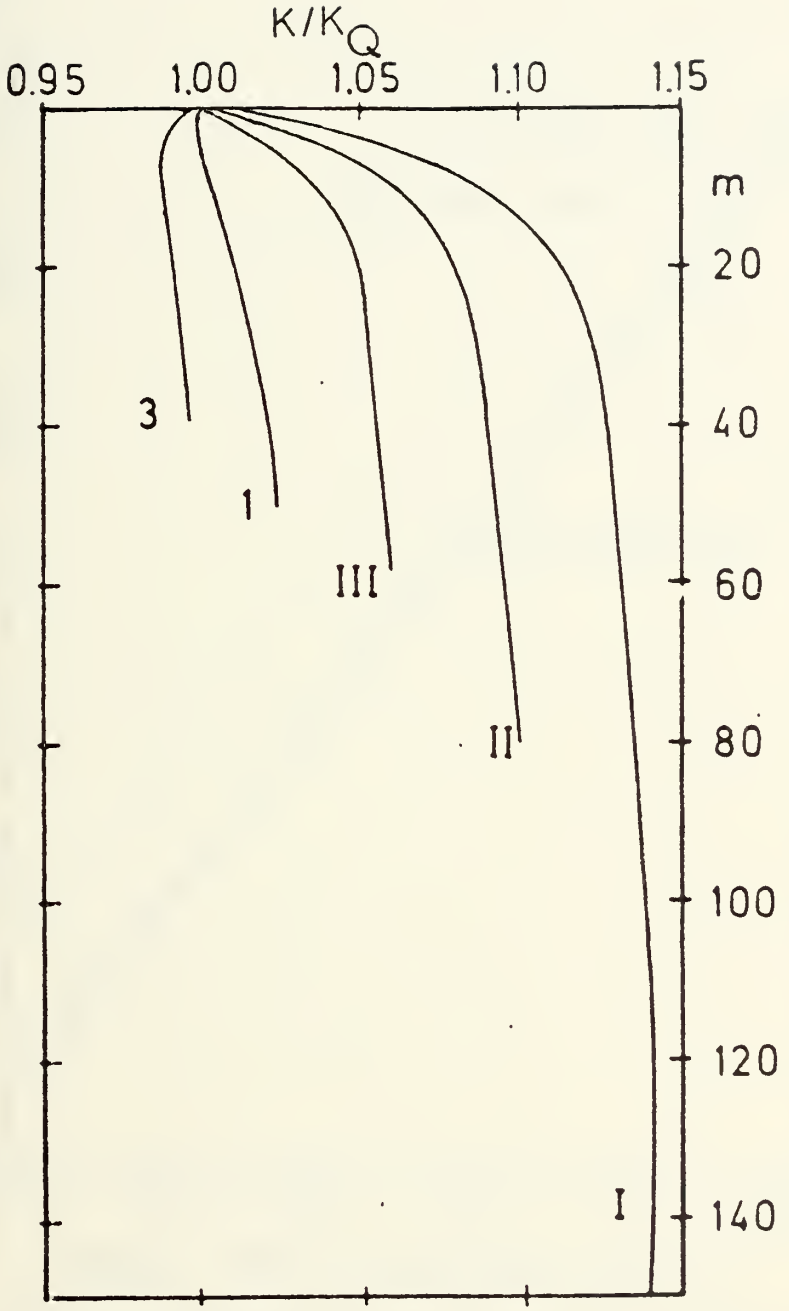


FIGURE 8. THE RATIO OF IRRADIANCE TO QUANTUM IRRADIANCE IN THE SPECTRAL RANGE 350-700 nm AS A FUNCTION OF DEPTH IN DIFFERENT OPTICAL WATER MASSES (JERLOV, 1976).

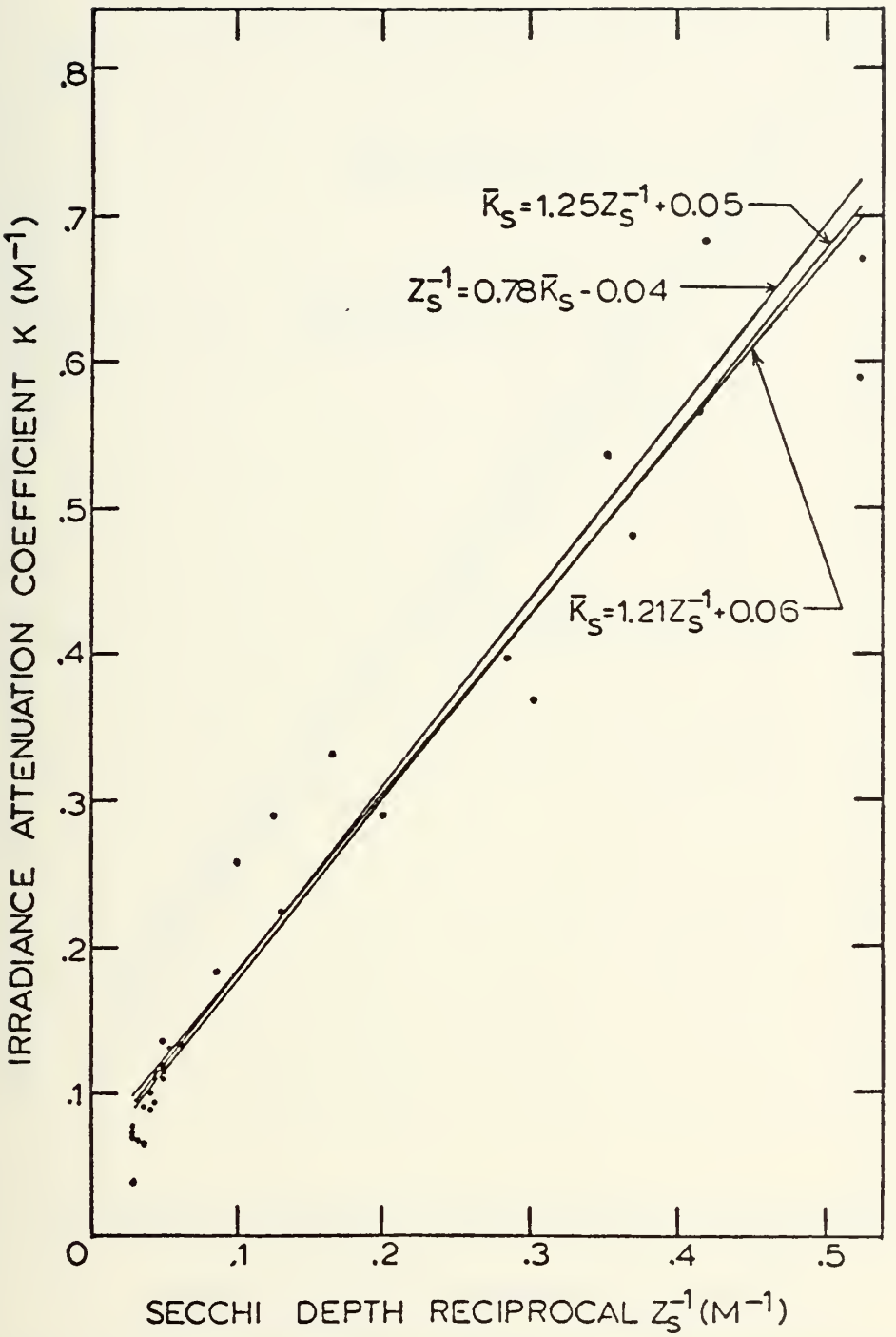


FIGURE 9. LINEAR REGRESSIONS OF $\bar{K}_s$ AND $Z_s$ FOR EASTERN PACIFIC COASTAL WATERS.

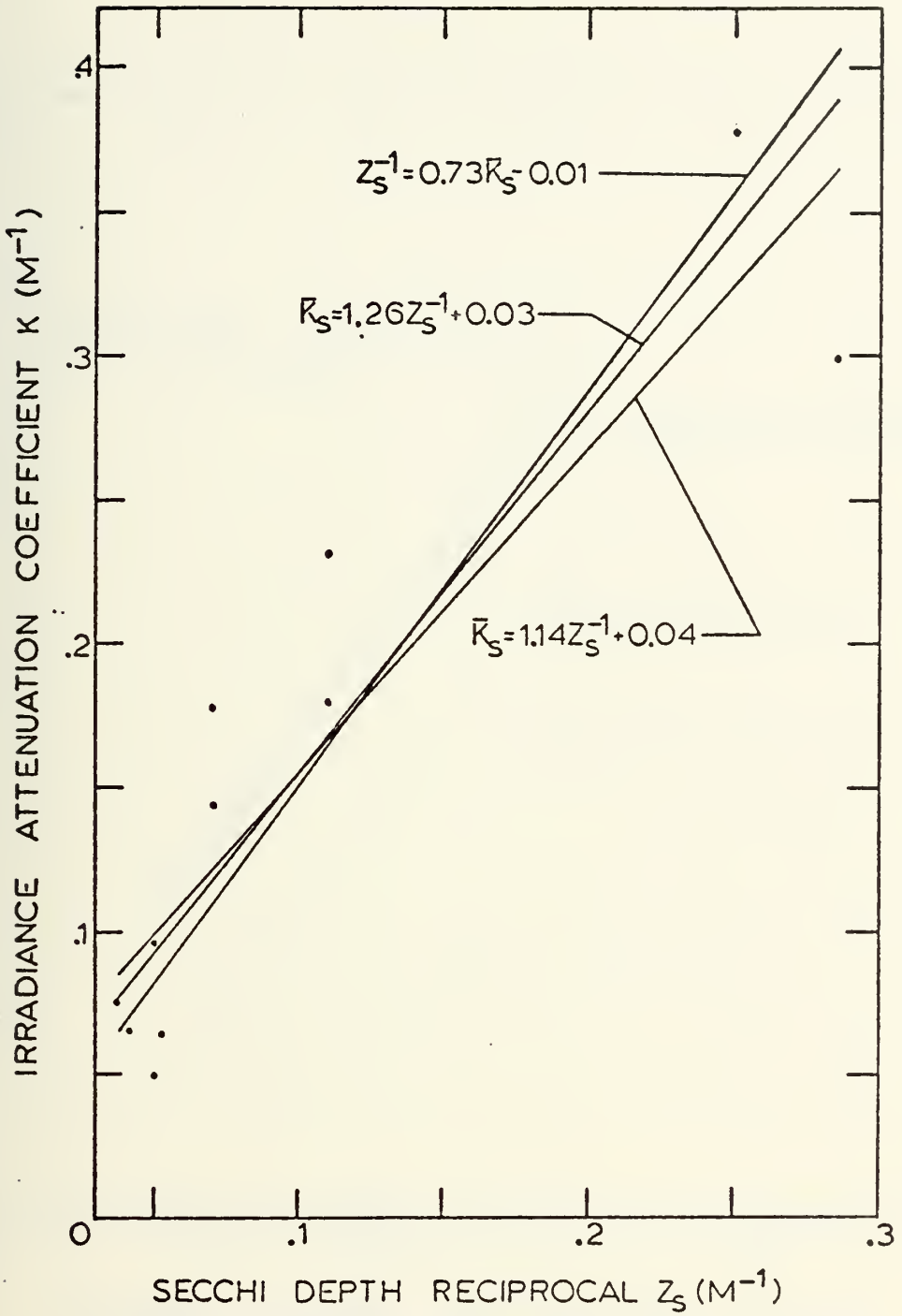


FIGURE 10. LINEAR REGRESSIONS OF $\bar{K}_s$ AND $Z_s$ FOR WESTERN GULF COASTAL WATERS.

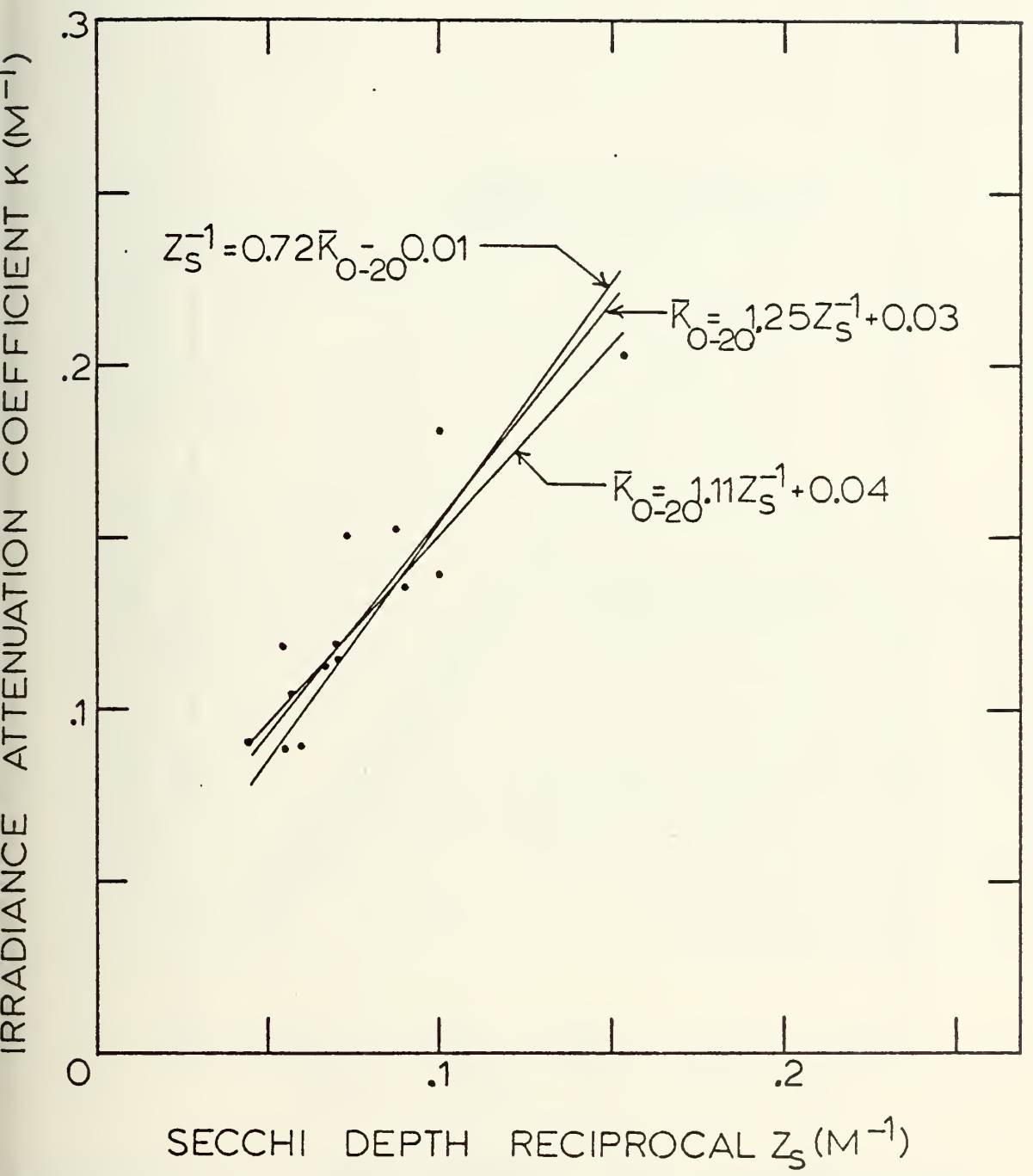


FIGURE 11. LINEAR REGRESSIONS OF $\bar{K}_s$ AND $Z_s$ FOR POOLE AND ATKINS DATA.

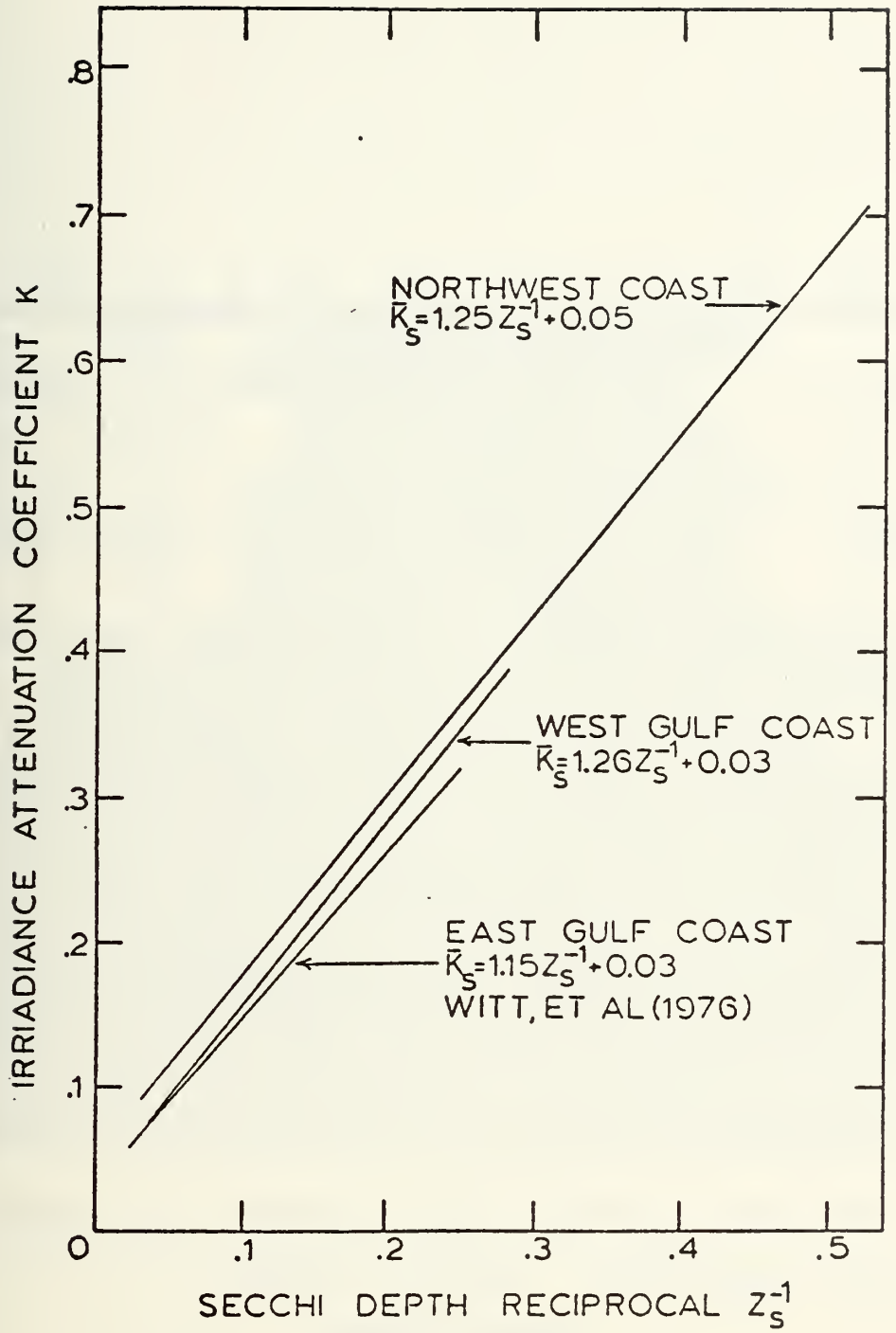


FIGURE 12. LINEAR REGRESSIONS USED TO CONVERT $Z_s$ TO $\bar{K}_s$ FOR SELECTED U.S. COASTAL WATERS.

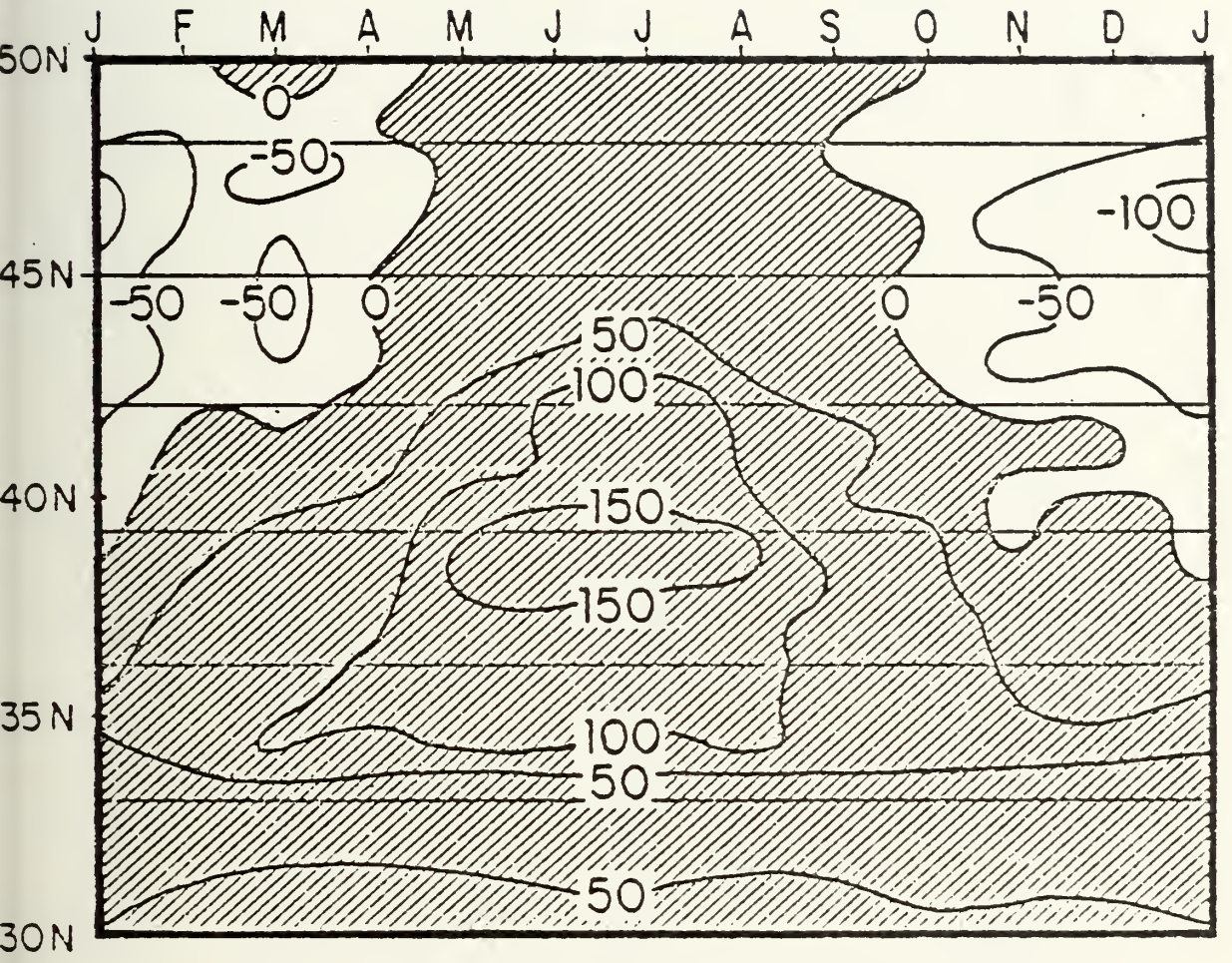


FIGURE 13 UPWELLING INDEX FOR THE U.S. WEST COAST ($m^3$/ sec / 100m)

BAKUN (1975)

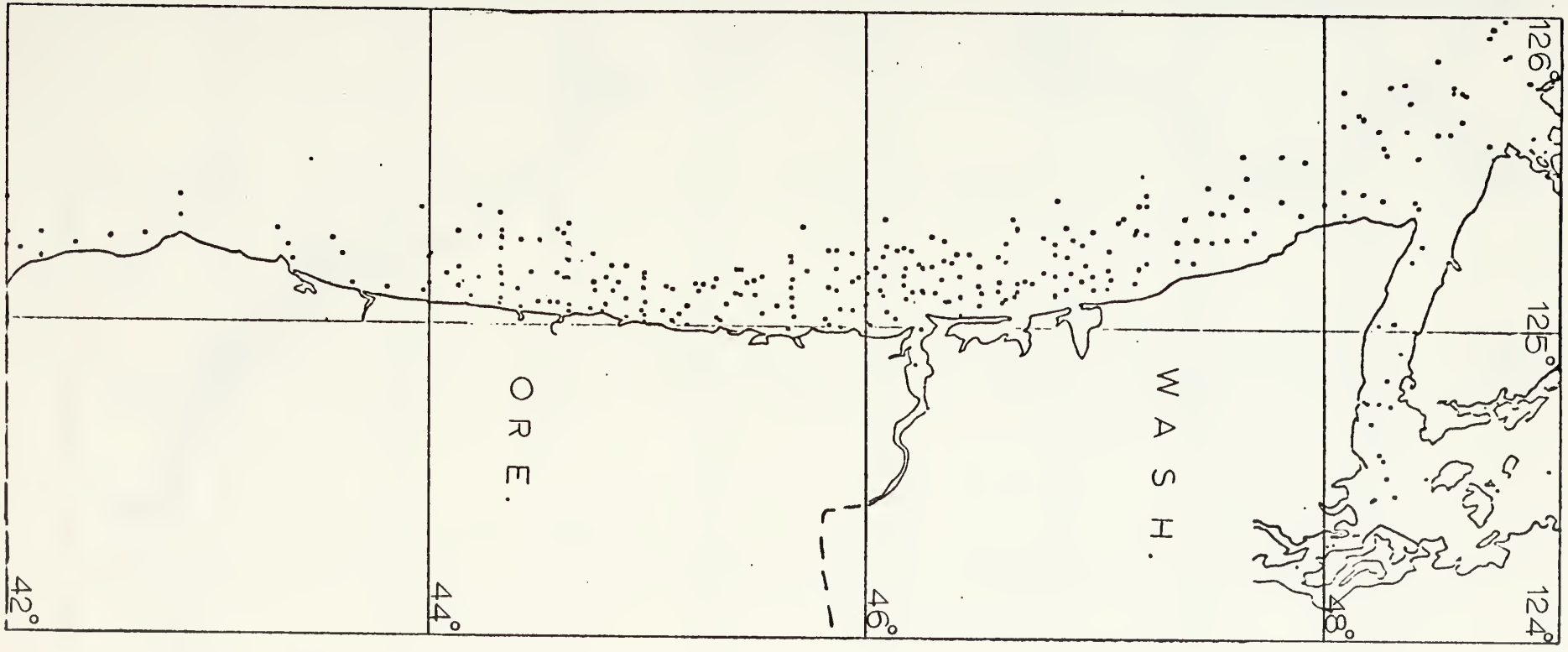


NORTHWEST COAST POSITION PLOT FIGURE 14

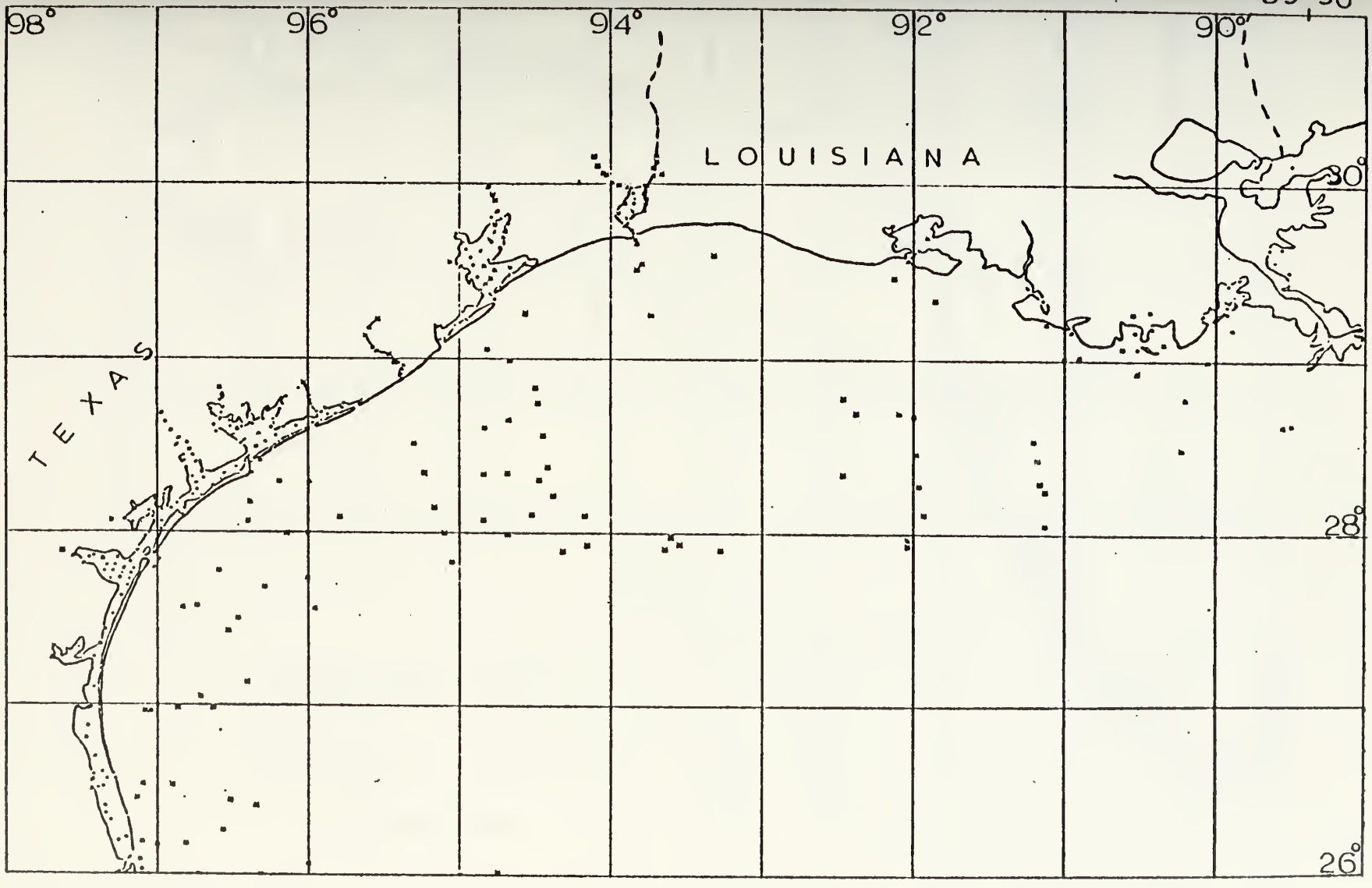


FIGURE 15 WESTERN GULF POSITION PLOT

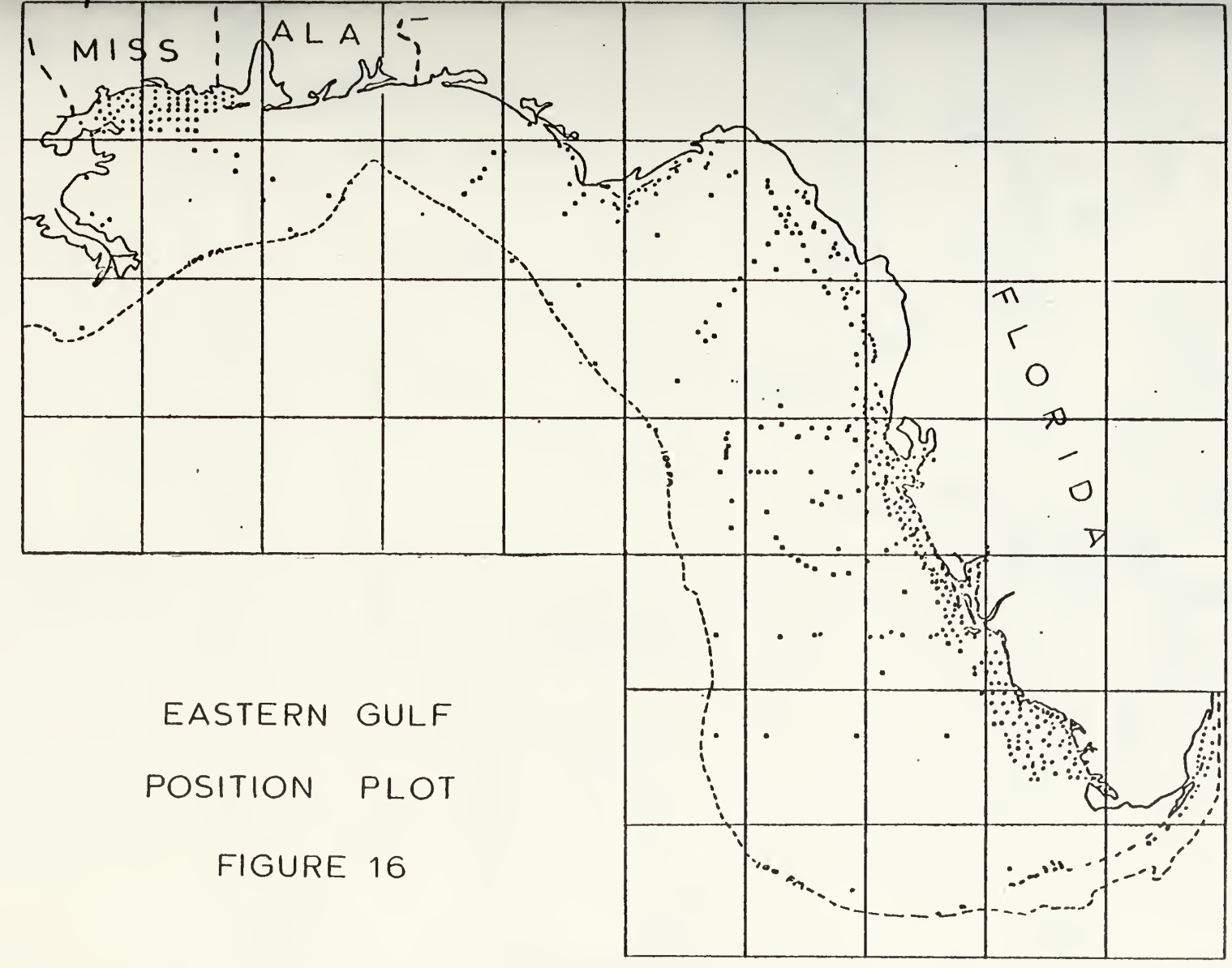


EASTERN GULF

POSITION PLOT

FIGURE 16

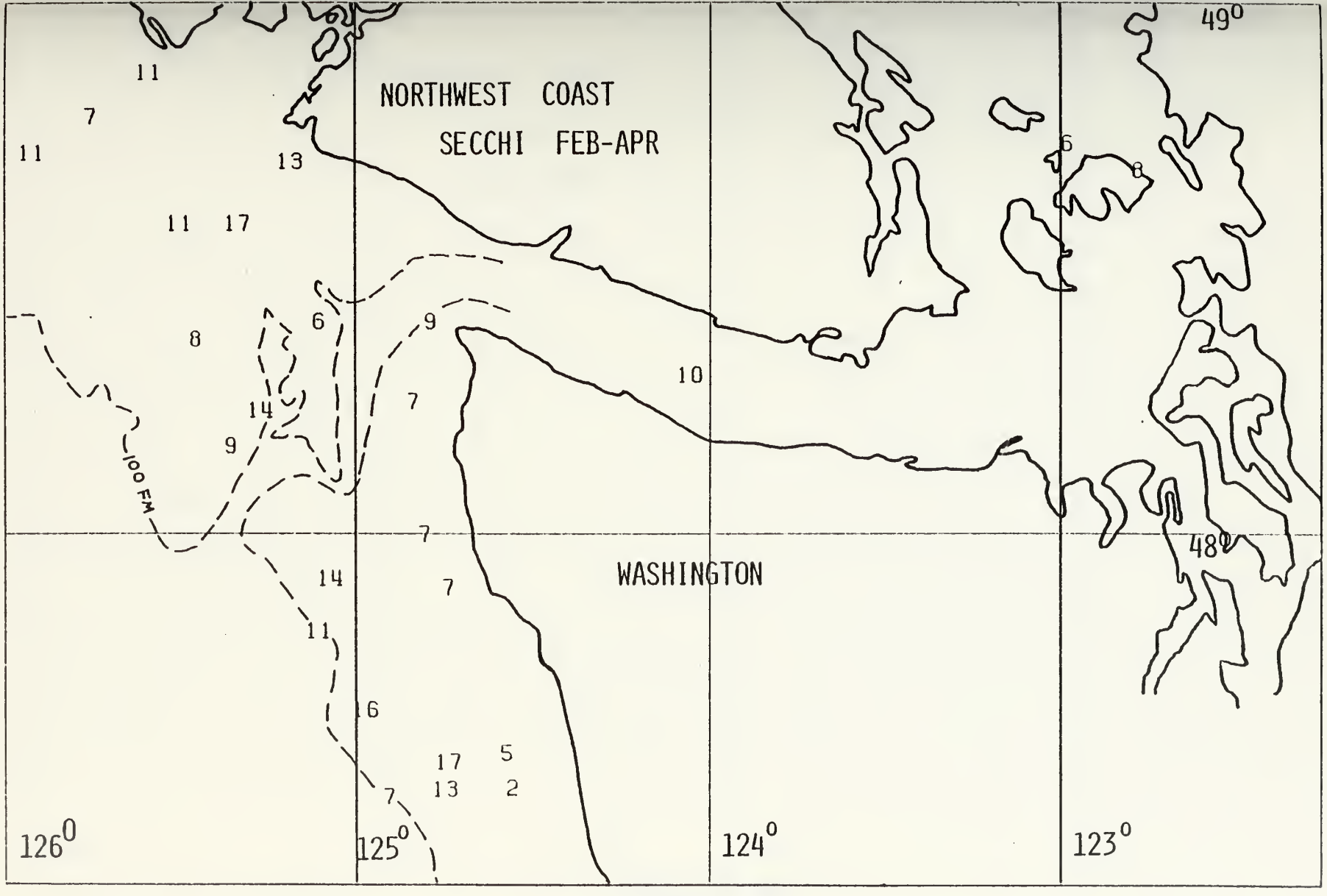
NORTHWEST COAST
SECCHI FEB-APR
WASHINGTON
100 FM
49°
48°
126°
125°
124°
123°
11
7
11
13
11
17
8
6
9
14
9
7
10
7
14
7
11
16
17
5
13
2
7
6
8

FIGURE 17

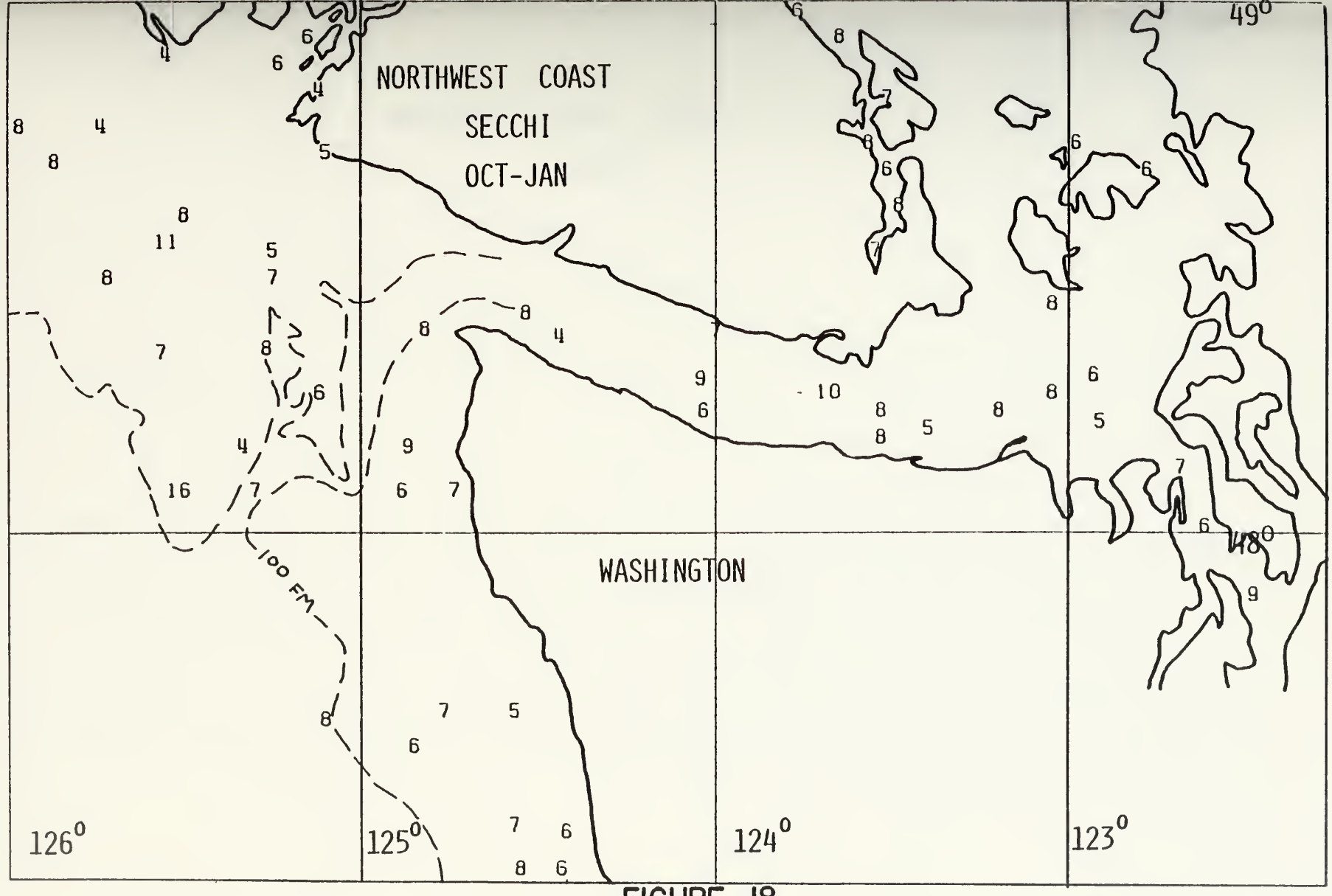
NORTHWEST COAST
SECCHI
OCT-JAN
WASHINGTON
100 FM
49°
48°
126°
125°
124°
123°

FIGURE 18

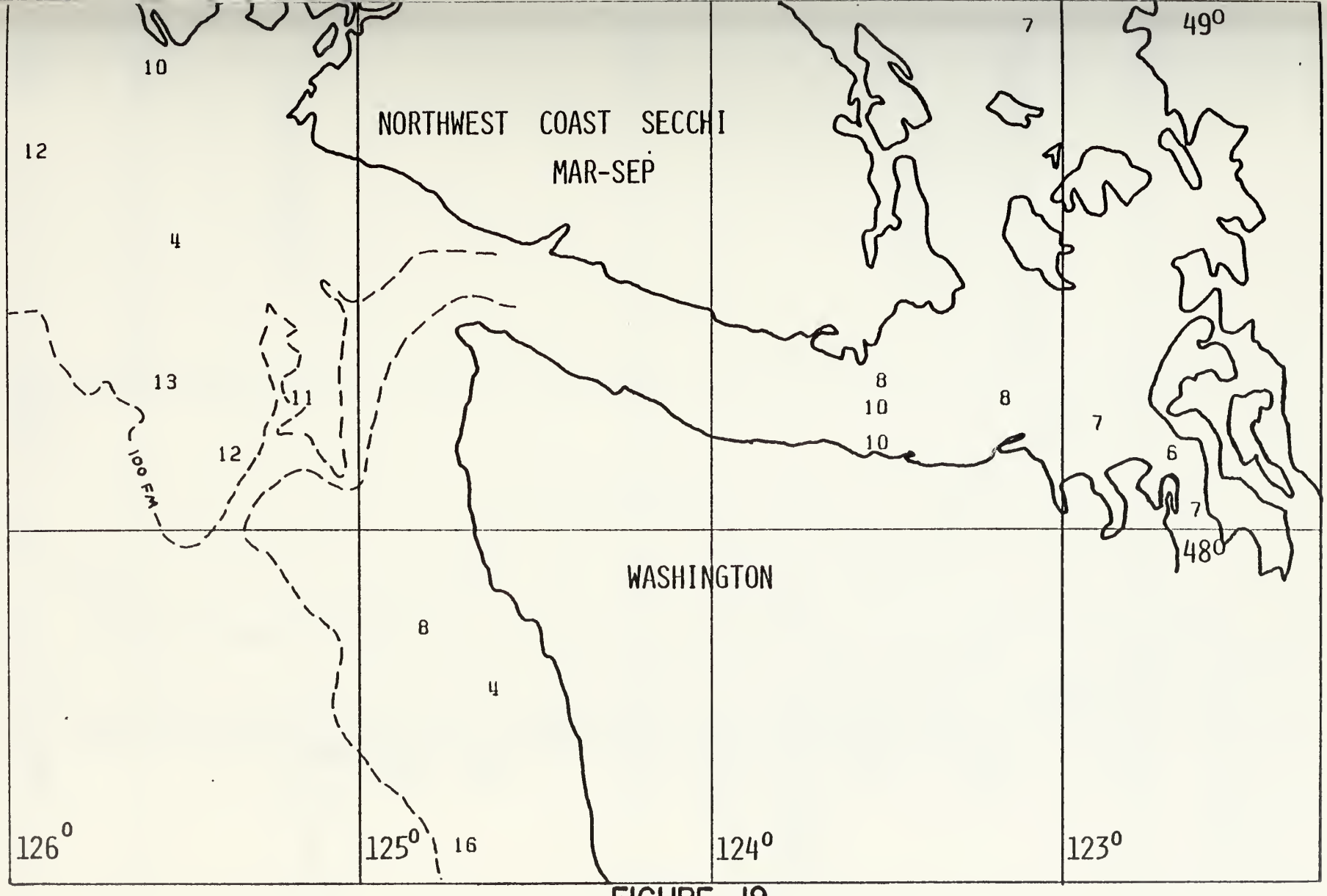
NORTHWEST COAST SECCHI
MAR-SEP
WASHINGTON
100 FM
10
12
4
13
11
12
8
10
10
8
7
6
7
7
8
4
16
49°
48°
126°
125°
124°
123°

FIGURE 19

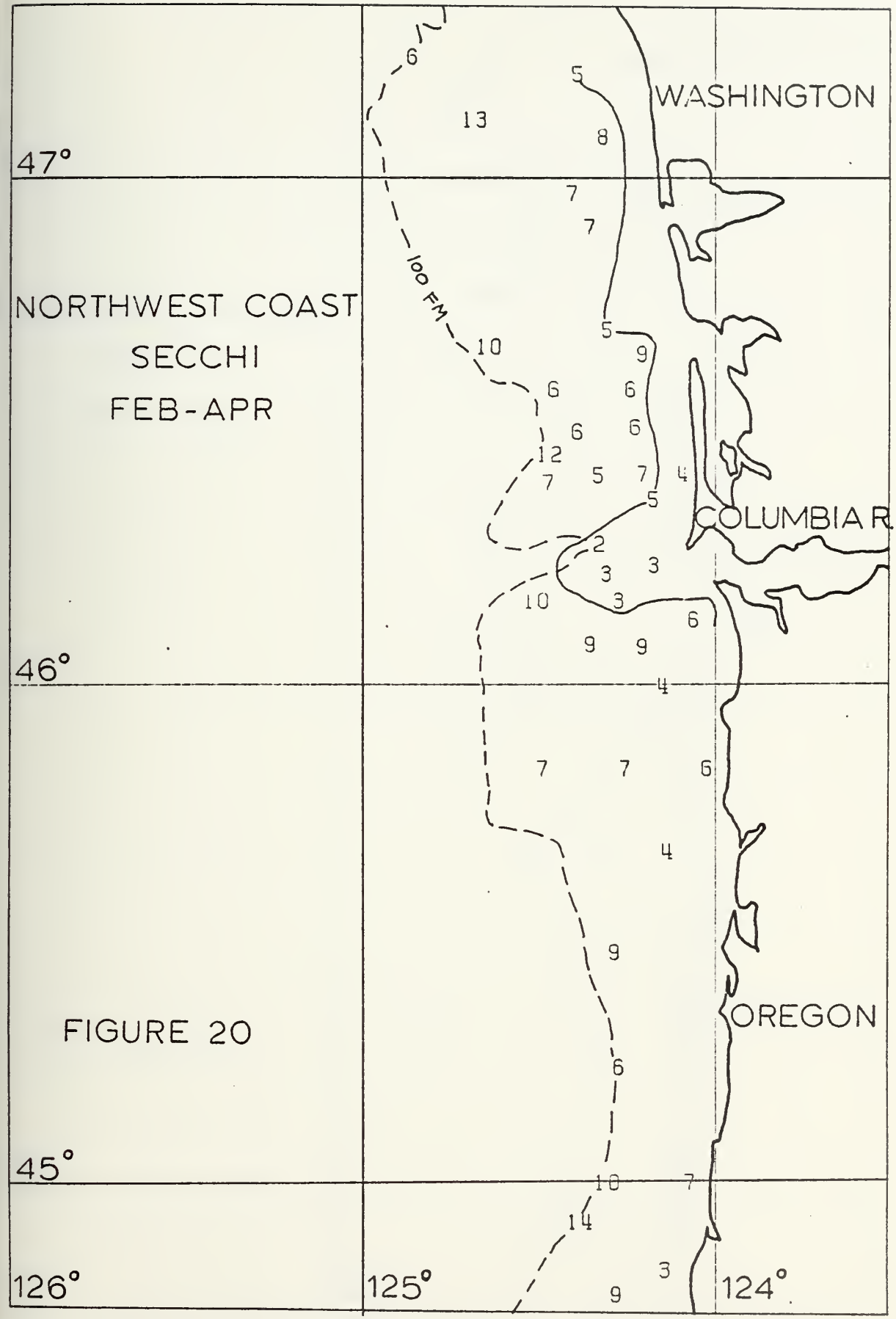
NORTHWEST COAST
SECCHI
FEB-APR
47°
46°
45°
126°
125°
124°
WASHINGTON
OREGON
COLUMBIA R.
100 FM
6
5
13
8
7
7
5
10
9
6
6
6
6
12
7
5
7
4
5
2
3
3
10
3
6
9
9
4
7
7
6
4
9
6
10
7
14
3
9

FIGURE 20

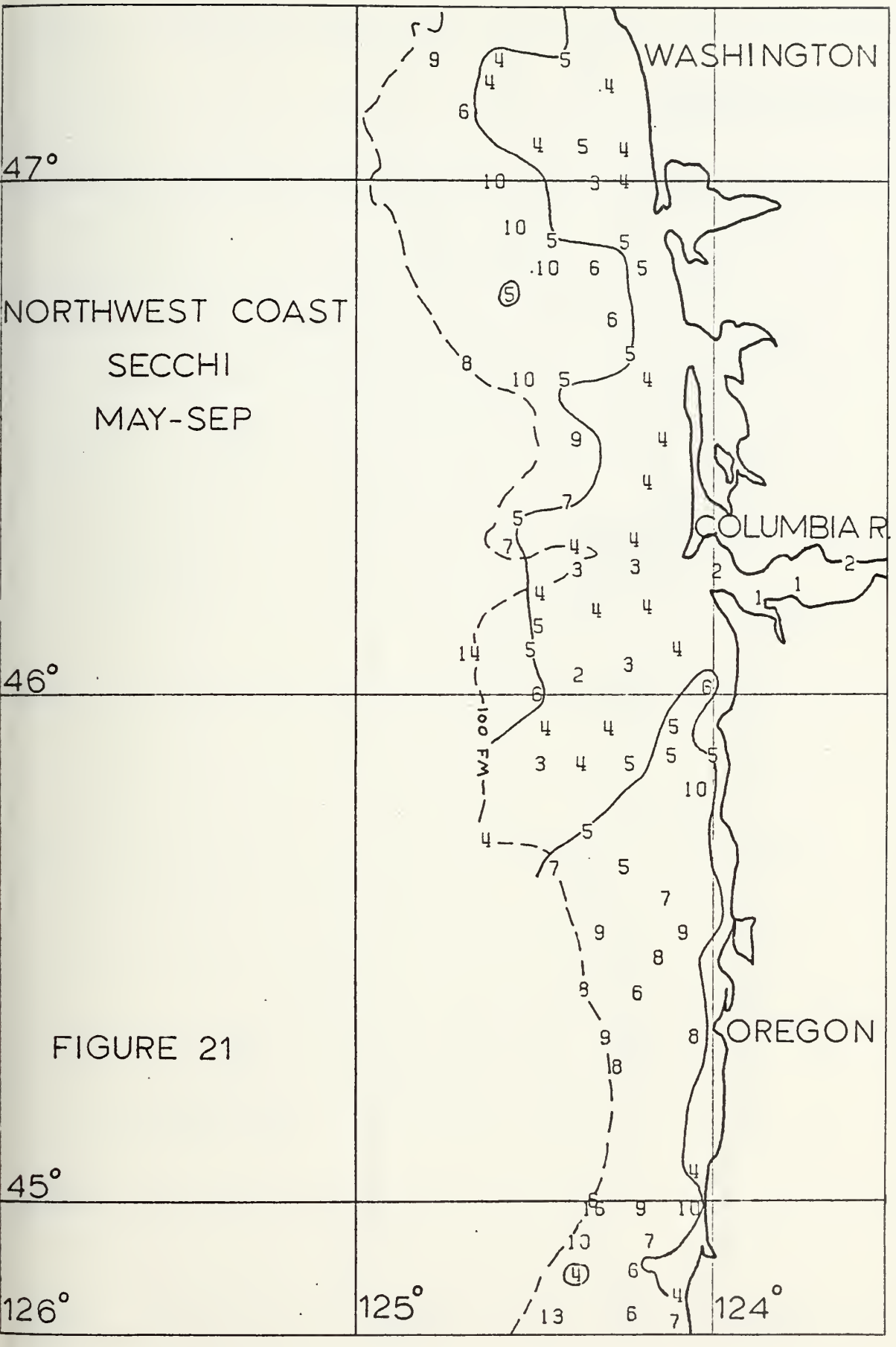
NORTHWEST COAST
SECCHI
MAY-SEP
WASHINGTON
COLUMBIA R.
OREGON
100 FM
47°
46°
45°
126°
125°
124°

FIGURE 21

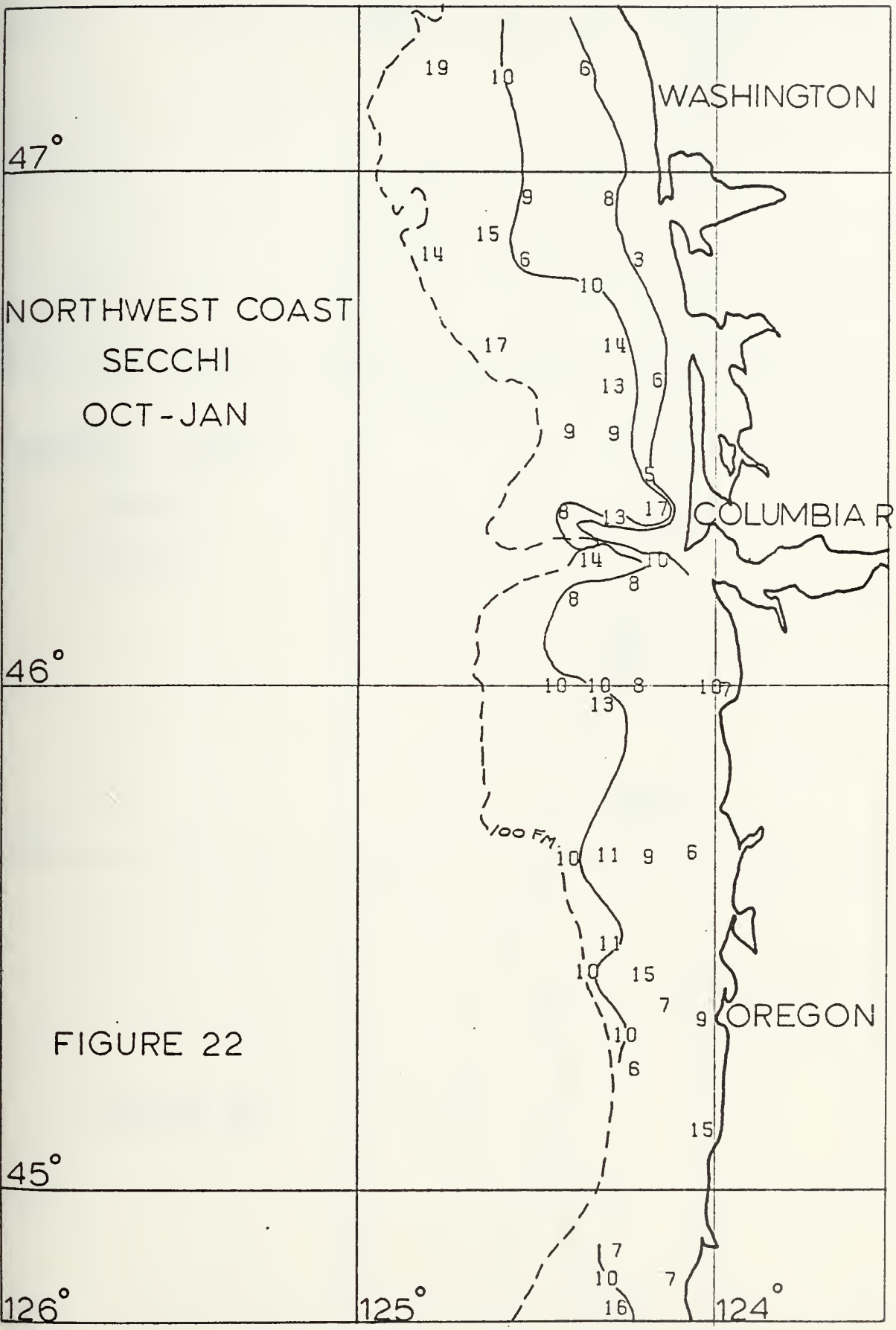
NORTHWEST COAST
SECCHI
OCT-JAN
WASHINGTON
COLUMBIA R
OREGON
100 FM
47°
46°
45°
126°
125°
124°
19
10
6
9
8
15
14
6
3
10
17
14
13
6
9
9
5
8
13
17
14
10
8
8
10
10
8
10
7
13
10
11
9
6
11
10
15
7
9
10
6
15
7
10
7
16

FIGURE 22

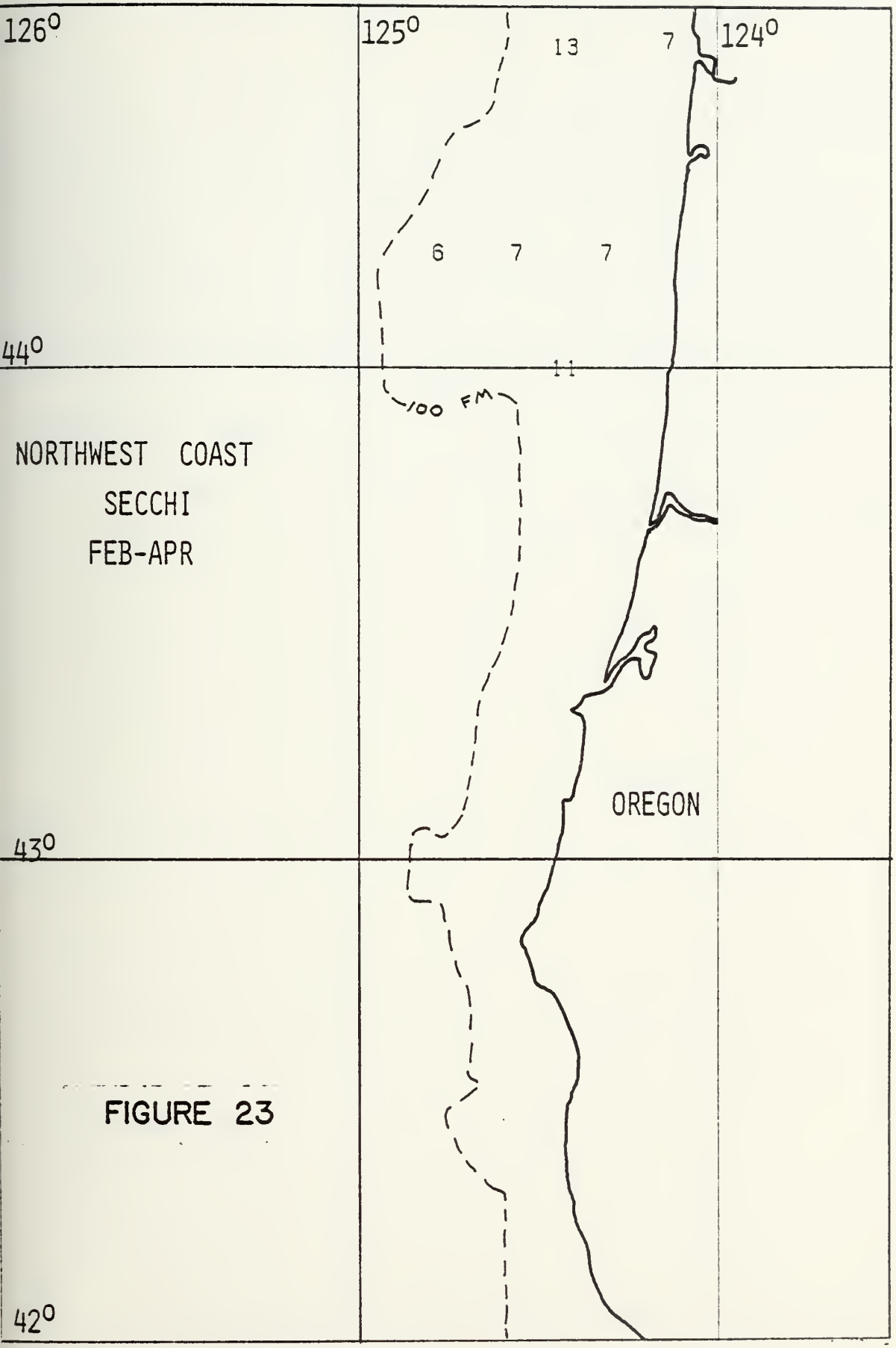
126°
125°
124°
44°
43°
42°
13
7
6
7
7
11
100 FM
NORTHWEST COAST
SECCHI
FEB-APR
OREGON

FIGURE 23

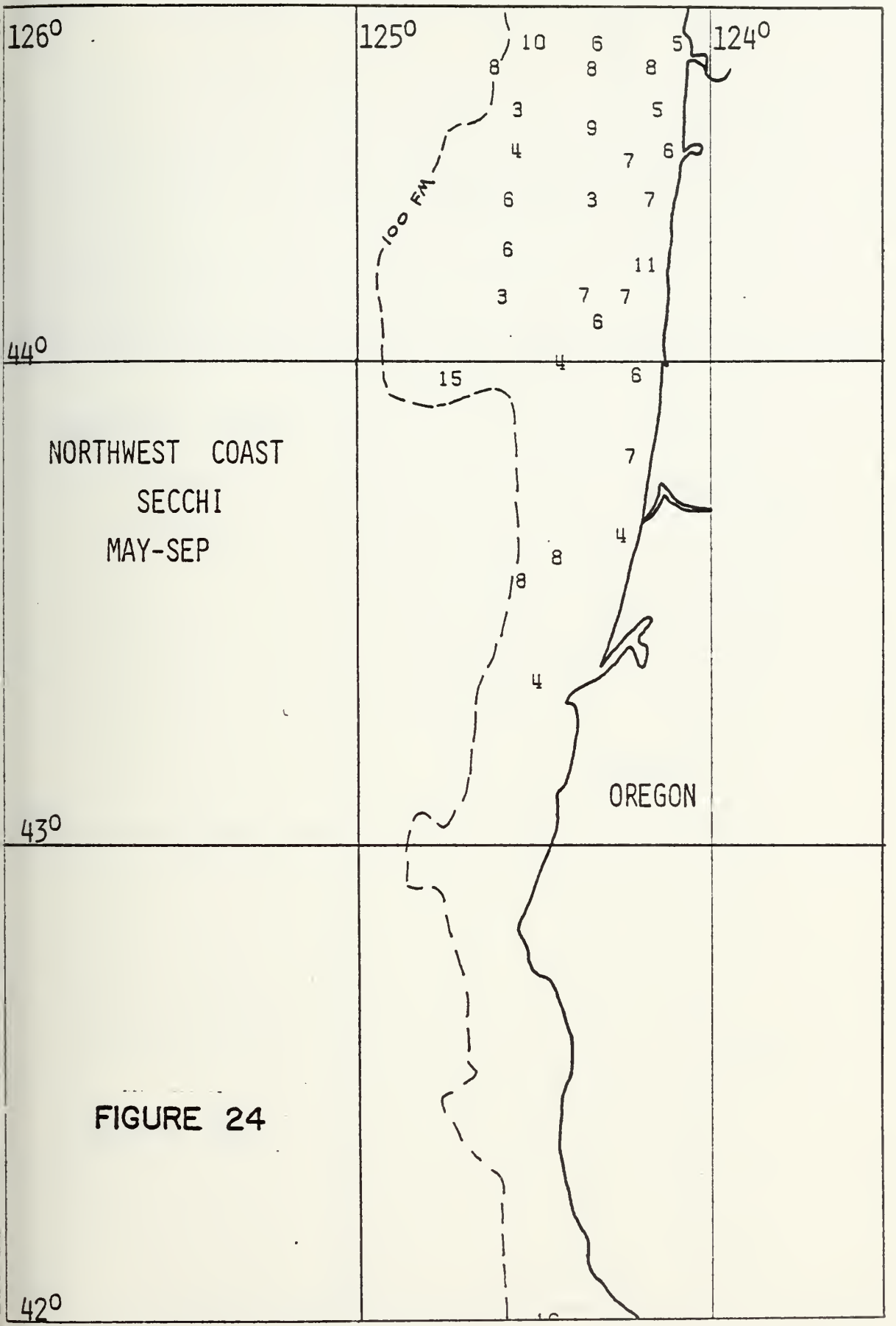
126°
125°
124°
44°
43°
42°
100 FM
NORTHWEST COAST
SECCHI
MAY-SEP
OREGON

FIGURE 24

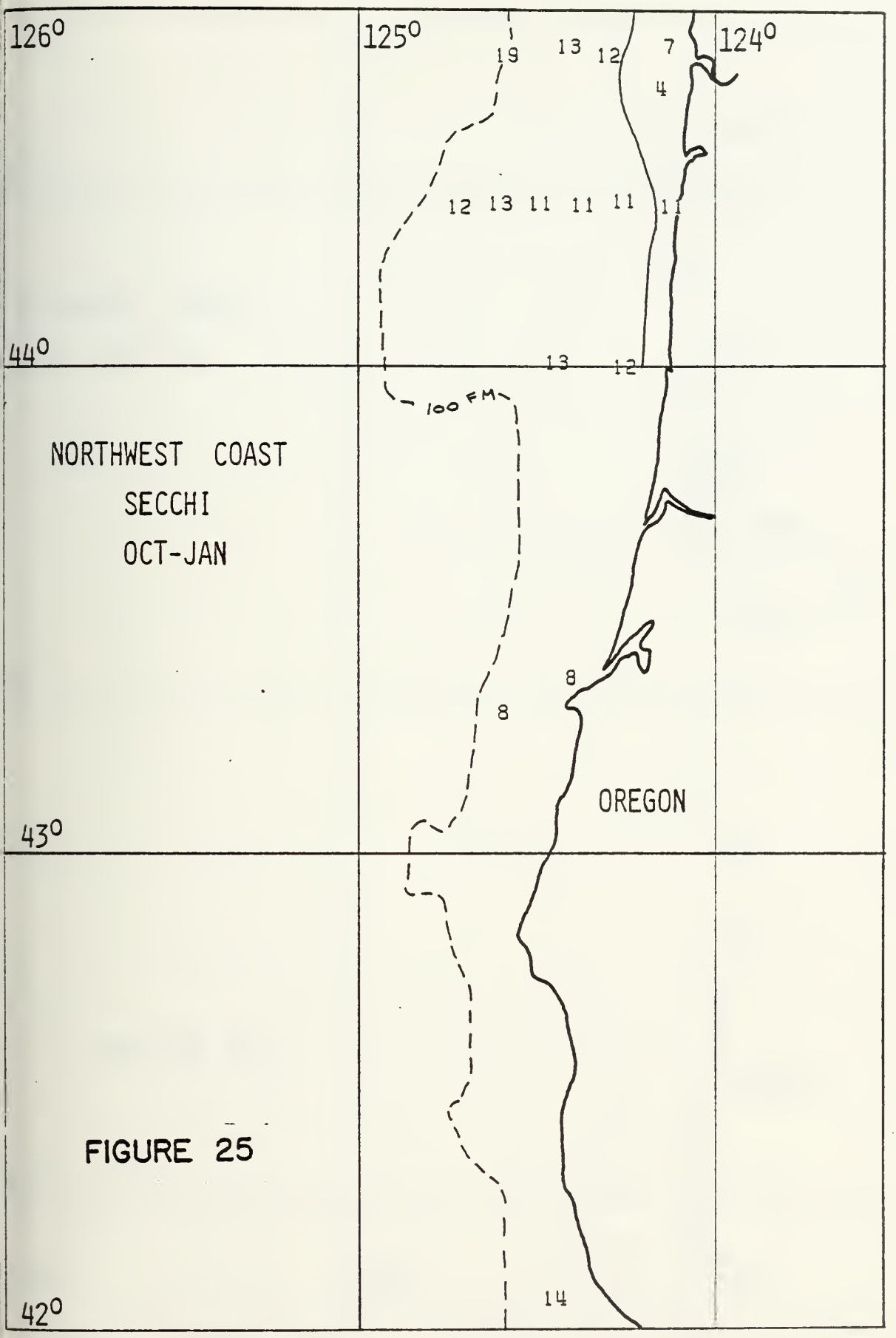
126°
125°
124°
44°
43°
42°
19
13
12
7
4
12
13
11
11
11
11
13
12
100 FM
8
8
OREGON
14
NORTHWEST COAST
SECCHI
OCT-JAN

FIGURE 25

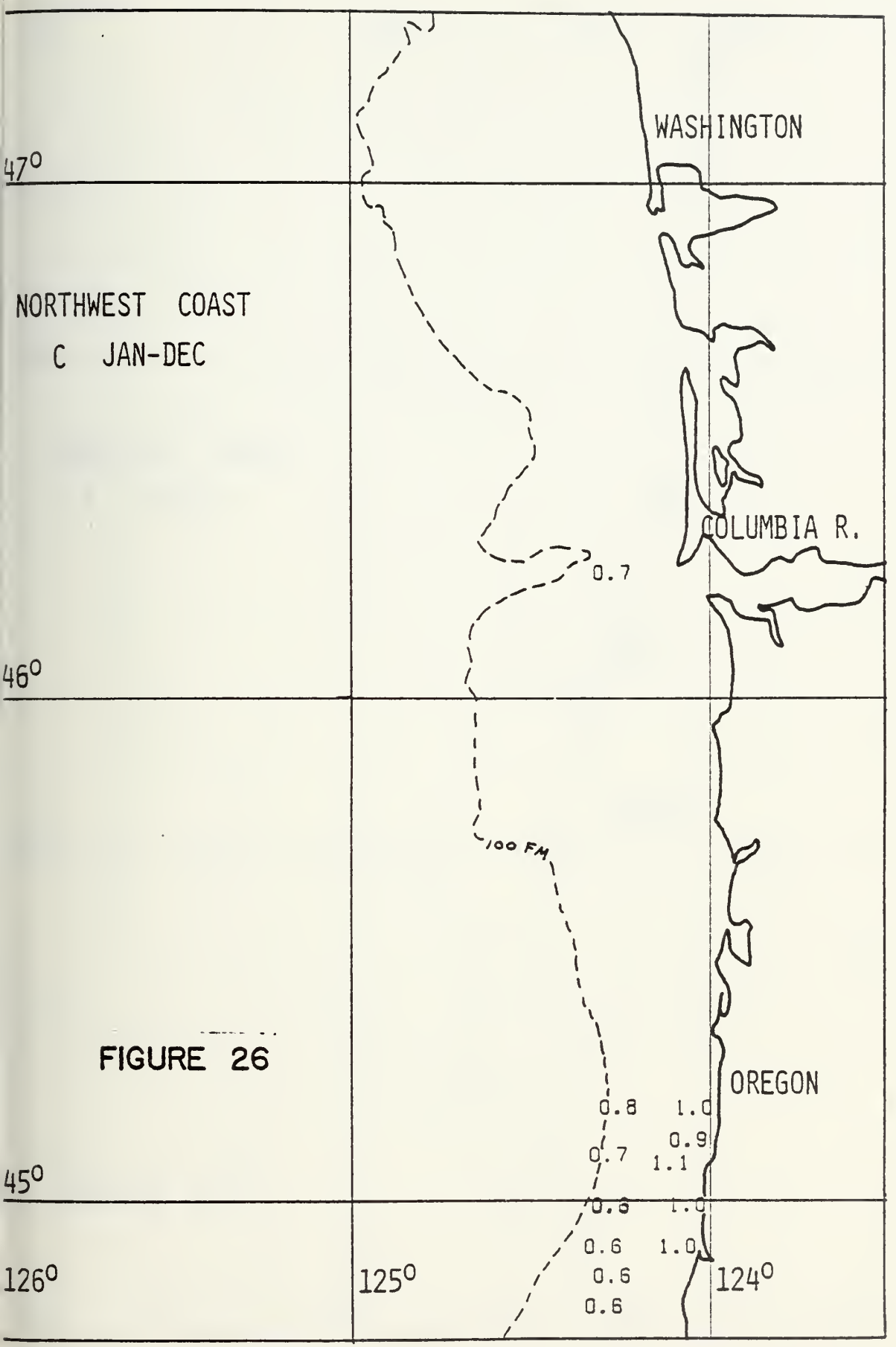
NORTHWEST COAST
C JAN-DEC
WASHINGTON
COLUMBIA R.
OREGON
47°
46°
45°
126°
125°
124°
0.7
100 FM
0.8
1.0
0.9
0.7
1.1
0.6
1.0
0.6
1.0
0.6
0.6

FIGURE 26

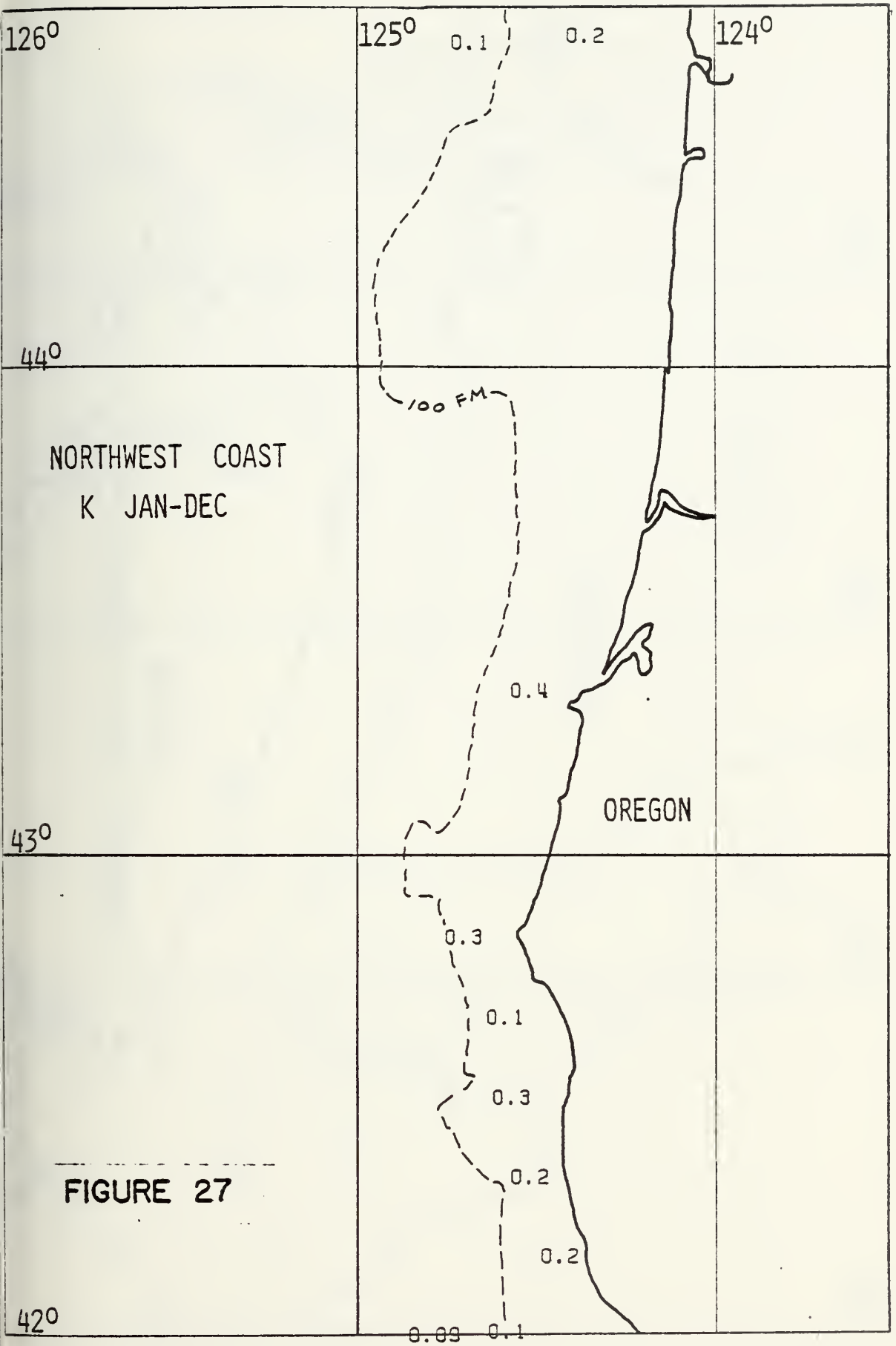
126°
125°
124°
44°
43°
42°
0.1
0.2
100 FM
NORTHWEST COAST
K JAN-DEC
0.4
OREGON
0.3
0.1
0.3
0.2
0.2
0.09
0.1

FIGURE 27

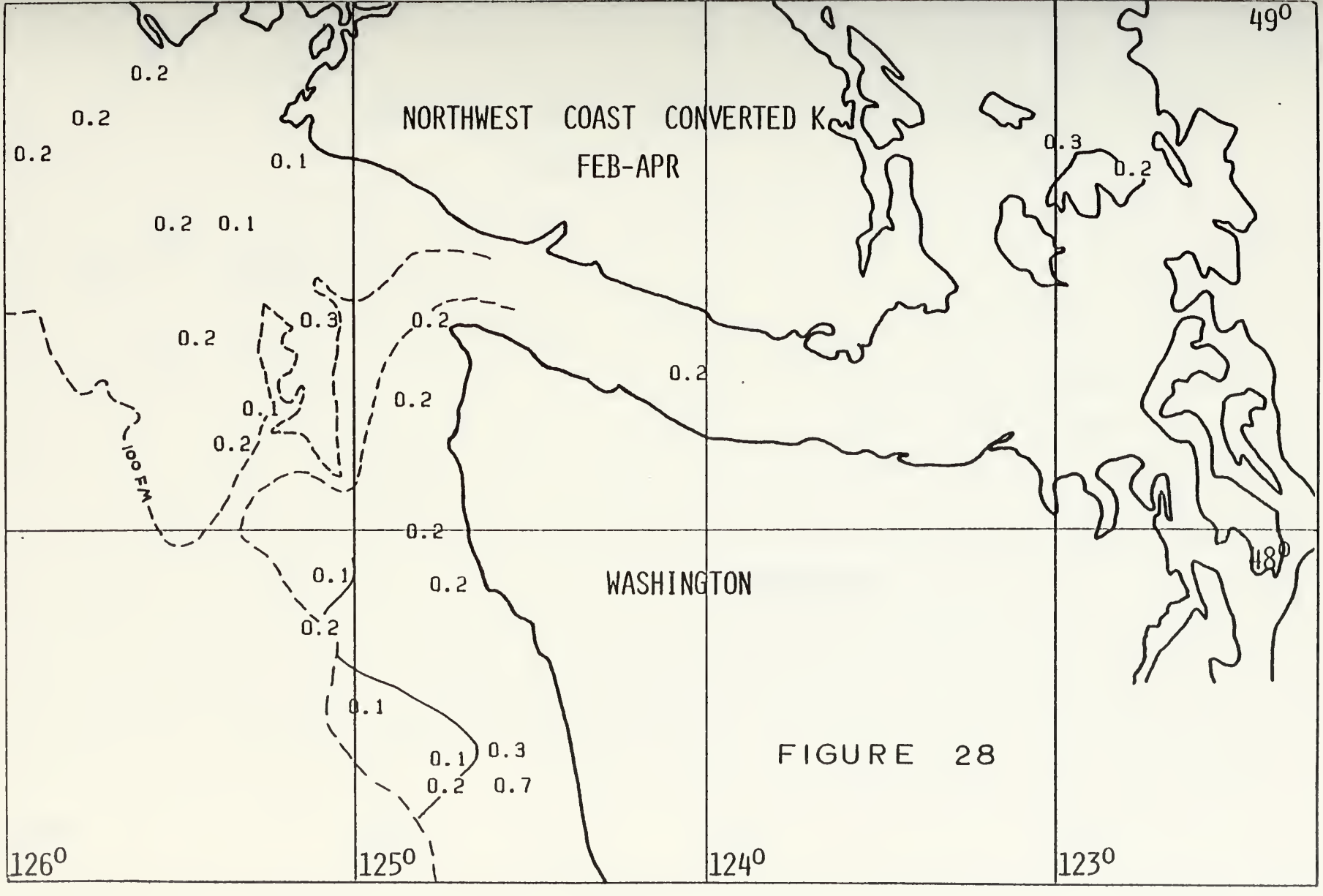
NORTHWEST COAST CONVERTED K
FEB-APR
WASHINGTON
100 FM
0.2
0.2
0.2
0.1
0.2
0.1
0.3
0.2
0.2
0.2
0.2
0.2
0.2
0.1
0.2
0.2
0.1
0.1
0.3
0.2
0.7
0.3
0.2
49°
48°
126°
125°
124°
123°

FIGURE 28

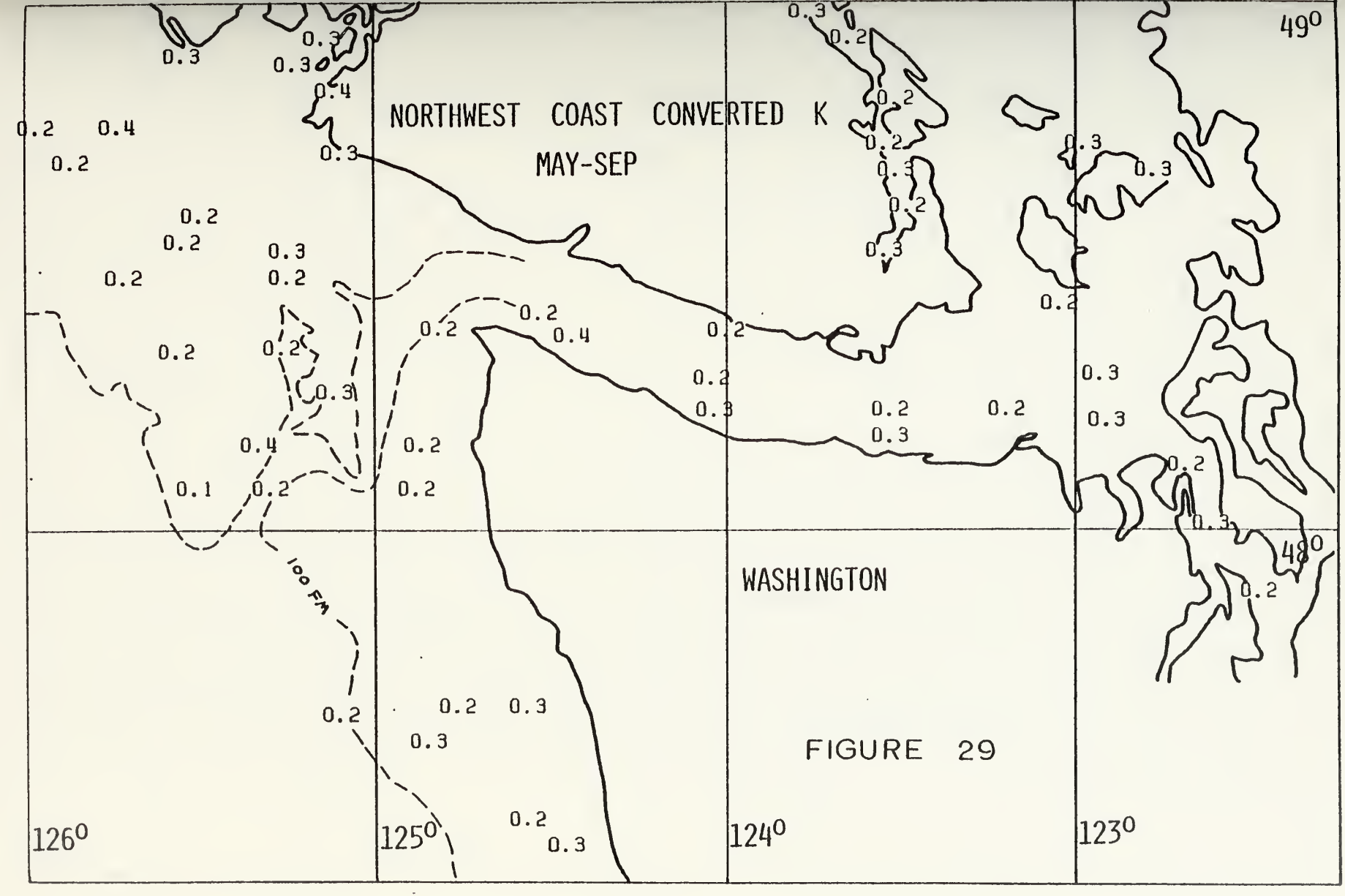
NORTHWEST COAST CONVERTED K
MAY-SEP
WASHINGTON
100 FM
49°
48°
126°
125°
124°
123°

FIGURE 29

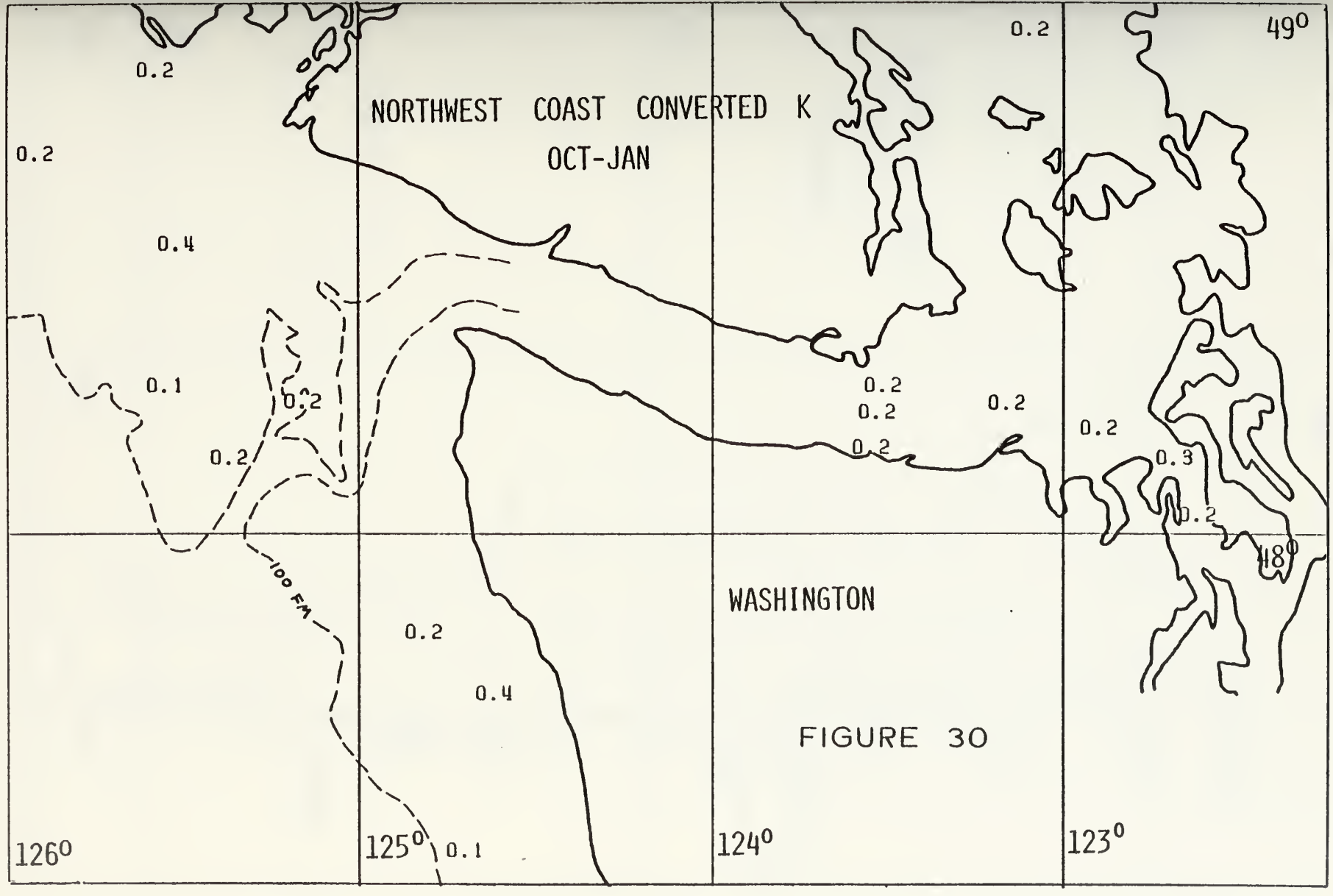
NORTHWEST COAST CONVERTED K
OCT-JAN
0.2
0.2
0.4
0.1
0.2
0.2
0.2
0.2
0.2
0.2
0.2
0.3
0.2
0.2
0.4
0.1
100 FM
WASHINGTON
49°
48°
126°
125°
124°
123°

FIGURE 30

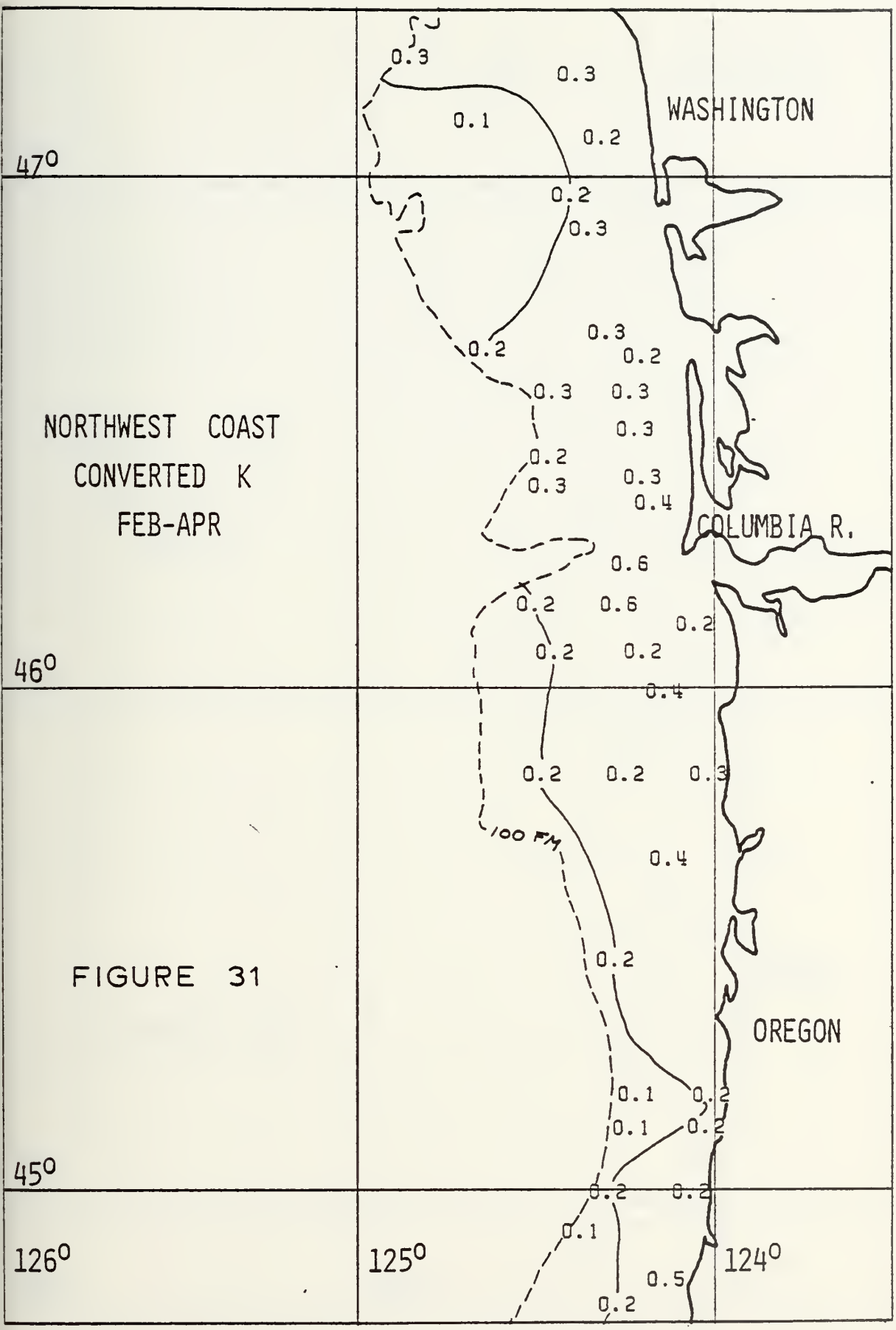
NORTHWEST COAST
CONVERTED K
FEB-APR
WASHINGTON
COLUMBIA R.
OREGON
100 FM
47°
46°
45°
126°
125°
124°
0.3
0.1
0.2
0.4
0.5
0.6

FIGURE 31

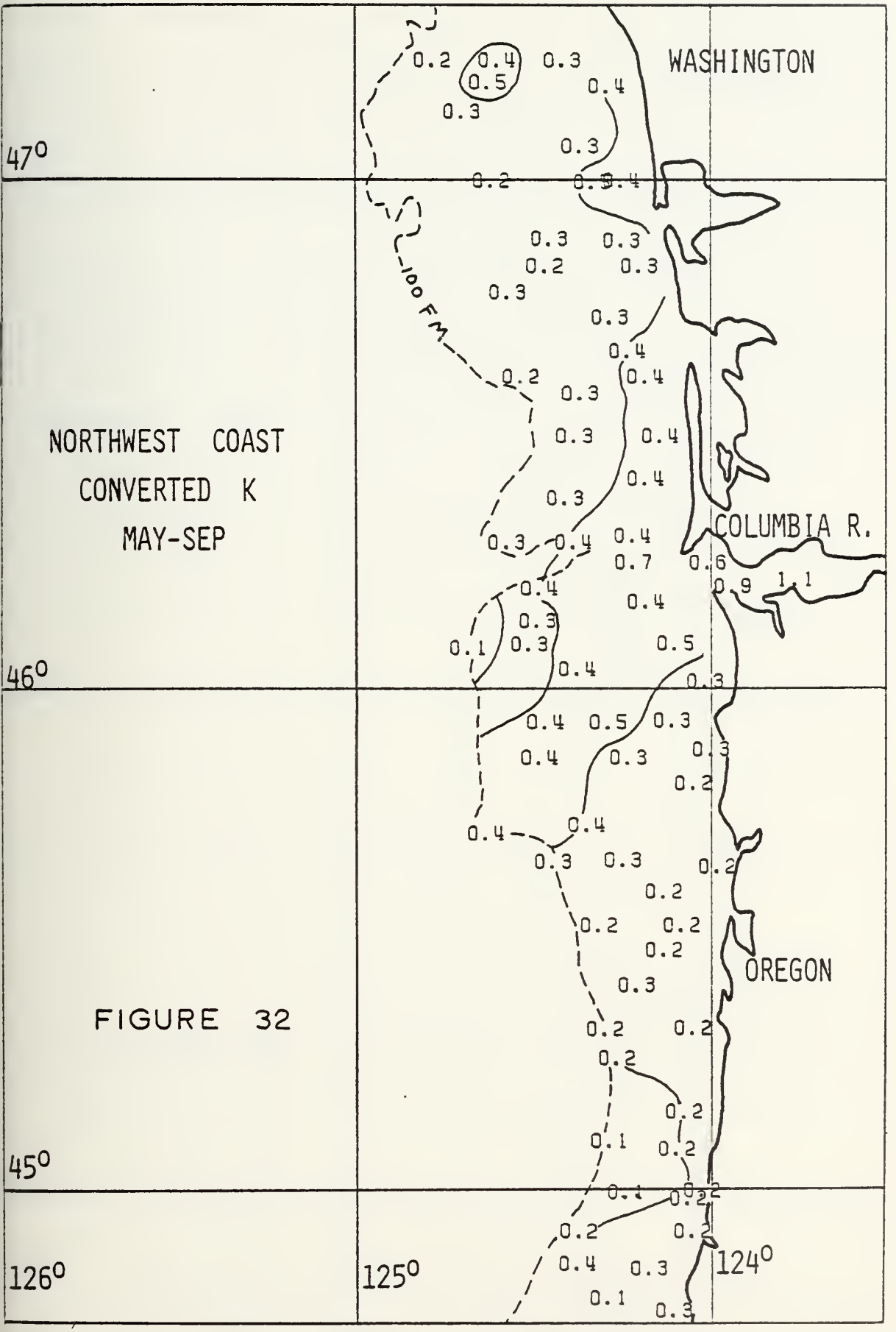
NORTHWEST COAST
CONVERTED K
MAY-SEP
WASHINGTON
COLUMBIA R.
OREGON
100 FM
47°
46°
45°
126°
125°
124°

FIGURE 32

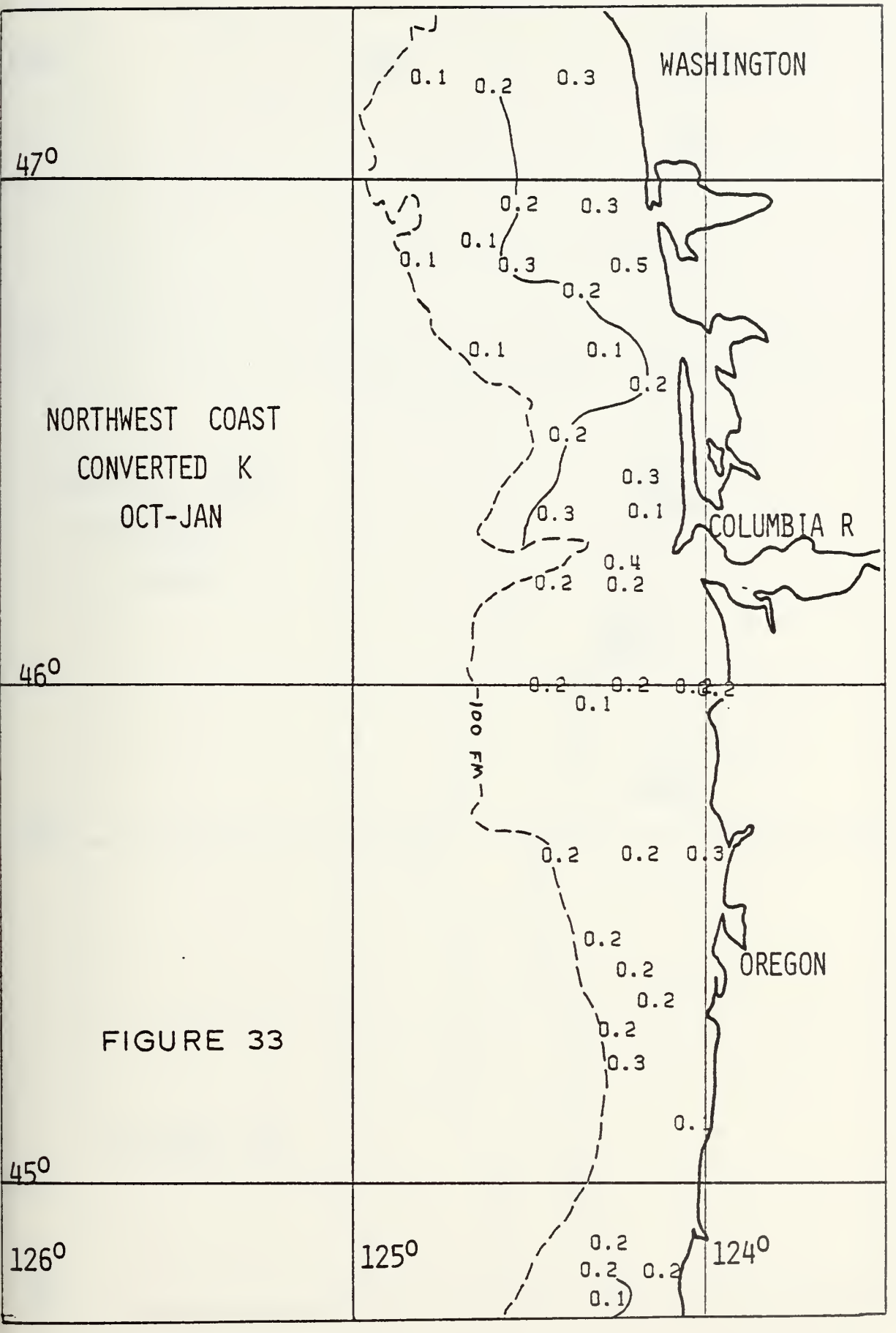
WASHINGTON
47°
NORTHWEST COAST
CONVERTED K
OCT-JAN
COLUMBIA R
46°
100 FM
OREGON
45°
126°
125°
124°

FIGURE 33

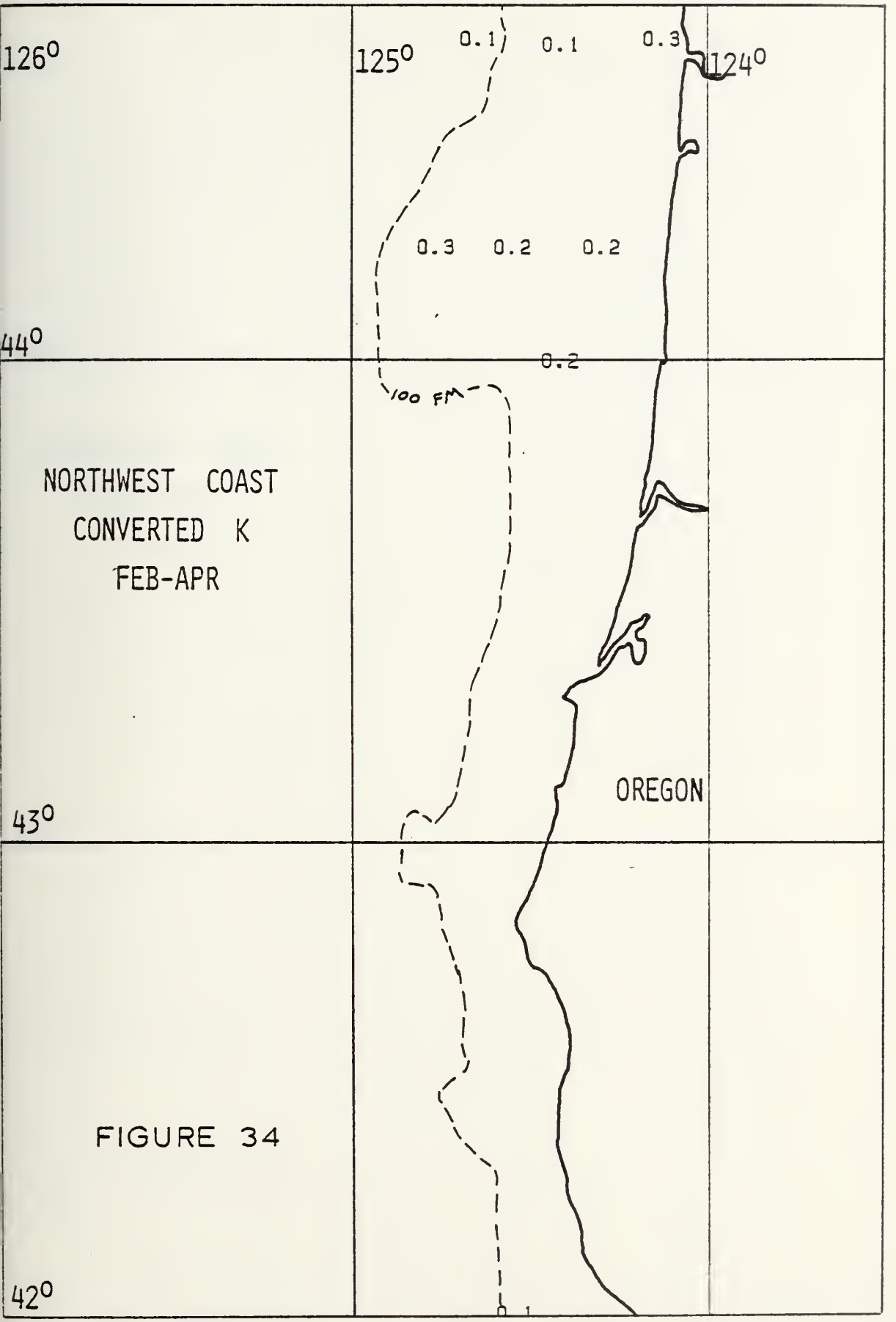
126°
125°
124°
44°
43°
42°
0.1
0.1
0.3
0.3
0.2
0.2
0.2
100 FM
NORTHWEST COAST
CONVERTED K
FEB-APR
OREGON

FIGURE 34

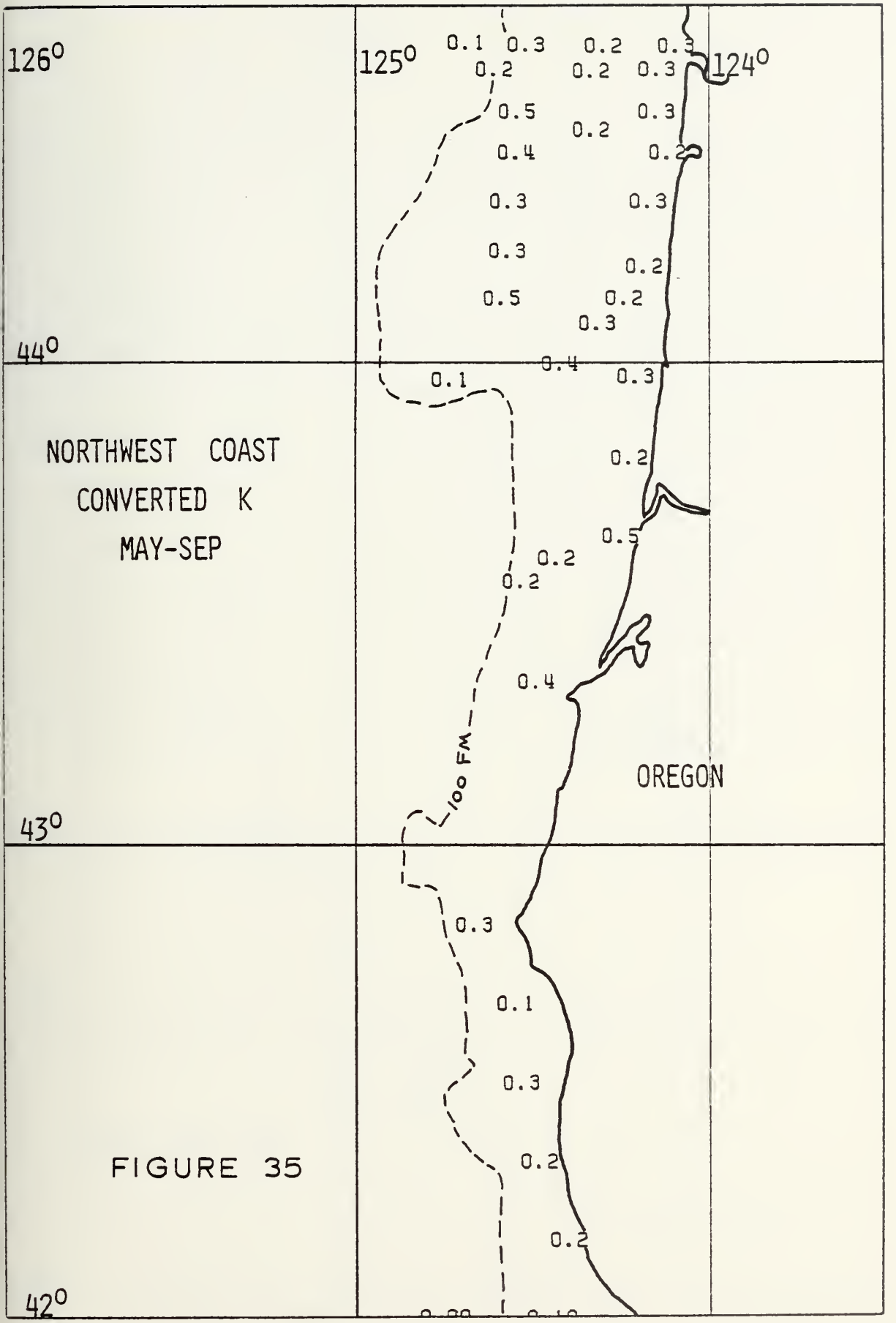
126°
125°
124°
44°
43°
42°
NORTHWEST COAST
CONVERTED K
MAY-SEP
100 FM
OREGON
0.1 0.3 0.2 0.3
0.2 0.2 0.3
0.5 0.3
0.2
0.4 0.2
0.3 0.3
0.3 0.2
0.5 0.2
0.3
0.4 0.3
0.1
0.2
0.5
0.2
0.2
0.4
0.3
0.1
0.3
0.2
0.2

FIGURE 35

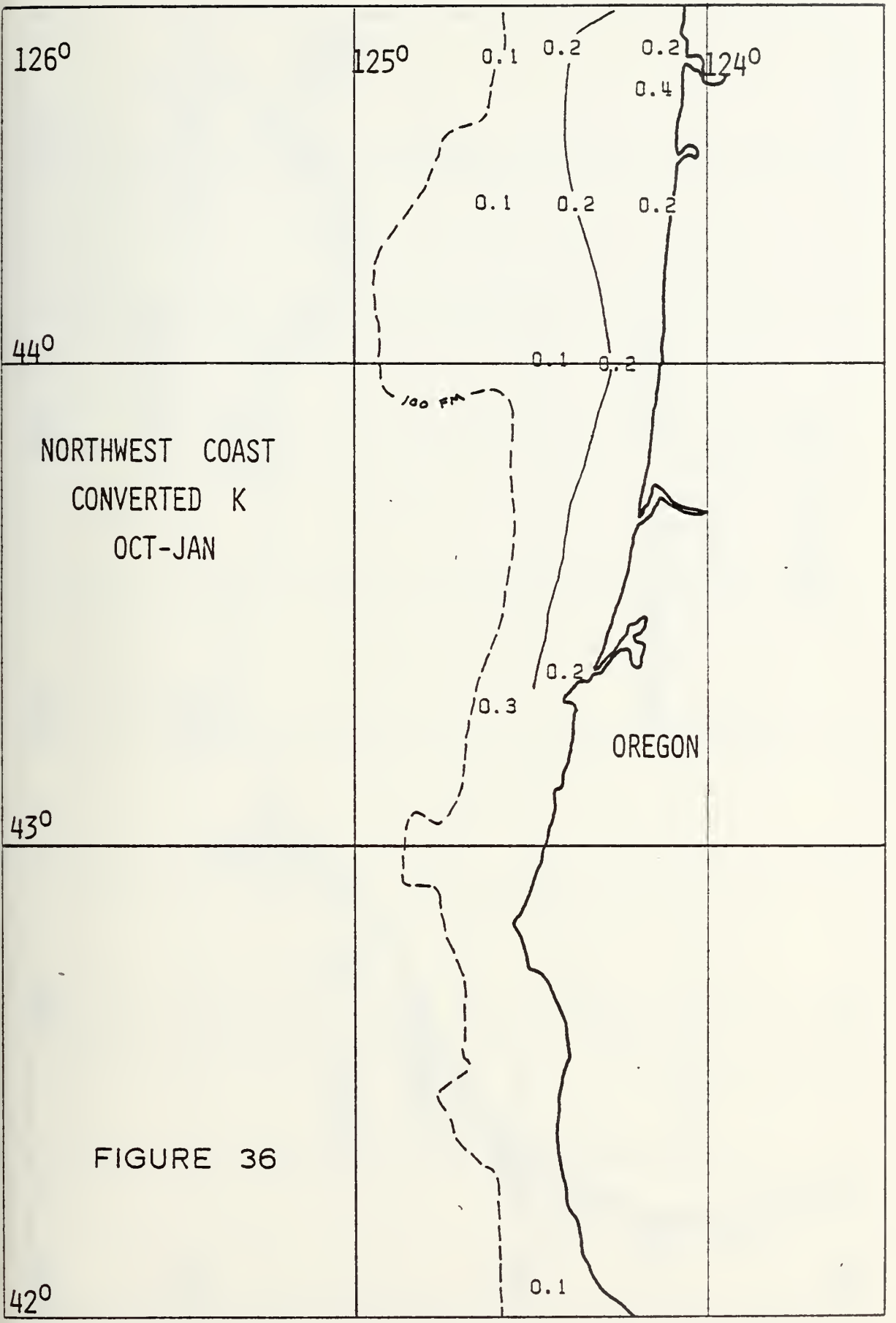
126°
125°
124°
44°
43°
42°
0.1
0.2
0.2
0.4
0.1
0.2
0.2
0.1
0.2
100 FM
NORTHWEST COAST
CONVERTED K
OCT-JAN
0.2
0.3
OREGON
0.1

FIGURE 36

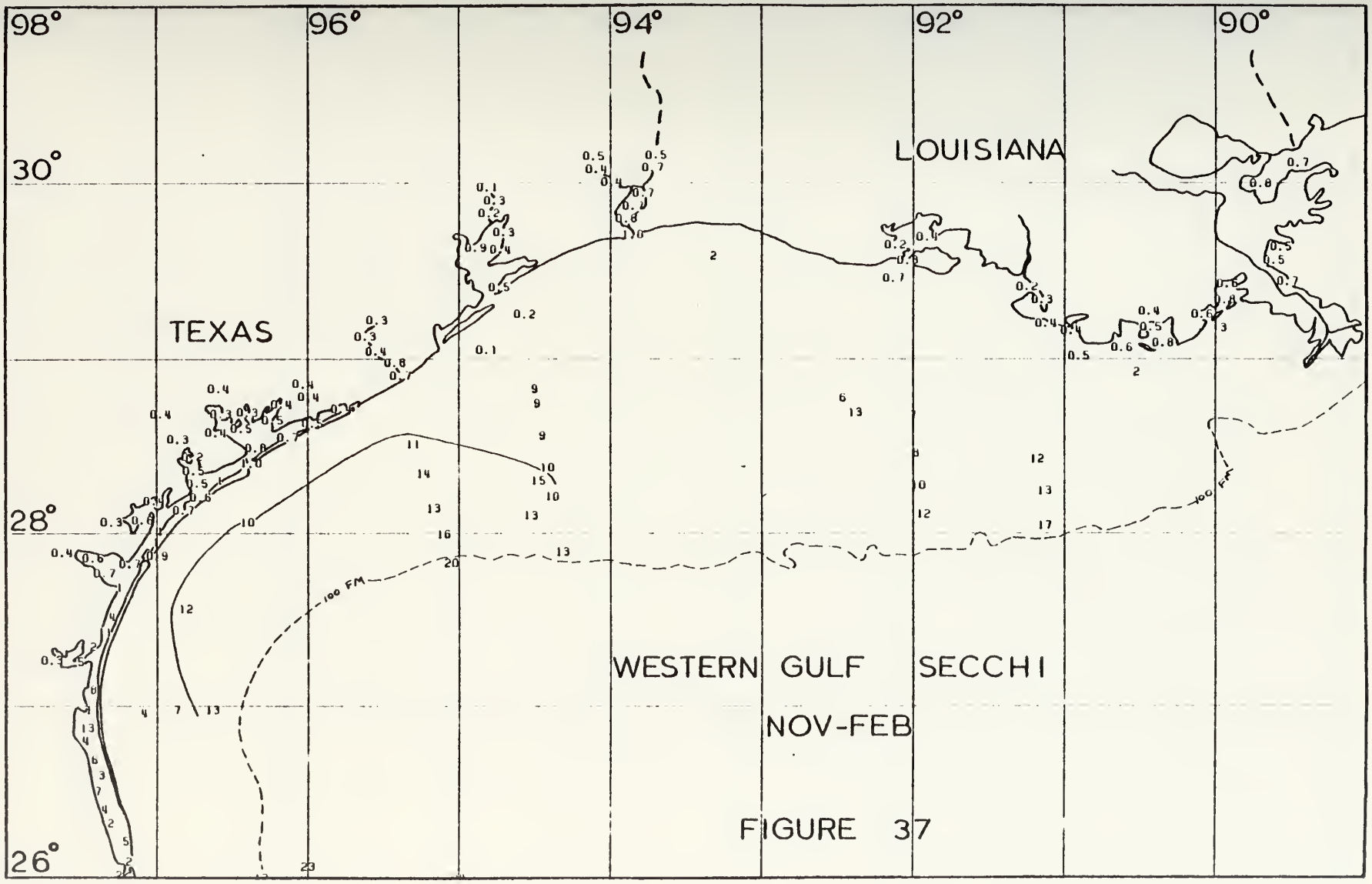


WESTERN GULF SECCHI

NOV-FEB

FIGURE 37

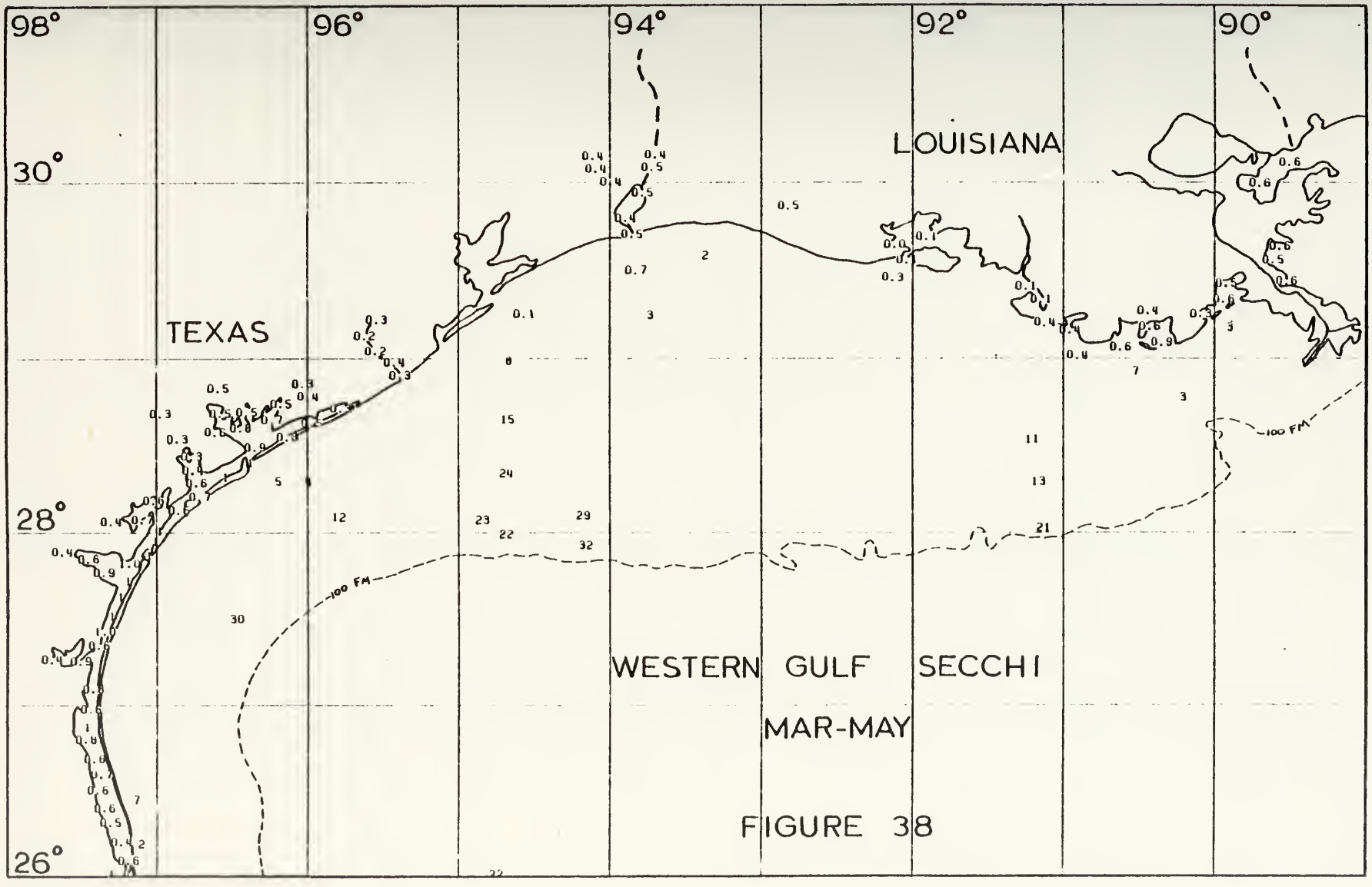
98°
96°
94°
92°
90°
30°
28°
26°
TEXAS
LOUISIANA
100 FM
100 FM
WESTERN GULF SECCHI
MAR-MAY

FIGURE 38

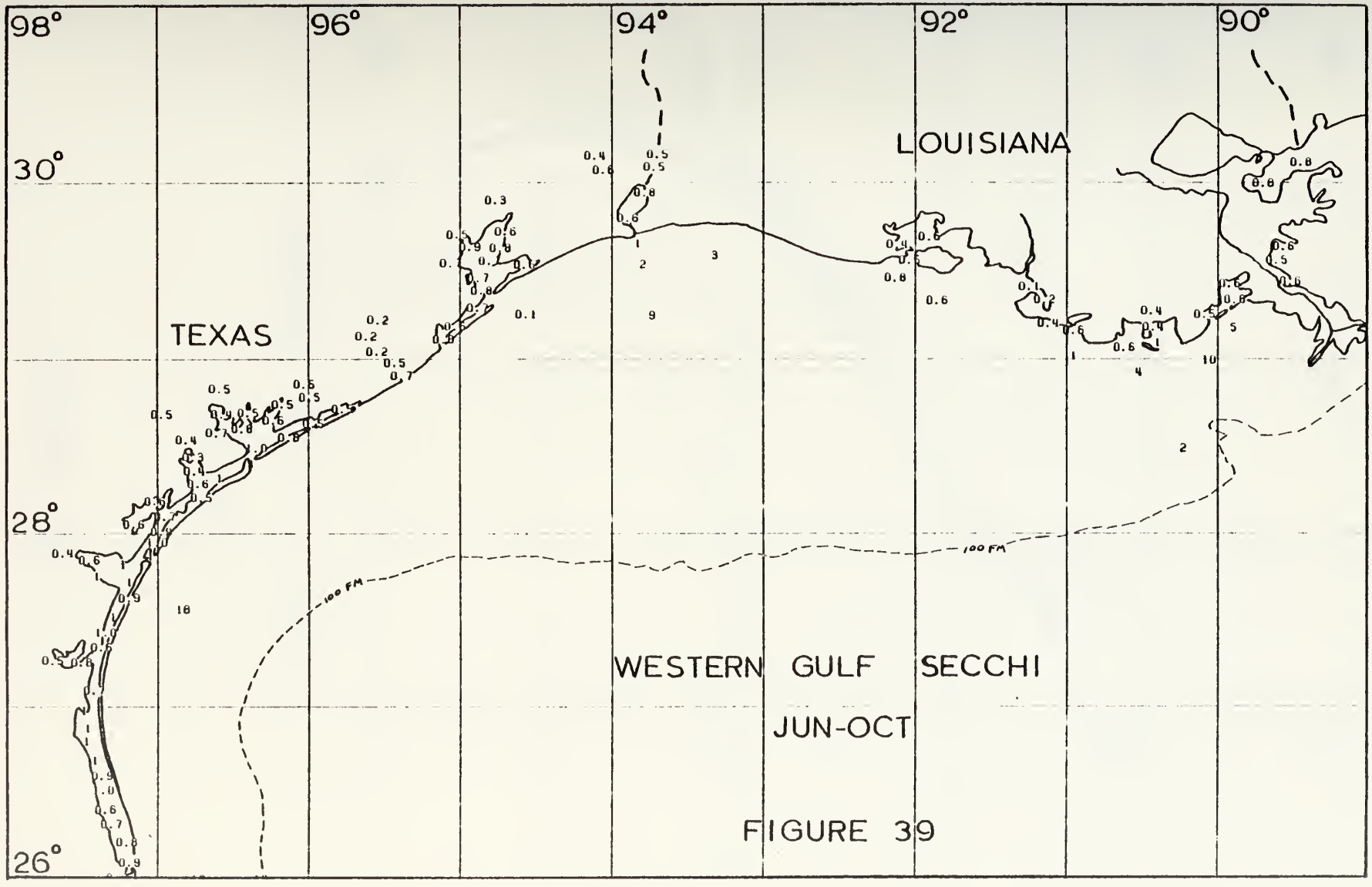


WESTERN GULF SECCHI

JUN-OCT

FIGURE 39

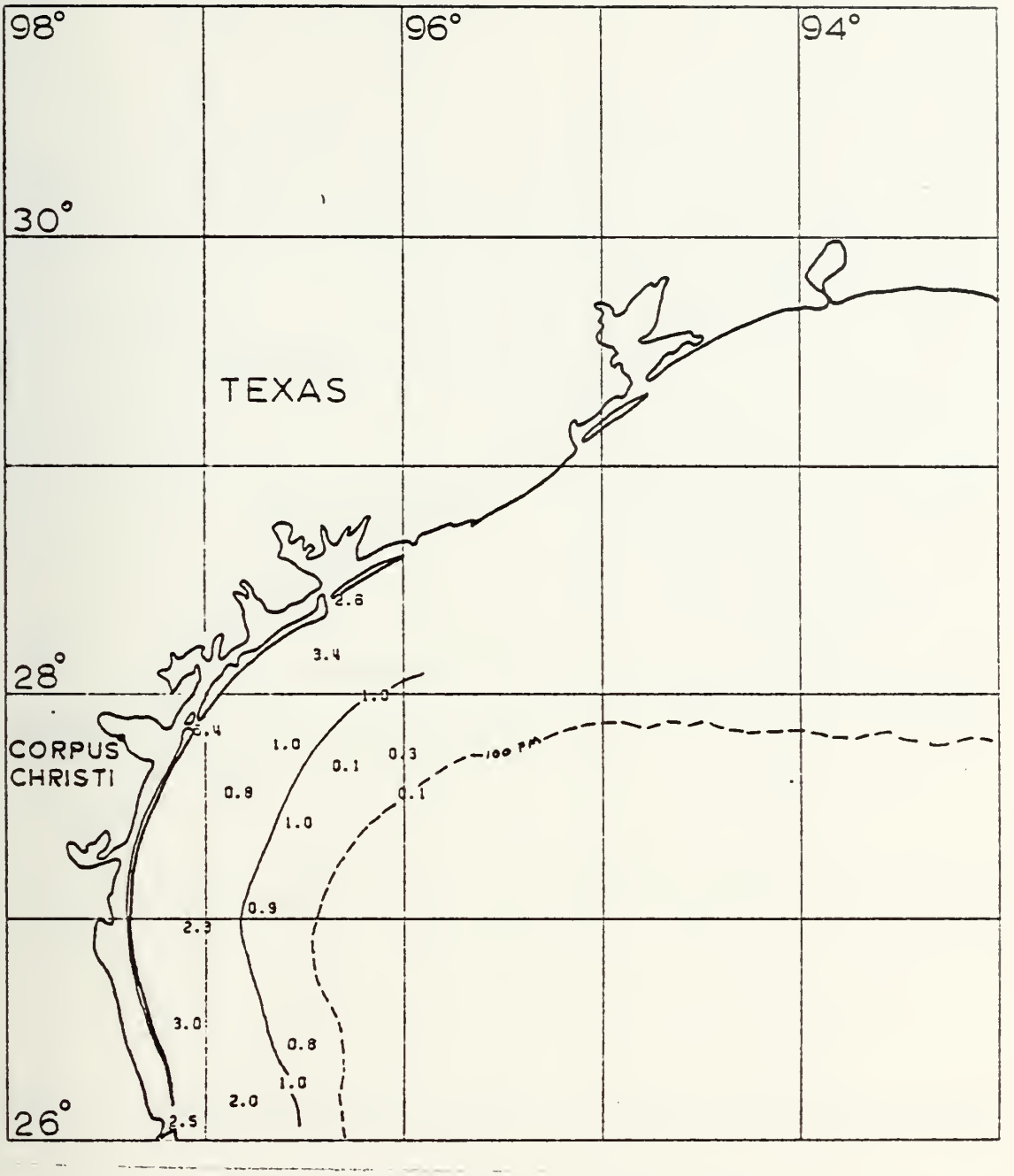


WESTERN GULF C-DATA

NOV-FEB

FIGURE 40

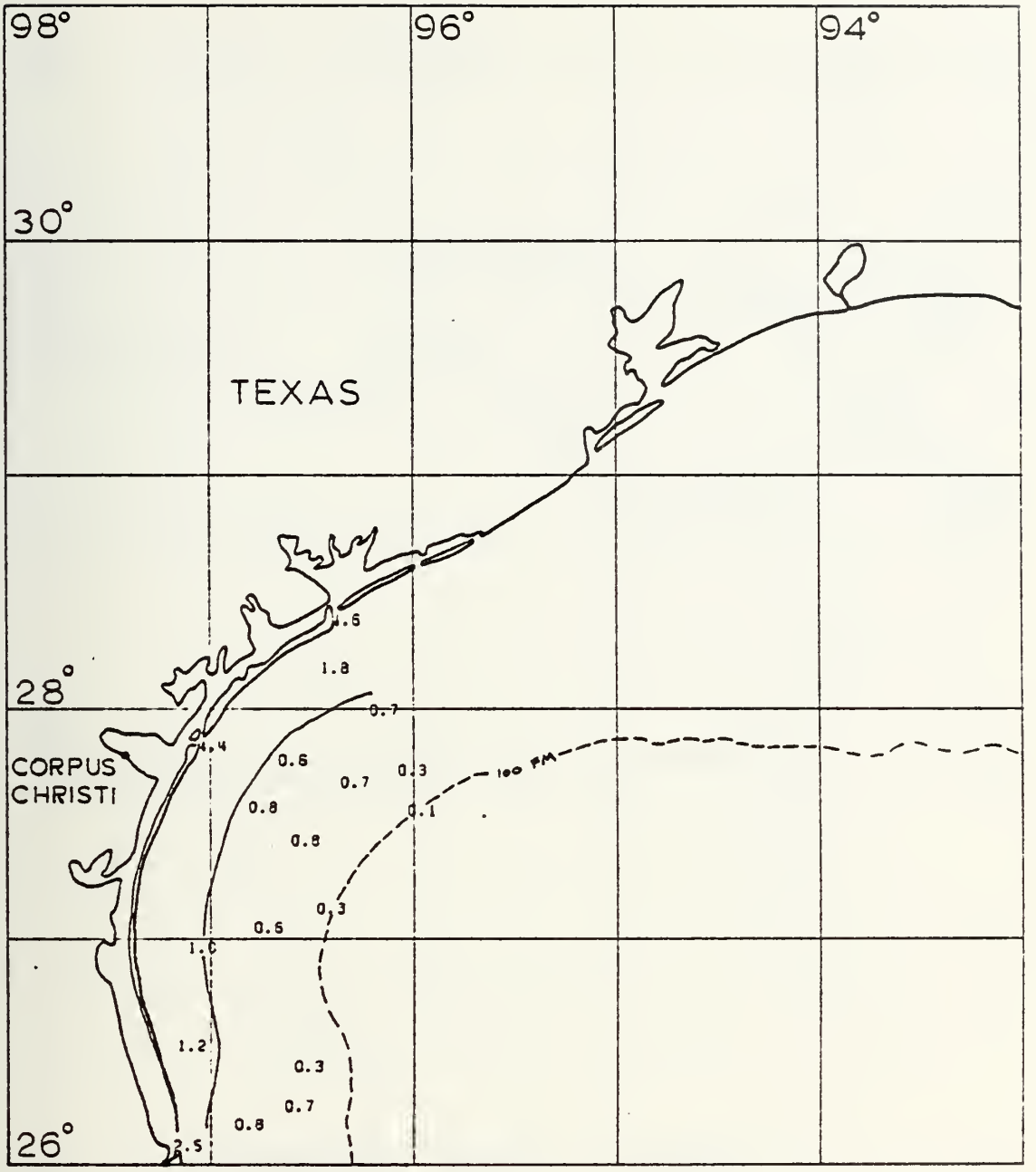


WESTERN GULF C-DATA

MAR-MAY

FIGURE 41

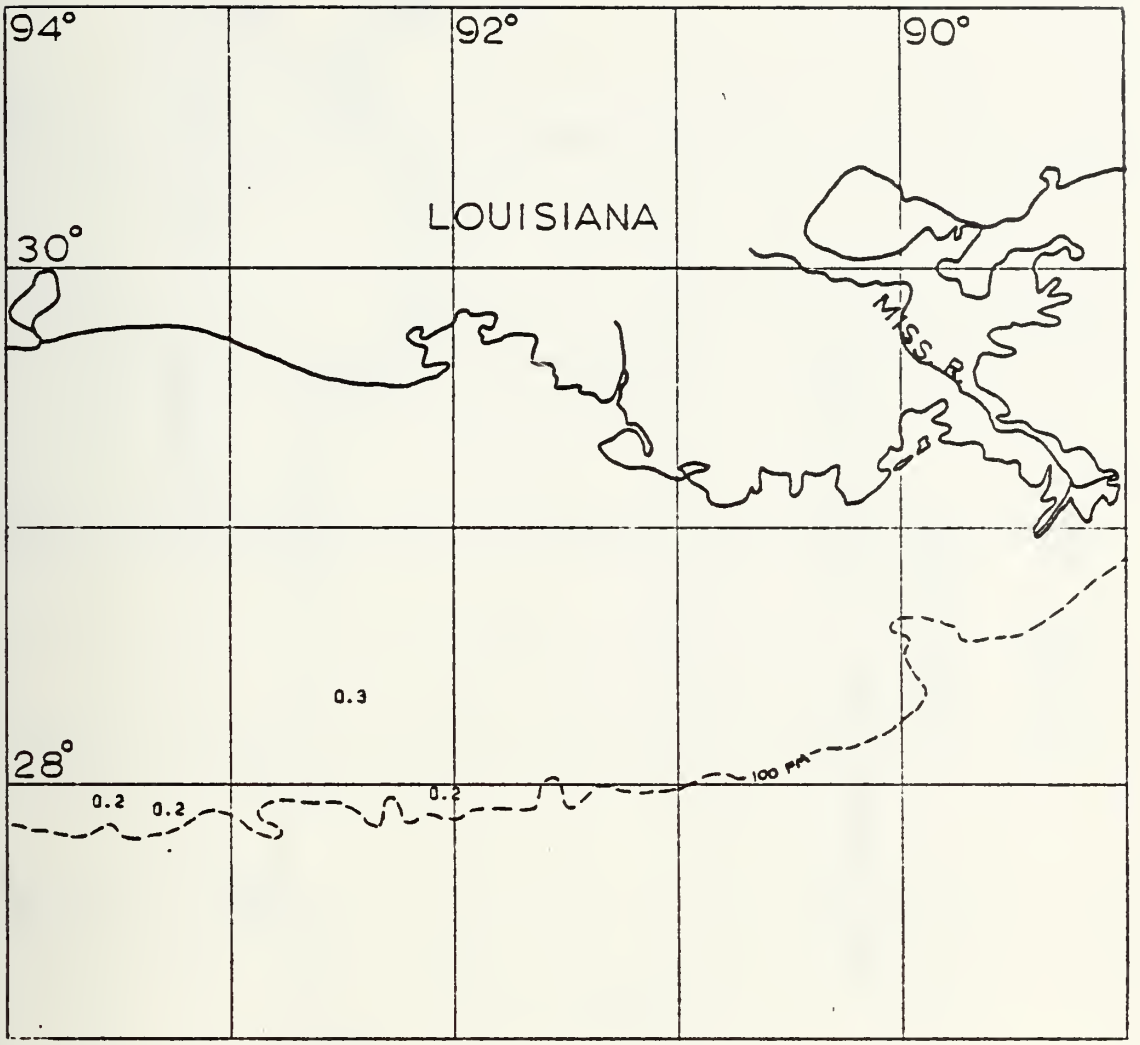


WESTERN GULF K-DATA

JAN-DEC

FIGURE 42

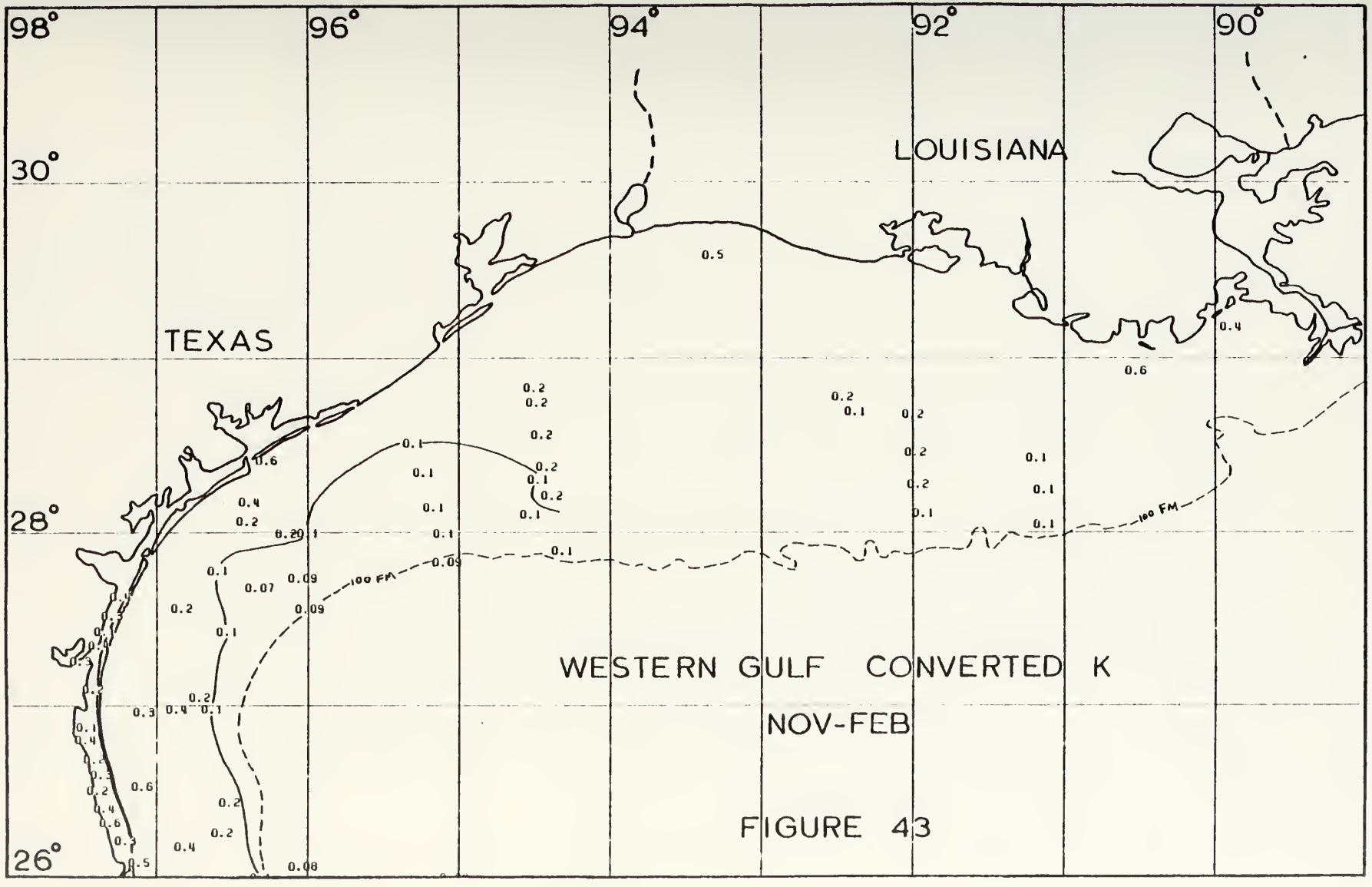


WESTERN GULF CONVERTED K

NOV-FEB

FIGURE 43

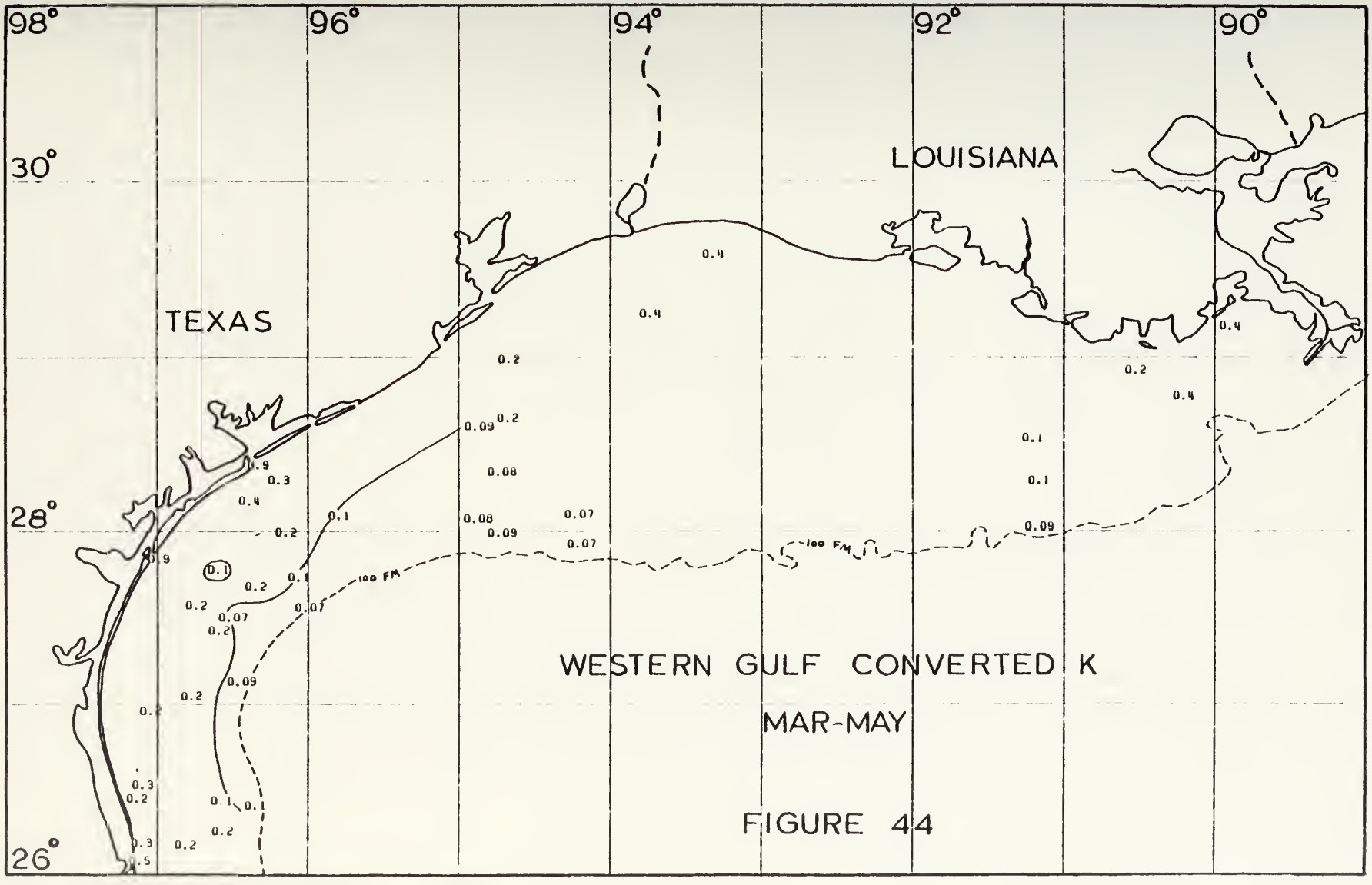


WESTERN GULF CONVERTED K

MAR-MAY

FIGURE 44

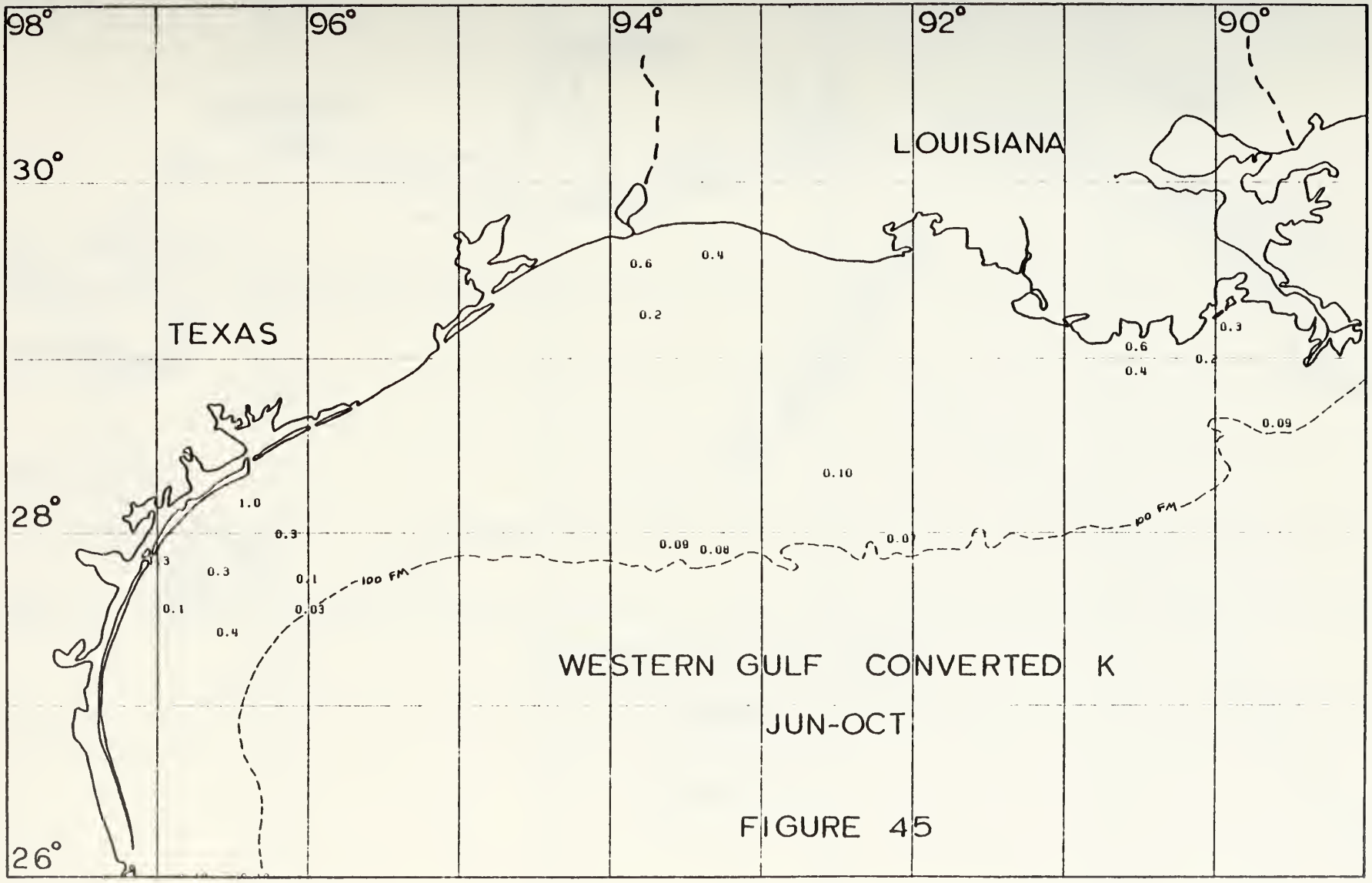


WESTERN GULF CONVERTED K

JUN-OCT

FIGURE 45

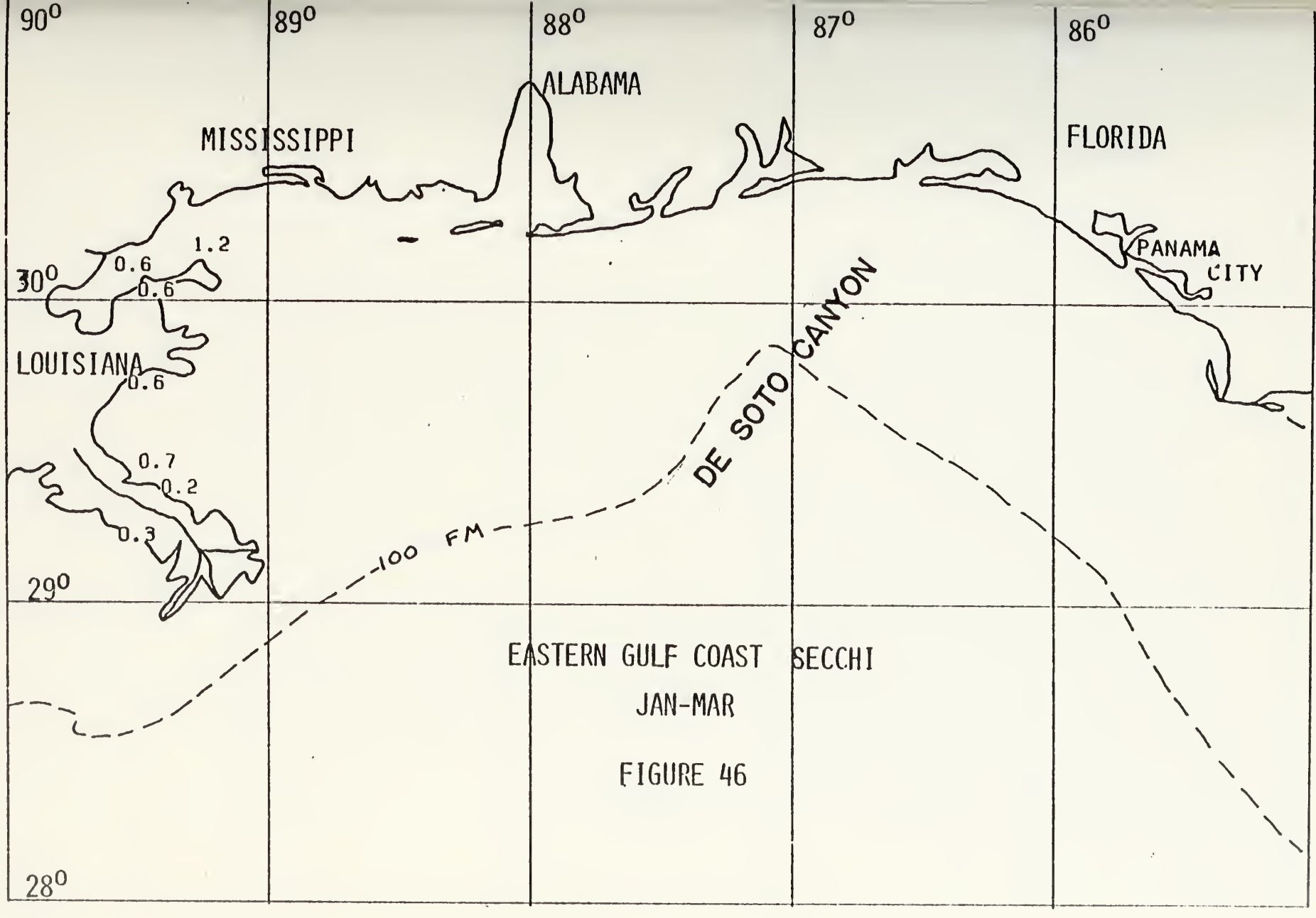


EASTERN GULF COAST SECCHI

JAN-MAR

FIGURE 46

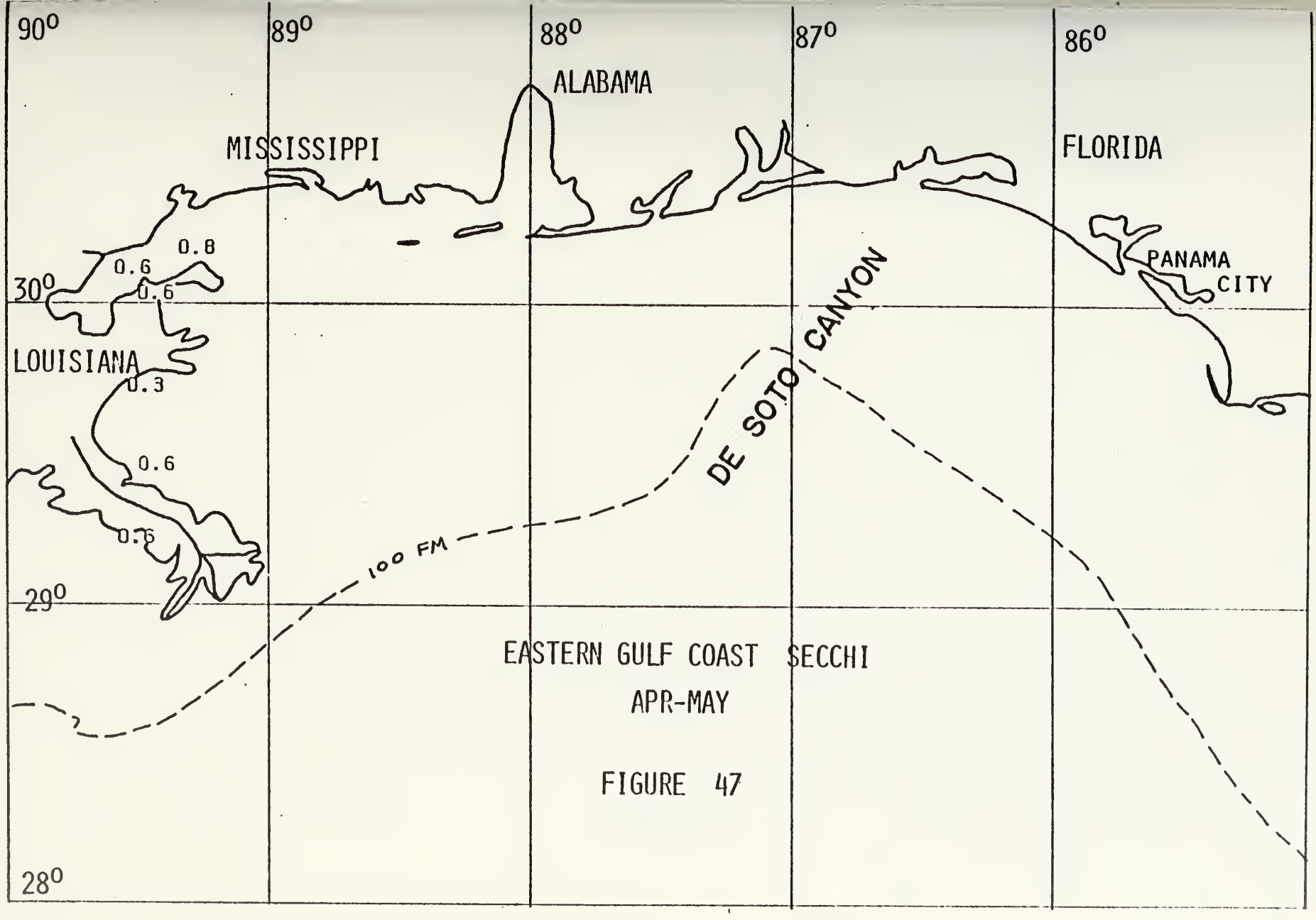


EASTERN GULF COAST SECCHI
APR-MAY

FIGURE 47

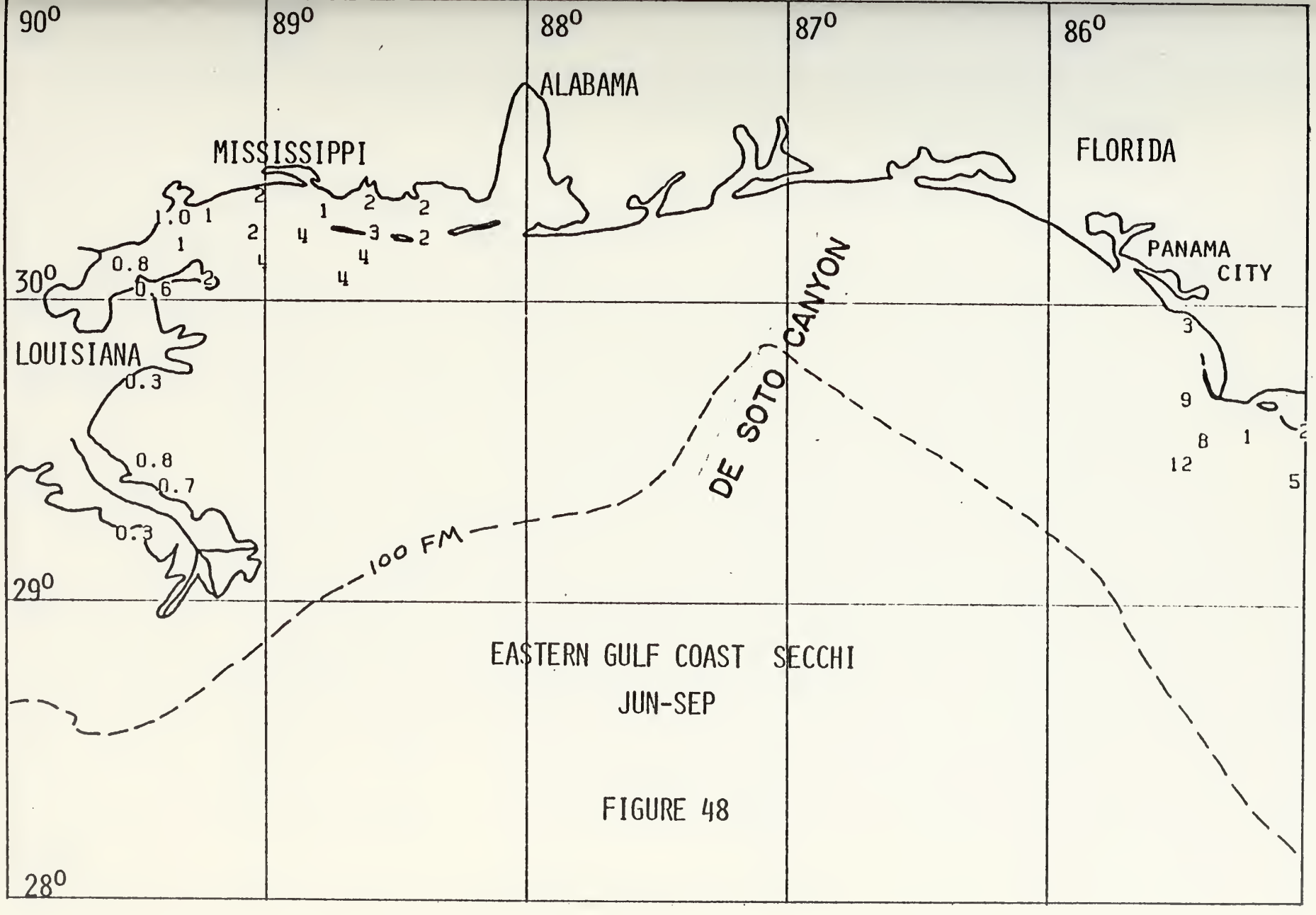
90°
89°
88°
87°
86°
ALABAMA
MISSISSIPPI
FLORIDA
PANAMA CITY
30°
LOUISIANA
DE SOTO CANYON
100 FM
29°
28°
1.0
0.8
0.6
0.3
0.8
0.7
0.3
EASTERN GULF COAST SECCHI
JUN-SEP

FIGURE 48

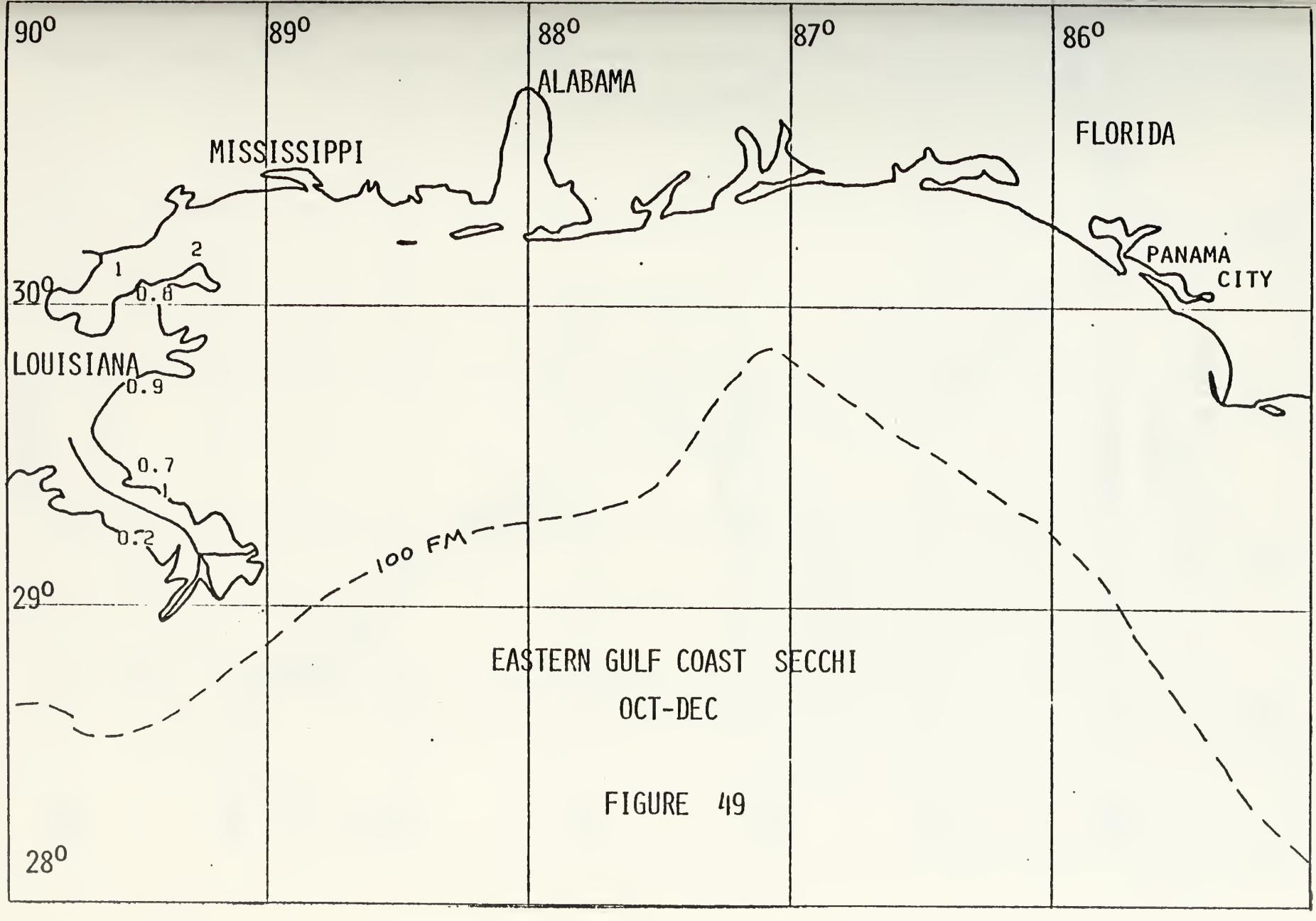


EASTERN GULF COAST SECCHI
OCT-DEC

FIGURE 49

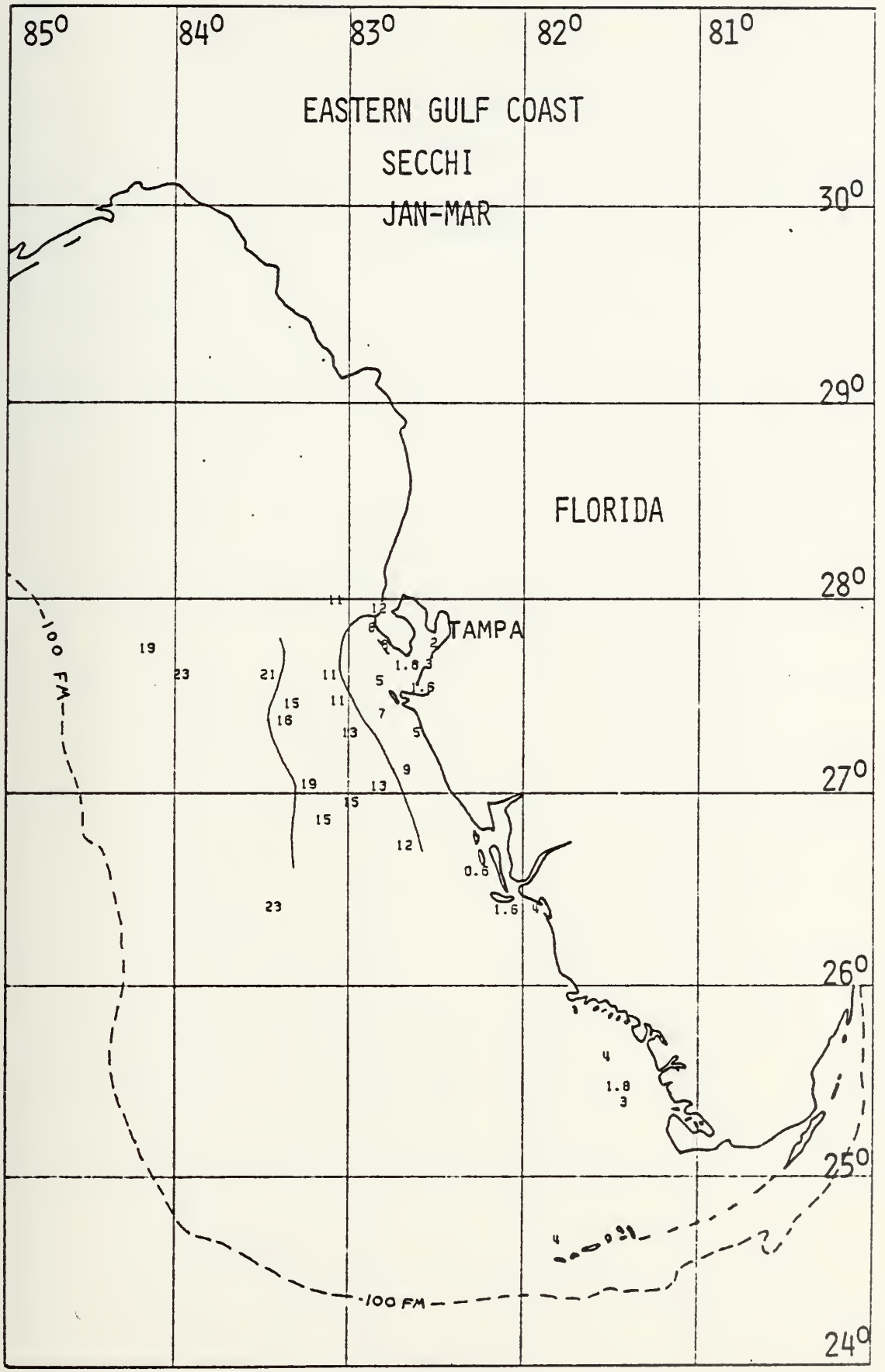
85°
84°
83°
82°
81°
EASTERN GULF COAST
SECCHI
JAN-MAR
30°
29°
FLORIDA
28°
TAMPA
27°
26°
25°
24°
100 FM
100 FM

FIGURE 50

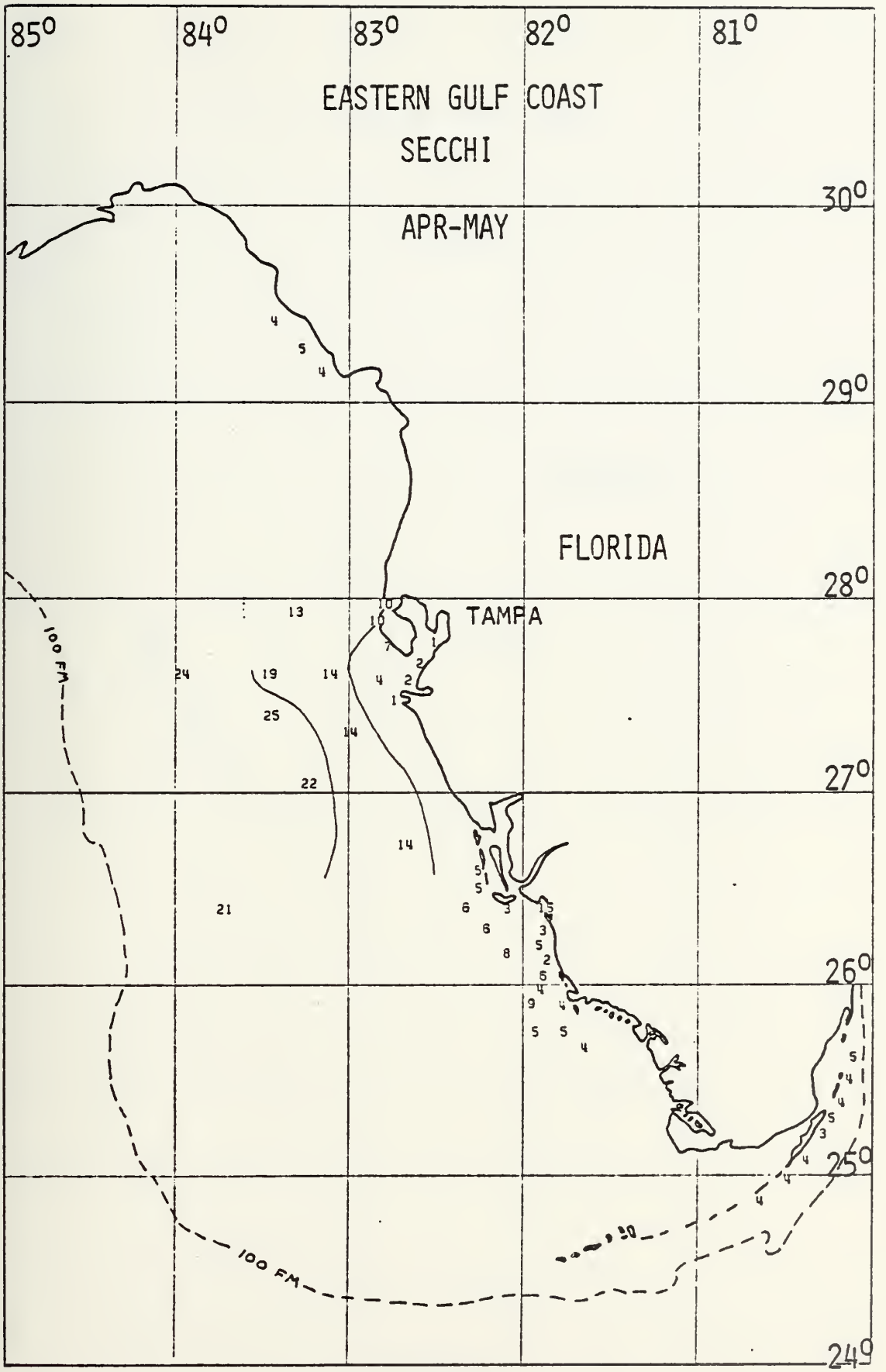
85°
84°
83°
82°
81°
EASTERN GULF COAST
SECCHI
APR-MAY
30°
29°
28°
27°
26°
25°
24°
FLORIDA
TAMPA
100 FM
100 FM

FIGURE 51

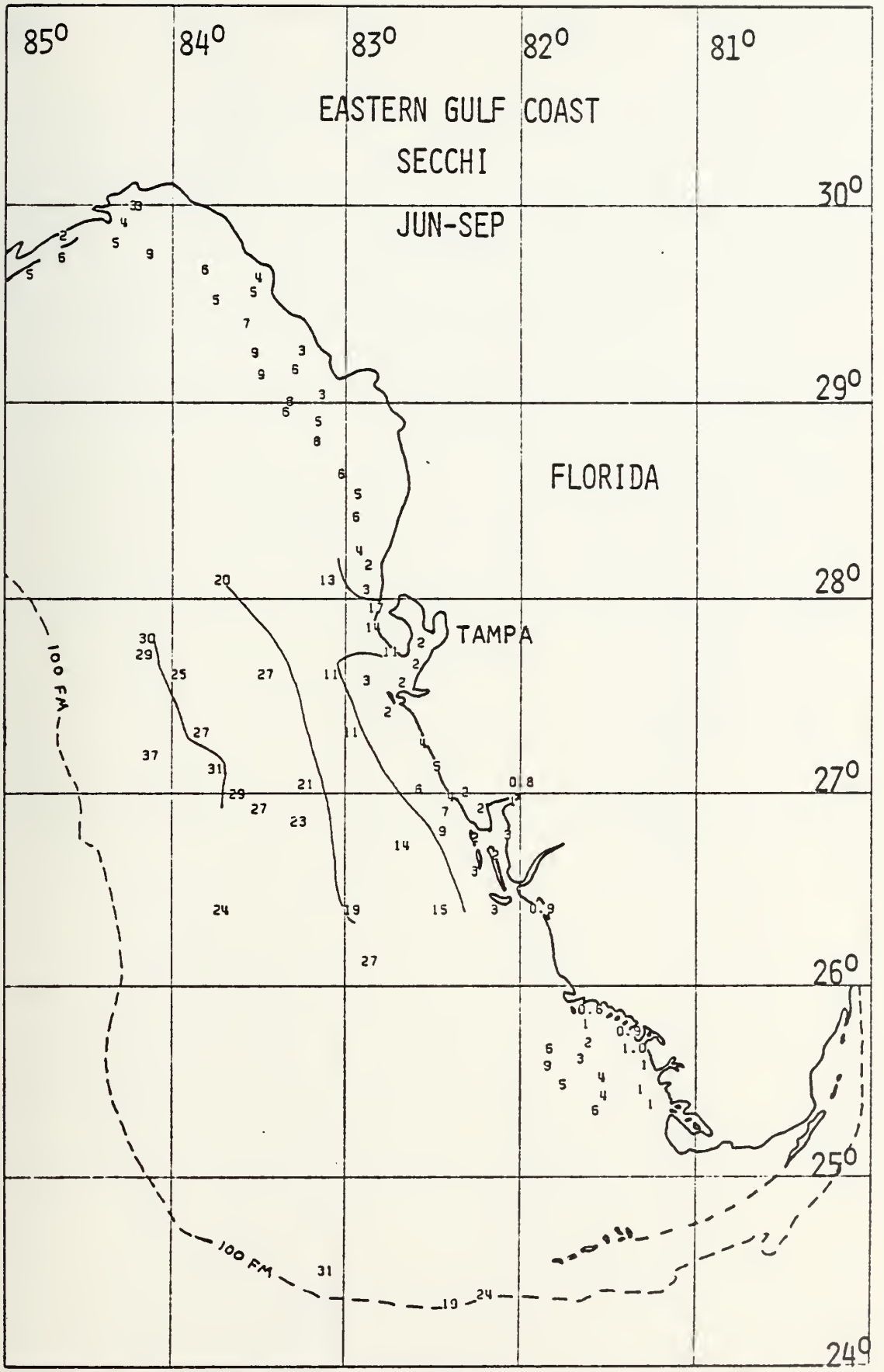
85°
84°
83°
82°
81°
EASTERN GULF COAST
SECCHI
JUN-SEP
30°
29°
28°
27°
26°
25°
24°
FLORIDA
TAMPA
100 FM
100 FM

FIGURE 52

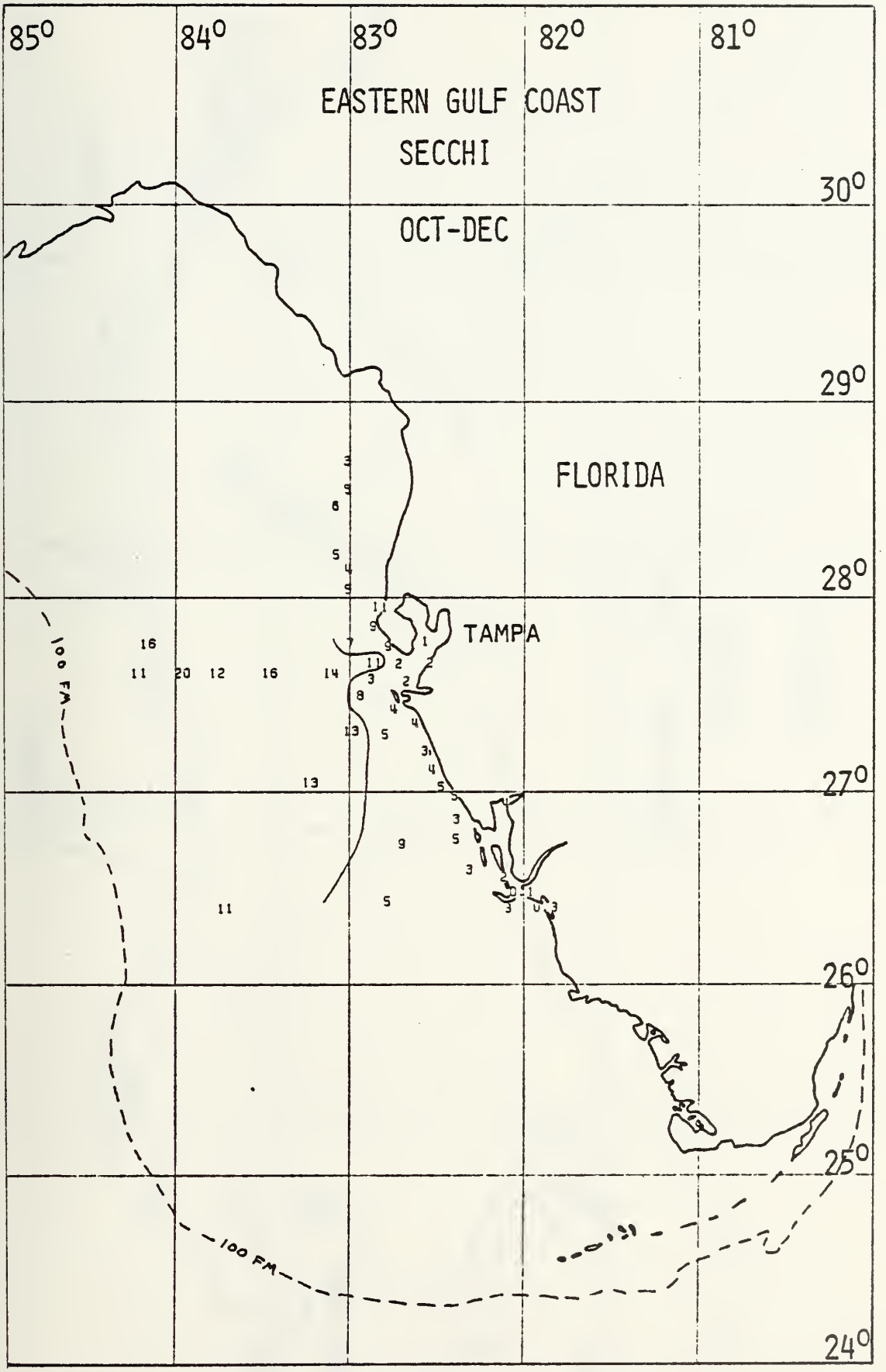
85°
84°
83°
82°
81°
EASTERN GULF COAST
SECCHI
OCT-DEC
30°
29°
28°
27°
26°
25°
24°
FLORIDA
TAMPA
100 FM
100 FM

FIGURE 53

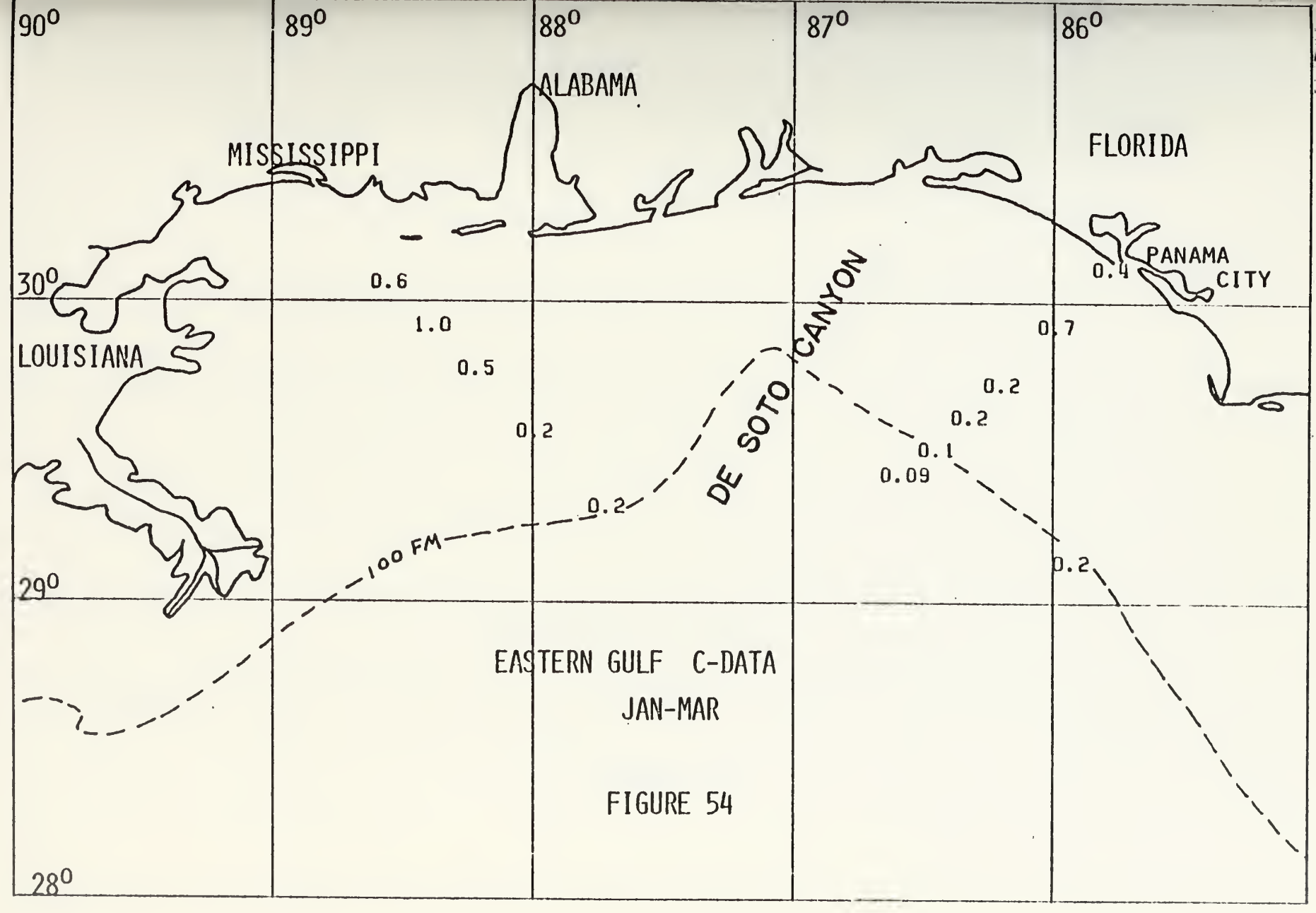
90°
89°
88°
87°
86°
ALABAMA
MISSISSIPPI
FLORIDA
PANAMA CITY
30°
LOUISIANA
0.6
1.0
0.5
0.2
0.4
0.7
0.2
0.2
0.1
0.09
0.2
DE SOTO CANYON
100 FM
29°
28°
EASTERN GULF C-DATA
JAN-MAR

FIGURE 54

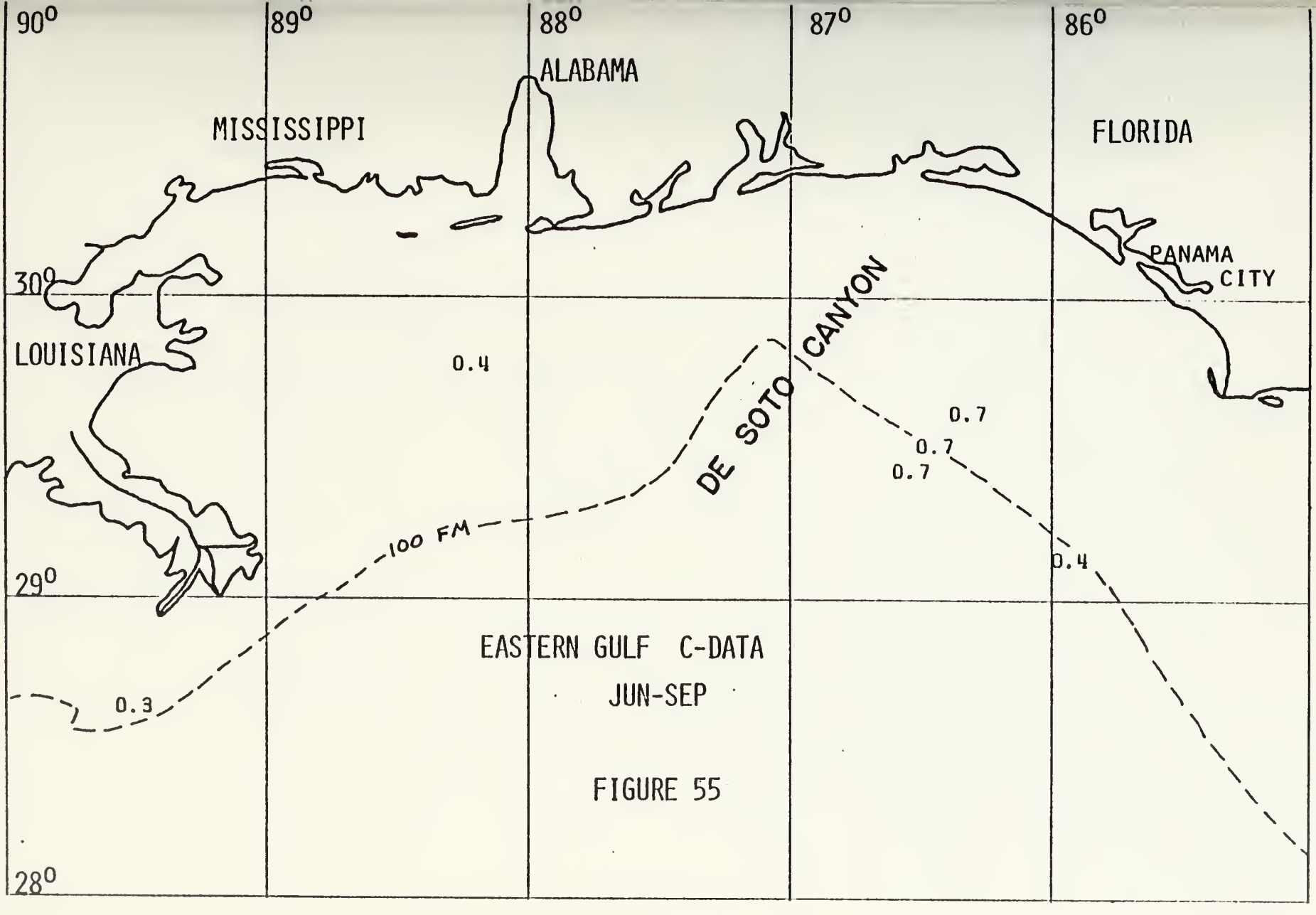


EASTERN GULF C-DATA

JUN-SEP

FIGURE 55

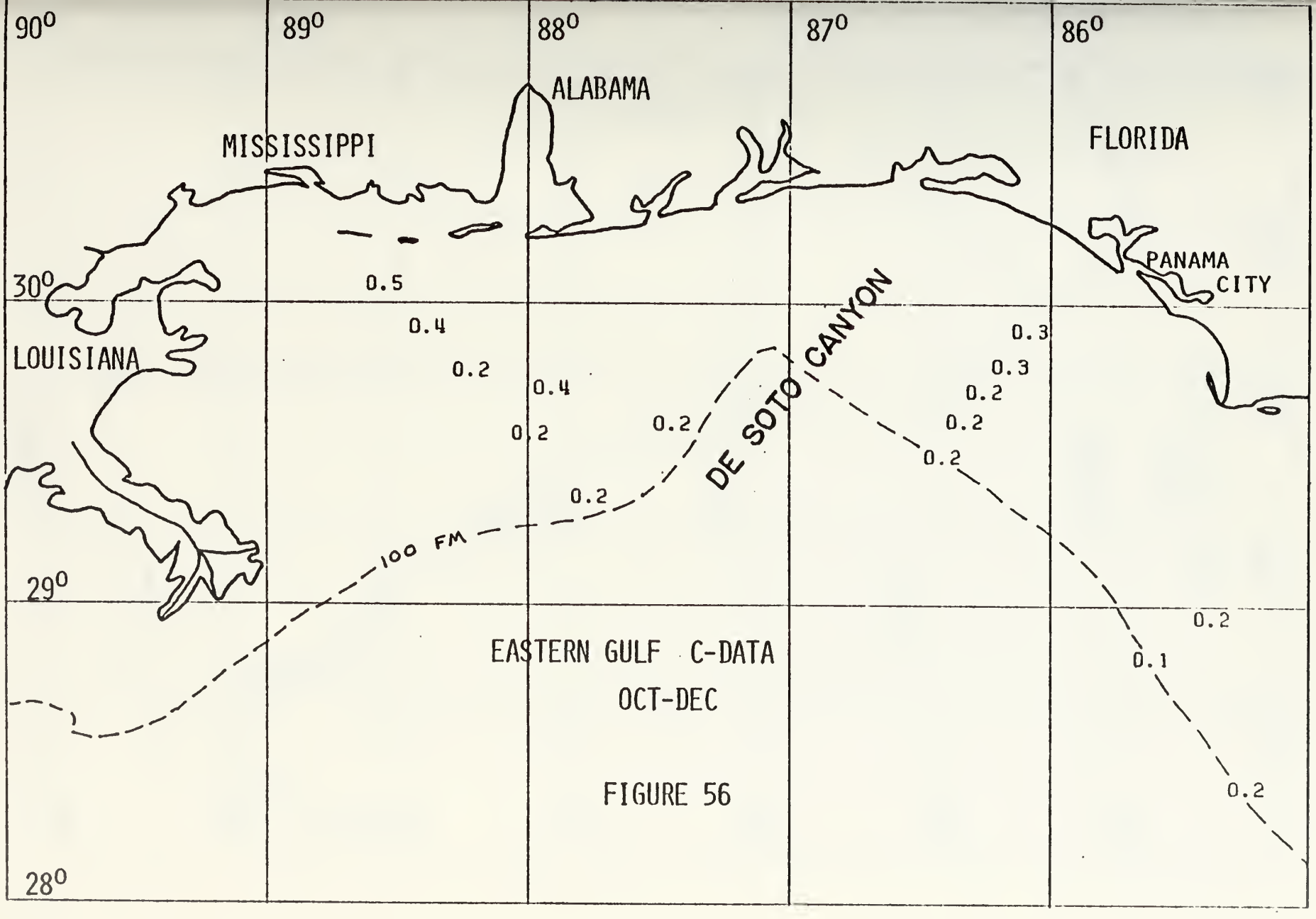
90°
89°
88°
87°
86°
ALABAMA
MISSISSIPPI
FLORIDA
PANAMA CITY
30°
LOUISIANA
0.5
0.4
0.2
0.4
0.2
0.2
0.2
DE SOTO CANYON
0.3
0.3
0.2
0.2
0.2
100 FM
29°
0.2
0.1
0.2
EASTERN GULF C-DATA
OCT-DEC
28°

FIGURE 56

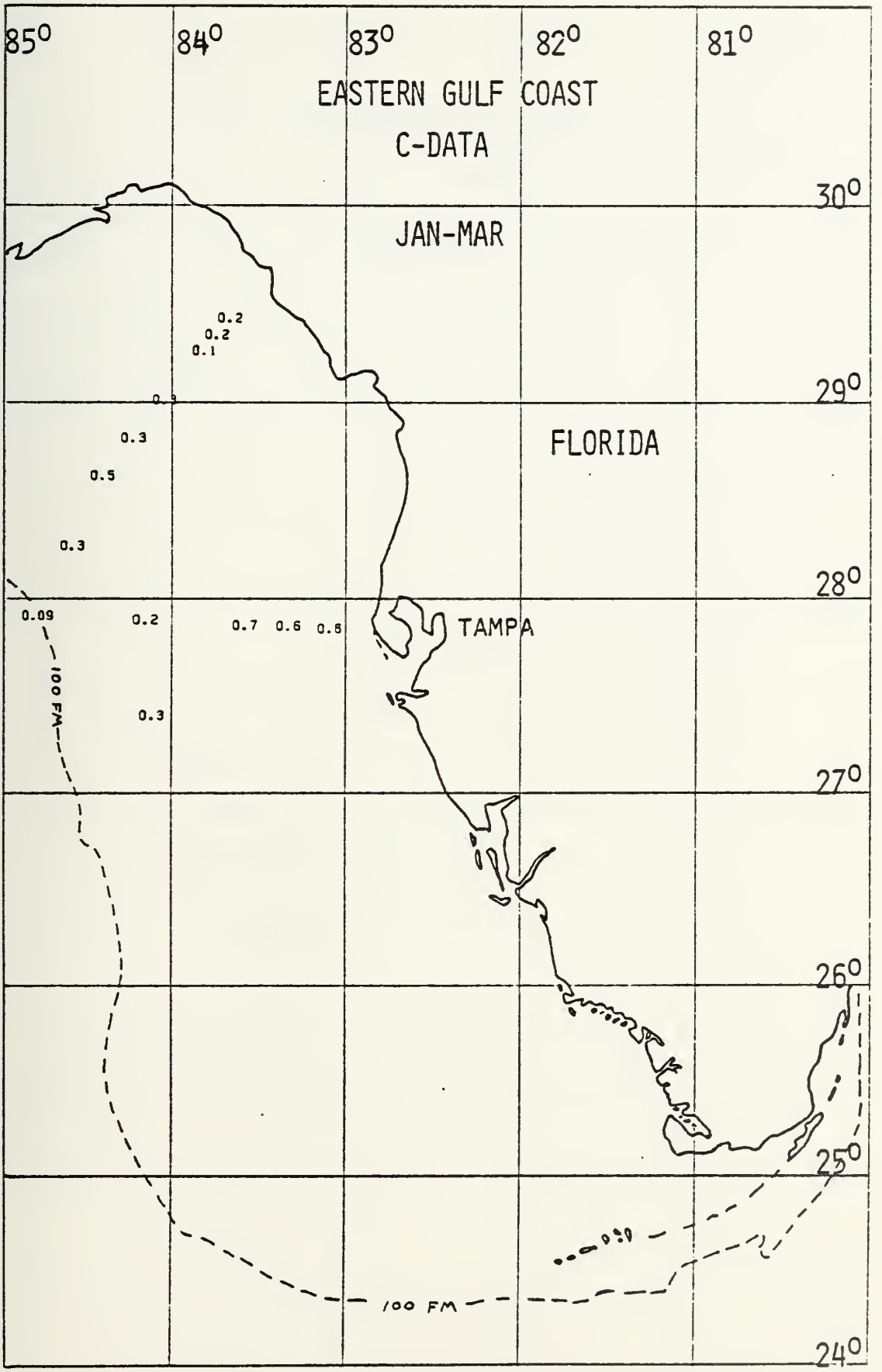
85°
84°
83°
82°
81°
EASTERN GULF COAST
C-DATA
JAN-MAR
30°
29°
28°
27°
26°
25°
24°
FLORIDA
TAMPA
0.2
0.2
0.1
0.3
0.5
0.3
0.09
0.2
0.3
0.7
0.6
0.6
100 FM
100 FM

FIGURE 57

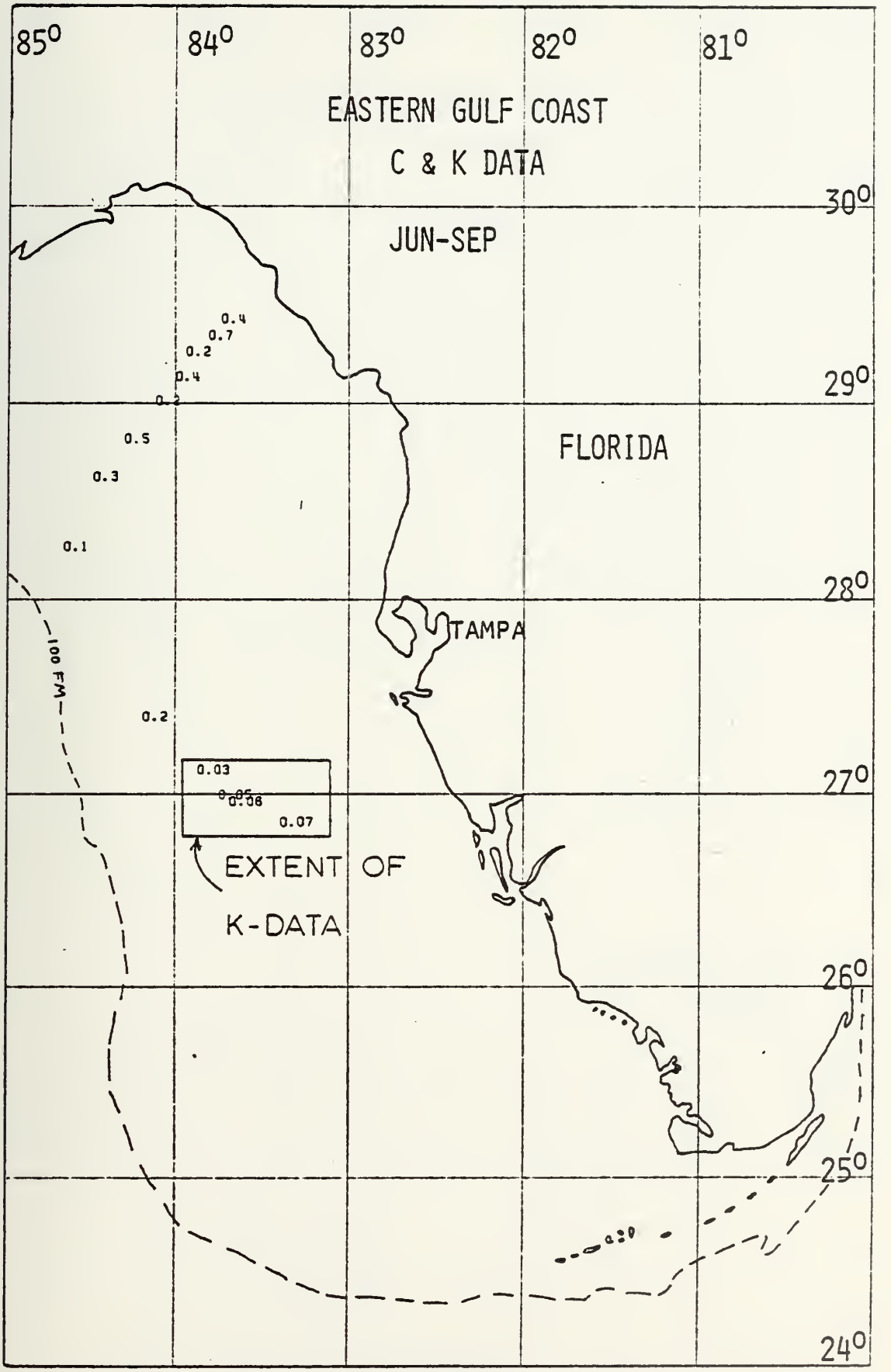
85°
84°
83°
82°
81°
EASTERN GULF COAST
C & K DATA
JUN-SEP
30°
29°
28°
27°
26°
25°
24°
FLORIDA
TAMPA
0.4
0.7
0.2
0.4
0.2
0.5
0.3
0.1
0.2
100 FM
0.03
0.06
0.07
EXTENT OF
K-DATA

FIGURE 58

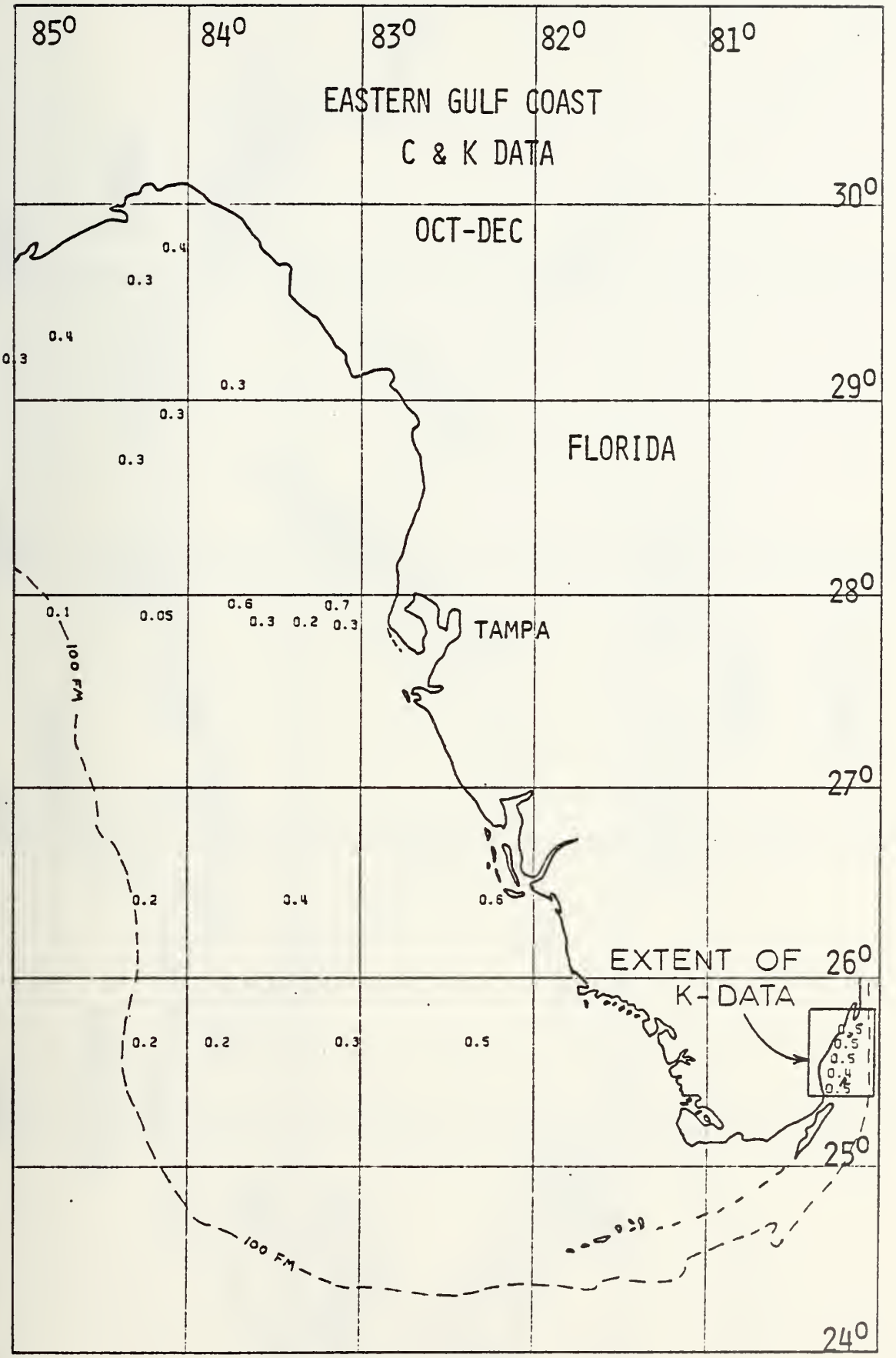
85°
84°
83°
82°
81°
EASTERN GULF COAST
C & K DATA
30°
OCT-DEC
0.4
0.3
0.4
0.3
0.3
29°
0.3
0.3
FLORIDA
28°
0.1
0.05
0.6
0.3
0.2
0.7
0.3
TAMPA
100 FM
27°
0.2
0.4
0.6
EXTENT OF
K-DATA
26°
0.2
0.2
0.3
0.5
0.5
0.5
0.5
0.4
0.5
25°
100 FM
24°

FIGURE 59

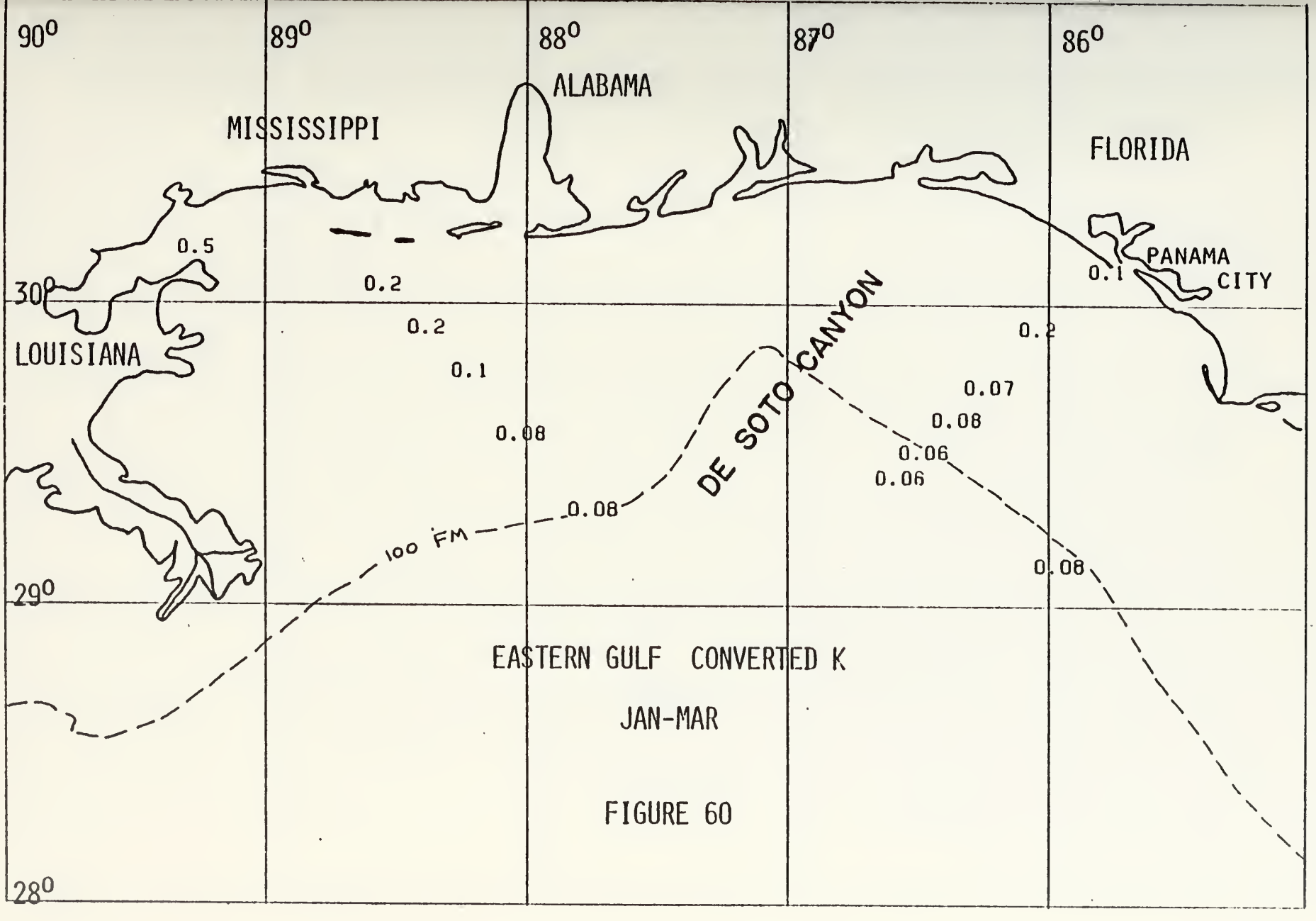
90°
89°
88°
87°
86°
ALABAMA
MISSISSIPPI
FLORIDA
PANAMA CITY
0.5
0.2
0.1
30°
0.2
0.2
LOUISIANA
0.1
0.08
DE SOTO CANYON
0.07
0.08
0.06
0.06
0.08
100 FM
0.08
29°
EASTERN GULF CONVERTED K
JAN-MAR
FIGURE 60
28°

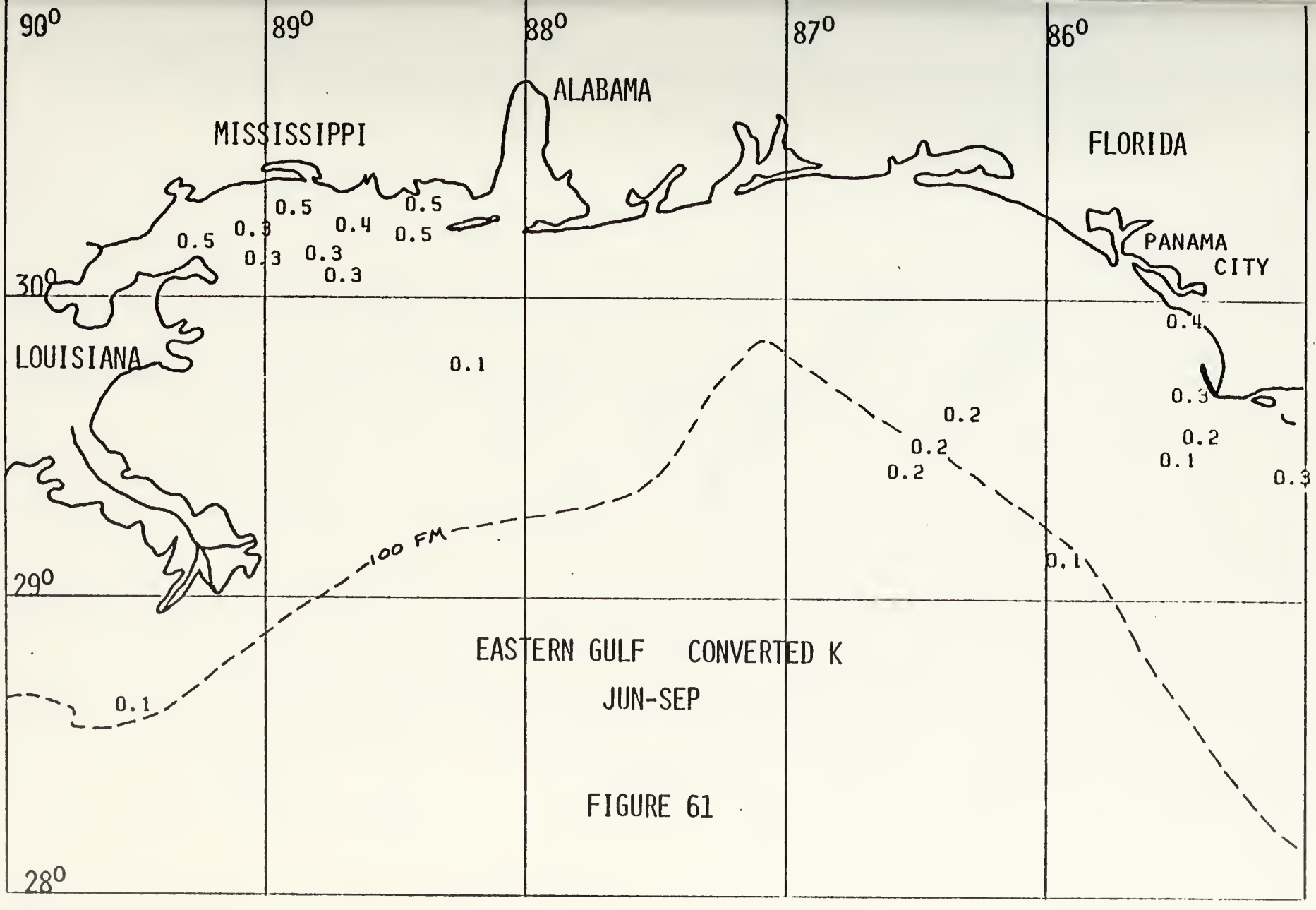


EASTERN GULF CONVERTED K

JUN-SEP

FIGURE 61

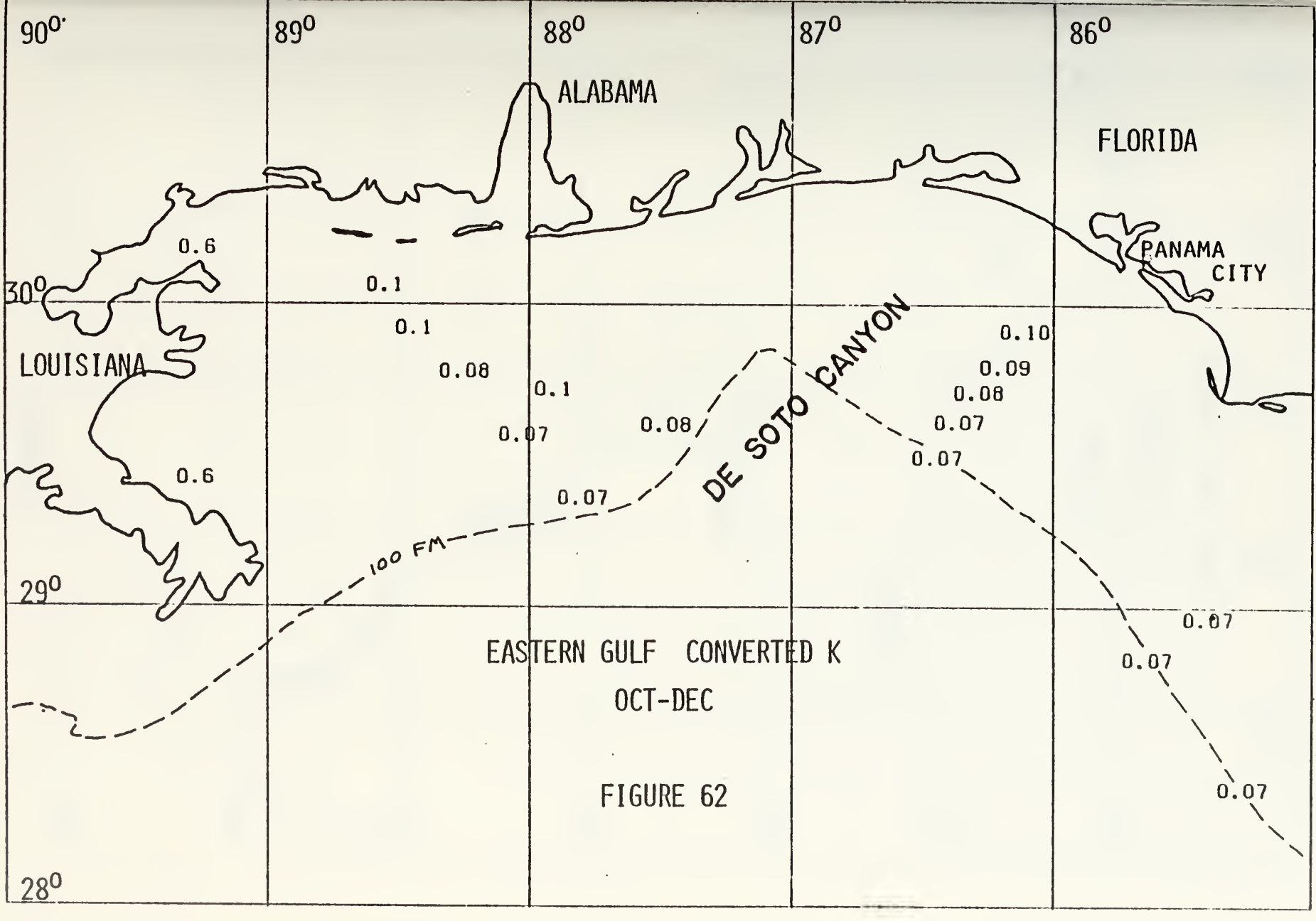


EASTERN GULF CONVERTED K
OCT-DEC

FIGURE 62

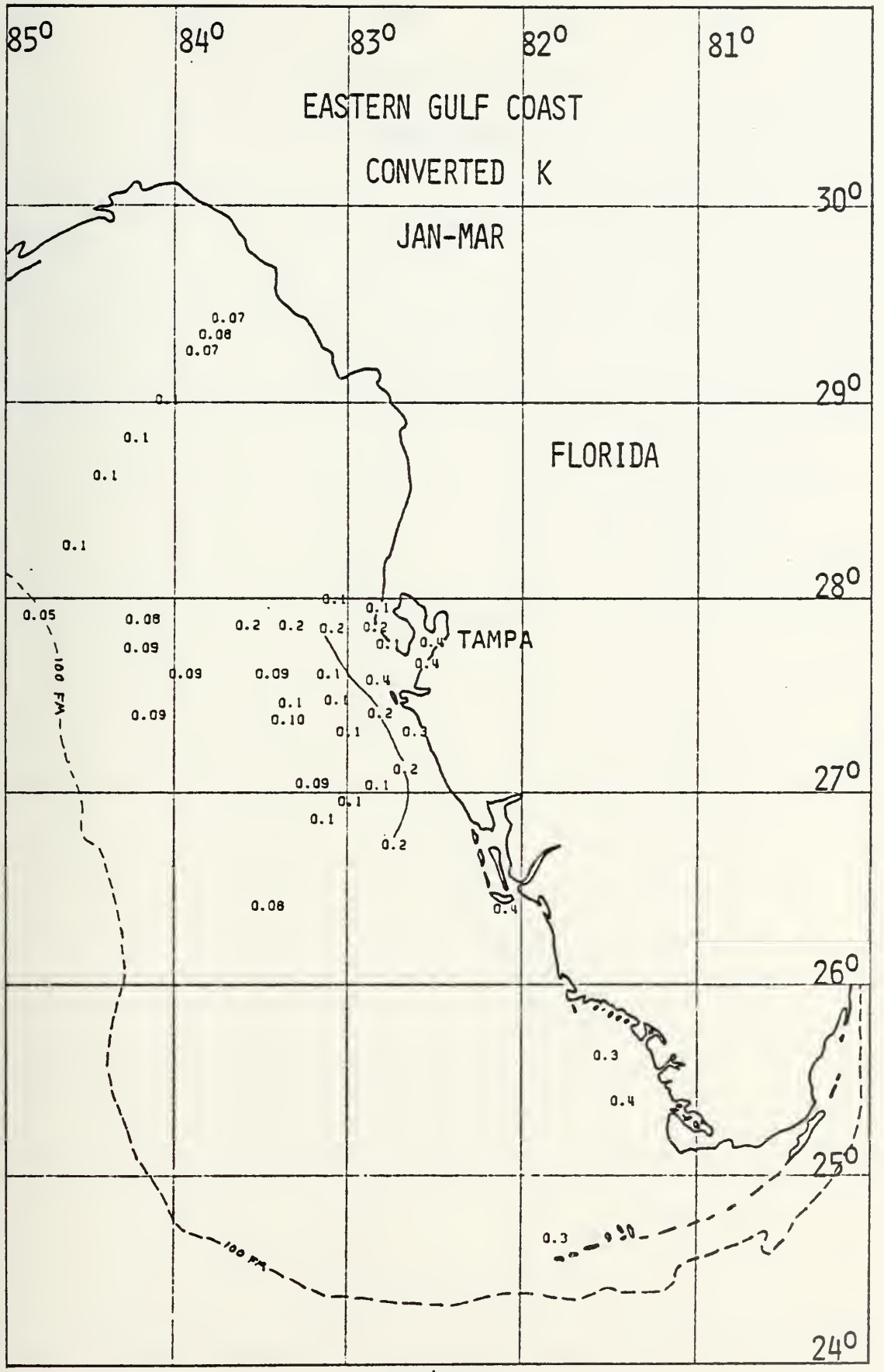
85°
84°
83°
82°
81°
EASTERN GULF COAST
CONVERTED K
JAN-MAR
30°
29°
28°
27°
26°
25°
24°
FLORIDA
TAMPA
100 FM
100 FM

FIGURE 63

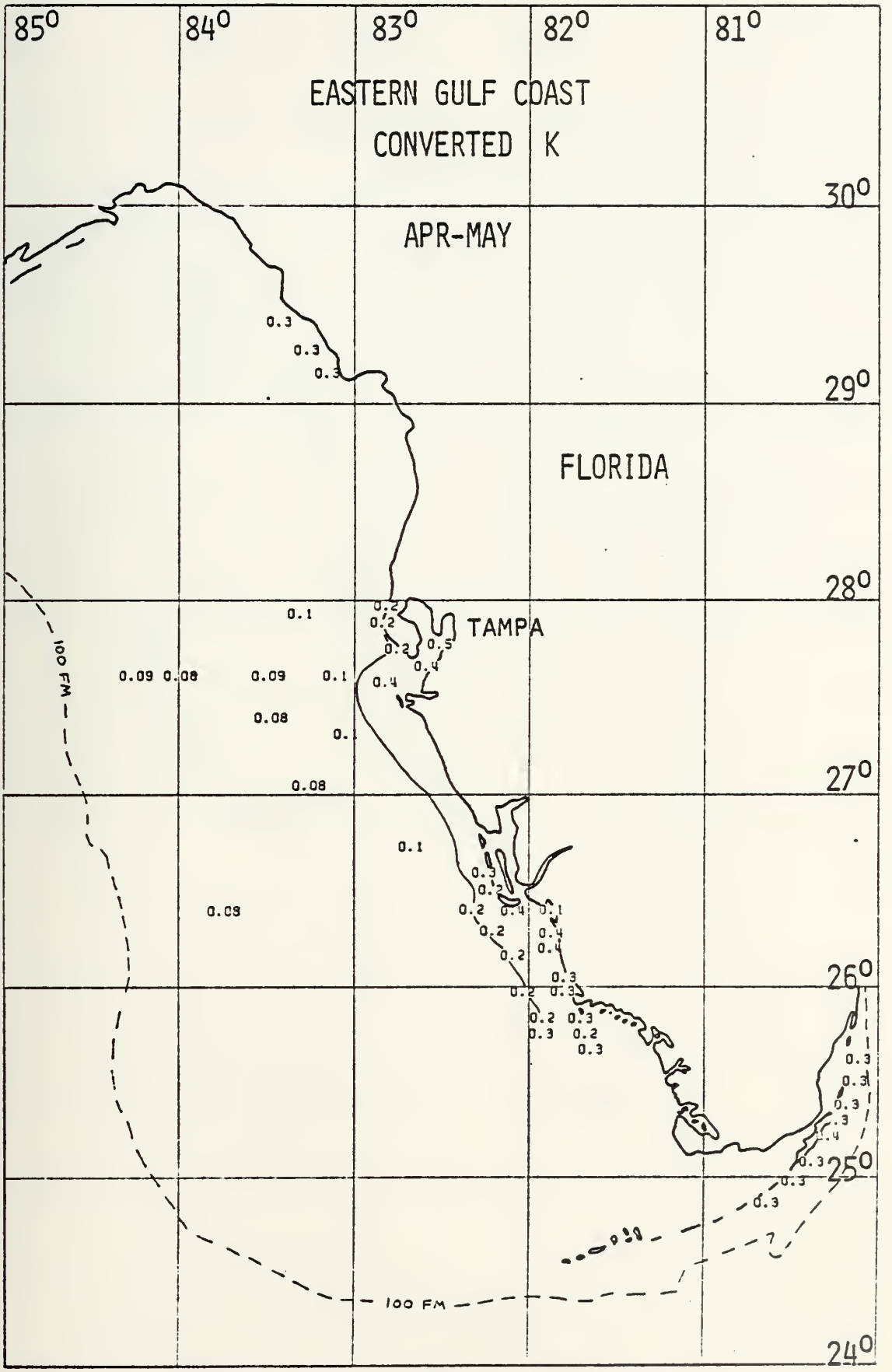
85°
84°
83°
82°
81°
EASTERN GULF COAST
CONVERTED K
APR-MAY
30°
29°
FLORIDA
28°
TAMPA
27°
26°
25°
24°
100 FM
100 FM

FIGURE 64

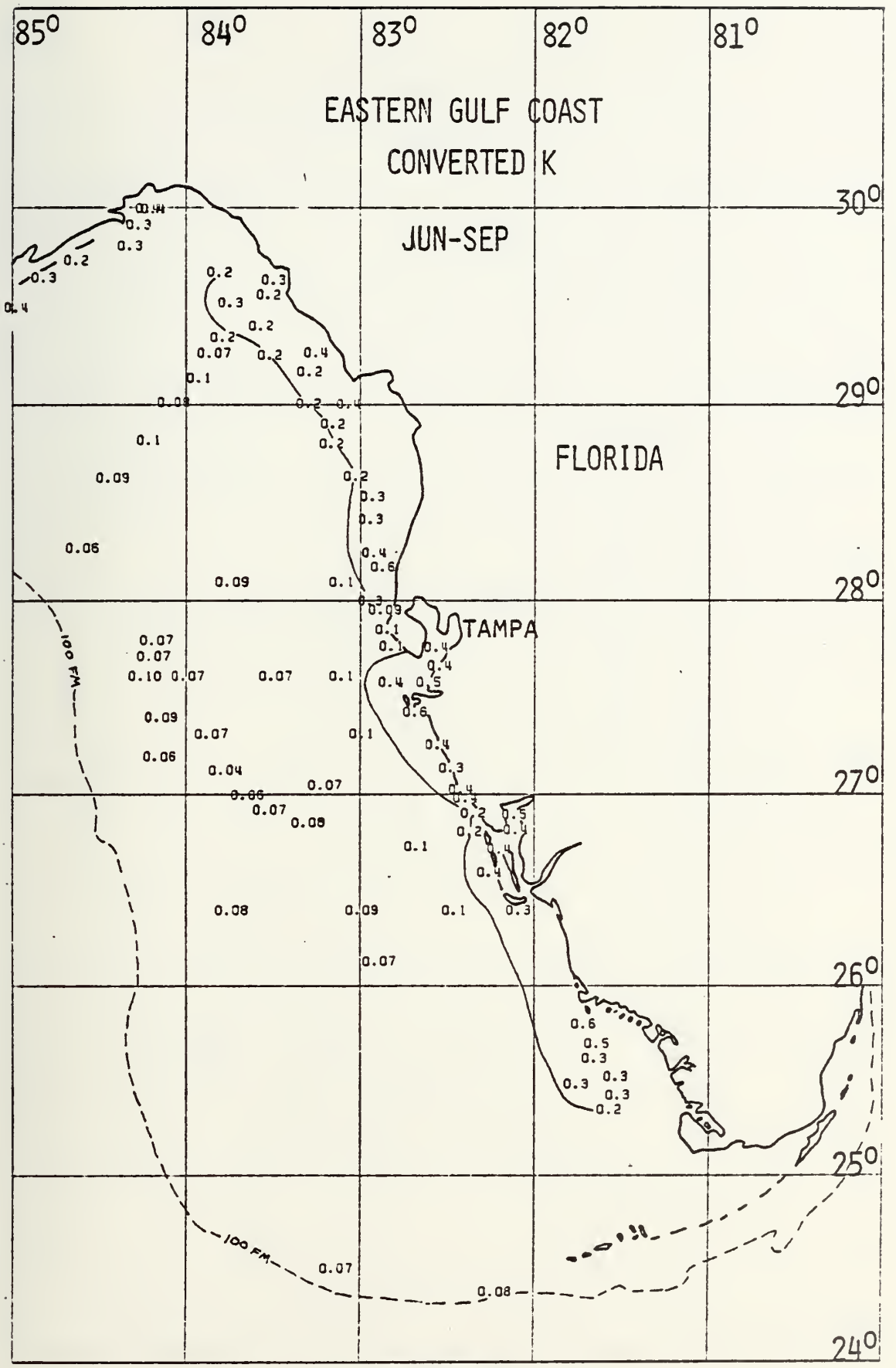
85°
84°
83°
82°
81°
EASTERN GULF COAST
CONVERTED K
JUN-SEP
30°
29°
28°
27°
26°
25°
24°
FLORIDA
TAMPA
100 FM
100 FM

FIGURE 65

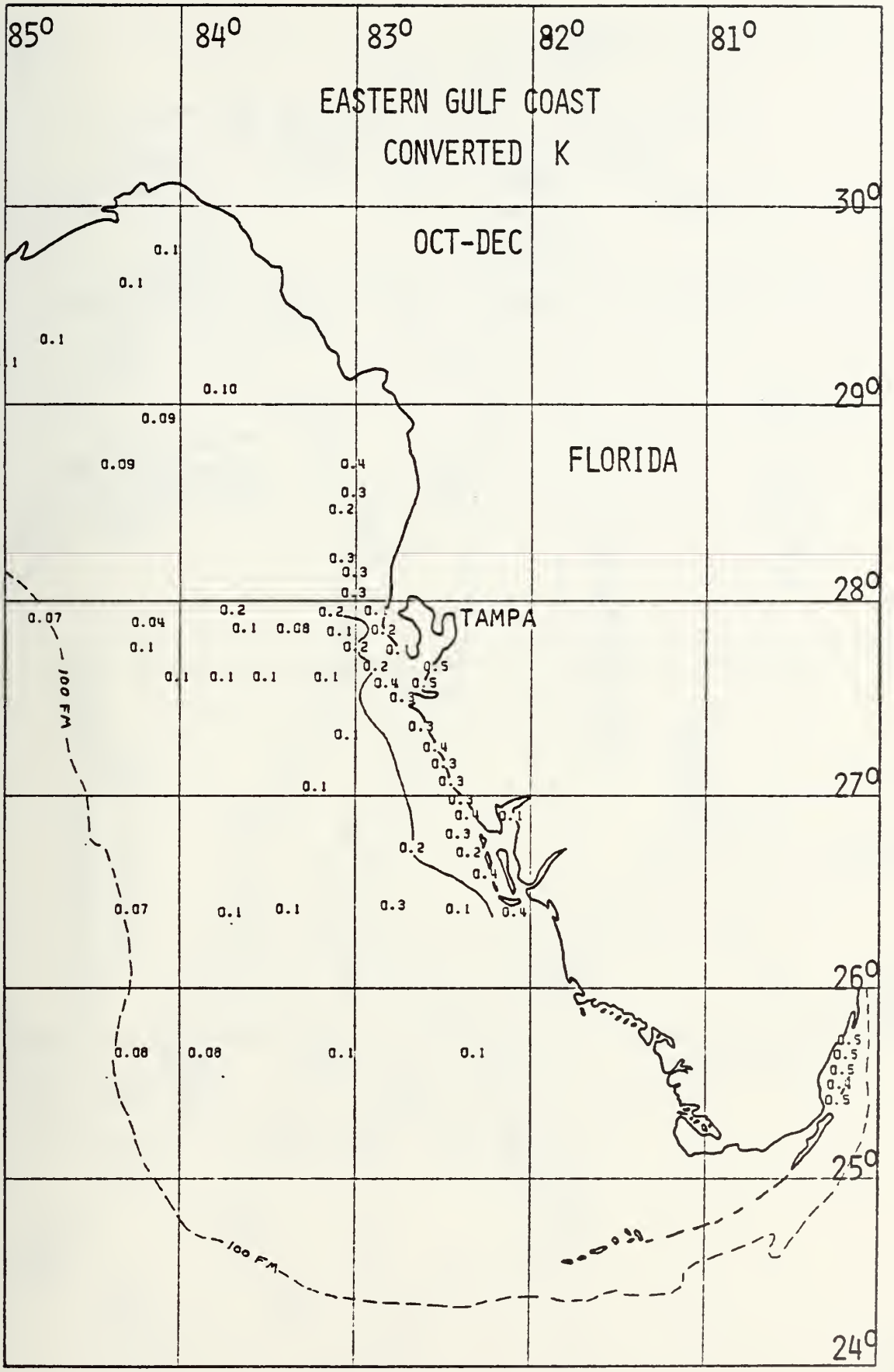
85°
84°
83°
82°
81°
EASTERN GULF COAST
CONVERTED K
OCT-DEC
30°
29°
28°
27°
26°
25°
24°
FLORIDA
TAMPA
100 FM
100 FM

FIGURE 66

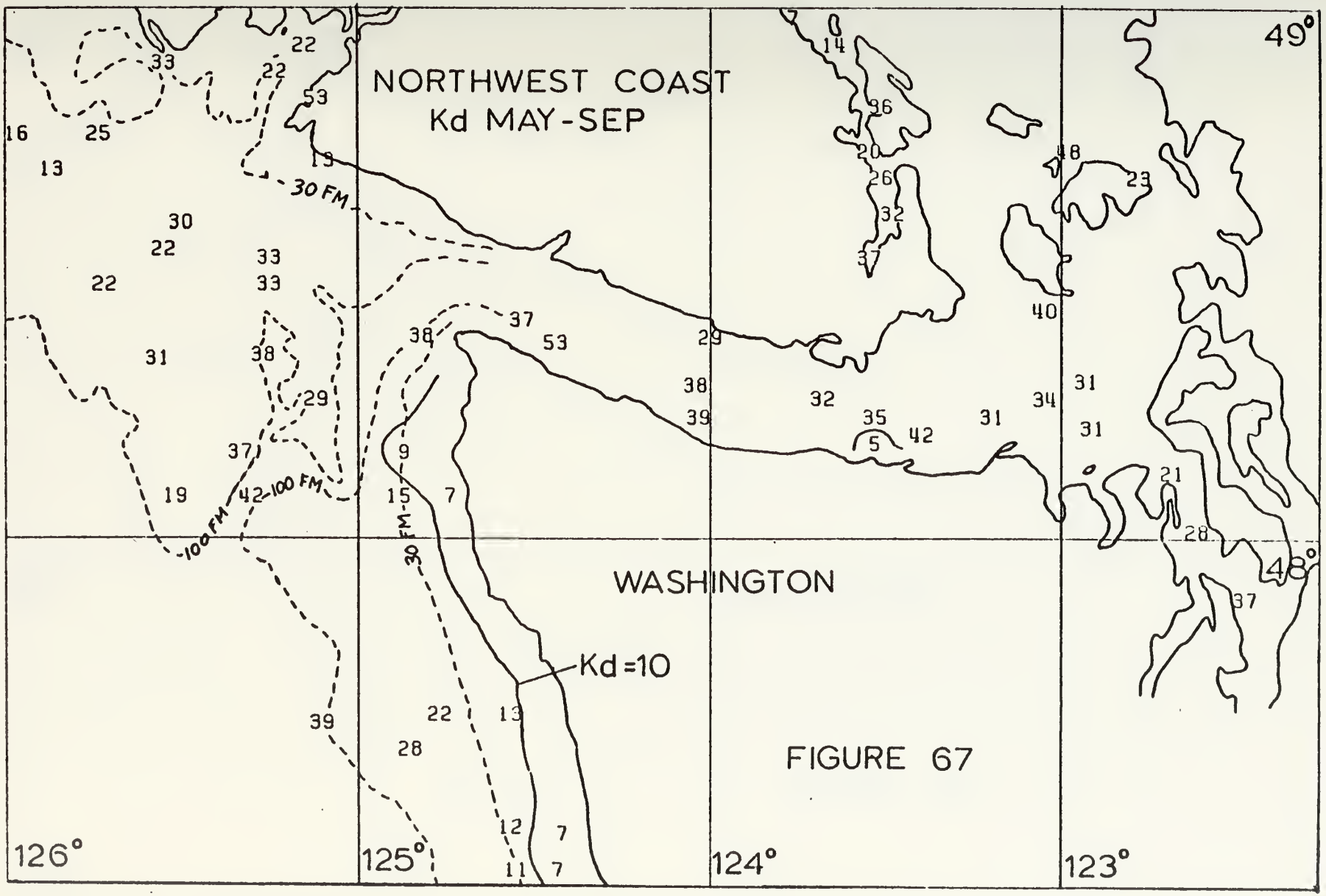
NORTHWEST COAST
Kd MAY-SEP
WASHINGTON
30 FM
100 FM
100 FM
30 FM
Kd =10
49°
48°
126°
125°
124°
123°

FIGURE 67

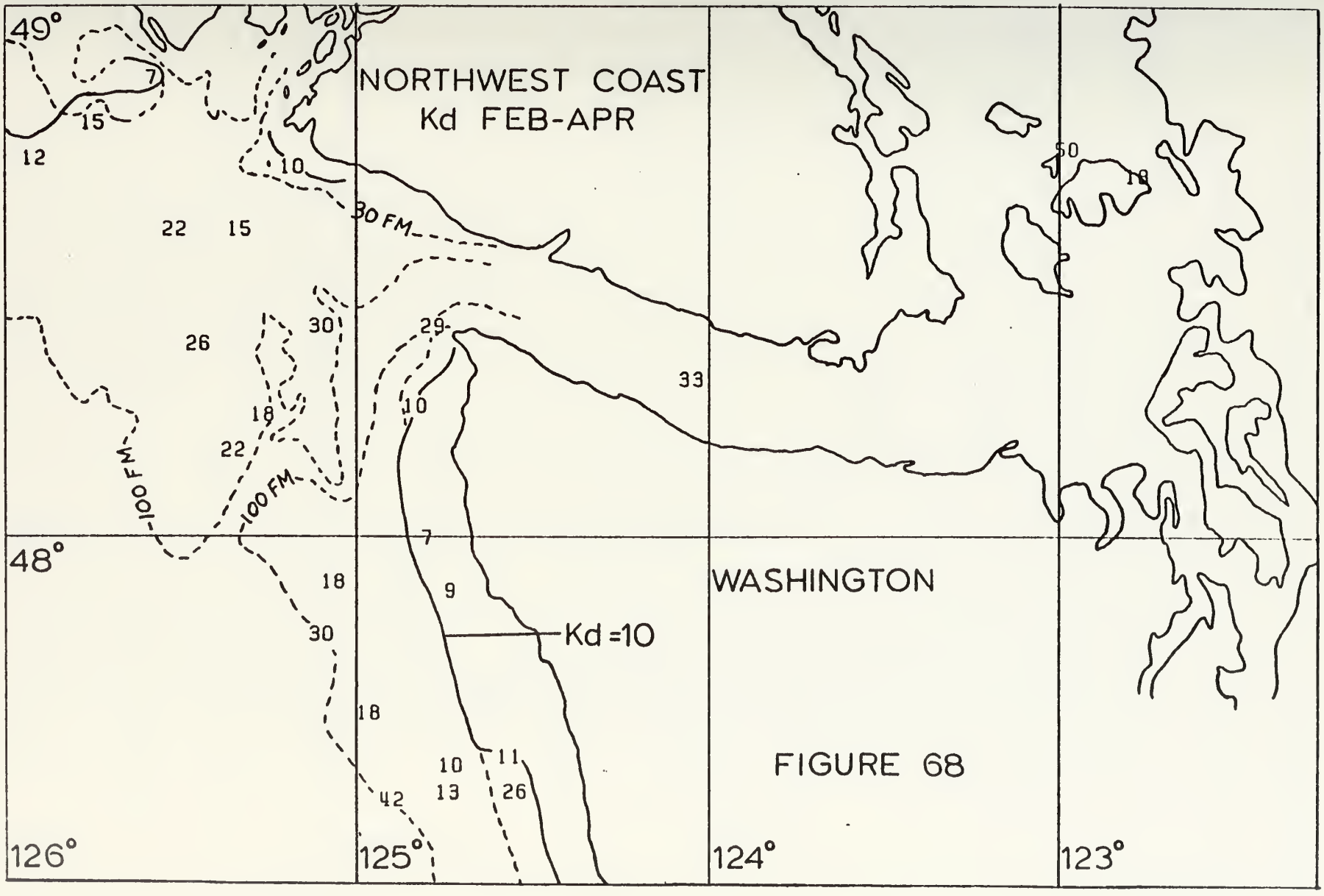
NORTHWEST COAST
Kd FEB-APR
49°
48°
126°
125°
124°
123°
WASHINGTON
Kd =10
30 FM
100 FM
100 FM
7
15
12
10
22
15
26
30
18
22
29
10
33
7
9
18
30
18
10
11
13
26
42
50
18

FIGURE 68

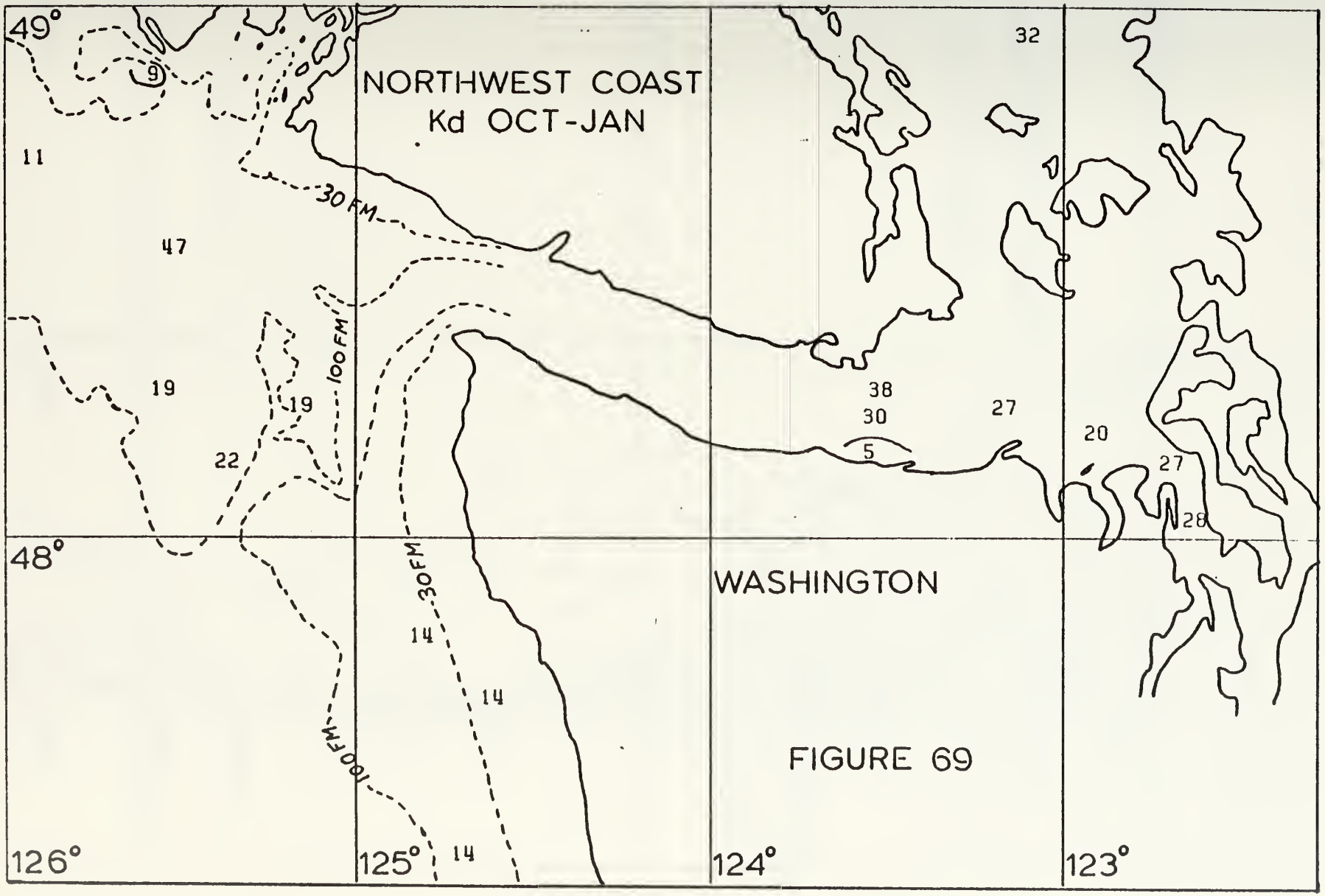
NORTHWEST COAST
Kd OCT-JAN
WASHINGTON
49°
48°
126°
125°
124°
123°
30 FM
100 FM
30 FM
100 FM
9
11
47
19
19
22
14
14
14
32
38
30
5
27
20
27
28

FIGURE 69

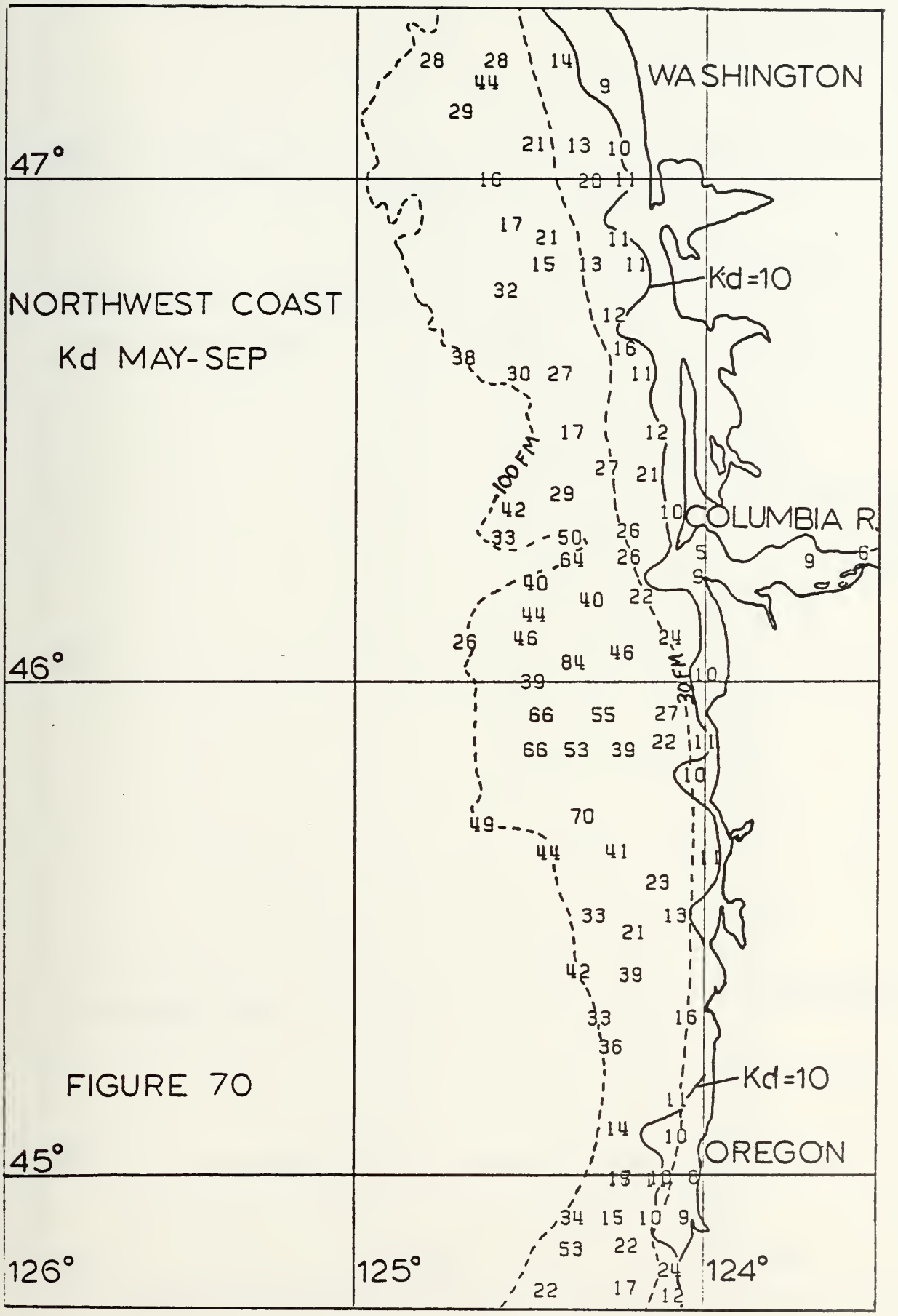
NORTHWEST COAST
Kd MAY-SEP
WASHINGTON
COLUMBIA R.
OREGON
Kd=10
Kd=10
100 FM
30 FM
47°
46°
45°
126°
125°
124°

FIGURE 70

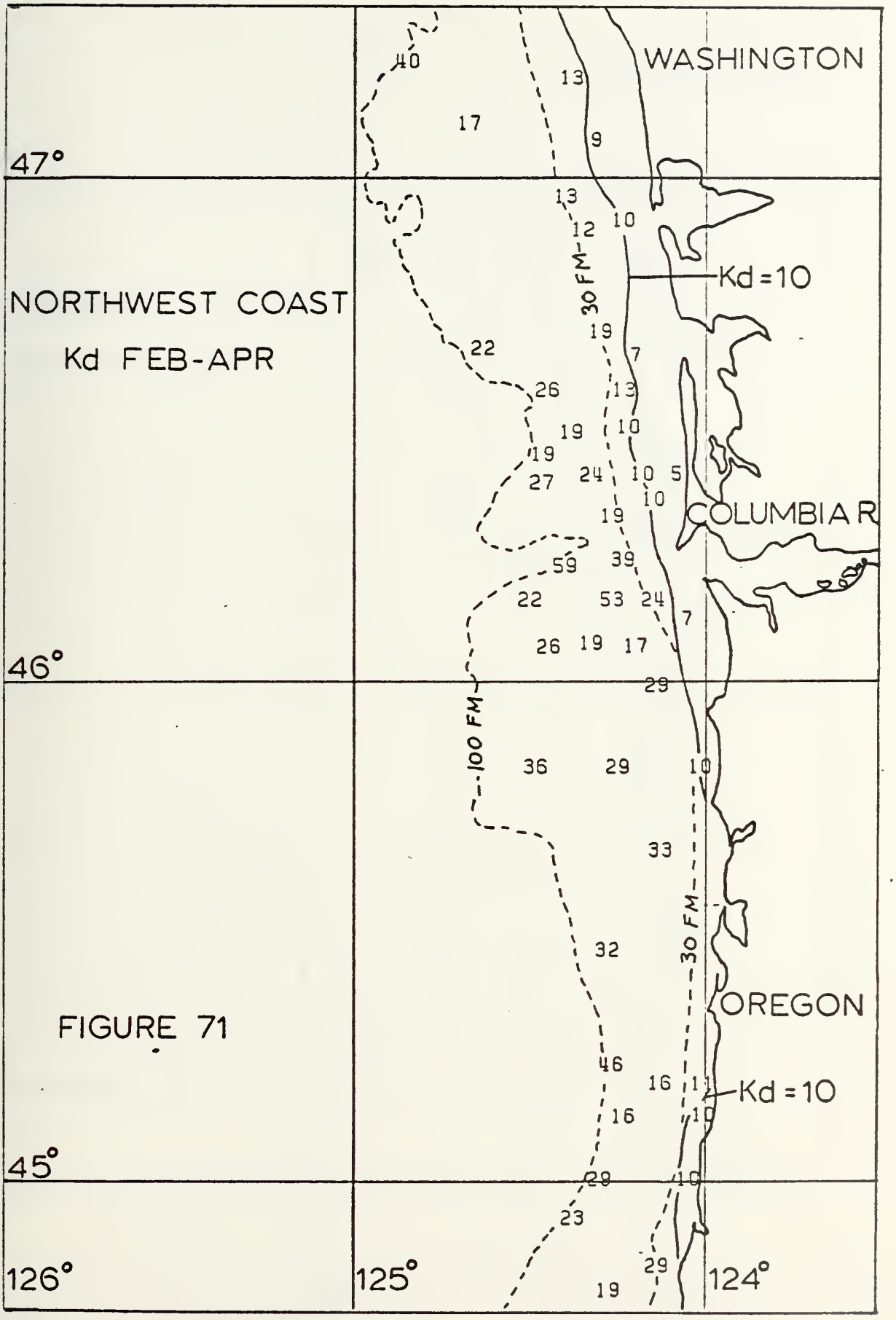
NORTHWEST COAST
Kd FEB-APR
WASHINGTON
OREGON
COLUMBIA R
Kd = 10
Kd = 10
30 FM
100 FM
30 FM
47°
46°
45°
126°
125°
124°
40
13
17
9
13
12
10
22
26
19
7
13
19
10
19
27
24
10
5
10
19
59
39
22
53
24
7
26
19
17
29
36
29
10
33
32
46
16
11
16
10
29
10
23
29
19

FIGURE 71

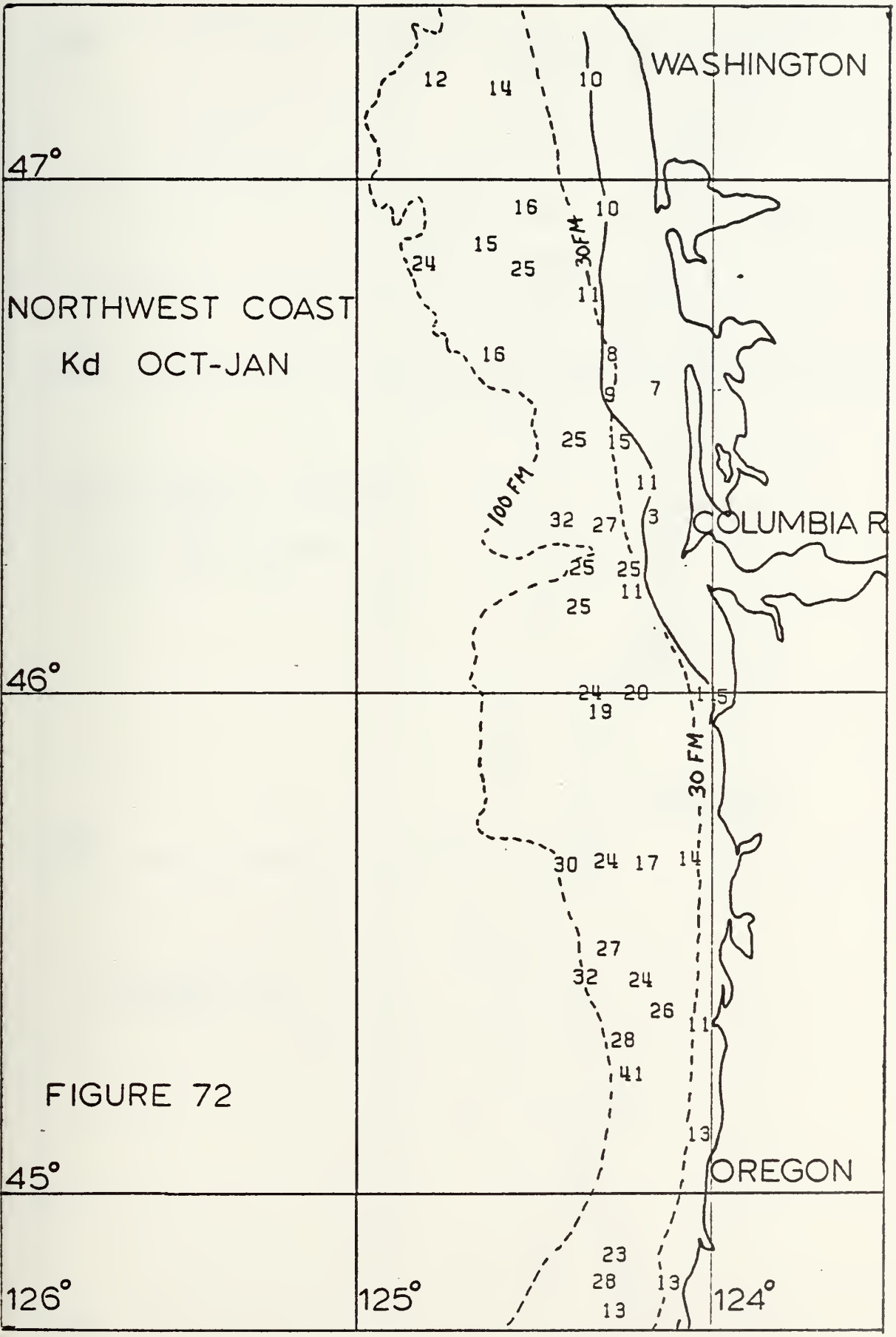
WASHINGTON
47°
NORTHWEST COAST
Kd OCT-JAN
30 FM
100 FM
COLUMBIA R
46°
30 FM
OREGON
45°
126°
125°
124°

FIGURE 72

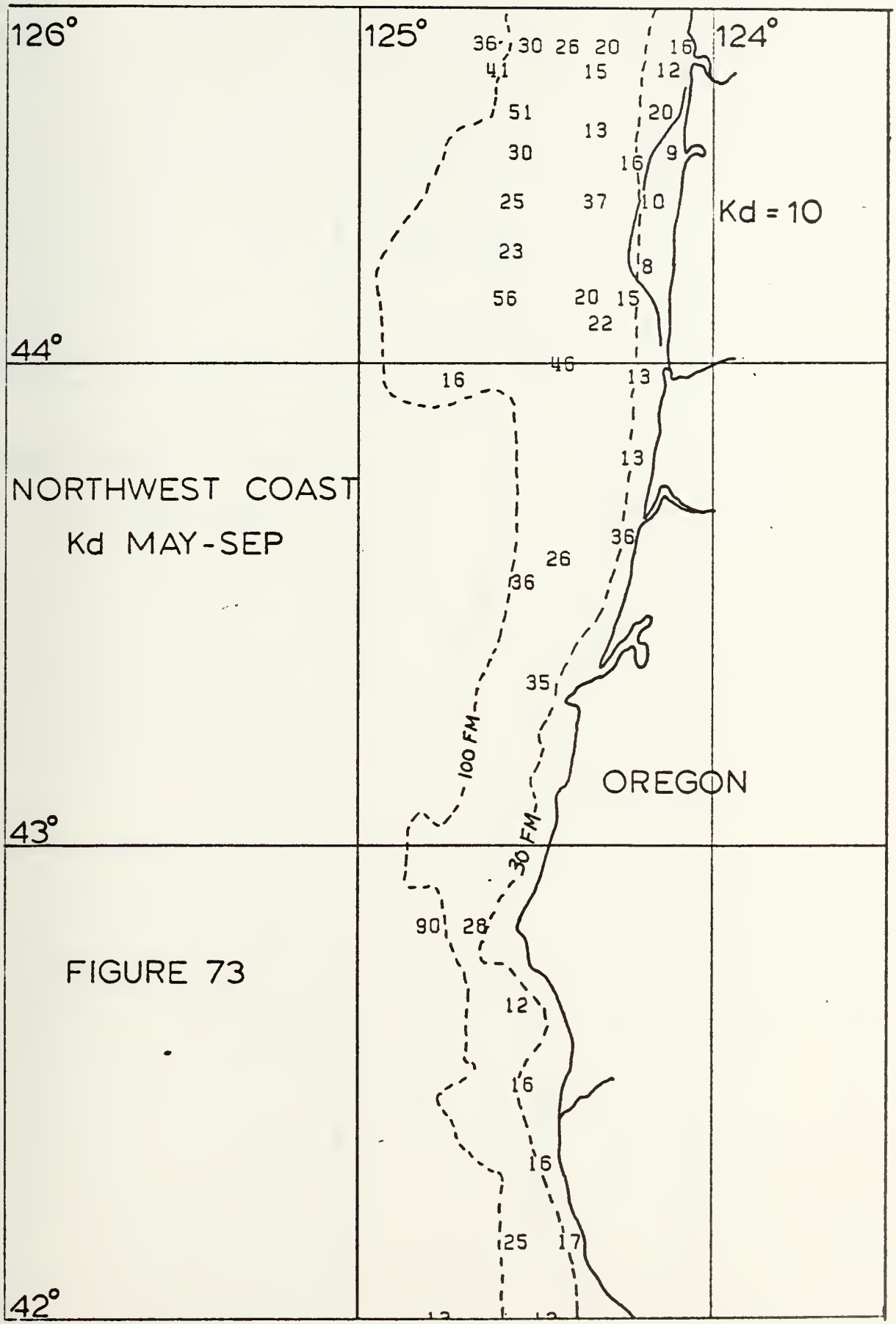
126°
125°
124°
44°
43°
42°
36
30
26
20
16
41
15
12
51
13
20
30
16
9
25
37
10
23
8
56
20
15
22
46
16
13
13
36
26
36
35
100 FM
30 FM
OREGON
90
28
12
16
16
25
17
Kd = 10
NORTHWEST COAST
Kd MAY-SEP
FIGURE 73

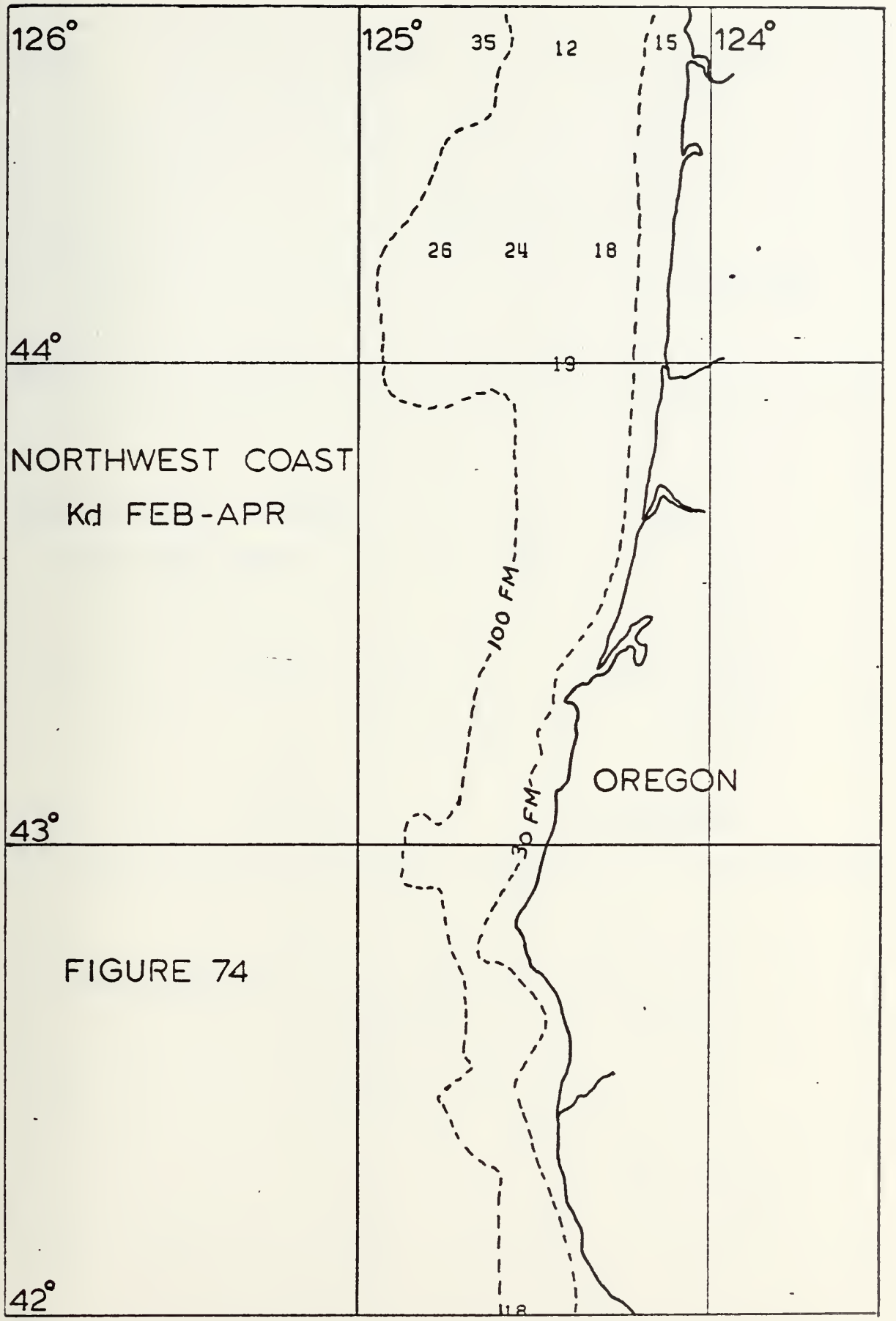
126°
125°
124°
44°
43°
42°
35
12
15
26
24
18
19
NORTHWEST COAST
Kd FEB-APR
100 FM
30 FM
OREGON
18

FIGURE 74

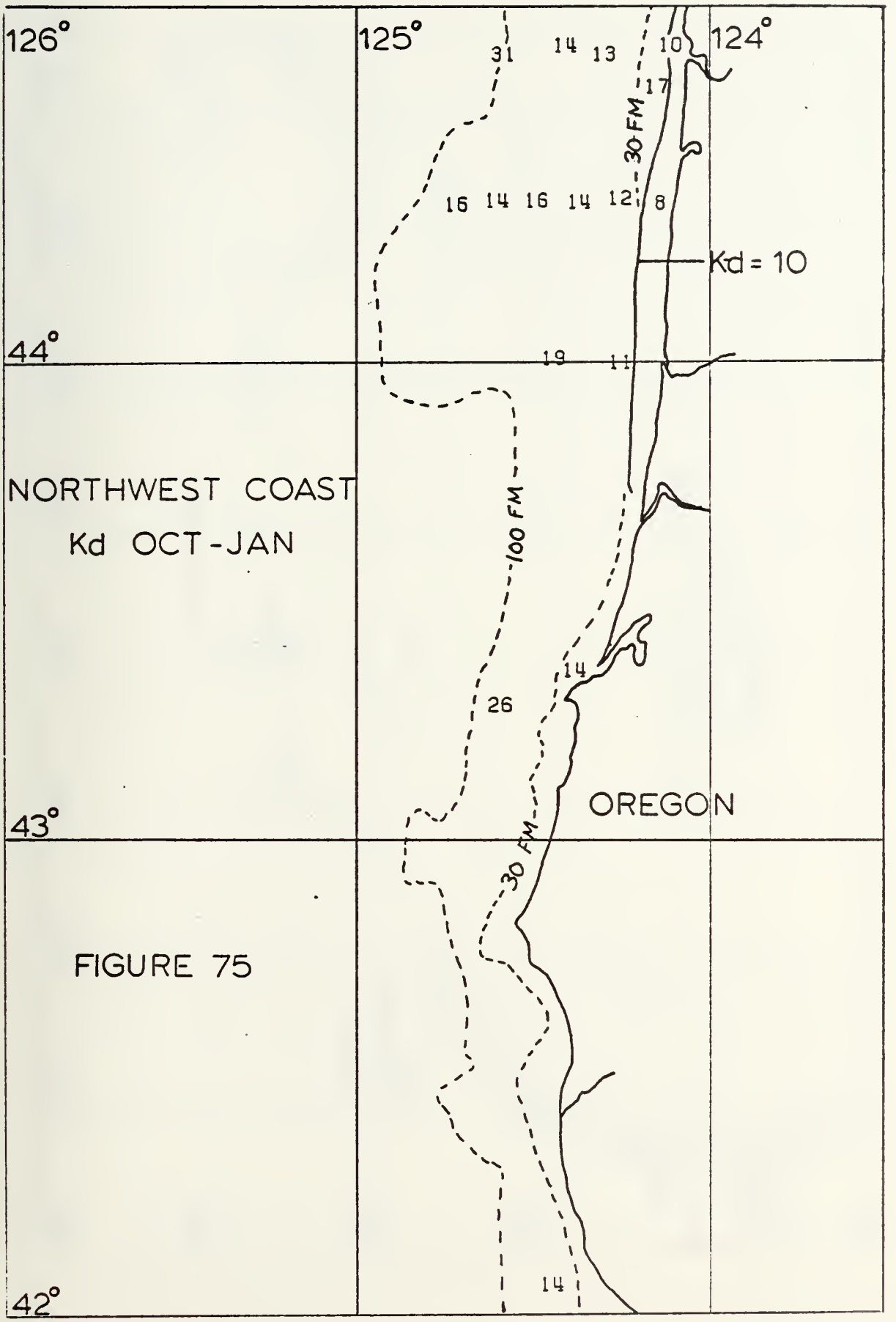
126°
125°
124°
44°
43°
42°
31
14
13
10
17
30 FM
16
14
16
14
12
8
Kd = 10
19
11
NORTHWEST COAST
Kd OCT-JAN
100 FM
14
26
OREGON
30 FM
14

FIGURE 75

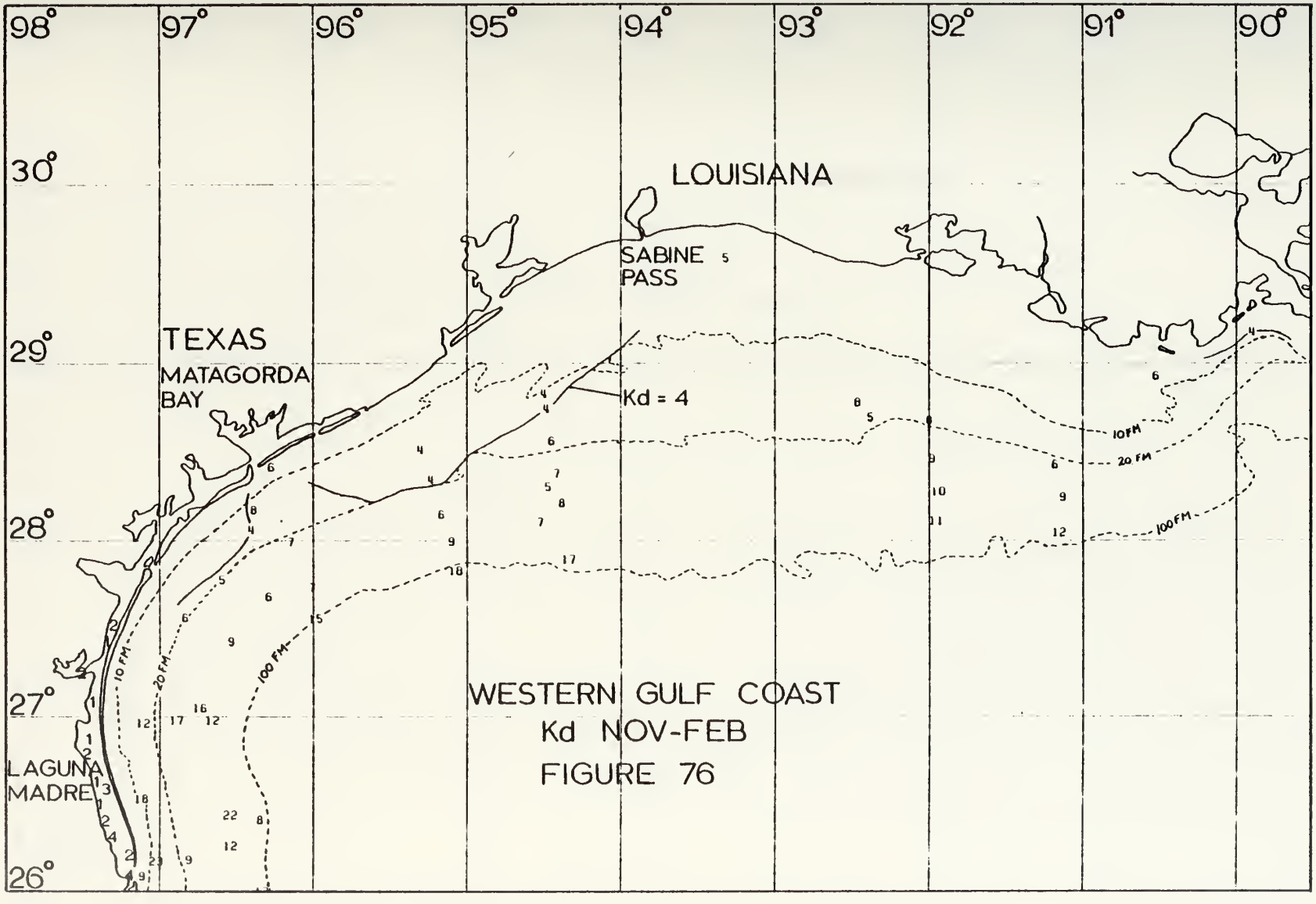
98°
97°
96°
95°
94°
93°
92°
91°
90°
30°
29°
28°
27°
26°
LOUISIANA
SABINE PASS
TEXAS
MATAGORDA BAY
Kd = 4
10 FM
20 FM
100 FM
LAGUNA MADRE
WESTERN GULF COAST
Kd NOV-FEB
FIGURE 76

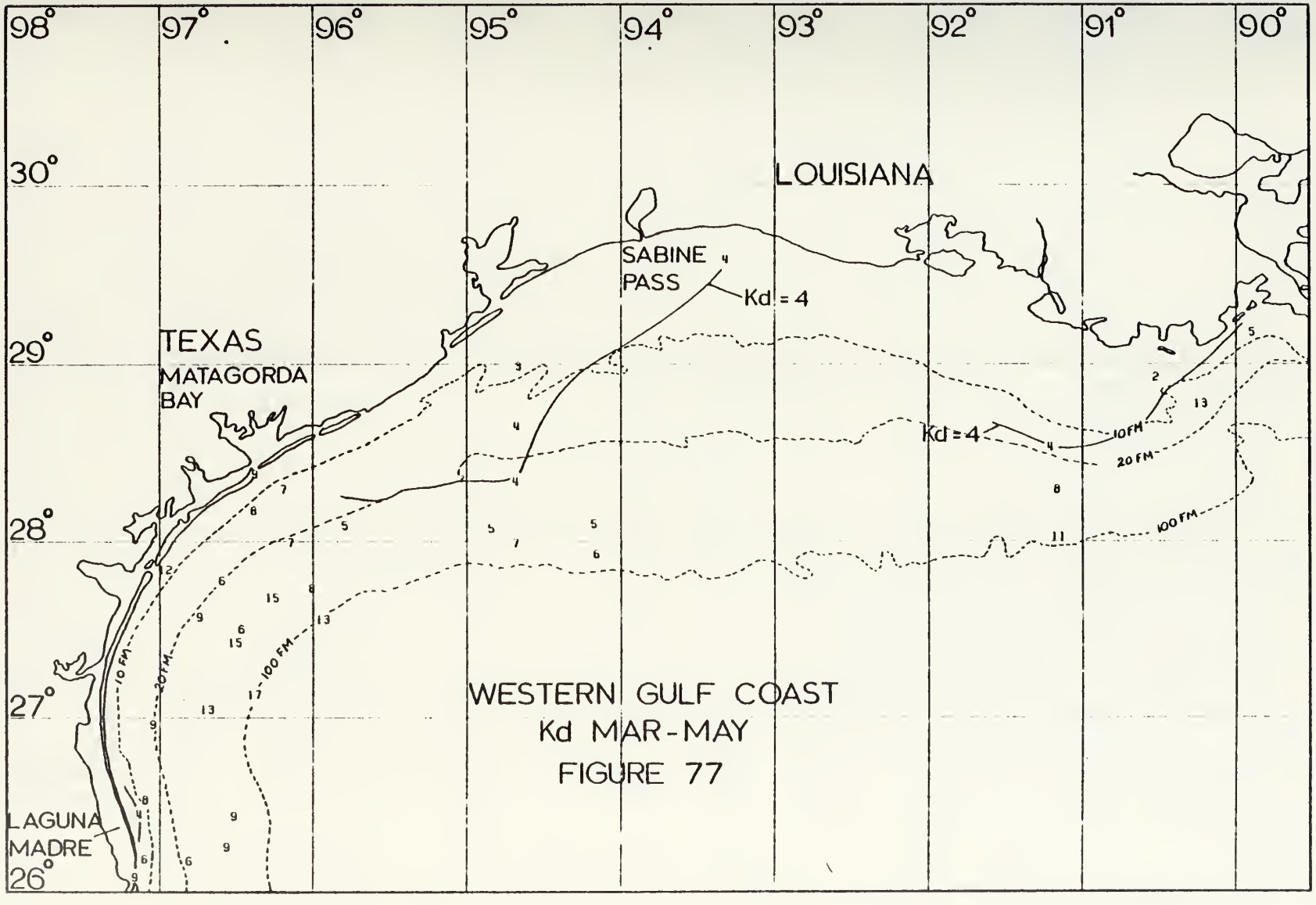
98°
97°
96°
95°
94°
93°
92°
91°
90°
30°
29°
28°
27°
26°
LOUISIANA
TEXAS
SABINE PASS
Kd = 4
MATAGORDA BAY
Kd = 4
10 FM
20 FM
100 FM
LAGUNA MADRE
WESTERN GULF COAST
Kd MAR-MAY
FIGURE 77

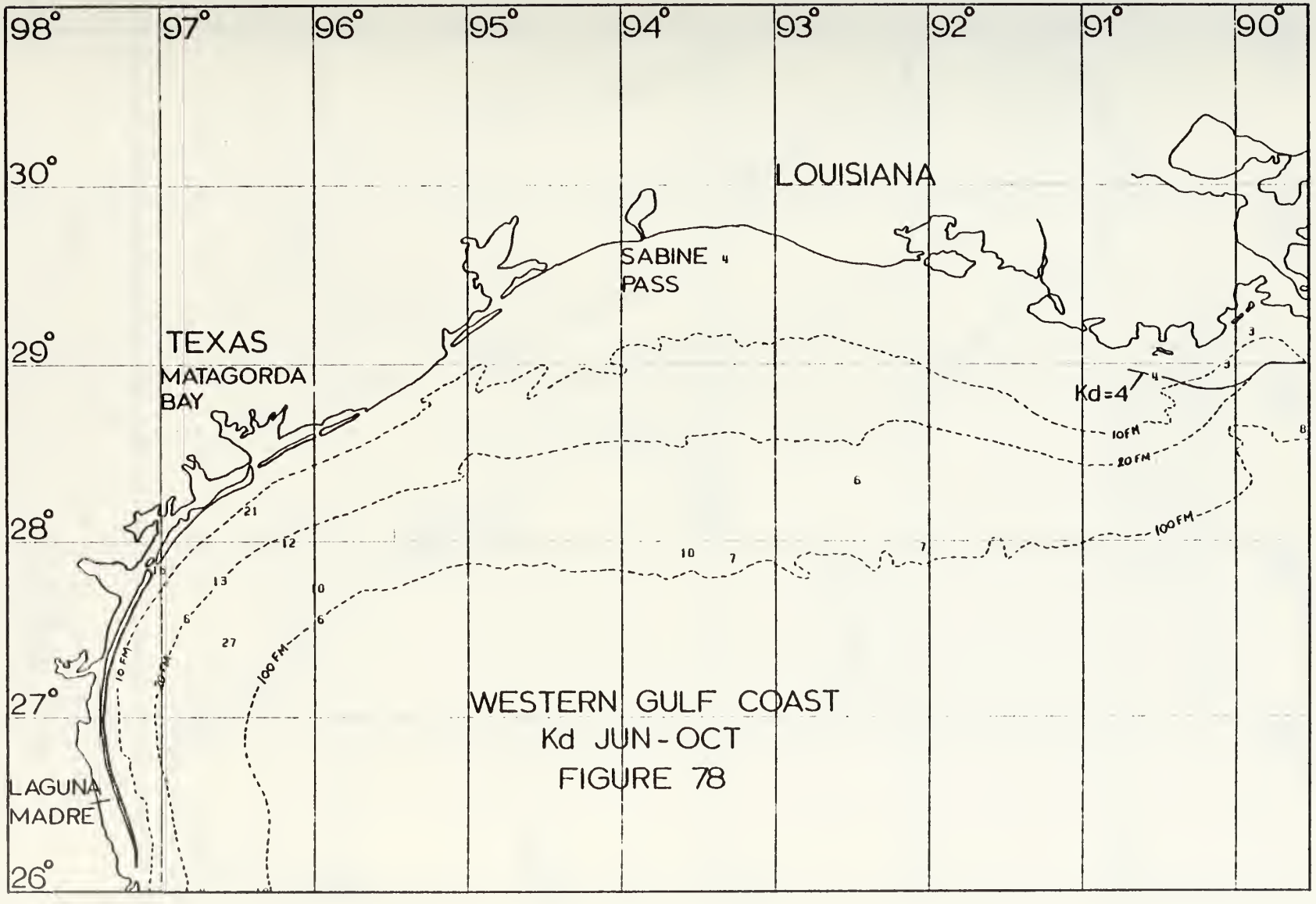
98°
97°
96°
95°
94°
93°
92°
91°
90°
30°
29°
28°
27°
26°
LOUISIANA
SABINE PASS
TEXAS
MATAGORDA BAY
LAGUNA MADRE
Kd=4
10FM
20FM
100FM
WESTERN GULF COAST
Kd JUN-OCT
FIGURE 78

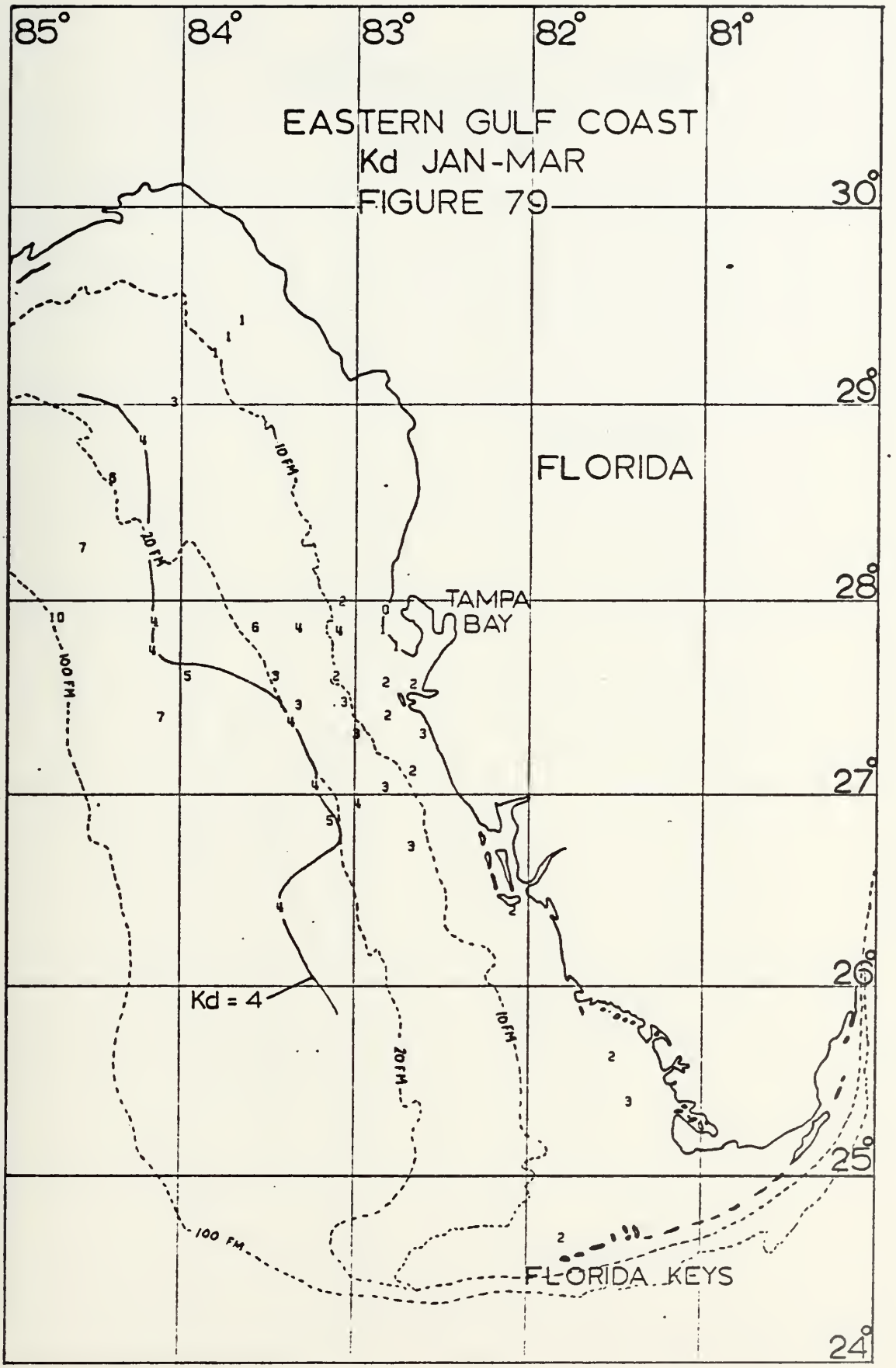
85°
84°
83°
82°
81°
EASTERN GULF COAST
Kd JAN-MAR
FIGURE 79
30°
29°
FLORIDA
28°
TAMPA
BAY
27°
26°
Kd = 4
10 FM
20 FM
100 FM
25°
FLORIDA KEYS
24°

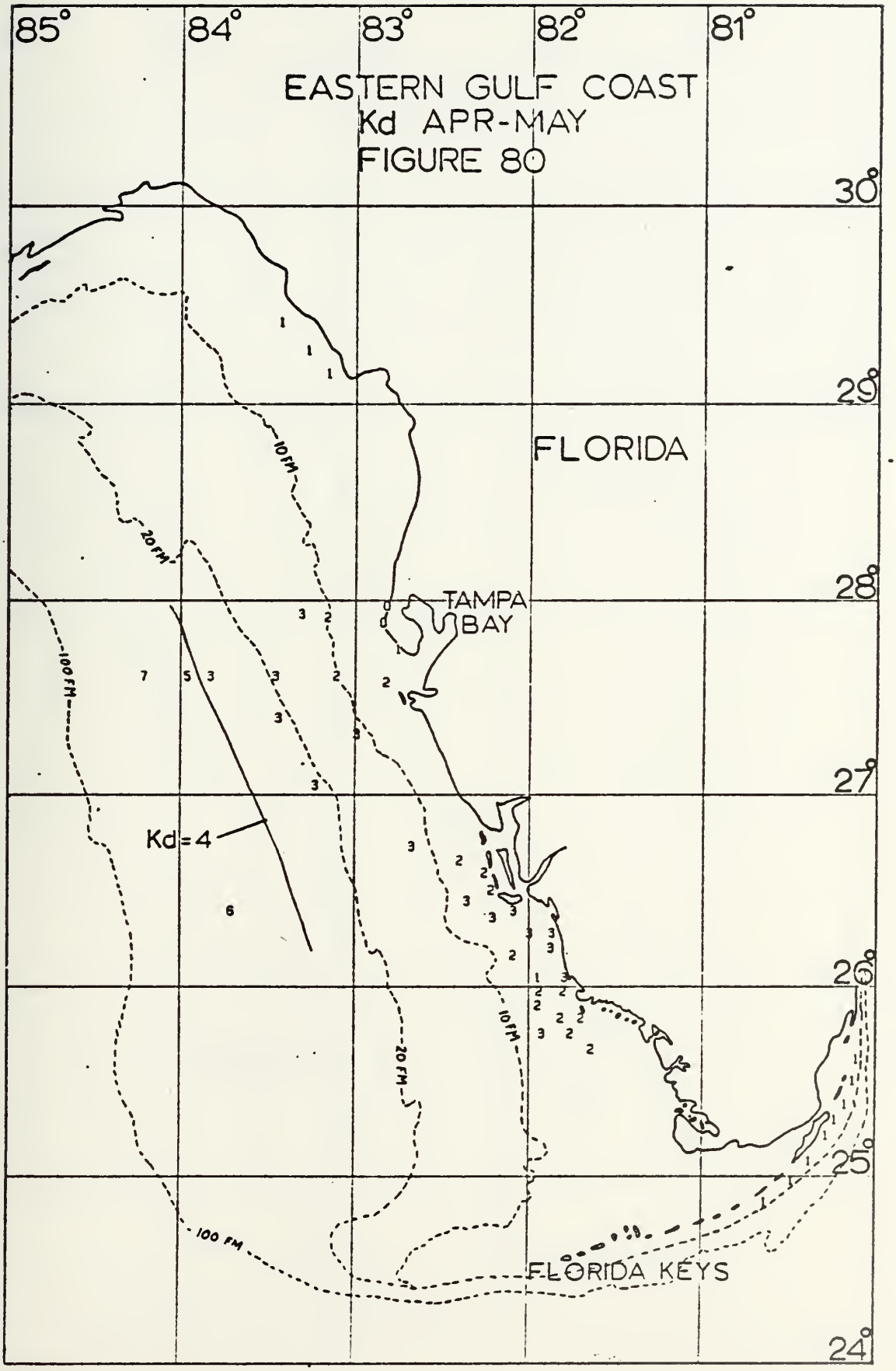
85°
84°
83°
82°
81°
EASTERN GULF COAST
Kd APR-MAY
FIGURE 80
30°
29°
28°
27°
26°
25°
24°
FLORIDA
TAMPA BAY
10 FM
20 FM
100 FM
Kd = 4
FLORIDA KEYS

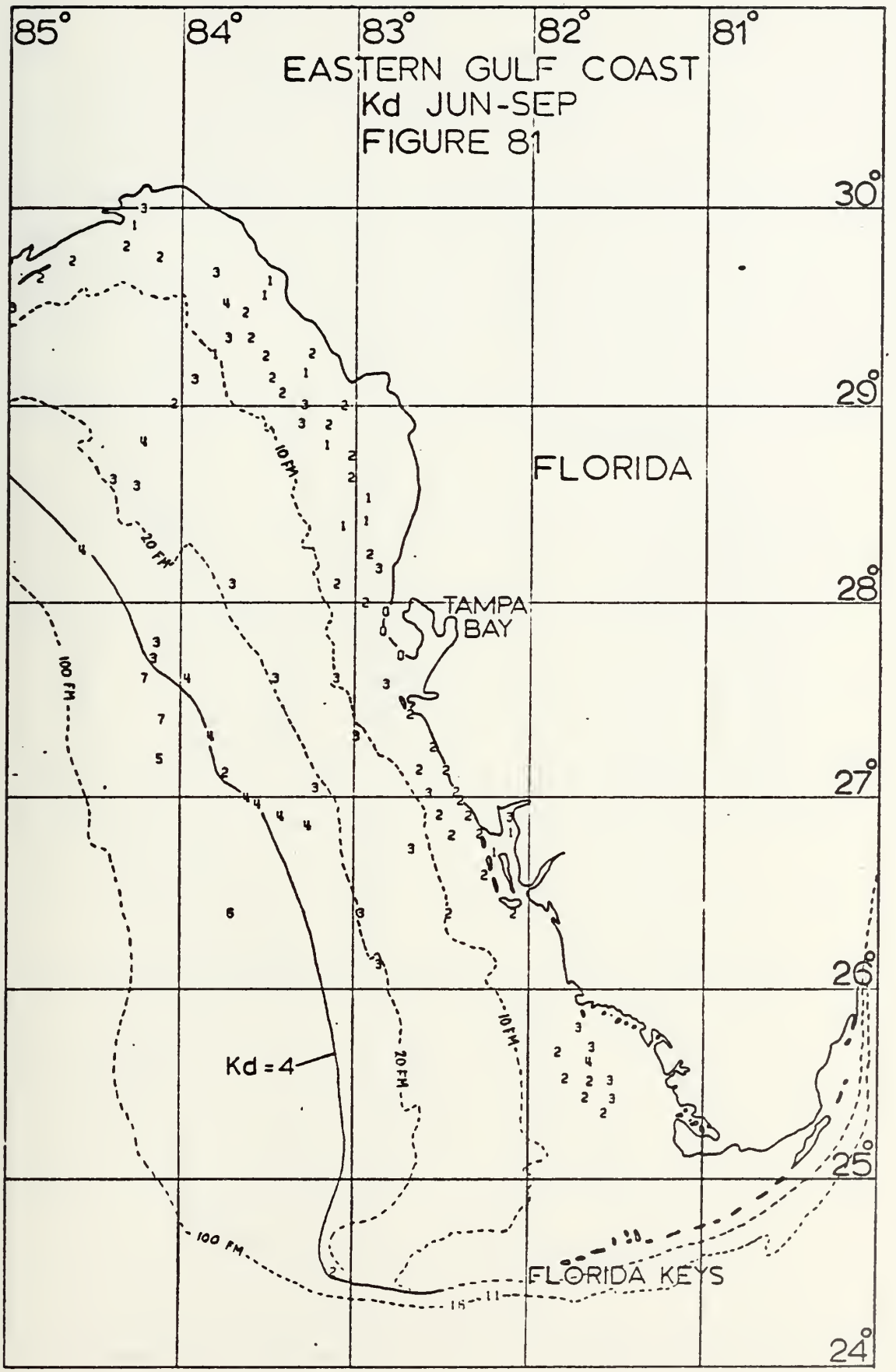
85°
84°
83°
82°
81°
EASTERN GULF COAST
Kd JUN-SEP
FIGURE 81
30°
29°
28°
27°
26°
25°
24°
FLORIDA
TAMPA BAY
10 FM
20 FM
100 FM
Kd = 4
FLORIDA KEYS

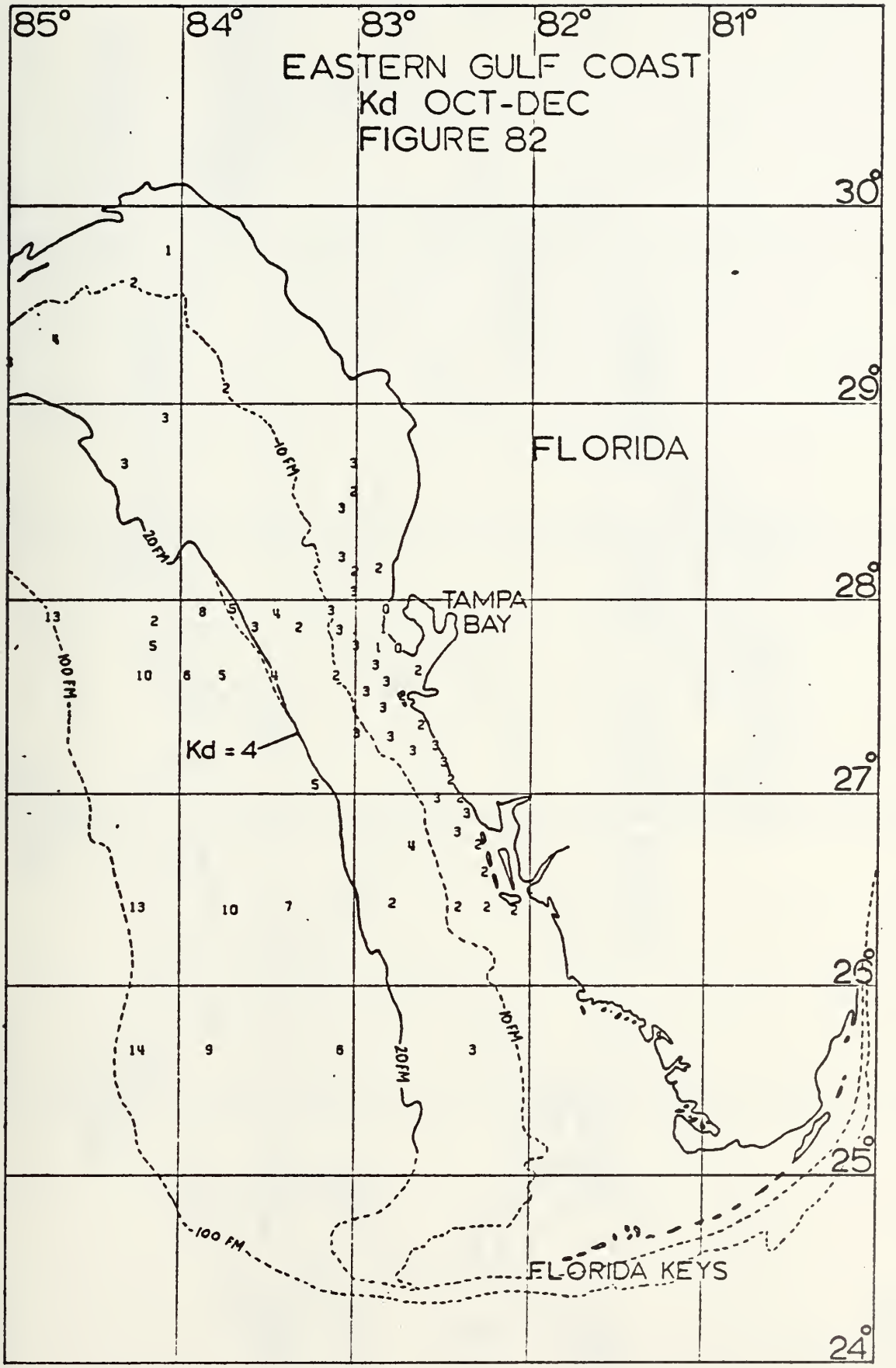
85°
84°
83°
82°
81°
EASTERN GULF COAST
Kd OCT-DEC
FIGURE 82
30°
29°
28°
27°
26°
25°
24°
FLORIDA
TAMPA BAY
Kd = 4
10 FM
20 FM
100 FM
FLORIDA KEYS

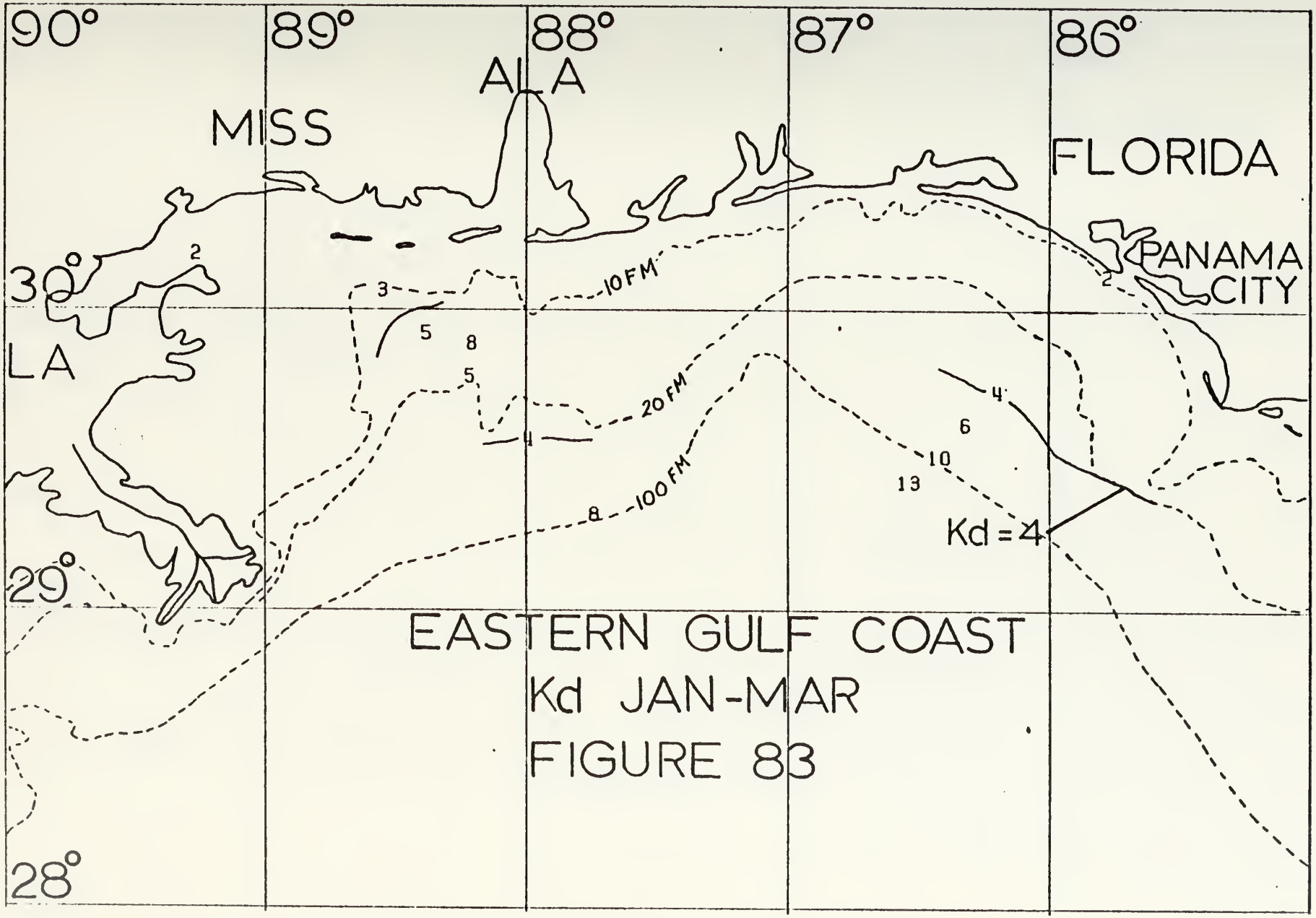


EASTERN GULF COAST
Kd JAN-MAR
FIGURE 83

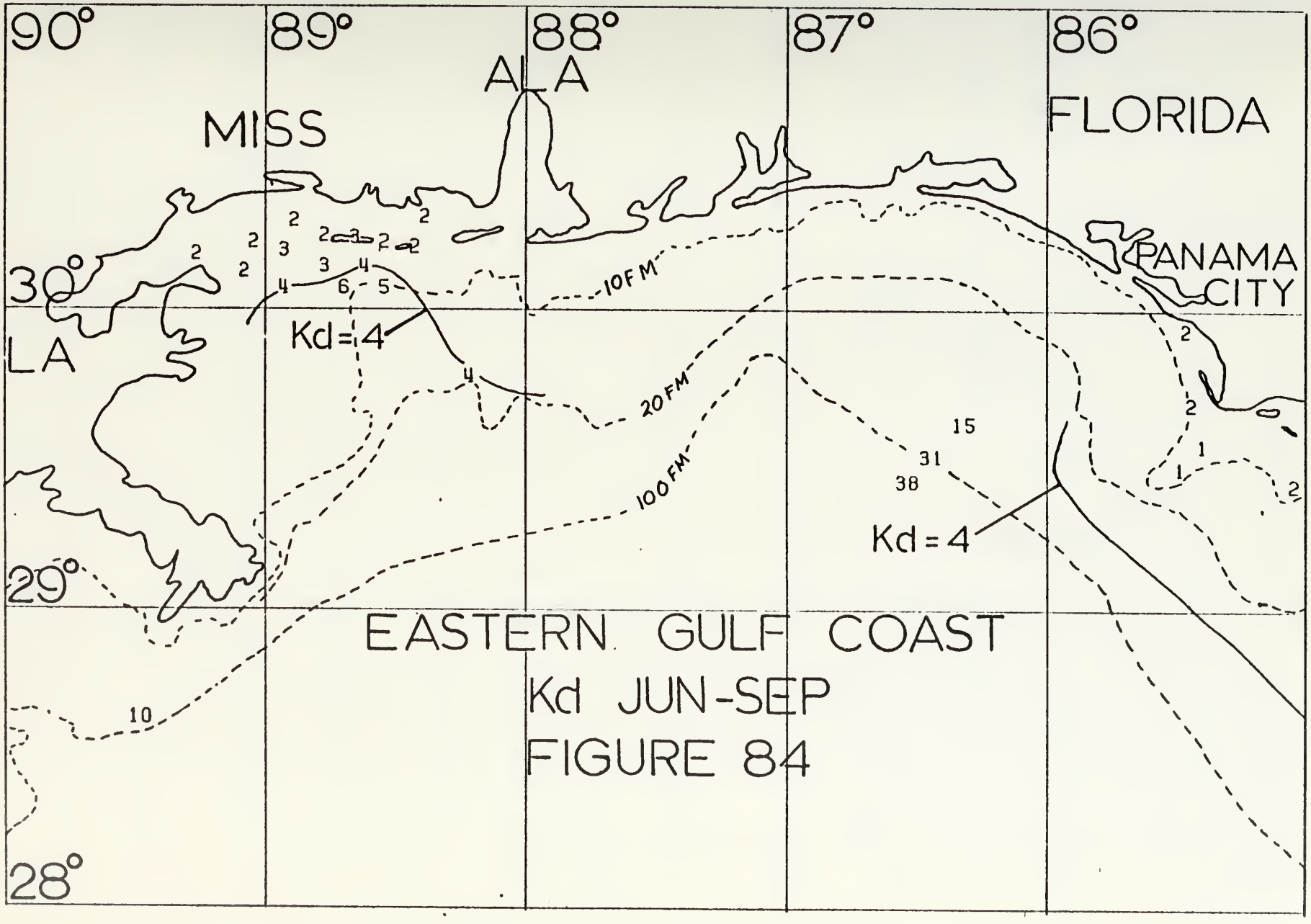
90°
89°
88°
87°
86°
MISS
ALA
FLORIDA
PANAMA CITY
30°
LA
29°
28°
10FM
20FM
100FM
Kd=4
Kd=4
EASTERN GULF COAST
Kd JUN-SEP
FIGURE 84

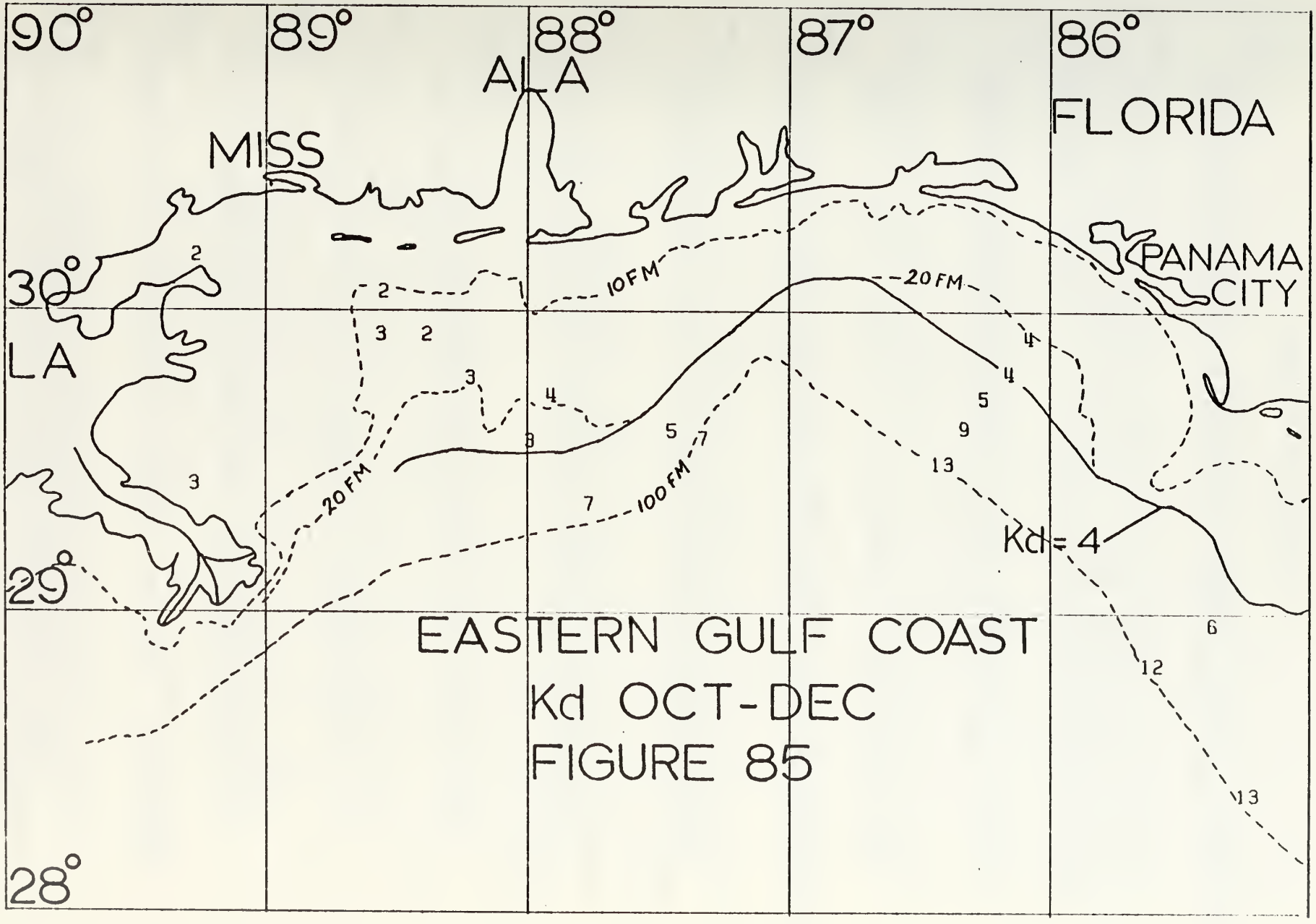


EASTERN GULF COAST

Kd OCT-DEC

FIGURE 85

LIST OF REFERENCES

Alexander, J.E., et al., BLM Contract No. 08550-CT5-30, Baseline Monitoring Studies, Mississippi, Alabama, Florida, Outer Continental Shelf, 1975-1976, Vol. IV, 28 June 1977.

Allan Hancock Foundation, University of Southern California, State of California, Resources Agency, State Water Quality Control Board, Publication No. 27, An Oceanographic and Biological Survey of the Southern California Mainland Shelf, 232 pages, 1963.

Avco Everett Research Laboratory, Inc., Contract No. 7-35373, Airborne Hydrography System, Limited Design Report, prepared for National Ocean Survey, January 1978.

Avco Everett Research Laboratory, Inc., NASA Contractor Report NASA CR-141407, Airborne Oceanographic Lidar System Final Report, October 1975.

Bakun, A., NOAA Technical Report NMFS SSRF-693, Daily and Weekly Upwelling Indices, West Coast of North America, 1967-73, 114 pages, August 1975.

Barret, B.B., et al., Technical Bulletin No. 27, A Study of Louisiana's Major Estuaries and Adjacent Offshore Waters, Louisiana Department of Wildlife and Fisheries, New Orleans, April 1978.

Barrett, B.B., Cooperative Gulf of Mexico Estuarine Inventory and Study, Louisiana, Phase II, Hydrology and Phase III, Sedimentology, Louisiana Wildlife and Fisheries Commission, New Orleans, 1971.

Berryhill, H.L., Jr., et al., U.S. Geological Survey Report USGS GD-78003, Environmental Studies, South Texas Outer Continental Shelf, 1976, Geology, 1976.

Berryhill, H.L., Jr., et al., U.S. Geological Survey Report USGS GD-78012, Environmental Studies, South Texas Outer Continental Shelf 1977, Geology, 1 February 1978.

Boone, C.G., et al., Environmental Laboratory, U.S. Army Engineer Waterways Experiment Station, Technical Report D-77-30, Aquatic Disposal Field Investigations Columbia River Disposal Site, Oregon, pp. 15-21, May 1978.

Bright, D., NASA SP-375, "NAVOCEANO's Lidar Program," The Use of Lasers for Hydrographic Studies, pp. 9-10, 12 September 1973.

Brown, P.J., Correlation Coefficients Calculated on a World Wide Basis Between Observed Secchi Depths and Other Simultaneously Measured Standard Oceanographic Parameters, M.S. Thesis, U.S. Naval Postgraduate School, 123 pages, March 1973.

Callaway, R. and McGary, J.W., U.S. Fish and Wildlife Service, Special Scientific Report, Fisheries No. 315, Northeastern Pacific Albacore Survey, Part 2, Oceanographic and Meteorological Observations, July 1959.

Carder, K.L., and Haddad, K.D., Final Report to Bureau of Land Management, Contract AA550-CT7-34, "Transmissometry on the Eastern Gulf of Mexico Shelves, MAFLA Outer Continental Shelf Baseline Environmental Survey, 1977-1978, Vol. II-B, 1979.

Carlson, P.R., et al., U.S. Geological Survey, Principal Sources and Dispersal Patterns of Suspended Particulate Matter in Nearshore Surface Waters of the Northeast Pacific Ocean, pp. 1-139, 10 February 1975.

Crandall, C.J., "Coastal Aerial Photo-Laser Survey (CAPS)," International Hydrographic Review, Vol. 53, No. 1, pp. 53-64, January 1976.

Drake, D.E., Distribution and Transport of Suspended Matter, Santa Barbara Channel, California, Ph.D. Thesis, University of Southern California, Los Angeles, 1972.

El-Sayed, S.Z., Unpublished data of Texas A&M University cruises 71-A-6, 72-A-12, and 73-A-12, Personal correspondence with Dr. Tucker.

Enabnit, D., National Ocean Survey, Code C611, Personal letter to Dr. Tucker, Subject: Optical Oceanography and Laser Hydrography, 29 January 1979.

Enabnit, D., "Status of Airborne Laser Hydrography," Proceedings of the National Ocean Survey Hydrographic Survey Conference, 6th Annual Conference, Seattle, Washington, 8-12 January 1979.

Erb, R.B., NASA TM X-58118, The Erts-1 Investigation (ER-600): Vol. II Erts-1 Coastal/Estruarine Analysis (Report for period July 1972-June 1973), July 1974.

Ferguson, G.D., "Blue-Green Lasers for Underwater Applications," Ocean Optics, Vol. 64, Proceedings of the Society of Photo-Optical Instrumentation Engineers, pp. 150-156, 19-20 August 1975.

Frederick, M.A., An Atlas of Secchi Disc Transparency Measurements and Forel-Ule Color Codes for the Oceans of the World, M.S. Thesis, U.S. Naval Postgraduate School, September 1970.

Geraghty, J.J., et al, Water Information Center Publication, Water Atlas of the United States, plates 24 and 25, 1973.

Godcharles, M.F., and Jaap, W.C., Special Scientific Report No. 40, Florida Department of Natural Resources Marine Research Laboratory, Fauna and Flora in Hydraulic Clam Dredge Collections from Florida West and Southeast Coasts, December 1973.

Goddard Space Flight Center, NASA, The Nimbus 7 User's Guide, August 1978.

Gordon, H.R. and Dera, J., "Irradiance Attenuation Measurements in Sea Water off Southeast Florida," Bulletin of Marine Science, Vol. 19, No. 2, pp. 279-285, 1969.

Gordon, H.R. and Wouters, A.W., "Some Relationships between Secchi Depth and Inherent Optical Properties of Natural Waters," Applied Optics, Vol. 17., No. 21, pp. 3341-3343, 1978.

Grady, J.R., National Marine Fisheries Service letter to M. van Norden, Naval Postgraduate School, Subject: Secchi Measurements off Louisiana and Texas collected during five cruises of the Gus III, January to May 1966, 20 April 1979.

Graham, J.J., "Secchi Disc Observations and Extinction Coefficients in the Central and Eastern North Pacific Ocean," Limnology and Oceanography, 11(2), pp. 184-190, 1966.

Guenther, G.C. and Enabnit, D.B., "Laser Bathymetry for Near-Shore Charting Applications (A Status Report)," paper presented at 9th International Conference on Cartography, International Cartographic Association, College Park, Maryland, 1 August 1978.

Hickman, G.D., Hogg, J.E., and Ghovanlou, A.H., Sparcom Inc., Technical Report No. 1, Pulsed Neon Laser Bathymetric Studies using Simulated Delaware Bay Waters, pp. 1-79, September 1972.

Holmes, R.W., "The Secchi Disc in Turbid Coastal Waters," Limnology and Oceanography, 15(5), pp. 688-694, 1970.

Houck, M., Naval Oceanographic Research and Development Agency, personal communication with John Murdock, Naval Postgraduate School, Subject: Projected Number of Irradiance Attenuation Lengths to be Attained by the HALS System, 11 September 1979.

Hunter, R.E., NASA SP-327, "Distribution and Movement of Suspended Sediment in the Gulf of Mexico off the Texas Coast," Symposium on Significant Results Obtained from the Earth Resources Technology Satellite-1, Vol. I: Technical Presentations Section B, 5-9 March 1973.

Ichiye, T., Kuo, H, and Carnes, M.R., Texas A&M University, Contribution No. 601, Assessment of Currents and Hydrography of the Eastern Gulf of Mexico, 15 September 1973.

Jarman, J.W., NASA SP-356, "Erts Program of the U.S. Army Corps of Engineers," Third Earth Resources Technology Satellite Symposium, Vol. II, Summary of Results, December 10-14, 1973, pp. 62-75, May 1974.

Jerlov, N.G., Marine Optics, Elsevier Oceanography Series, No. 5, New York: Elsevier Scientific Publishing Co., 1976.

Joyce, E.A., and Williams, J., Memoirs of the Hourglass Cruises, Vol. I, Part I, Florida Department of Natural Resources, 50 pages, March 1969.

Kamykowski, D., et al., Supplemental Report to Bureau of Land Management Contract No. AA550-CT6-17, "Biological Characterization of the Nepheloid Layer," Chapter 15, Environmental Studies of South Texas Outer Continental Shelf, Biology and Chemistry, 1978.

Kamykowski, D., et al, Final Report 1977, Contract AA550-CT7-11, "Phytoplankton and Productivity," Chapter 11, Environmental Studies of South Texas Outer Continental Shelf, Biology and Chemistry, January 1979.

Karl, H.A., Processes Influencing Transportation and Deposition of Sediment on the Continental Shelf, Southern California, Ph.D. Thesis, University of Southern California, Los Angeles, November 1976.

Krumboltz, H., "Experimental Investigation of System Attenuation Coefficient for HALS," Naval Air Development Center Report (Draft Copy), 7 August 1979.

Manheim, F.T., Steward, R.G., and Carder, K.L., Final Report to Bureau of Land Management, Contract 08550-CT5-30, "Transmissometry and Particulate Matter Distribution in the Eastern Gulf of Mexico Shelves, MAFLA Survey, 1975-1976," MAFLA Monitoring Study, 1976, Vol. I, 1977.

Maul, G.A., and Gordon, H.R., "On the Use of the Earth Resources Technology Satellite (Landsat-1) in Optical Oceanography," Remote Sensing of Environment, Vol. 4, pp. 95-128, 1975.

McGrail, D.W., Huff, D., and Jenkins, S., Final Report to Bureau of Land Management, Contract AA550-CT7-15, "Current Measurements and Dye Diffusion Studies," Northwestern Gulf of Mexico Topographic Features Study, December 1978.

National Ocean Survey, The Office of Marine Technology, Airborne Laser Hydrography, A Briefing Prepared for the Director of the National Ocean Survey, Rockville, Maryland, 11 May 1979.

Naval Ocean Research and Development Activity, Hydrographic Airborne Laser Sounder (HALS), Base Line System, prepared by NORDA for DMA, pp. 1-33, 30 November 1978.

Otto, L., "Light Attenuation in the North Sea and the Dutch Wadden Sea in Relation to Secchi Disc Visibility and Suspended Matter," Netherlands Journal of Sea Research, Vol. 3(1), pp. 28-51, 1966.

Pak, H., Oregon State University, letter to M. van Norden, Naval Postgraduate School, Subject: Optical Data of R/V Yaquina Cruises Y7408-B and Y7504-C, 9 April 1979.

Pak, H., Secchi Data of Oregon State University Cruises 1968-1971, Personal correspondence with Dr. Tucker, November 1974.

Pak, H. and Zaneveld, R.V., "Bottom Nepheloid Layers and Bottom Mixed Layers Observed on the Continental Shelf off Oregon," Journal of Geophysical Research, Vol. 82, No. 27, pp. 3921-3931, 20 September 1977.

Perret, W.S., et al., Cooperative Gulf of Mexico Estuarine Inventory and Study, Louisiana, Phase I Area Description and Phase IV Biology, Louisiana Wild Life and Fisheries Commission, New Orleans, Louisiana, 1971.

Pirie, D.M. and Steller, D.D., California Coast Nearshore Processes Study Progress Report, 1 March-31 August 1973, U.S. Army Engineering District, San Francisco, California, prepared for Goddard Space Flight Center, September 1973.

Poole, H.H. and Atkins, W.R.G., "Photo-electric Measurements of Submarine Illumination throughout the Year," Journal of the Marine Biological Association of the United Kingdom, Vol. 16, pp. 297-324, 1929.

Pruter, A.T. and Alverson, D. L., editors, The Columbia River Estuary and Adjacent Ocean Waters, University of Washington Press, Seattle, Washington, 1972.

Rattman, W. and Cunningham, L., "The Pulsed Light Airborne Depth Sounder (PLADS)," Marine Geodesy: A Practical View, A Second Symposium on Marine Geodesy, 3-5 November 1969, Marine Technology Society, pp. 101-108, 1969.

Rouse, L.J. and Coleman, J.M., "Circulation Observations in the Louisiana Bight using LANDSAT Imagery," Remote Sensing of Environment, Vol. 5, No. 1, pp. 55-66, 1976.

Saloman, C.H. and Collins, L.A., NOAA NMFS DR90, NOAA 74111312, Hydrographic Observations in Tampa Bay and Adjacent Waters 1972, National Fisheries Service, Seattle, Washington, 181 pages, August 1974.

Saloman, C.H., Physical, Chemical, and Biological Characteristics of Nearshore Zone of Sand Key, Florida, Prior to Beach Restoration, Vol. I, National Marine Fisheries Service, Panama City, Florida, June 1974.

Shannon, J.G., "Correlation of Beam and Diffuse Attenuation Coefficients Measured in Selected Ocean Waters," Ocean Optics, Vol. 64, Proceedings of the Society of Photo-Optical Instrumentation Engineers, pp. 3-11, 19-20 August 1975.

Shannon, J.G., Naval Air Development Center, personal communication with M. van Norden, Subject: Relationships for Converting Secchi and Beam Attenuation Measurements to Irradiance Attenuation Coefficients, 7 August 1979.

Shideler, G. L., "Physical Characteristics of Suspended Sediments, South Texas Continental Shelf," U.S. Geological Survey Open File Report 79-362, 1972.

Small, L.F., Oregon State University, personal correspondence with M. van Norden, Naval Postgraduate School, Subject: Irradiance Attenuation data collected off Oregon 1962-1965, 4 April 1979.

Small, L.F. and Curl, H., Jr., "The Relative Contribution of Particulate Chlorophyll and River Tripton to the Extinction of Light Off the Coast of Oregon," Limnology and Oceanography, Vol. 13, No. 1, pp. 84-91, January 1968.

Stevenson, W.H., and Pastula, E.J., Investigation Using Data from Erts-1 to Develop and Implement Utilization of Living Marine Resources, Final Report 1 July 1972-4 October 1973, National Marine Fisheries Service, Bay St. Louis, Mississippi, 198 pages, December 1973.

Tyler, J.E., "The Secchi Disc," Limnology and Oceanography, Vol. 13, No. 1, pp. 1-6, January 1968.

U.S. Naval Hydrographic Office, H.O. Publication No. 570, Atlas of Surface Currents Northeast Pacific Ocean, 1967.

U.S. Naval Oceanographic Office, American Practical Navigator, originally by Nathaniel Bowditch, Washington, DC: Government Printing Office, 1966.

U.S. Naval Oceanographic Office, SP-189II, Environmental-Acoustics Atlas of the Caribbean Sea and Gulf of Mexico, Vol. II, pp. 145-168, August 1972.

U.S. Naval Weather Service Command, Summary of Synoptic Meteorological Observations, Vol. 6, 474 pages, May 1970.

Williams, J., John Hopkins University, Technical Report 45, Reference 68-15, The Meaningful Use of the Secchi Disc, November 1968.

Winzler and Kelly, Report prepared for Department of Interior, A Summary of Knowledge of the Central and Northern California Coastal Zone and Offshore Areas, Vol. I, Physical Conditions Book 1, Eureka, California, August 1977.

Witt, A.K., U. S. Naval Air Development Center, Johnsville, Pennsylvania, personal communication to authors, July 1979.

York, G.L., Statistical Studies of World-Wide Secchi Data, M.S. Thesis, U.S. Naval Postgraduate School, March 1974.

Zaneveld, J.R., et al., Oregon State University, School of Oceanography Ref. 78-13, Optical Hydrographic and Chemical Observations in the Monterey Bay Area During May and September 1977, August 1978.

INITIAL DISTRIBUTION LIST

| | No. Copies |
|---|---|
| Defense Documentation Center<br>Cameron Station<br>Alexandria, VA 22314 | 2 |
| Library, Code 0142<br>Naval Postgraduate School<br>Monterey, CA 93940 | 2 |
| Chairman, Code 68<br>Department of Oceanography<br>Naval Postgraduate School<br>Monterey, CA 93940 | 3 |
| Dr. Stevens P. Tucker, Code 68Tx<br>Department of Oceanography<br>Naval Postgraduate School<br>Monterey, CA 93940 | 5 |
| Director<br>Naval Oceanography Division (OP952)<br>Navy Department<br>Washington, DC 20350 | 1 |
| Office of Naval Research<br>Code 480<br>Naval Ocean Research and Development Activity<br>NSTL Station<br>Bay St. Louis, MS 39522 | 1 |
| Dr. Robert E. Stevenson<br>Scientific Liaison Office, ONR<br>Scripps Institution of Oceanography<br>La Jolla, CA 92037 | 1 |
| Commanding Officer<br>Fleet Numerical Weather Central<br>Monterey, CA 93940 | 1 |
| Dr. Murray Brown<br>Bureau of Land Management, OSC<br>Hale Boggs Fed. Bldg., Suite 841<br>500 Camp Street<br>New Orleans, LA 70130 | 1 |
| Mr. Gerald L. Shideler<br>U.S. Geological Survey<br>P.O. Box 6732<br>Corpus Christi, TX 78411 | 1 |

Commanding Officer 1
Naval Environmental Prediction Research Facility
Monterey, CA 93940

Commander 1
Oceanographic Systems Pacific
Box 1390
Pearl Harbor, Hawaii 96860

Commanding Officer 1
Naval Ocean Research and Development Activity
NSTL Station
Bay St. Louis, MS 39522

Commander 1
Naval Oceanography Command
NSTL Station
Bay St. Louis, MS 39522

Commanding Officer 1
Naval Oceanographic Office
NSTL Station
Bay St. Louis, MS 39522

Mr. Maxim F. van Norden 5
Code 8412
U.S. Naval Oceanographic Office
NSTL Station
Bay St.Louis, MS 39522

Mr. John Shannon, Code 3012 1
Naval Air Development Center
Warminster, PA 18974

Mr. H. Krumboltz, Code 3010 1
Naval Air Development Center
Warminster, PA 18974

Mr. Steven E. Litts, Code HYAI 5
DMAHTC
6500 Brookes Lane
Washington, DC 20315

Mr. David B. Enabnit 2
National Oceanic and Atmospheric Administration
National Ocean Survey
Rockville, MD 20852

Mr. Mike Cooper, Code 772 1
Naval Coastal Systems Lab
Panama City, FL 32407

Mr. Richard M. Wargelin, Code 2000 1
U.S. Naval Oceanographic Office
NSTL Station
Bay St. Louis, MS 39522

Mr. Jim Hammock 1
DMAHTC
6500 Brookes Lane
Washington, DC 20315

Mr. Albert Pressman, Code 335 1
Naval Ocean Research and Development Activity
NSTL Station
Bay St. Louis, MS 39522

Library 1
DMA H/TC
6500 Brookes Lane
Washington, DC 20315

U.S. Naval Oceanographic Office 1
Library, Code 4103
NSTL Station
Bay St. Louis, MS 39522

Mr. Jimmy C. Stribling, Code 8412 1
U.S. Naval Oceanographic Office
NSTL Station
Bay St. Louis, MS 39522

CDR Donald Nortrup, Code 68Nr 1
Department of Oceanography
Naval Postgraduate School
Monterey, CA 93940

Mr. K. Petri, Code 3012 1
Naval Air Development Center
Warminster, PA 18974

Mr. James E. Gillis, Code ST 1
DMA H/TC
6500 Brookes Lane
Washington, DC 20315

Mr. Max Houck, Code 302 1
Naval Ocean Research and Development Activity
NSTL Station
Bay St. Louis, MS 39522

Mr. Duane Bright, Code 302 1
Naval Ocean Research and Development Activity
NSTL Station
Bay St. Louis, MS 39522

CDR Van K. Nield, Code SST 1
Defense Mapping Agency HQ
Bldg. 56, U.S. Naval Observatory
Washington, DC 20305

Dr. Boyd Olson, Code 02 — 1
U.S. Naval Oceanographic Office
NSTL Station
Bay St. Louis, MS 39522

Mr. Robert Higgs, Code 8000 — 1
U.S. Naval Oceanographic Office
NSTL Station
Bay St. Louis, MS 39522

Mr. David Jenkins, Code 8400 — 1
U.S. Naval Oceanographic Office
NSTL Station
Bay St. Louis, MS 39522

Mr. Larry Bourquin, Code 8400 — 1
U.S. Naval Oceanographic Office
NSTL Station
Bay St. Louis, MS 39522

Mr. Dodd Ouellette, Code 8410 — 1
U.S. Naval Oceanographic Office
NSTL Station
Bay St. Louis, MS 39522

Mr. W. Henry Odum, III — 2
Environmental Data Service
National Oceanographic Data Center
Washington, DC 20235

Mr. Louis Hoelman, WH553 — 1
Environmental Protection Agency
Washington, DC 20460

Mr. Andrew Bakun — 1
National Marine Fisheries Service
c/o Fleet Numerical Weather Central
Monterey, CA 93940

John Murdock, Code 8412 — 1
U.S. Naval Oceanographic Office
NSTL Station
Bay St. Louis, MS 39522

Dr. Hasong Pak — 1
School of Oceanography
Oregon State University
Corvallis, Oregon 97331

Thesis
V23
c.1
van Norden
186201
The transparency of selected U.S. coastal waters with applications to laser bathymetry.